



Estimation of Biomass and Carbon Stock in Para rubber Plantation in East Thailand Using Object-based Classification from THAICHOTE Satellite Data

Kitsanai Charoenjit

► To cite this version:

Kitsanai Charoenjit. Estimation of Biomass and Carbon Stock in Para rubber Plantation in East Thailand Using Object-based Classification from THAICHOTE Satellite Data. Environmental Engineering. Université Pierre et Marie Curie - Paris VI, 2015. English. NNT : 2015PA066170 . tel-01207535

HAL Id: tel-01207535

<https://theses.hal.science/tel-01207535>

Submitted on 1 Oct 2015

HAL is a multi-disciplinary open access archive for the deposit and dissemination of scientific research documents, whether they are published or not. The documents may come from teaching and research institutions in France or abroad, or from public or private research centers.

L'archive ouverte pluridisciplinaire **HAL**, est destinée au dépôt et à la diffusion de documents scientifiques de niveau recherche, publiés ou non, émanant des établissements d'enseignement et de recherche français ou étrangers, des laboratoires publics ou privés.

THÈSE

PRÉSENTÉE A

Université Pierre et Marie Curie

ÉCOLE DOCTORALE : Géosciences, ressources naturelles et environnement

LABORATOIRE : Institut des Sciences de la Terre de Paris (ISTeP)

Par Kitsanai CHAROENJIT

POUR OBTENIR LE GRADE DE

DOCTEUR

**Estimation of Biomass and Carbon Stock in Para rubber
Plantation in East Thailand Using Object-based Classification
from THAICHOTE Satellite Data**

Co-directeurs de recherche : Pierpaolo ZUDDAS et Pascal ALLEMAND

Date de soutenance : 18 Juin 2015

Devant un jury composé de :

Dr.	Bernard RIERA	CNRS, France.	Rapporteur
Prof.	Christophe DELACOURT	UBO, France.	Rapporteur
Dr.	Bruno GALBRUN	UPMC, France	Examineur
Prof.	Pierpaolo ZUDDAS	UPMC, France.	Directeur de thèse
Prof.	Pascal ALLEMAND	UCBL, France.	Co-directeur de thèse
Assoc.Prof.	Sura PATTANAKIAT	Mahidol University, Thaïlande.	Invité
Assist.Prof.	Katavut PACHANA	Burapha University, Thaïlande.	Invité

I dedicate this work to Faculty of Geoinformatics - Burapha University, Pimpan, Suraphong and Arommanee

“Genius is one percent inspiration and ninety-nine percent perspiration.”

Thomas Alva Edison

ACKNOWLEDGEMENTS

I want to firstly acknowledge my PhD thesis supervisors for their contribution and involvement in this work. Prof. Pierpaolo Zuddas (University Pierre and Marie CURIE: UPMC) and Prof. Pascal Allemand (Université Claude Bernard Lyon 1: UCBL) for they trust, continuous support and guidance along the years.

I am indebted to the Franco-Thai Scholarship Program and Faculty of Geoinformatics, Burapha University for the 3 years scholarship award.

I am very grateful to the members of the examining committee Dr. Bernard Riera (Museum National d'Histoire Naturelle: CNRS UMR MNHN 7179), Prof. Christophe Delacourt (Université de Bretagne Occidentale: UBO), Dr. Bruno Galbrun (University Pierre and Marie CURIE: UPMC), Assoc.Prof. Sura Pattanakiat (Mahidol University: MU), and Assist.Prof. Katavut Pachana (Burapha University: BUU), whose valuable comments improved the content and presentation of this contribution.

I would like to thank the team of GIREN, Mahidol University and Asscociat.Prof. Prasong Saguantam, Faculty of forestry, Kasetsart University. Without their untiring efforts and hard work for establishing the biomass and carbon forest inventory, this study would not have been possible. I also would like to thank the Geo-Informatics and Space Technology Development Agency (GISTDA) for providing THAICHOTE satellite data without charge.

Institut des Sciences de la Terre de Paris (UPMC-ISTeP), Dr. Marc de Rafélis and Dr. Gabrielle Rousselle are thanked for support the office equipments in Paris.

I share my greatest feelings to my “Charoenjit” family, to Arommanee’s specially for their unconditional love, generosity and support. I will always recall my time spent in their UPMC, Paris.

EXTENDED SUMMARY

CO₂ is the most abundant atmospheric gas related to the global warming. CO₂ is responsible for more than half of the radiative forces associated with the greenhouse effect. The forest plantation could play an important role in carbon budget and thus be part of the Clean Development Mechanism (CDM) of the Kyoto Protocol. Para rubber (*Hevea brasiliensis*) is a perennial tree of economic importance in Indonesia, Malaysia and particularly in Thailand for producing latex to the world-market. The Para rubber has high biomass, high growth rate and strong potential of carbon storage.

This study explored to the improve efficiency of measurements of carbon stock by remote sensing techniques on Para rubber plantations in East Thailand. Current methods of carbon stock estimations use classical pixel based classification on middle-resolution images and thus produce results with a large uncertainty. In this study, the method use very high resolution images from the THAICHOTE satellite, associated to field measurements to estimates the carbon stock and its evolution in the Mae num Prasae watershed. Using object based classifications, the plantations have been mapped and their age and girth have been estimated from a parametric model derived from spectral, textural, 3D information and field data.

The results of this study show that these data can be used to map Para rubber plantation and distinguish age classes of trees in the plantations. The study propose that textural information is more useful than spectral information to capture tree canopy architecture and thus the age of the canopy. One spectral of Global Environment Monitoring (GEMI) and four textural information of Homogeneity, Dissimilarity, Contrast and Variance were used in the fit model for estimating the Para rubber tree girth and age while the 3D information (canopy height model: CHM) was not appropriated to build the image classification information. The model equation has been obtained from multiple linear regression analysis with correlation coefficient of $R^2=0.87$ and thus can be used with confidence on the study area.

Around 154 km² of the 232 km² of the studied area are covered by Para rubber plantations. The class of age of each plantation has been estimated to be 33% of the crop

surface belong to the young class (from 4 to 12 years), 34% of the crop surface belong to the middle class (from 12 to 18 years) and 33% belong to the old class (older than 18 years). The total amount of biomass and carbon stocks are 2.23 Megatons and 0.99 Megatons C respectively with uncertainty of 11%. In 2011, the total area sequestered 121 tCO₂ by Para rubber plantations. Such a value is two orders of magnitude higher than carbon sequestered in the ocean.

Keywords: Carbon stock estimation, Object based classification, Para rubber plantation, THAICHOTE satellite, Mae num Prasae watershed/East Thailand

RESUMÉ ÉTENDU

Le CO₂ est le gaz atmosphérique le plus abondant lié au réchauffement global. Il est responsable de plus de la moitié des forces radiatives liées à l'effet de serre. La plantation de forêts pourrait jouer un rôle important dans le budget de carbone et donc faire partie du Clean Development Mechanism (CDM) du Protocole de Kyoto. Para rubber (*Hevea brasiliensis*) est un arbre à feuilles persistantes qui représente une importance économique considérable en Indonésie, en Malaisie et plus particulièrement en Thaïlande. Il sert à la production de latex pour le marché mondial. Para rubber plantation possède une biomasse élevée, un taux de croissance élevé et un fort potentiel de stockage de carbone.

Cette étude a été effectuée pour améliorer l'efficacité des mesures de stockage de carbone par des techniques de télédétection dans les plantations de Para rubber en Thaïlande. Les estimations des méthodes actuelles de stockage de carbone s'opèrent à l'aide de la classification classique basée sur le système des pixels basée sur des images de moyenne résolution et produit donc des résultats d'une grande incertitude. En revanche, dans cette étude, la méthode utilisée est basée sur des images de très haute résolution provenant du satellite THAICHOTE, associés à des mesures sur le terrain pour des estimations de stockage de carbone et de son évolution dans le bassin versant de Mae Num Prasae. L'utilisation de l'objet en fonction des classifications, les plantations cartographiées, leur âge et leur circonférence ont été estimées à partir d'un modèle paramétrique dérivé de données spectrales, de texture, d'information et de terrain 3D.

Les résultats de cette étude montrent que ces données peuvent être utilisées pour cartographier les plantations de Para rubber et distinguer les classes d'âge des arbres dans les plantations. L'étude propose une information de texture plus utile que l'information spectrale pour capturer l'architecture des arbres du couvert et donc l'âge de la canopée. Un spectrale de Global Environment Monitoring (GEMI) et quatre informations texturales de Homogeneity, Dissimilarity, Contrast and Variance ont été utilisées dans l'ajustement du modèle pour estimer la circonférence et l'âge des arbres tandis que le modèle d'hauteur de la canopée (Canopy Height Model: CHM) des informations 3D n'était pas autorisée pour construire l'information de classement d'images. L'équation du modèle a été obtenue à partir de l'analyse

de régression linéaire, multiplié avec un coefficient de corrélation de $R^2 = 0,87$ et peut donc être utilisée en toute confiance sur la zone d'étude.

Environ 154 km² des 232 km² de la zone étudiée sont couverts par des plantations de *Hevea brasiliensis*. La classe d'âge de chaque plantation a été estimée comme suivant : 33% de la surface des cultures appartient à la classe jeune (4 à 12 ans), 34% appartient à la classe moyenne (12 à 18 ans) et 33% appartient à la classe âgée (plus de 18 ans). La quantité totale de la biomasse et des stocks de carbone s'élève à 2,23 mégatonnes et 0,99 mégatonnes C, respectivement avec une incertitude de 11%. En 2011, la superficie totale séquestrée était de 121 tCO₂ par des plantations de Para rubber. Cette valeur représente deux ordres de grandeur plus élevée que le carbone emmagasiné dans l'océan.

Keywords: Carbon stock estimation, Object based classification, Para rubber plantation, THAICHOTE satellite, Mae Num Prasae watershed/East Thailand

CONTENTS

	Page
ACKNOWLEDGEMENTS	ii
ABSTRACT (ENGLISH)	iii
ABSTRACT (FRENCH)	v
LIST OF CONTENTS	vii
LIST OF TABLES	ix
LIST OF FIGURES	xi
DEFINITION OF TERMS	xii
LIST OF ABBREVIATION	xv
CHAPTER I INTRODUCTION	1
1.1 Introduction	1
1.2 Remote sensing Classification Problem on Forest Biomass Estimation	2
1.3 State-of-the-art-of forest biomass estimation on large-surface	4
1.4 Related studies	5
1.5 Objectives of the Study	9
1.6 Hypothesis	10
1.7 Scope of the Study	10
1.8 Conceptual Framework	11
1.9 Structure of Thesis	12
CHAPTER II LITERATURE REVIEW	15
2.1 Para rubber plantation	15
2.2 Forest carbon cycle	17
2.3 Ground forest biomass stock inventory	19
2.4 General information of Remote sensing used in this study	20

CONTENTS (continue)

	Page
CHAPTER III DATA AND METHODS	37
3.1 Study Processes	39
3.2 Field data	39
3.3 Satellite Image Preprocessing	43
3.4 Image Classification	47
3.5 Para rubber plantation Surface Extraction	55
CHAPTER IV RESULTS AND DISCUSSIONS	60
4.1 Field data	61
4.2 Ground Biomass and Carbon Stocks Estimation	63
4.3 THAICHOTE Satellite Image	65
4.4 Image Classification	69
4.5 Map of Para rubber plantation limit	76
4.6 Tree girth model (TGM) and Para rubber tree Classification	77
4.7 Estimation of Biomass and Carbon Stock	89
4.8 Result's Discussion	94
CHAPTER IV CONCLUSIONS AND PERSPECTIVES	99
5.1 Conclusions	99
5.2 Perspectives	101
REFERENCES	102
APPENDIX	107
A.1 Field measurement: Tree height measurement using Haga altimeter	108
A.2 Field measurement: Data sheet for collecting forest inventory data	110
A.3 The input dataset for tree girth modeling (TGM) and Histogram	111
A.4 Articles publication	131

LIST OF TABLES

Table	Page
2-1 Para rubber productivity of the world in 2011	16
2-2 Performed percentage carbon and elements on parts of RRIM 600	21
2-3 (a) THAICHOTE performance., (b) THAICHOTE payload optical instruments characteristics	24
2-4 Textural information equations	30
3-1 Data sources	44
3-2 Gain and Bias in each band of THAICHOTE data used in the study	46
3-3 The parameters input to the model	47
3-4 Distance from Earth to the Sun (Astronomical Unit)	47
3-5 Textural formula	51
4-1 Field data collected from December 2011 to April 2012: view from ground and view from THAICHOTE satellite data (band composite RGB:NIR, Red, Green) for the Para rubber ages used in this study	62
4-2 The rate capacity of carbon sequestration, biomass and carbon stock obtained by single tree stand of Para rubber tree	64
4-3 Statistical of THAICHOTE satellite data. It was corrected radiometry using COST model (reflectance data)	65
4-4 The rate capacity of carbon sequestration, biomass and carbon stock obtained by individual tree stand of Para rubber tree., Veg.1-3 is vegetation1-3	66
4-5 Statistical of image classification layers obtained by spectral and textural information	70
4-6 Statistical of image characteristics measured at the emplacement where field data were acquired association to the girth and age of trees of each plantation...	78

LIST OF TABLES (Continue)

Table	Page
4-7 Pearson's correlation between tree girth and layer parameters measured at field plot positions	81
4-8 Model summary	83
4-9 Excluded Variables	84
4-10 Area summary of the Para rubber plantation	86
4-11 Confusion matrix of para rubber classification	86
4-12 Biomass and Carbon stocked in study area 2011	90
4-13 Model summary of TGM#3	95
4-14 The rate of carbon storage at rotation age in Eucalyptus (<i>E. camaldulensis</i>), Teak (<i>Tectona grandis</i>) and Para rubber plantation RRIM 600 (<i>Hevea brasiliensis</i>)	98

LIST OF FIGURES

Figure	Page
1-1 (a).THAICHOTE false-color image (RGB: NIR,Red,Blue, spatial resolution of 2 m., (b). Rubber age class map derived from pixel based classification with coverage by salt-pepper noise and misclassified some age class of rubber plantation., (c). Rubber age class map derived from object based classification.	3
1-2 State of the art of forest biomass estimation on large-surface	4
1-3 The Mae num Prasae watershed	11
1-4 Conceptual Framework	12
1-5 Structure of Thesis	14
2-1 Para rubber plantation (RRIM 600)	16
2-2 Diagram showing the processes and fluxes maintaining or modifying the different C stocks in a forest, and the fluxes of the other key greenhouse gases, CH ₄ and N ₂ O. Green arrows indicate C flux into the forest and between various C stocks; red arrows indicate C fluxes out of the forest	18
2-3 Organization of a biomass measurement...	20
2-4 Relationship between girth (cm) at 1.7 meter above ground and dry weight biomass per tree RRIM 600 age 2 - 25 years...	21
2-5 (a) THAICHOTE performance., (b) Spectral signature of THAICHOTE	25
2-6 Example illustration of the probability matrix generation...	29
2-7 Top-down view of a simple stereo system highlighting significance of correspondence problem	32
2-8 “Normal Case” configuration for calculation of object space coordinates	34
2-9 Object-oriented image analysis: the generic procedure	36
3-1 Study process	38
3-2 The equipment of forest field measurements...	40

LIST OF FIGURES (continue)

Figure	Page
3-3 Sample plot measurements...	41
3-4 The processes of Image Classification	48
3-5 The processes of textural information	50
3-6 The processes of 3D information	53
3-7 The processes of Para rubber surface extraction	55
4-1 The Mae num Prasae watershed on THAICHOTE satellite data (yellow boundary)	61
4-2 The relationship between tree age and girth ($R^2 = 0.96$)	61
4-3 Planting layout of Para rubber plantation in study area	63
4-4 The biomass and carbon stocked in single tree of Para rubber	64
4-5 THAICHOTE satellite natural color (R, G, B) image corrected	65
4-6 THAICHOTE satellite false color (NIR, G, B) image corrected.	66
4-7 The sample reflectance data in the study area obtained by THAICHOTE image	67
4-8 The spectral signature obtained by THAICHOTE satellite image non-corrected according to Water vegetation and bare soil object	68
4-9 The spectral signature obtained by THAICHOTE satellite image corrected according to Water vegetation and bare soil object	68
4-10 Example layers of Spectral information (Single bands)...	71
4-11 Example layers of Spectral information (Vegetation indexes)., (a) ARVI., (b) GEMI., (c) IRVI., (d) MSAVI2...	72
4-12 Example layers of Spectral information (Vegetation indexes)., (e) NDVI., (z) THAICHOTE false color image (NIR, G, B).	72

LIST OF FIGURES (continue)

Figure	Page
4-13 Example layers of Textural information (Texture measures)., (a) CON., (b) DIS., (c) HOMO., (d) ASM., (z) THAICHOTE false color image (NIR, G, B).	72
4-14 Example layers of Textural information (Texture measures)., (e) ENT., (f) Mean., (g) Var., (h) Cor., (z) THAICHOTE false color image (NIR, G, B).	73
4-15 Example images of THAICHOTE stereo pair data segmentation	74
4-16 Example layers of 3D information...	75
4-17 Example map of Para rubber plantations extracted from the multi-scale segmentation. Yellow polygon is Para rubber plantation limits	76
4-18 Example map of Para rubber plantations limit extracted from the multi-scale segmentation (Yellow polygon) and the manual digitization (Green polygon)	77
4-19 The graphics obtained from mean, skewness and kurtosis of the image classification layers of each age class of Para rubber plantation.	80
4-20 Pearson's correlation coefficient graph	82
4-21 (a) TGM#1 derived from a spectral information, (b) TGM#2 derived from a combination of spectral and textural information	85
4-22 Map of Para rubber age class	87
4-23 (a) Bar graphs: biomass, carbon stock and uncertainties data. (b) The rate of CO ₂ sequestration by Para rubber of each age class	91
4-24 Map of Para rubber carbon stock.	92
4-25 (a) Para rubber plantation limits (segmentation)., (b) Bar graph: textural information and age class map	97

DEFINITION OF TERMS

Allometric equation – the forest-biomass inventory technique for dry biomass determination. It has been developed by establishing a relationship between the various physical parameters of the trees such as the diameter at breast height, height of the tree trunk, branch, total height of the tree, crown diameter, tree species [17].

Biomass – the total amount of living organic matter in trees expressed as oven dry tons per unit area [27].

Forest plantation – a forest established by planting or seeding in the process of afforestation and reforestation consisting of introduce or indigenous species [26].

Carbon sequestration – the process of increasing the carbon content of a carbon pool [26]. In the study, carbon sequestered by each age class was the carbon density or carbon stored in the biomass of Para rubber tree over its age, in unit tC ha⁻¹ yr⁻¹.

Carbon stock – the absolute quantity of carbon held within a pool at a specified time [26]. In the study carbon stock is use to imply the amount of carbon stored by Para rubber plantation.

Object based image analysis (OBIA) – it is a state-of-the-art of remote sensing classification techniques on very high resolution image. The advantage of a spatial resolution with pixel sizes significantly smaller than the average size of the object of interest comes with the disadvantage of an abundance of spatial detail and the accordingly huge amount of data to be processed. To overcome this drawback, the OBIA approach has proven to be an alternative to the pixel based image analysis and a large number of publications suggest that better results can be expected [46].

LIST OF ABBREVIATION

3D	Three Dimension
C	Carbon
ARVI	Spectral information: Atmospherically Resistant Vegetation Index
ASM	Textural information: Angular Second Moment
CHM	Canopy Height Model
CON	Textural information: Contrast
COR	Textural information: Correlation
DIS	Textural information: Dissimilarity
DSM	Digital Surface Model
DTM	Digital Terrain Model
ENT	Textural information: Entropy
GEMI	Spectral information: Global Environment Monitoring Index
HOMO	Textural information: Homogeneity
IPVI	Spectral information: Infrared Percentage Vegetation Index
MEAN	Textural information: Mean
MSAVI2	Spectral information: Modified Soil Adjusted Vegetation Index 2
NDVI	Spectral information: Normalized Difference Vegetation Index
VAR	Textural information: Variance
VI_s	Vegetation Indexes

INTRODUCTION

CHAPTER I

INTRODUCTION

1.1 Introduction

CO₂ is the most abundant atmospheric gas related to the global warming. CO₂ is responsible for more than half of the radiative forces associated with the greenhouse effect [1]. Forest may play an important role in the short carbon dioxide cycle. In particular tropical forests have the potential capacity to sequester and to conserve carbon permanently [2, 3]. This is the reason why the Clean Development Mechanism recommended by the Kyoto Protocol advocates evaluating tree capacity of CO₂ storage in humid tropical forest plantations [4]. Para rubber is a perennial tree of economic importance in Indonesia, Malaysia and particularly in Thailand for producing latex to the world-market [5]. The Para rubber has high biomass, high growth rate and strong potential of carbon storage [6, 7].

Today, very high resolution (VHR) sensors on board of satellites can map tropical forest plantations providing valuable data to evaluate forest biomass and carbon stocks evolution. VHR data has overcome the limitation of spatial resolution of the medium-low resolution sensors such as Landsat 8 OLI (15 m) or MODIS (250 m). These sensors cannot capture the tree characteristics such as crown canopy. Therefore, estimation of plantation biomass and carbon stocks from low resolution remote sensing data was inaccurate [8]. THAICHOTE satellite camera (previously named THEOS) is a high resolution sensor on 2 m resolution. It is the first Earth observation satellite of Thailand. Its data are potentially an important data source for biomass and carbon stocks estimation on large surfaces.

However, the monitoring of forest carbon stock is a complex task. Numerous approaches have been proposed to estimate biomass [8-15]. The spectral information contained in satellite data is classically used [11-15]. The methods developed with these data

cannot differentiate the biomass according to the tree species or tree age [8-10]. Recently, methods based on the texture measurement were developed to obtain better results than using only spectral information [8-10]. Field data and remote sensing data were linked using common regression analysis [8, 9], with most studies relating visible and near-infrared (NIR) wave range, vegetation indices and texture analysis.

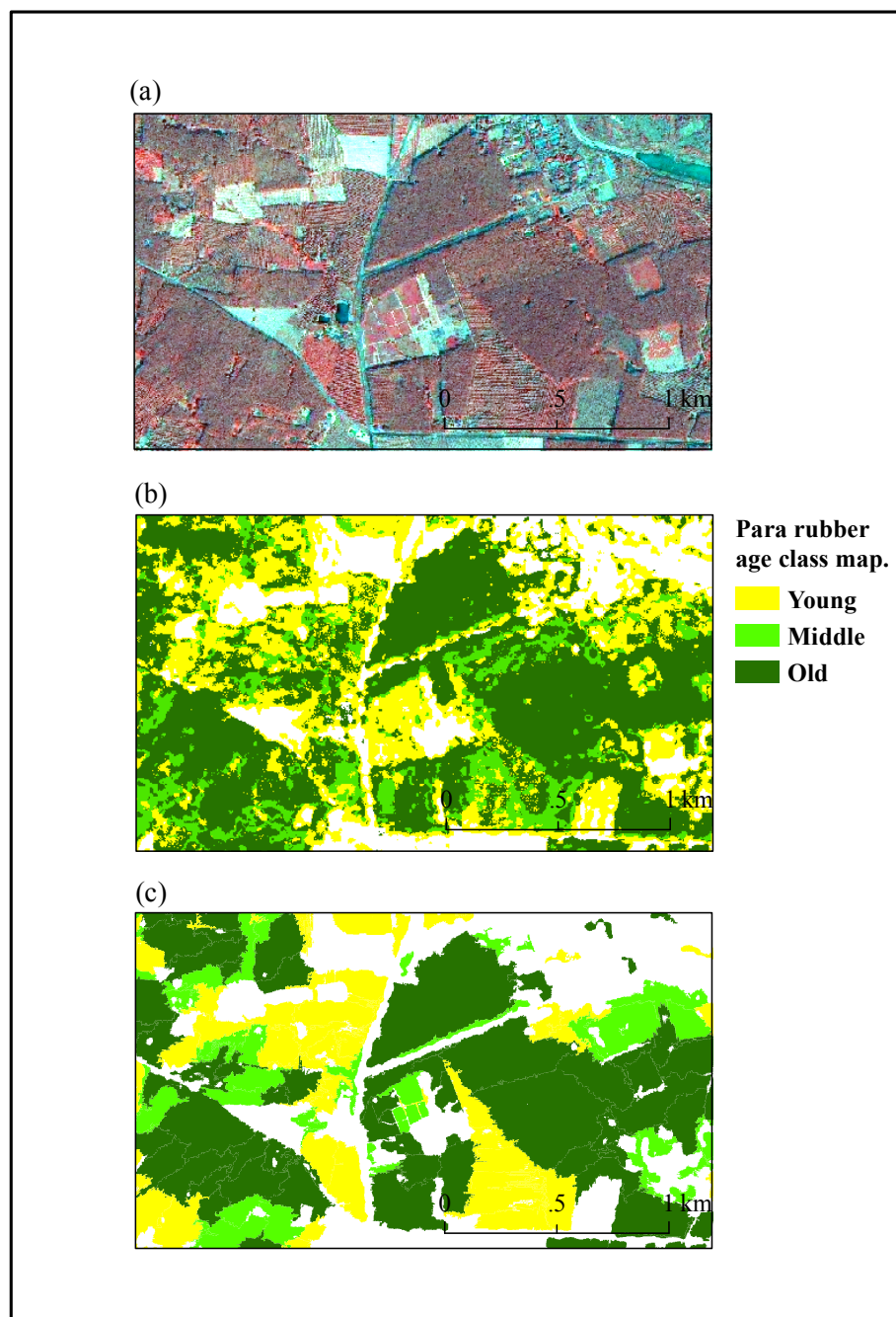
1.2 Remote sensing Classification Problems on Forest Biomass Estimation

This study have identified two major problems in biomass estimation by remote sensing classification techniques. The first problem is the noise in the image classification. Image noise is a critical problem of remote sensing classification on VHR data. Figure 1-1 shows “salt-pepper noise” on Para rubber plantation mapping. THAICHOTE false-color imagery (Figure 1-1(a)) was classified by classical pixel-based technique (Figure 1-1(b)). The result is inaccurate in terms of geometry of class boundary (or plantation limit) and the age data of Para rubber plantation. The legacy technique is derived from supervised and unsupervised methods for assigning a class label to individual pixel based on distance or similarity measures in feature space [16]. This approach has been used simple spectral information in order to class identification. By contrast, the object based classification (object based image analysis: OBIA) overcome limitation from pixel based classification. Figure 1-1(c) revised the Para rubber plantation mapping derived from OBIA approach. OBIA process is done in two steps: image segmentation and modeling for object identification. Segmentation in remote sensing can remove image noise while the model can identify the object by analyzing more information such as reflectance distribution, shape, size, and texture [16].

The second problem is the poor-quality relationship between field data and VHR data when using spectral information for biomass estimation. Recently, methods based on the texture measurement were developed to obtain better results than those using only spectral information. The texture of image is a good description of the forest canopy architecture. It was shown to have a certain relation with biomass volume [8, 9]. Classical pixel based classification is not a good candidate to determine the characteristics of the canopy. Most of the previous works were used as simple spectral information for forest biomass estimation

using medium resolution satellite images [11-15]. Consequently, the established relationships between field data and remote sensing data were weak.

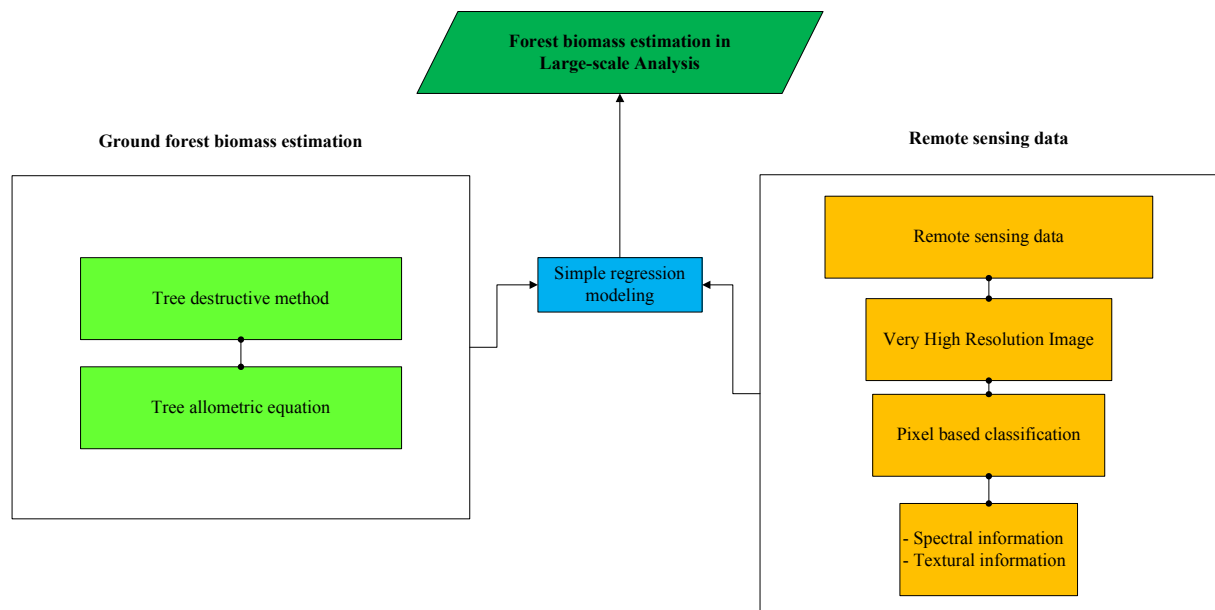
Figure 1-1 (a). THAICHOTE false-color image (RGB: NIR, Red, Blue, spatial resolution of 2 m., (b). Rubber age class map derived from pixel based classification with coverage by salt-pepper noise and misclassified some age class of rubber plantation., (c). Rubber age class map derived from object based classification.



1.3 State-of-the-art of forest biomass estimation at large-surface

The Figure 1-2 shows a brief story of the state of the art of forest biomass estimation at large-surface estimation which the ground forest biomass estimation and remote sensing data via optical satellite are purposed.

Figure 1-2 State of the art of forest biomass estimation on large-surface.



The Ground forest biomass inventory used the destructive method involves harvesting of all the trees in the known area and measuring the weight of the different components of the harvested tree like the tree trunk, leaves and branches root and measuring the weight of these components after they are oven dried. Therefore, the destructive method has been addressed by the tree allometry. The allometric equation is developed by establishing a relationship between the various physical parameters of the trees such as the diameter at breast height, height of the tree trunk, branch, total height of the tree, crown diameter and tree species [17]. Despite, the Ground forest biomass method provided accurately the forest biomass estimation but this method is limited to estimate biomass on large-surface analysis, using more time and resource consuming.

Currently, the estimation of forest biomass on large-surface is used the integration of ground data and remote sensing data. The very high resolution (VHR) optical sensors on board of satellites is mapped forest plantation surfaces and provided valuable data to evaluate forest biomass and carbon stocks evolution. The classical pixel based and spectral information were used for forest surface identification. Nevertheless, the classical technique on the remote sensing classification is inappropriated and provided large-uncertainty data. Recently, methods based on the texture measurements were developed to obtain better results than using only spectral information [8-10]. Finally, ground data and remote sensing data are linked using common regression analysis [8, 9], with most studies relating visible and near-infrared (NIR) wave range, vegetation indices and textural information for minimization uncertainty data on forest biomass estimation at large-surface.

1.4 Related Studies

A brief story of previously works is reviewed. This section realized to forest biomass estimation and forest surface classification using optical satellite data. Several approaches are used to estimate the forest biomass and land use land cover mapping. The goal of this study is realized to improving for the works of S. Noiruksar, (2011) [14], J. Nilubon, (2007) [13] and C.O. Iglesias, (2012) [12] where investigation on biomass estimation in Teak, Para rubber and Eucalyptus plantations respectively and the state-of-the-art as object-based classification on spectral, textural information and canopy height information are applied.

Classical pixel-based classifications obtained by spectral information on satellite medium-resolution is first reviewed and then the textural information is combined. The canopy high information can be improved the forest biomass estimation. This section, the canopy high information obtained by LiDAR and Photogrammetry is reviewed. Therefore the land use land cover mapping is addressed classification by object-based technique.

- **Classical pixel-based classifications and Spectral information**

S. Noiruksar, (2011) [14] studied the estimation of ground biomass in Teak plantation of North Thailand using remote sensing. Landsat 5 TM was used to classify Teak plantations into two age stages, the primary stage (3-7 years old) and the rotation stage (25-38 years old).

The biomass allometric equation and spectral information of Advanced Vegetation Index (AVI), Bare Soil Index (BI) and Water Index (WI) were used for estimation the carbon sequestration. The result indicated to the primary stage and the rotation stage of Teak could store about 6.60 and 38.50 tons of carbon per hectare, respectively.

J. Nilubon, (2007) [13] studied the age class identification of Para rubber plantation in Krabi (South Thailand) using Landsat 5 TM. The tree age classes of Para rubber were defined to Harvest stage (>7-20 years old), Mature stage (>20-24 years old), and Logging stage (more than 24 years old). The hierarchical (expert) model and forest inventory were used to age class classification. Spectral information of Water Index (WI), Bare Soil Index (BI), Normalized Difference Vegetation Index (NDVI), and Advance Vegetation Index (AVI) were combined in the hierarchical (expert) model for classify age class. Then, the biomass was estimated using biomass allometric equation. The result given to overall accuracy of average lower than 75% in each age class and estimated biomass of all Para rubber plantations was 10,603,272.879 tons in Krabi province.

C.O. Iglesias, (2012) [12] studied the carbon sequestration and storage capacity of *Eucayptus* plantation in Sra Kaew province (East Thailand) using Remote sensing. The hybrid classification obtained by manual digitization and hierarchical classification was used in the age class identification. Five age classes classified as 1, 2, 3, 4 and 5 year were established based on the rotation length and end-use of Eucalyptus in Thailand. Using values of Normalized Difference Vegetation Index (NDVI), Bare Soil Index (BI) and Water Index (WI) an age class model was developed on Landsat 5 TM. The total area of eucalyptus plantations in Sra Kaew has the capacity to store carbon at 364 555.78 tons per year and an annual carbon sequestration rate of 111 874.48 tons carbon. Thus, eucalyptus plantations in Sra Kaew can remove 411 250.59 tons carbon dioxide per year from the atmosphere.

- **Classical pixel-based classifications on integration of spectral and textural information**

Mongkolsawat et al., (2010) [18] studied the estimating area of Rubber plantation in North Thailand using Satellite data and physical data. SPOT and THEOS (THAICHOTE) obtained from period 2006-2009 were used. Differentiation and classification of Rubber tree was derived from the difference in the cover patterns, resulting 3 classes of the tree age: less

than 5, 5-10 and over 10 years. The result indicated that areas planted to rubber tree accounting for about 1,480.19, 384.25, and 379.36 km² for <5, 5-10 and > 10 years of plant ages respectively.

S. Eckert, (2012) [8] studied the Improved Forest Biomass and Carbon Estimations in northeast Madagascar Using Texture Measures from WorldView-2 Satellite Data. Degraded forest and non-degraded forest stratum were determined. The result shown to: Pearson's correlation coefficients revealed that (a) texture measures correlated more with biomass and carbon than spectral parameters, and (b) correlations were stronger for degraded forest than for non-degraded forest. For degraded forest, the texture measures of Correlation, Angular Second Moment, and Contrast, derived from the red band, contributed to the best estimation model, which explained 84% of the variability in the field data (relative RMSE = 6.8%). For non-degraded forest, the vegetation index EVI and the texture measures of Variance, Mean, and Correlation, derived from the newly introduced coastal blue band, both NIR bands, and the red band, contributed to the best model, which explained 81% of the variability in the field data (relative RMSE = 11.8%). These results indicate that estimation of tropical rainforest biomass/carbon, based on very high resolution satellite data, can be improved by (a) developing and applying forest stratum-specific models, and (b) including textural information in addition to spectral information.

Sarker et al., (2011) [9] studied the improved forest biomass estimates using ALOS AVNIR-2 texture indices. That research investigates the potential of high resolution optical data from the ALOS AVNIR-2 sensor for biomass estimation in a mountainous, subtropical forested region using four different types of image processing techniques including 1) spectral reflectance and simple spectral band ratio, 2) commonly used vegetation indices, 3) texture parameters and 4) ratio of texture parameters. Simple linear and stepwise multiple regression models were developed between biomass data from 50 field plots. The results suggest that the performance of biomass estimation can be improved significantly using the combination of texture parameters and band ratio of high resolution optical data.

- **Canopy height information**

A. Benzie, (2013) [19] studied the Canopy Height Modeling for Improved Forest Biomass Inventory in Ontario Canada. Using LiDAR and Semi Global Matching (SGM) on stereo photogrammetry method. The study found, height values modeled by LiDAR and SGM were strong correlated. The study recommended to incorporate the canopy height modeled and forest field-based to examination of forest biomass volume.

Zhang et al., (2014) [20], studied the Estimation of forest aboveground biomass in California using canopy height and leaf area index estimated from satellite data. They present a new remote sensing based approach for estimating live forest aboveground biomass (AGB) based on a simple parametric model that combines high-resolution estimates of leaf area index (LAI) from the Landsat Thematic Mapper sensor and canopy maximum height from the Geoscience Laser Altimeter System (GLAS) sensor onboard ICESat, the Ice, Cloud, and land Elevation Satellite. The study shown a high-resolution approach to map forest aboveground biomass at regional-to-continental scales and assess sources of uncertainties in the estimates.

- **Object-based classification**

Guo et al., (2007) [21] studied the Object-Based Classification Approach in Mapping Tree Mortality Using High Spatial Resolution Imagery in California. They developed an object-based approach, including an image segmentation process and a knowledge-based classifier, to detect individual tree mortality in imagery of 1 m spatial resolution. The combined segmentation and classification methods provided an easy and intuitive way to incorporate human knowledge into the classification process. The results shown that, the object-based approach significantly outperformed a pixel-based maximum likelihood classification method in mapping the tree mortality on high-spatial-resolution multispectral imagery.

Kim et al., (2009) [22] studied the use of a geographic object-based image analysis (GEOBIA) approach with the incorporation of object-specific grey-level co-occurrence matrix (GLCM) texture measures in Guilford Courthouse National Military Park, North Carolina. Imagery was obtained from a multispectral IKONOS image for delineation of deciduous, evergreen, and mixed forest types in the studied. A series of automated segmentations was

produced at a range of scales, each resulting in an associated range of number and size of objects (or segments). They found, an overall accuracy of 79 percent with a Kappa of 0.65 was obtained at the optimal segmentation scale of 19. The addition of object-specific GLCM multiple texture analysis improved classification accuracies up to a value of 83 percent overall accuracy and a Kappa of 0.71 by reducing the confusion between evergreen and mixed forest types. Some misclassification still remained because of local segmentation quality, a visual assessment of the texture-enhanced GEOBIA classification generally agreeable with manually interpreted forest types.

1.5 Objectives of the Study

The goal of this study is to improve the Para rubber biomass and carbon stocks estimation of estimation using object-based classification combining both spectral and textural information from a THAICHOTE satellite image that was acquired in December 2011 over the Mae num Prasae watershed, Thailand. The objective points can be written in below:

- To develop the empirical model for identification of Para rubber tree girth and age using linear multiple regression on both spectral and textural information from THAICHOTE satellite data.
- To identify the Para rubber plantation age class map using Object based classification from THAICHOTE satellite data.
- To estimates the biomass and carbon stock in Para rubber plantations over the Ma num Prasae watershed, East Thailand.

1.6 Hypothesis

Objective	Research Question	Research Hypothesis
1	The textural information can be improved the relationship of Para rubber plantation biomass between field and remote sensing data.	H1: Yes, the textural information is significant for improving the relationship between field and remote sensing data.
2	The precision-measuring of Para rubber biomass and carbon stock can be done using the object based classification	H1: The object based classification can be applied and minimized uncertainty data for estimating the Para rubber biomass and carbon stock.

1.7 The Study Limitation

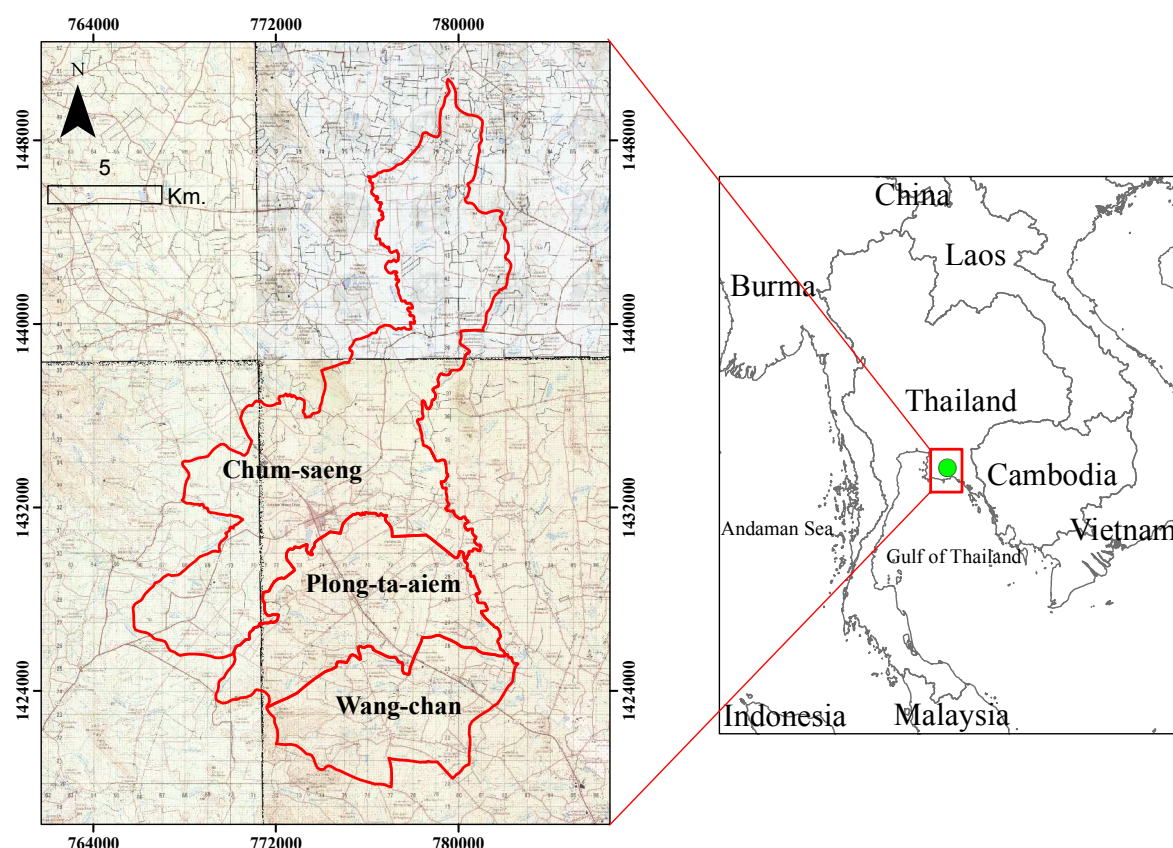
- Biomass-allometric equation and default value of carbon conversion is applied to estimate biomass and carbon stocks of Para rubber clones RRIM 600 (Commercial rubber tree breed was developed by Rubber Research Institute of Malaysia No.600).
- The THAICHOTE optical satellite data 2011 is used in the major source of the study.
- A study area is the Mae num Prasae watershed is located in Rayong province of the eastern of Thailand. It consist three sub-districts of Chum-saeng, Plong-ta-aiem and Wang-chan. Geo-location is located near 12°58'22"N/101°32'56"E and covering a surface of 232 km².

The average elevation of the watershed is around 43 m above MSL and the average slope is 6°. Rainfalls occur around 120 days per year and cumulated rain is 1,900 mm. The average temperature is 28 °C and humidity ranges from 60 to 90%.

Para rubber plantation is a major source of agriculture productivity economy for Thailand. Around 34% of surface of Rayong province was occupied by Para rubber

plantations surface (2011). This province is 7th order of Thailand for latex production performing [5]. The Mae num Prasae watershed is shown in Figure 1-3.

Figure 1-3 The Mae num Prasae watershed (georeferenced on UTM WGS 1984 Z48N).



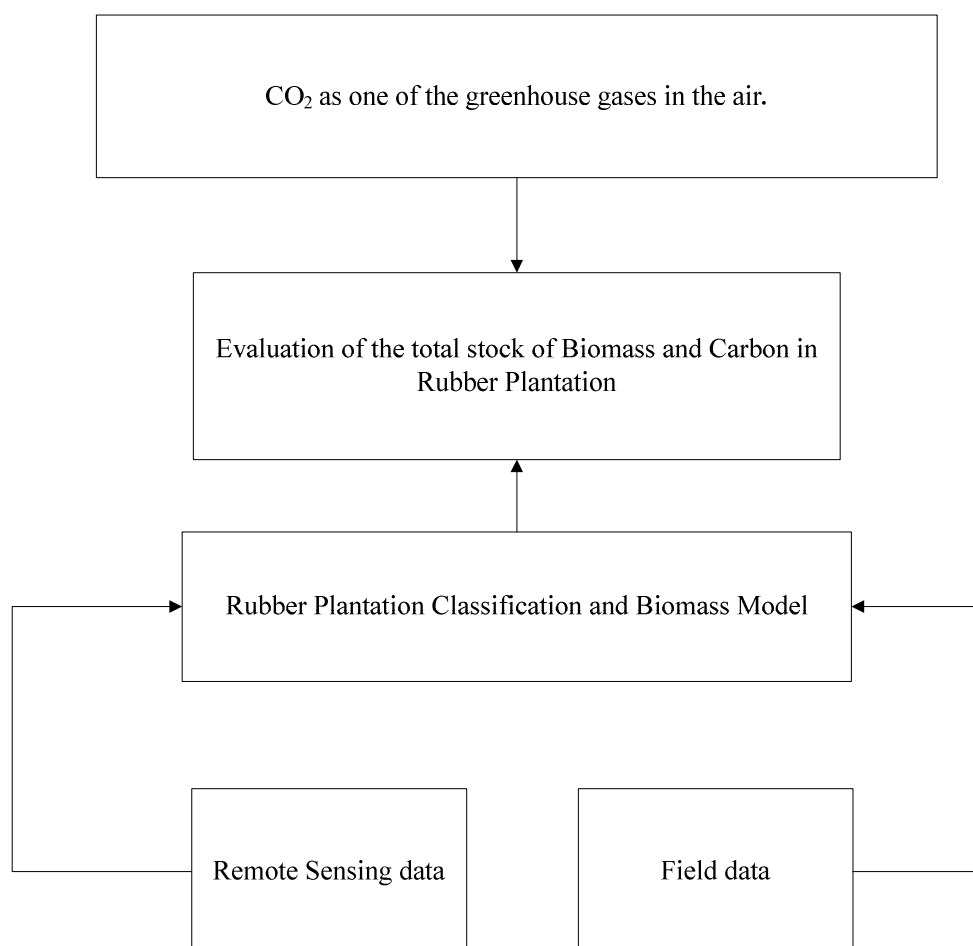
1.8 Conceptual Framework

Figure 1-4. shows the concept of the carbon dioxide elimination using the forest plantation. The carbon can be stored in the Para rubber tree, capturing by the leaves thru photosynthesis process with the aid of light and water these are processed and stored in the stems of trees as biomass.

The field data and remote sensing technique were used for estimating biomass and carbon stock in the large scale. The ages of Para rubber plantation were first classified and then the study used the biomass modeling (called Tree Girth Model: TGM) for estimating

biomass and carbon stock. Therefore, the total stock of Para rubber plantation's biomass and carbon in the Mae num Prasae watershed was evaluated using field and remote sensing data.

Figure 1-4 Conceptual Framework.



1.9 Structure of Thesis

Chapter I Introduction: introduce to global warming and forest as a tool for playing on clean development mechanism, problematic on remote sensing classification for biomass and carbon stocks estimation. The state-of-the-art of forest biomass estimation at large-surface and the related works are first described and then Objectives of the study, Study Limitation are identified.

Chapter II Literature Review: introduce to the general information of Para rubber plantation, Forest Carbon cycle and Ground forest biomass inventory. Then the general information of remote sensing used in this study are described associated to Remote sensing for vegetation indices, texture measurement, 3D terrain model and Object based classification.

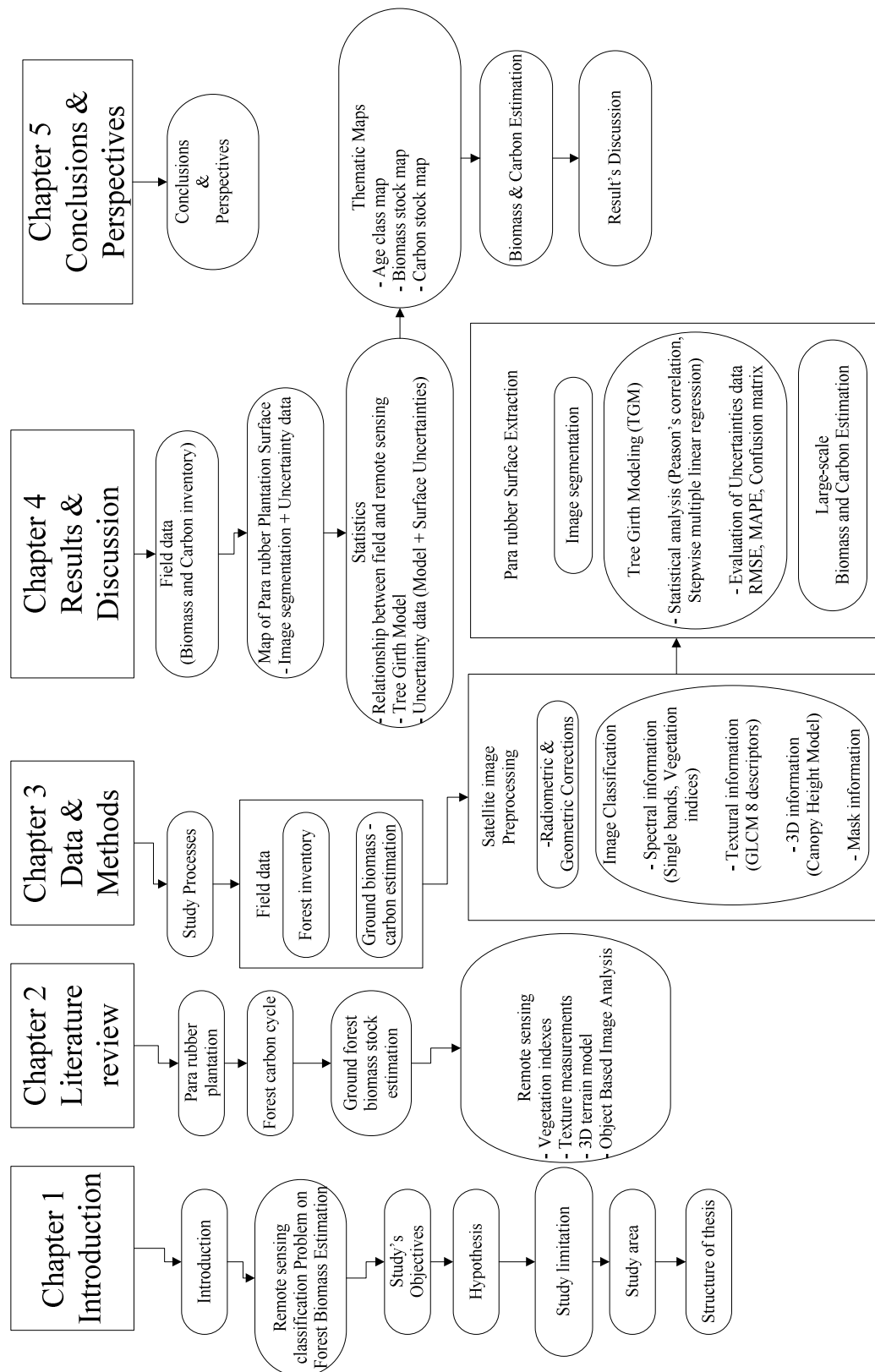
Chapter III Data and Methods: THAICHOTE satellite data and GIS database are included to the material setting. The method defined into 4 board parts. Forest inventory and Ground Biomass and Carbon estimation are combined in Part 1. The image processing is employed using 3 steps of Satellite Image Preprocessing (Part 2), Image Classification (Part 3) and Para rubber Surface Extraction (Part 4). Finally, the total biomass and carbon stock at large surface are estimated.

Chapter IV Results and Discussion: the results are explained in the following area: Field data, Ground Biomass and Carbon Stock Estimation, THAICHOTE image corrected, Image classification, Relationship between field data and remote sensing data, Para rubber surface extraction and Biomass and Carbon Stock Estimation over the Mae num Prasae watershed. Finally, the results of the study is discussed. The discussion are the limitation of the study method for estimate biomass and carbon stock such as the best parametric model for linking the field data and remote sensing data, comparison of this resulted and other studied, uncertainty data of biomass and carbon estimation and THAICHOTE image.

Chapter V Conclusions and Perspectives: Conclusions explained the parameterization for biomass estimation, the correlation of spectral and textural information from THAICHOTE satellite data, total amount of the surface of Para rubber age class, total capacity of biomass and carbon stock and the rate of CO₂ sequestration by Para rubber plantation and further work.

The thesis structure is shown in Figure 1-4.

Figure 1-4 Structure of Thesis.



LITERATURE REVIEW

CHAPTER II

LITERATURE REVIEW

Chapter II reviewed to the general information of Para rubber plantation, Forest carbon cycle and Ground biomass-carbon stock inventory. Then the general of remote sensing used in this study is described.

2.1 Para rubber plantation

2.1.1 General Characteristics

Hevea brasiliensis is a rapid-growing species that can reach 40 m in height and 35 cm in diameter. Its trunk is cylindrical with a narrow base and a gray-green bark and irregular branches. Its leaves are compound, trifoliate, and alternate. They have a dark green upper face, a light green lower face, and marked venation (Figure 2-1). Commonly known as the rubber tree or the Para rubber tree, *Hevea brasiliensis* is a native tree species of the Amazon (Brazil, Bolivia, Peru, Colombia, Guyana, and Suriname). The rubber tree is found in tropical America from Mexico to Sao Paulo, in Africa from Mozambique to Madagascar, in southern India, Sri Lanka, and throughout Southeast Asia, the Thailand, Philippines, Indonesia, and New Guinea. Commercial rubber plantations are found between 24 degrees north latitude in China to 25 degrees south latitude in the state of Sao Paulo, Brazil [23].

2.1.2 Limiting Factors

In the study area, the rubber clone of *Hevea brasiliensis* RRIM 600 (Rubber Research Institute of Malaysia No.600) is planted (Figure 2-1). Rubber tree life cycle is around 25 to 30 years, after which the latex production from rubber decreases. Replanting is thus necessary to maintain latex production. *Hevea brasiliensis* needs a rainfall of 2,000 mm (or more) with no

severe dry season and a 125-150 raining days per year. The minimum and maximum temperature should be 20°C and 35°C respectively and atmospheric humidity should be 80-90 % with moderate wind, and bright sunshine for about 2,000 hours in a year [24].

Figure 2-1 Para rubber plantation (RRIM 600).



2.1.3 Para rubber productivity

Para rubber is a perennial tree of economic importance in Indonesia, Malaysia and particularly in Thailand for producing latex to the world-market. The Para rubber has high biomass, high growth rate and strong potential of carbon storage [6, 20]. Thailand is the leader of rubber producer in the world that produces around 3.5 million tons per year or 37% of the world annual production [5]. The world product of Para rubber was listed in Table 2-1.

Table 2-1 Para rubber productivity of the world in 2011.

Country	Product average (1,000 ton)
Thailand	3,527.30
Indonesia	3,093.00
Malaysia	996.3
India	892.7

Estimation of Biomass and Carbon Stock in Para rubber plantation in East Thailand Using Object-based Classification from THAICHOTE Satellite Data

China	710.7
Sri lanka	157.8
Liberia	64.5
Nigeria	55.3

2.2 Forest carbon cycle

The forest C (carbon) cycle, the contribution made by woodland to the C balance at any scale depends on the rate at which CO₂ is removed from the atmosphere and the quantity of C retained in the woodland. The C stocks in the forest include the above and below-ground components of trees, understorey and the soil. Trees take up CO₂ from the atmosphere during photosynthesis following basic chemical equation (The tree use Sunlight + CO₂ + Water and Nutrients). Much of the carbon that is taken up by the tree through photosynthesis is released again as CO₂ through above-ground and root respiration, which provides the energy for tissue growth and maintenance.

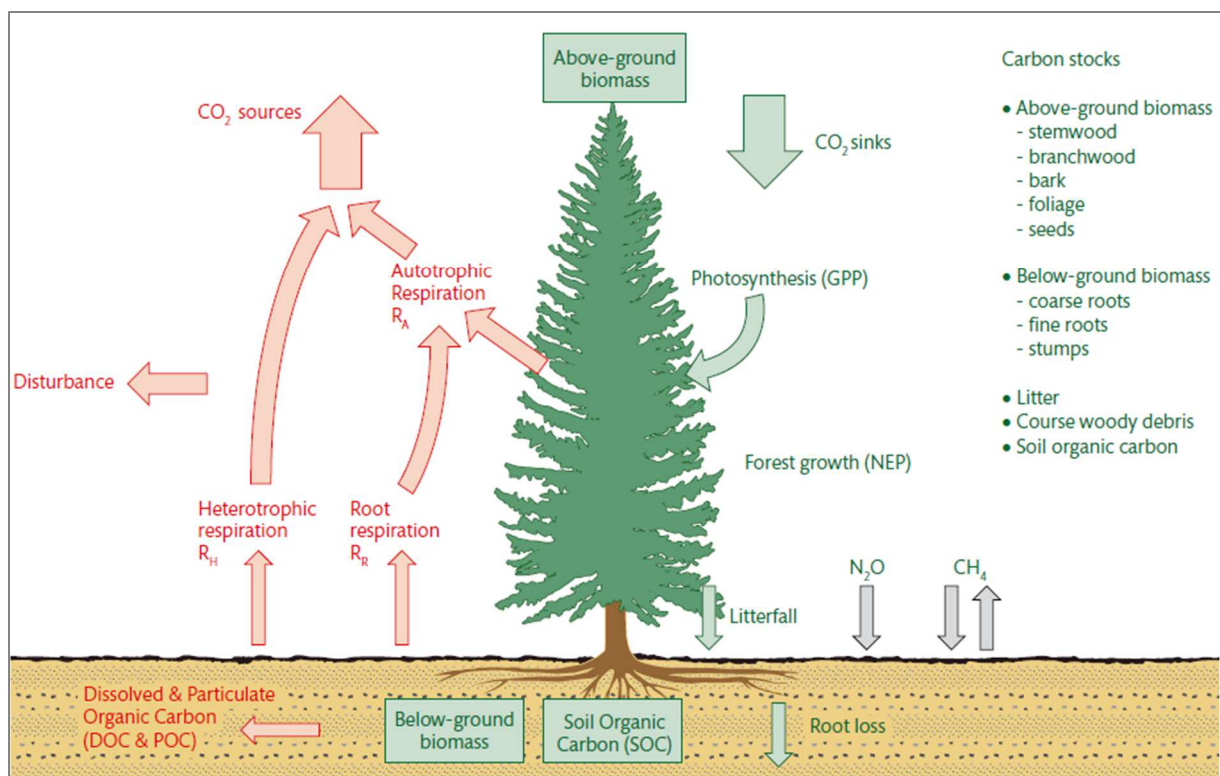
The remaining carbon is partitioned between or allocated to leaf, root, seed, stem and branch biomass. Most of the carbon in trees is in the stem approximately 50%, with substantial amounts in branches and below ground in roots. Decomposition of these litter and root exudation components releases CO₂. This flux of CO₂ is often referred to as soil respiration, usually include the respiration of the roots and any soil invertebrates. During decomposition the organic carbon remains in a wide variety of different components of soil organic carbon (SOC). Soil microbial activity can also result in the net release of the greenhouse gases CH₄ and N₂O, although only the former is formally part of the carbon cycle. However, the mass of carbon exchanged via methane fluxes is normally very much smaller than that in CO₂ exchanges, so is usually ignored for C balances.

Several terms are conventionally used to represent the different CO₂ fluxes in the system, the net primary productivity (NPP) is the difference between the gross primary productivity (GPP) and the respiration by the trees and other vegetation (autotrophic respiration, RA), and the net ecosystem productivity (NEP) is the difference between NPP and the respiration by animals and micro-organisms (heterotrophic respiration, RH). NEP is

therefore the rate of carbon accumulation in the system [25]. Forest carbon cycle is shown in Figure 2-2.

The world's forests area of 3,500 million hectare constitute 30 percent of the total land area [26]. The world's forests, 57 percent are mostly tropical located in developing countries [26]. According to S. Brown, (1997) [27] and GEO 3, (2003) [28], carbon pools in the world's forest are estimated at 348 Gt C in its vegetation and 478 Gt C in soil. The amount of carbon that can be conserved and sequestered by forest sector practices by 2050 is equivalent to 11 to 15 percent of the total fossil fuel emission [27]. This is because trees are long-live plants that develop large biomass thereby capturing large amounts of carbon over a growth cycles of many decades [26]. The mitigation potential of forests found in Asian countries as mentioned in the IPCC Report 2001 [29] is estimated at about 26.5 Gt carbon.

Figure 2-2 Diagram showing the processes and fluxes maintaining or modifying the different C stocks in a forest, and the fluxes of the other key greenhouse gases, CH₄ and N₂O. Green arrows indicate C flux into the forest and between various C stocks; red arrows indicate C fluxes out of the forest. [25]

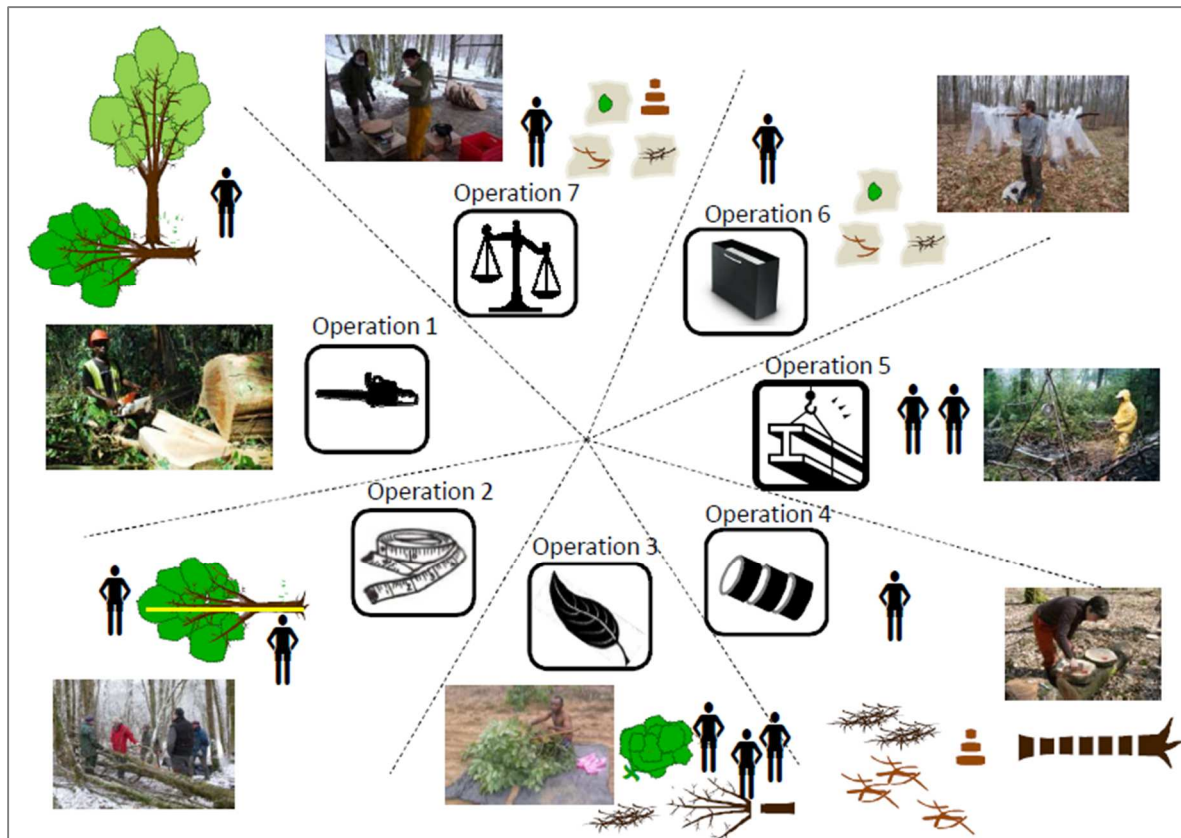


2.3 Ground forest biomass-carbon stock inventory

Woody biomass and wood volumes are important indicators that provide a comprehensive measure of the capacity a forest ecosystem to sequester carbon [26] since it is assumed that about 50 percent of the biomass is carbon [27]. As defined in Chapter II, biomass refers to the total amount of organic living matter in trees expressed as oven-dry tons per unit area. It represents the potential amount of carbon pools in forest land and that can be added to the atmosphere as carbon dioxide once the forest is burned.

The Ground biomass and carbon determination, Using destructive method involves harvesting of all the trees in the known area and measuring the weight of the different components of the harvested tree like the tree trunk, leaves and branches root and measuring the weight of these components after they are oven dried. The method has a limitation of a small area or small tree sample sizes. Although this method determines the biomass accurately for a particular area, it is time and resource consuming, strenuous, destructive, and it is not feasible for a large scale analysis. Then, the destructive method has been addressing by the use of biomass allometric equation. It has been developed by establishing a relationship between the various physical parameters of the trees such as the diameter at breast height, height of the tree trunk, branch, total height of the tree, crown diameter, tree species [17]. The steps of allometric equation process were shown in Figure 2-3. The majority of the biomass equations are in the form $Y = aX^b$, where Y is the weight of stem or branches or leaves (kg), X is the $DBH^2 \cdot Ht$ ($cm^2 \cdot m$) and a, b are constant value of equation [30]. The existing biomass equations were selected from the geographical regions closest to sample area.

Figure 2-3 Organization of a biomass measurement site with 7 different operations. Operation 1, site preparation and felling of the trees, operation 2, measurement of felled trees: stem profile, marking for cross-cutting, operation 3, stripping of leaves and limbing, operation 4, cross-cutting into logs and disks, operation 5, weighing of logs and brushwood, operation 6, sampling of branches, operation 7, sample weighing area. [30]

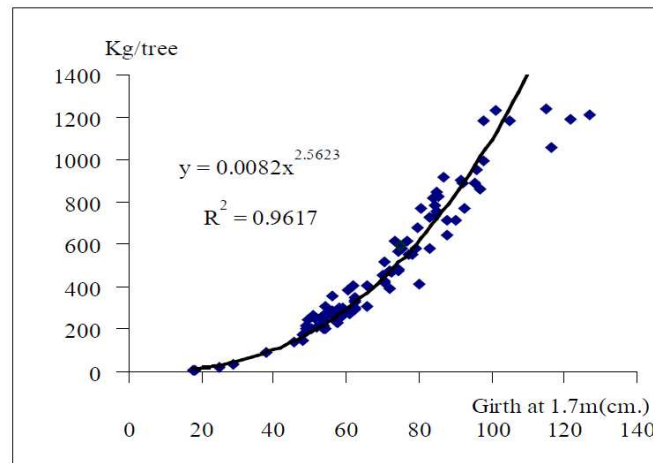


2.3.1 Allometric equation for *Hevea brasiliensis* (clone RRIM 600)

Several allometric relationship method are used for biomass estimation in *Hevea brasiliensis*-rubber clone using girth and height parameters to inputting data. The confident of allometric equation is published in range between $R^2 > 0.9$. This Chapter II is describe the tree allometric equation published by Chantuma *et al.*, 2004 as cite by ref. [7] for estimate a total weight biomass of *Hevea brasiliensis*-rubber clone RRIM 600. It was shown in Figure 2-4 a relationship between 95 trees rubber girth and total biomass. The biomass equation declared relationship between total dry matter (branch, trunk, leaf and roots) and girth of trees: $Y = 0.0082X^{2.5623}$, a coefficient of determination $R^2 = 0.9617$, Y is the tree dry biomass (kg), X is

girth (cm) at 1.7 m above ground. This equation was developed by measurements realized on plots located in North, North East, South and East of Thailand.

Figure 2-4 Relationship between girth (cm) at 1.7 meter above ground and dry weight biomass per tree RRIM 600 age 2 - 25 years, number of samples equals 95 trees. [7]



2.3.2 Carbon concentration of *Hevea brasiliensis* (clone RRIM 600)

The average 44.52 percentage of Carbon concentration of RRIM 600 biomass was found by the study of Chantuma *et al.*, 2004 [7] where measured by auto analyzer equipment (Table 2-2). The maximum of Carbon concentration is shown in Seed kernel endosperm part (57.27%) while the minimum is shown in Bark tap root part (39.45%).

Table 2-2 Performed percentage carbon and elements on parts of RRIM 600. [7]

Part of Para rubber tree (RRIM 600)	% C
Wood 0-3 meter above ground	44.5
Bark 0-3 meter above ground	41.02
Wood 9-12 meter above ground	45.3
Bark 9-12 meter above ground	42.5
Wood lateral root	45.88
Bark lateral root	41.51
Wood tap root	44.39

Bark tap root	39.45
Fibrous root	42.83
Mature stem branch	43
Young stem branch	43.97
Leaf laminar	47.95
Petiole leaf	45.4
Bark fruit	44.87
Hard fruit wall carpel	41.02
Seed shell	46
Seed kernel endosperm	57.27
average	44.52

2.4 General information of remote sensing used in this study

As defined in Chapter II, the remote sensing techniques are realized to the optical satellite data. Remote sensing is the measurement or acquisition of information of some property of an object or phenomenon, by a recording device that is not in physical or intimate contact with the object or phenomenon under study [31]. Various land cover absorbs and emits energy, which is recorded by sensors in the remote sensing device. The energy emitted by land covers called electromagnetic radiation differs among land covers giving certain features of the earth distinguishable characteristics as recorded in the satellite image.

Remote sensing using electromagnetic radiation has four components: a source, interactions with the earth's surface, interaction with the atmosphere and sensor [32]. Electromagnetic energy reaching the earth's surface from the sun is reflected, transmitted or absorbed. Reflected energy travels upwards through, and interacts with, the atmosphere; that the part of it which enters the field of view of the sensors is detected and converted into a numerical value that transmitted to a ground receiving station on the earth.

The characteristics of imaging remote sensing instrument can be summarized in term of their spatial, spectral, and radiometric resolutions. The spatial resolution is the ability to measure property (instantaneous field of view (IFOV)). The IFOV is defined as the area on

the ground. The term of spectral resolution refers to the width of these spectral bands measured in micrometers (μm) or nanometers (nm). The width and numbers of spectral bands determine the degree of discriminating power. The third important property, radiometric resolution refers to the number of digital quantization levels used to express the data collected by sensor. The greater the number of quantization levels the greater the detail in the information collected by the sensor. The different solutions of an earth observing system should be selected with the aim of investigation in mind [33].

2.4.1 THAICHOTE satellite data

THAICHOTE (previously name THEOS), THEOS is an Earth observation mission of Thailand, under development at EADS Astrium SAS, Toulouse, France. In July 2004, EADS Astrium SAS signed a contract for delivery of THEOS with GISTDA (Geo-Informatics and Space Technology Development Agency) of Bangkok, Thailand. GISTDA is Thailand's leading national organization (i.e., space agency) in the field of space activities and applications. The Thai Ministry of Science and Technology is funding the program.

The THEOS cooperative agreement includes the production and launch of one optical imaging satellite, as well as the development of the ground segment necessary to operate and control the satellite directly from Thailand. The contract also specifies on-the-job training of Thai engineers as part of the EADS Astrium development team. Also as part of the THEOS program, GISTDA earned the right to receive data from the SPOT-2, 4 and 5 spacecraft of CNES in Thailand, which have many features similar to those of THEOS [34].

The prime objective of THEOS is to provide Thailand with an affordable access to space (i.e., a state-of-the-art Earth observation satellite for the near future), and to spawn through this program's operational experience the country's own capability and infrastructure an indigenous potential for the development of future space missions.

The science objectives call for the provision of:

- Panchromatic (2 m) and multispectral (15 m) imagery from THEOS observations, and
- The generation of geo-referenced image products and image processing capabilities for applications in the fields of cartography, land use, agricultural monitoring, forestry management, coastal zone monitoring and flood risk management.

The THAICHOTE performance and payload characteristics are shown in Table 2-3 and Figure 2-5.

Table 2-3 (a) THAICHOTE performance., (b) THAICHOTE payload optical instruments characteristics.

(a)

Orbit Type	Circular SSO low earth orbit
Attitude	822 km
Number of Orbits per Day	14+5 / 26 orbits per day
Local Equator Crossing Time	10.00 am (descending)
Orbit Period	101 minutes
Orbit inclination	98.7
Orbit Cycle	26 days (369 orbits)
Distance Between Passes (at Equator)	108 km (between 2 closest passes), 2,800 km (between 2 consecutive passes)
Coverage Area	Radius more than 2000 km from Ground Station

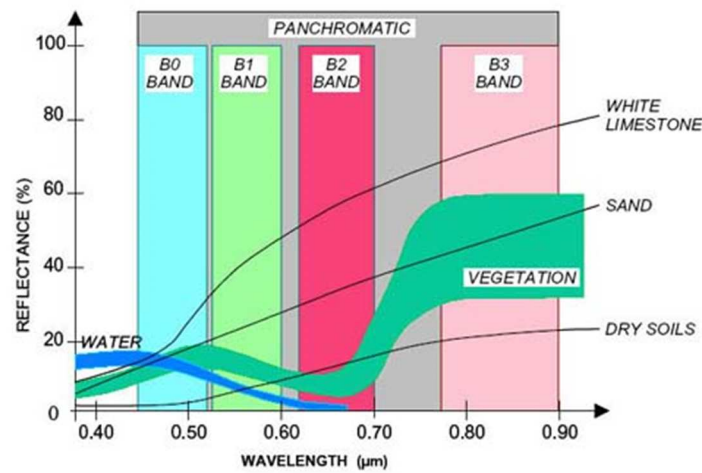
(b)

Parameter	Panchromatic (Pan) Camera	Multispectral (MS) Camera
Spectral range	0.45 to 0.90 μm	B1 (blue): 0.45-0.52 μm B2 (green): 0.53-0.60 μm B3 (red): 0.62-0.69 μm B4 (NIR): 0.77-0.90 μm
Spatial resolution	2 m GSD	15 m GSD
Swath width	22 km (nadir)	90 km (nadir)
Image dynamics	8 bits among 12 bits	8 bits among 12 bits

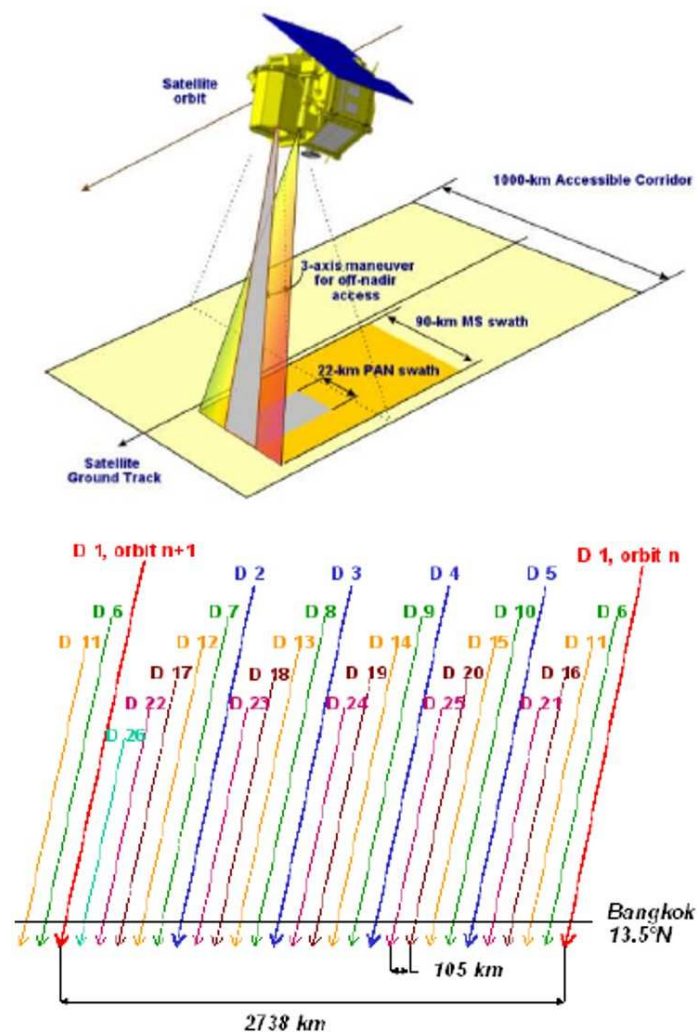
Source: Geo-Informatics and Space Technology Development Agency (GISTDA).

Figure 2-5 (a) Spectral signature of THAICHOTE., (b) THAICHOTE performance.

(a)



(b)



Source: Geo-Informatics and Space Technology Development Agency (GISTDA).

2.4.2 Remote sensing of vegetation

Plants have adapted their internal and external structure to perform photosynthesis. This structure and its interaction with electromagnetic energy have a direct impact on how leaves and canopies appear spectrally when recorded using remote sensing instruments [35]. Chlorophyll is the most important plant pigment absorbing blue and red light. Thus, the spectral reflectance curve rises in green wave bands. In addition, there are many factors that cause difference spectral such as percent canopy closure, temporal characteristics, managed phenological cycles, etc.

2.4.2.1 Broadband greenness Vegetation indexes

Broadband greenness vegetation indexes (VIs) are among the simplest measures of the general quantity and vigor of green vegetation. They are combinations of reflectance measurements that are sensitive to the combined effects of foliage chlorophyll concentration, canopy leaf area, foliage clumping, and canopy architecture. These VIs are designed to provide a measure of the overall amount and quality of photosynthetic material in vegetation, which is essential for understanding the state of vegetation for any purpose.

Broadband greenness VIs compare reflectance measurements from the reflectance peak of vegetation in the near-infrared range to another measurement taken in the red range, where chlorophyll absorbs photons to store into energy through photosynthesis. Use of near-infrared (NIR) measurements, with much greater penetration depth through the canopy than red, allows sounding of the total amount of green vegetation in the column until the signal saturates at very high levels. Because these features are spectrally quite broad, many of the broadband greenness indices can work effectively, even with image data collected from broadband multispectral sensors, such as AVHRR, Landsat TM, THAICHOTE, QUICKBIRD. Applications include vegetation phenology (growth) studies, land-use and climatological impact assessments, and vegetation productivity modeling [36]. Basic example of broadband greenness Vis indexes obtained by NIR and Red ratio from THAICHOTE data are listed in below.

- **Normalized Difference Vegetation Index (NDVI)**

The Normalized Difference Vegetation Index: NDVI [37] is image enhancing the green vegetation obtained by transformation of the visible (red) and near-infrared bands of satellite information. The NDVI values range from -1 to 1. Healthy vegetation will have a high NDVI value. Bare soil and rock will have NDVI values near zero. Clouds, water, and snow are negative NDVI values. The NDVI is calculated with the following Equation (2-1).

$$\frac{\text{NIR} - \text{RED}}{\text{NIR} + \text{RED}} \quad (2-1)$$

- **Atmospherically Resistant Vegetation Index (ARVI)**

The Atmospherically Resistant Vegetation Index: ARVI [38] is image enhancing according to the factor resistant to the atmospheric (eg. aerosol). The result of this index ranges from -1 to 1. The common range for green vegetation is 0.2 to 0.8. The ARVI is calculated using Equation (2-2).

$$\frac{\text{NIR} - 2(\text{RED}) - \text{BLUE}}{\text{NIR} + 2(\text{RED}) - \text{BLUE}} \quad (2-2)$$

- **Global Environment Monitoring Index (GEMI)**

The Global Environment Monitoring Index: GEMI [39] is eliminated the need for a detailed atmospheric correction by constructing a stocked atmospheric correction for the vegetation index. The result of GEMI is shown in range from -1 to 1. The GEMI is calculated using Equation (2-3).

$$\frac{n(1-0.25n)-\text{RED}-0.125}{1-\text{RED}} \quad \text{where : } n = \frac{2[(\text{NIR}^2-\text{RED}^2)+1.5(\text{NIR})]}{1-\text{RED}} \quad (2-3)$$

- **Infrared Percentage Vegetation Index (IPVI)**

The Infrared Percentage Vegetation Index : IPVI [40] this index as a way of improving calculation speed. It also is restricted to positive values between 0 and 1, which eliminates the need for storing a sign for the vegetation index values, and it eliminates the conceptual strangeness of negative values for vegetation indices. The IPVI is calculated using Equation (2-4).

$$\frac{\text{NIR}}{\text{NIR} + \text{RED}} \quad (2-4)$$

- **Modified Soil Adjusted Vegetation Index 2 (MSAVI 2)**

The Modified Soil Adjusted Vegetation Index 2 : MSAVI 2 [41] is adjusted vegetation indices that seek to address some of the limitation of NDVI when applied to areas with a high degree of exposed soil surface. The value of this index ranges from -1 to 1. The MSAVI2 is calculated using Equation (2-5).

$$\frac{2\text{NIR} + 1 - \sqrt{(2\text{NIR} + 1)^2 - 8(\text{NIR} - \text{RED})}}{2} \quad (2-5)$$

where:

RED = the THAICHOTE red band (0.62-0.69 μm)
 NIR = the THAICHOTE near infrared band (0.77-0.90 μm)

2.4.3 Texture measurement

The texture of an image is related to the statistical characteristics of association of pixels at a given scale. The texture of an image is a good descriptor of the forest canopy [8, 9]. The Grey-Level Co-occurrence Matrix (GLCM) texture measurement [42, 43] has been applied to satellite imagery. The GLCM is a tabulation of how often different combinations of pixel brightness values (grey levels) occur in the image. The GLCM is realized in 2 steps.

The first one is the generation of the co-occurrence matrix called probability matrix, and the second one is the computation of texture descriptors. The probability matrix characterizes the texture of an image by calculating how often pairs of pixel with specific values and in a specified spatial relationship occur in an image, creating a GLCM, and then extracting statistical measures from this matrix [43]. A sliding window was used to generate co-occurrence matrix. Four directions (0° , 45° , 90° , and 135°) of pixel neighborhood connections were considered. The probability matrix generation was illustrated in Figure 2-6.

Second one, the texture descriptors were computed from GCLM. The Haralick et al. [42] equations were used for texture measurements. These equations refer to 3 groups of descriptors that are: the contrast group (Contrast, Dissimilarity, and Homogeneity), the orderliness group (Angular second moment, Entropy) and the descriptive statistics group (Mean, Variance, and Correlation), (Table 2-4). Eight textural layers have been computed from the original image.

Figure 2-6 Example illustration of the probability matrix generation, considering east direction only (1 pixel offset from a reference pixel and its immediate neighbor) and summary total is 16 elements (sliding window 4x4 pixels). Frame work matrix was used to fill neighbor position (i,j). Twice in the original image the reference pixel is 0 and its eastern neighbor is also 0. Twice the reference pixel is 0 and its eastern neighbor is 1. Three times the reference pixel is 2 and its neighbor is also 2. The probability was computed which divide by sum of total elements of window.

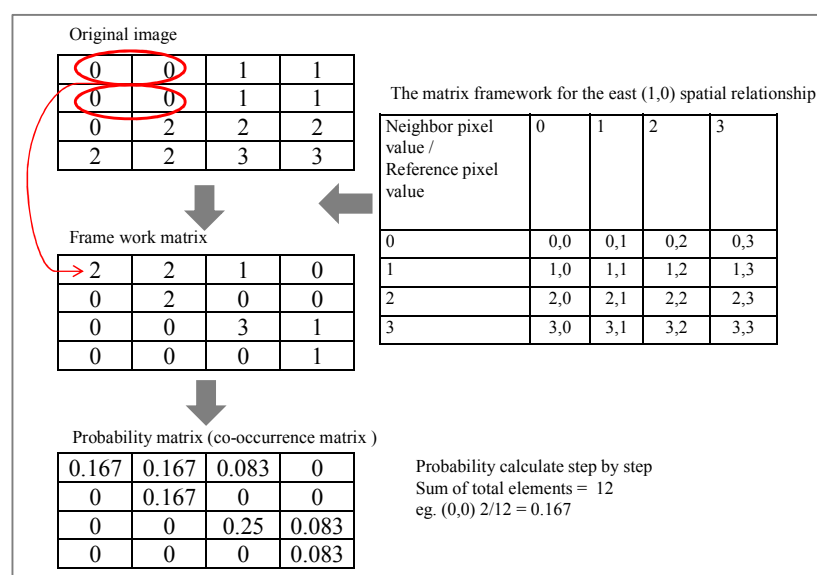


Table 2-4 Textural information equations. [42]

Texture group	GLCM descriptor	Formula	Description
Contrast	Contrast (CON)	$f_{\text{CON}} = \sum_{i,j=0}^{N-1} P_{i,j} i - j ^2$	Quadratic measure of the local variation in the image. High values indicate large differences between neighbouring pixels.
	Dissimilarity (DIS)	$f_{\text{DIS}} = \sum_{i,j=0}^{N-1} P_{i,j} i - j $	Linear measure of the local variation in the image.
	Homogeneity (HOM)	$f_{\text{HOM}} = \sum_{i,j=0}^{N-1} \frac{P_{i,j}}{1 + (i - j)^2}$	Measure of the uniformity of tones in the image. A concentration of high values along the GLCM diagonal denotes to a high homogeneity.
Orderliness	Angular Second Moment (ASM)	$f_{\text{ASM}} = \sum_{i,j=1}^{N-1} P_{i,j}^2$	Measure of the order in the image. It is related to the energy required for arranging the elements in the system.
	Entropy (ENT)	$f_{\text{ENT}} = \sum_{i,j=0}^{N-1} P_{i,j} (-\ln P_{i,j})$	Measure of the disorder in the image. It is inversely related to ASM.
Descriptive statistics	Mean	$f_{\mu i} = \mu_i \sum_{i,j=0}^{N-1} i(P_{i,j}),$ $f_{\mu j} = \mu_j \sum_{i,j=0}^{N-1} j(P_{i,j})$	Mean of the probability values from the GLCM. It is directly related to the image spectral

			heterogeneity.
	Variance (Var)	$f_{\text{variance}} = \sum_{i,j=0}^{N-1} P_{i,j} (i - \mu)^2$	Measure of the global variation in the image. Large values denote high levels of spectral heterogeneity.
	Correlation (Cor)	$f_{\text{correlation}} = \sum_{i,j=0}^{N-1} \left[\frac{(i - \mu_i)(j - \mu_j)}{\sqrt{(\sigma_i^2) + (\sigma_j^2)}} \right]$	Measure of the linear dependency between neighbouring pixels.

where:

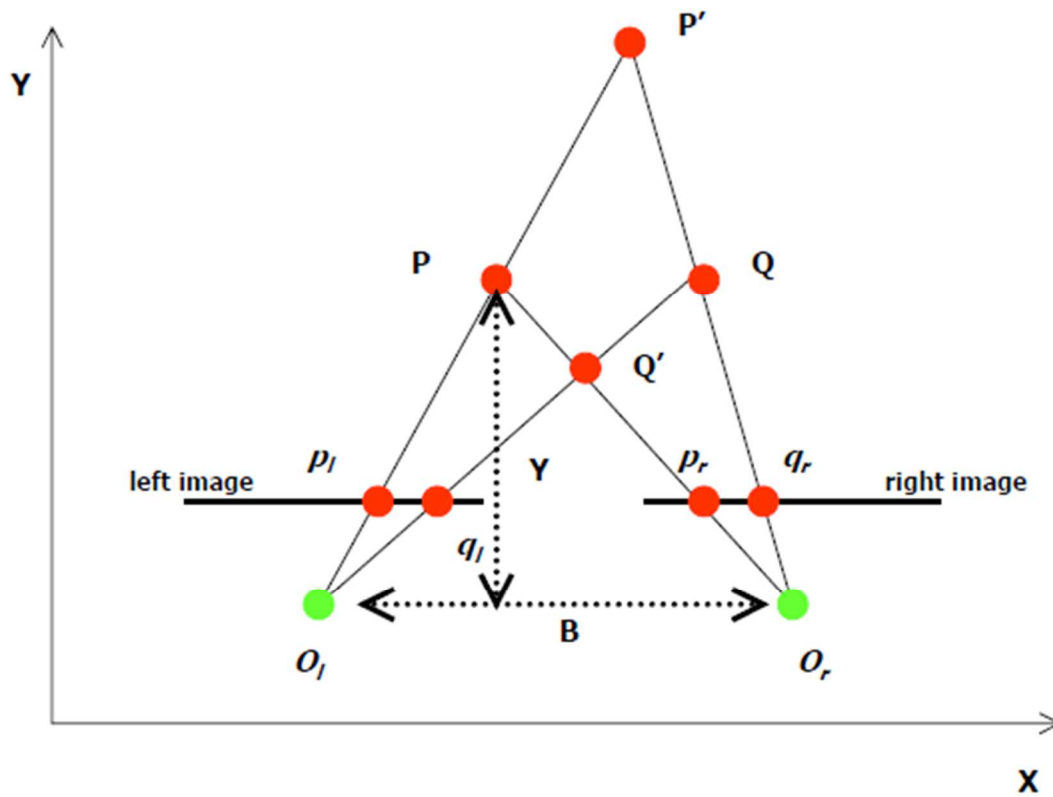
$P_{i,j}$	=	The probability matrix
i	=	Reference pixel
j	=	Neighborhood pixel
$\mu_i, \mu_j, \sigma_i, \sigma_j$	=	The mean and standard deviation of $P_{i,j}$ respectively

2.4.4 3D terrain model

2.4.4.1 A simple stereo system

A brief story of a simple stereo system is described [44]. The computation of object positions in space requires linking coordinates of points in 3-dimensional space with coordinates of their corresponding images points. Using the example of a simple stereo system (Figure 2-7) shown from a top down perspective, the determination of the position of P and Q in space can easily be seen through the process of triangulation.

Figure 2-7 Top-down view of a simple stereo system highlighting significance of correspondence problem. [45]



© Stephen Rawlinson 2002

Thus, the intersection of rays $O_l p_l - O_r p_r$ and $O_l q_l - O_r q_r$ leads to interpreting the image points as projections of P and Q . However, if (p_l, q_r) and (q_l, p_r) are the selected pairs of corresponding points, triangulation returns P' and Q' . Note that both interpretations, although radically different, are equally valid. Figure 2-8 also illustrates the triangulation of a single point P , determined from image coordinates p_l and p_r . The distance, B , between the centres of projection O_l and O_r , is referred to as the baseline of the stereo system. Letting x_l, x_r be coordinates of p_l, p_r with respect to the principal points c_l, c_r , f the camera constant or focal length, and Y the distance between P and the baseline. From the similar triangles (p_l, P, p_r) and (O_l, P, O_r) , the following equation can be derived in equation (2-6, 2-7).

$$\frac{B + x_r - x_l}{Y - f} = \frac{B}{Z} \quad (2-6)$$

Solving for Y yields the following:

$$Y = f \frac{B}{d}$$

where:

f	=	the camera constant (focal length)
B	=	distance of O_l and O_r referenced to the baseline
Z	=	depth information
d	=	$x_r - x_l$ and is referred to as the disparity or parallax

Parallax measures the difference in retinal position between the corresponding points in the two images. As such, depth is inversely proportional to parallax.

Equation 2-6 is the simple case (normal case) and although it is computationally attractive, it is rarely encountered in real world applications. In a 3-dimensional perspective and with the normal case assumption, any image object space (X_p, Y_p, Z_p) 3-dimensional coordinate corresponding to a feature contained within the left and right images can be calculated using the following sets of equations (2-7), (Figure 2-8).

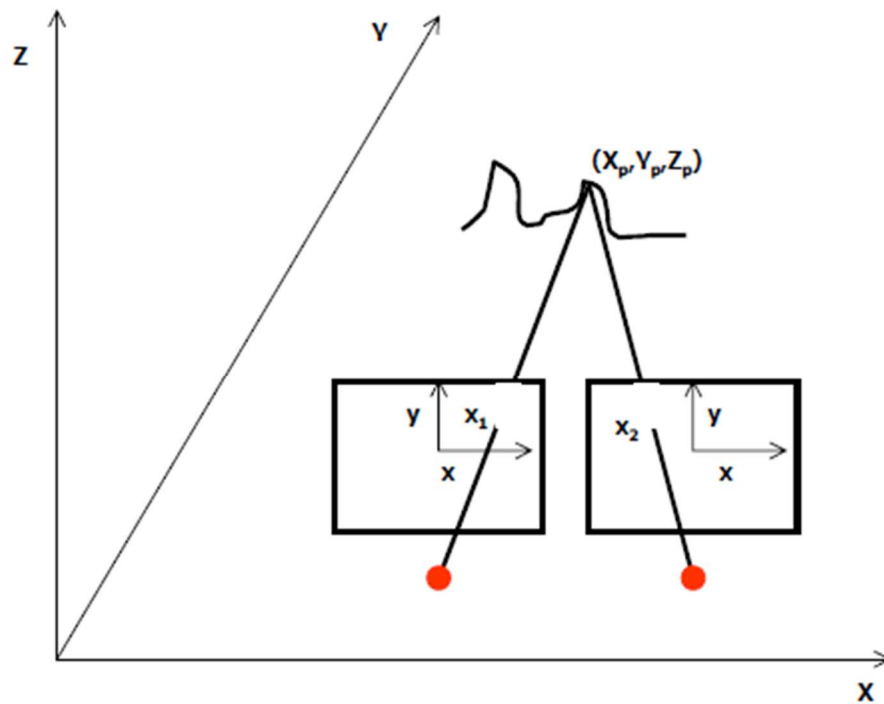
$$X_p = \frac{Y_p}{pd} x_1$$

$$Y_p = \frac{B_{pd}}{x_1 - x_2} \quad (2-7)$$

$$Z_p = \frac{Y_p}{pd} y$$

where:

x_1	=	x position of the object in the left image
x_2	=	x position of the object in the right image
pd	=	estimated principle distance
B	=	stereo base separation

Figure 2-8 “Normal Case” configuration for calculation of object space coordinates. [45]

© Stephen Rawlinson 2002

2.4.4.2 Implementation of a 3D terrain model on computer simulation

The Exelis Visual Information Solutions [45] has been explained the 3D terrain generation using stereo data. There are three steps in creating a 3D terrain model that are crucial to generating acceptable results: epipolar image creation, image matching, and 3D terrain geocoding.

- **Epipolar Image Creation:** Creating epipolar images is an essential processing step in Digital Elevation Model (DEM) extraction. Epipolar geometry describes the geometrical constraint between two frame images of a stereo pair. It represents the fact that a ground point and the two optical centers lie on the same plane. This means that for a given point in one image, its conjugate point in the other image must lie on a known line in the second image. By creating epipolar images, the search space for finding corresponding image points in automatic image matching is reduced.

- Image Matching: Image matching finds the conjugate points on both the left and right images which correspond to the same ground feature. The output of the image matching procedure is called a parallax image, in which the x-coordinate difference (along epipolar lines) between the left and right image is stored and is used to build the 3D terrain model. Thus, the quality of image matching largely determines the quality of the output 3D terrain.
- 3D terrain Geocoding: 3D terrain geocoding reprojects the 3D terrain model from the epipolar projection to an output map projection and units that you specify. This step involves filling failed pixels and resampling to a pixel spacing that you specify.

2.4.5 Object Based Image Analysis

The advantage of a spatial resolution with pixel sizes significantly smaller than the average size of the object of interest comes with the disadvantage of an abundance of spatial detail and the accordingly huge amount of data to be processed. To overcome this drawback, the object based image analysis (OBIA) approach has proven to be an alternative to the pixel based image analysis and a large number of publications suggest that better results can be expected [46]. The object-based approach suggests a two-staged approach. In the first step pixels are merged to object clusters, possibly in a multi-level object hierarchy, which then will be analyzed and classified in the second step.

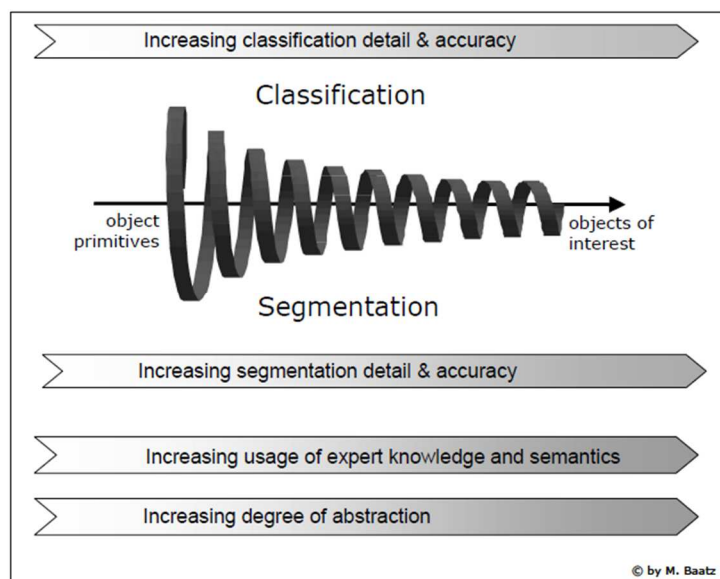
2.4.5.1 workflow

The workflow described here starts with object primitives as well. However, in contrast to the object-based workflow, it uses these objects not only as information carriers but also as building blocks for any further shape modification, merging, or segmentation procedures. In a whole sequence of processing steps, where segmentation steps alternate with evaluation and classification steps, these object primitives are constantly altered until they become the desired objects of interest. Because this strategy aims for correct shaping and classification of objects, and objects are also used at every step during the procedure as the central processing unit, serving both as information provider and as building blocks, this workflow consequently can be called “object-oriented image analysis”.

This workflow can be described best with a spiral and is illustrated in Figure 2-9. The entire process is iterative and starts in the first step with the creation of object primitives using any (knowledge-free) segmentation algorithm. The next step uses the object primitives in order to perform a first evaluation and classification, thus introducing semantics. Building on this result, the subsequent step allows refinement or improvement of the segmentation locally for a specific class. Thus, the whole process alternates iteratively between local object modification on the one hand and local object evaluation and classification on the other. By using such an iterative approach, different object classes can be addressed with different object modification strategies. During this process, the objects are altered from stage to stage until they represent the final target objects. Only the combination of correct shaping and correct classification characterizes the target objects; otherwise the results will be insufficient. The spiral in Figure 2-9 represents this alternation between segmentation and classification in the object-oriented approach.

As the analysis progresses, classification detail and accuracy are growing together with segmentation detail and accuracy. Whereas the process starts with rather simple and knowledge-free segmentation steps, more and more expert and domain knowledge is introduced and used in later steps. The more closely the process approximates the final target objects, the higher is the abstraction from the original image information [46].

Figure 2-9 Object-oriented image analysis: the generic procedure. [46]



DATA

&

METHODS

CHAPTER III

DATA AND METHODS

Classical methods are based on identification of Para rubber plantations from classification of spectral pixel information on remote sensing images. This study is to improve the classification by OBIA by combining both spectral and textural information from the images. The method developed here needs field data that will permit the building of a transfer equation model between field and remote sensing data. The girths of trees were measured in the field according to their age in 500 randomly chosen plots. In each plot, the characteristics of 10 to 15 trees were measured and evaluated. The biomass and the carbon storage for a single tree were estimated from already published allometric equations. In parallel, the Thaichote satellite image (2 m) was corrected from atmospheric artifacts and then classified according to the OBIA method.

The first step of OBIA consists of the image segmentation in order to identify the Para rubber plantations and to estimate the number of trees available per plantation. In a second step, textural and vegetation indices were constructed from the images using classical descriptors. The new images combined with the initial bands were used as inputs in a classification process to extract a numerical relation between the girths and ages of trees and the indicator values of the sampled plots. The empirical model obtained from a simple linear multiple regression technique was used to estimate the age of every plantation. Finally, the biomass and carbon stocked by Para rubbers in the Mae num Prasae watershed were estimated from the map of the plantation, the age estimated for each plantation and the relationship between the age and carbon stock for a single tree. The steps of process are described in Figure 3-1.

Figure 3-1 Study process.



3.1 Study Process

The study process was defined into 4 board parts (Figure 3-1). Firstly, the Field Data (Part 1) was collected using Forest inventory and Ground Biomass-Carbon estimation. Secondly, the remote sensing data obtained from THAICHOTE satellite data was applied to mapping of Para rubber plantation surface. Using 3 steps: Satellite Image Preprocessing (Part 2), Image Classification (Part 3) and Para rubber Surface Extraction (Part 4). The biomass and carbon stock of single trees were linked to the remote sensing data using linear multiple regression model. Finally, the total biomass and carbon stock at large surface were estimated.

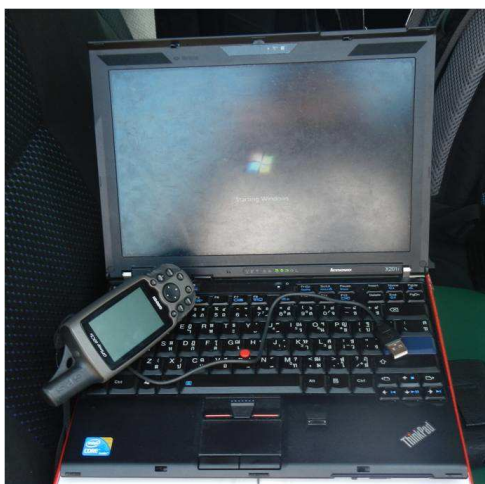
3.2 Field data

3.2.1 Field measurements

The study was applied the forest inventory technique (an equipment shown in Figure 3-2). In the field, diameter at breast height (DBH), tree height (see in appendix A1 for tree height measurement), girth (circulation) and age were measured on about 10 to 15 trees per plot (Figure 3-3(a)). Random plots were used for the forest inventory associated to tree age range from 4 to 25 years old. Every plot was collected geo-location using GPS handheld measured at center point of the plot. The study also measured the tree stand density. The age data was classified in 8 classes of 4, 8, 12, 16, 18, 20, 22 and 25 years old. DBH and tree girth were measured with a diameter tape at height 1.3 to 1.7 m above the ground according to the position of latex tapped skin on the trunk (Figure 3-3(b), 3-3(c)). Data was managed in a GIS database which included topographic map and satellite image projected in the Universal Transverse Mercator (UTM) 48N Zone on World Geodetic System 1984 (WGS84).

Figure 3-2 The equipment of forest field measurements. (a) a field computer notebook, (b) an altimeter (measuring tree height), (c) a diameter tape, (d) a field tape, (e) a GPS and (f) a Camera GPS.

(a)



(b)



(c)



(d)



(e)

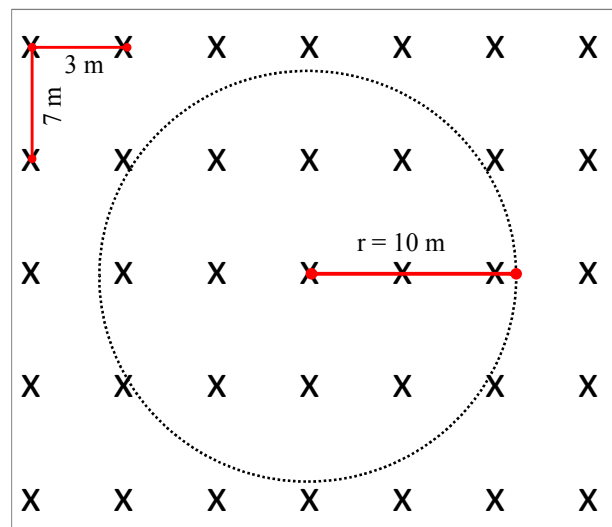


(f)



Figure 3-3 Sample plot measurements, (a) plot layout using a circle plot covered about 15 trees/sample plot., (b) and (c) shown the girth measurement on Para rubber plantation (DBH of 1.3 m and 1.7 m)

(a)



(b)



(c)



3.2.2 Ground biomass and carbon Estimation

Diameter from the field was used to determine the biomass of individual trees. The allometric equation developed for the rubber clone of *Hevea brasiliensis* (RRIM 600: Rubber Research Institute of Malaysia No.600) by Chuntuma et al., (2012) [7] was used in the estimate biomass of individual trees. The tree allometry was shown in Equation (3-1):

$$Y = 0.0082 X^{2.5623} \quad (3-1)$$

where:

Y = the tree dry biomass in kg.

X = the girth of tree in cm.

The coefficient of correlation (R^2) is 0.96. This equation was developed by measurements realized on plots located in North, North East, South and East of Thailand.

The factor conversion from Chuntuma et al., (2012) [7] for the average carbon content of every component of *Hevea brasiliensis* at 44.52% from dry biomass (kg) was applied. The carbon content value was used to determine the carbon density for all age classes of Para rubber plantation. The total amount of carbon stored was shown in Equation (3-2):

$$\text{Carbon density} = (\text{Biomass}) * (\%C) \quad (3-2)$$

where:

Carbon density = total amount of carbon stored in plantation expressed as tons of C (t C)

Biomass = total biomass (ton)

%C = carbon content at 44.52%

Therefore, the rate of carbon sequestration was calculated using by Sale et al., (2004) [1] in Equation (3-3):

$$\text{Carbon sequestration} = \frac{\text{Carbon Mass in 1 ha}}{\text{Age of trees}} \quad (3-3)$$

where:

Carbon sequestration = the amount of carbon sequestered or the quantity of carbon accumulated per year by each age class expressed as tons of C per hectare per year (t C ha⁻¹yr⁻¹)

Carbon Mass in 1 ha = total amount of carbon stored in plantation expressed as tons of C (t C)

Age = age of each tree (yr)

3.3 Satellite Image Preprocessing

3.3.1 Data sources

Three categories data were classified in the study. First category, multispectral, panchromatic and stereo pair from THAICHOTE data were major used in Para rubber biomass and carbon stock estimation. Second category, the mask information for Para rubber extraction was generated using GIS database and Third category, the Thailand topographic map and Digital Elevation Model (DEM) were used for THAICHOTE image correction. The data sources were listed in Table 3-1.

Table 3-1 Data sources.

Category data 1 : Multispectral data (spatial resolution 15 m.)					
Scene ID	Center of position	Bands	Cloud	Acquisition date	Sources
SCENE T1 M 2011/12/27 03:22:18.0 0265- 0323 3700	E101°31' 36" N12°53' 26"	1 (0.45-0.52 $\mu\text{m.}$) 2 (0.53-0.60 $\mu\text{m.}$) 3 (0.62-0.69 $\mu\text{m.}$) 4 (0.77-0.90 $\mu\text{m.}$)	<10%	December 27, 2011	GISTDA.
Panchromatic data (spatial resolution 2 m.)					
SCENE T1 P 2011/12/27 03:22:17.9 0265- 0324 5000	E101°31' 44" N12°53' 46"	0.45-0.90 $\mu\text{m.}$	<10%	December 27, 2011	GISTDA.
SCENE T1 P 2011/12/27 03:22:21.3 0265- 0324 5000	E101°28' 59" N12°41' 45"	0.45-0.90 $\mu\text{m.}$	<10%	December 27, 2011	GISTDA.
Stereo data					
Scene ID	Center of position	Viewing angle (degree)	Cloud	Acquisition date	Sources
SCENE T1 P 2012/04/03 03:37:41.4 0265- 0324 0	E101°32' 34" N12°54' 06"	along -37.465028° across 21.010437°	<20%	April 3,2012	GISTDA.
SCENE T1 P 2012/04/03 03:37:38.0 0265- 0324 0	E101°35' 32" N13°06' 05"	along -37.471443° across 21.013978°	<20%	April 3,2012	GISTDA.
SCENE T1 P 2012/04/03 03:34:28.3 0265- 0324 1200	E101°32' 44" N12°54' 53"	along 35.524439° across 21.101462°	<20%	April 3,2012	GISTDA.
SCENE T1 P 2012/04/03 03:34:24.9 0265-	E101°35' 38" N13°06' 55"	along 35.521264° across	<20%	April 3,2012	GISTDA.

0324 1200		21.101122°			
Category data 2 : Thailand topographic map scale 1:50,000 (series L7018)					
Map index			Sources		
5235II, 5335III, 5234I, 5334IV, 5234II, 5334III			Royal Thai Survey Department		
Digital Elevation Model (DEM)					
Product type	Spatial Resolution	Sources			
DEM	30	Global Digital Elevation Model (GDEM V.2)			
Category data 3 : GIS database from NSDI					
Product type	Scale	Sources			
Forest	1:50,000	Forest Department, Thailand.			
Land use	1:4,000	Land Development Department, Thailand.			
Road	1:50,000	Department of Highways, Thailand,			
Soil series	1:250,000	Land Development Department, Thailand.			
Admin boundary	1:50,000	Department of Provincial Administration, Thailand.			

3.3.2 Satellite Image Correction

On December 27, 2011 at 03:22 GMT during the dry season, THAICHOTE image was acquired where cloud cover was less than 10%. The image was first pan-sharpened and georeferenced using ortho-rectification method [47] in the Universal Transverse Mercator projection Zone 48 North on World Geodetic System 1984 ellipsoid (UTM WGS-1984 Z48N) and corrected from topographic distortion using ASTER Global Digital Elevation (GDEM Version 2). GDEM was revised spatial resolution from 30 m to 2 m using raster resample technique. Therefore, THAICHOTE image has been provided in 2 m spatial resolution and 4 single bands of Blue (0.45-0.52 μm), Green (0.53-0.60 μm), Red (0.62-0.69 μm) and Near Infrared (NIR, 0.77-0.90 μm).

The cosine of the solar zenith corrections (COST) [48] was used to correct the radiometry of the image. The sun azimuth was 143.21° and the sun elevation was 44.5710°. The inputs to the model are the Earth-Sun Distance, sun elevation angle, and digital number

(DN) values for each band. The parameters input were shown in Table 3-2, 3-3 and 3-4. The image DN value was first transferred to spectral radiance value using Equation (3-4):

$$L_{\lambda} = \text{Gain (DN)} + \text{Bias} \quad (3-4)$$

where:

L_{λ}	=	Spectral radiance at the sensor's aperture ($\text{Mw} \cdot \text{cm}^{-2} \cdot \text{ster}^{-1} \cdot \mu\text{m}^{-1}$)
DN	=	Digital number (8-bit, 0-255)
Gain	=	Absolute calibration gain of each band ($\text{mW} \cdot \text{cm}^{-2} \cdot \mu\text{m}^{-1}$)
Bias	=	Absolute calibration bias of each band ($\text{mW} \cdot \text{cm}^{-2} \cdot \mu\text{m}^{-1}$)

Table 3-2 Gain and Bias in each band of THAICHOTE data used in the study.

Band	Gain	Bias
Blue	3.42038	0
Green	2.12232	0
Red	2.07681	0
NIR	1.67119	0

Then, the spectral radiance value was applied to COST model (assumed to have a reflectance of 1% or called $L_{\lambda\text{Haze}}$) that following Equation (3-5):

$$\rho_{\lambda} = \frac{\pi \cdot (L_{\lambda} - L_{\lambda\text{Haze}}) \cdot d^2}{ESUN_{\lambda} \cdot \cos \theta_s} \quad (3-5)$$

where:

ρ_{λ}	=	Planetary reflectance (unitless)
π	=	Mathematical constant approximately equal to 3.14159
L_{λ}	=	Spectral radiance at the sensor's aperture ($\text{mW} \cdot \text{cm}^{-2} \cdot \mu\text{m}^{-1}$)
$L_{\lambda\text{Haze}}$	=	A haze correction ($L_{\lambda} - L_{\lambda 1\%}$) as in Table 3-3
d	=	Distance from earth to sun (Astronomical Unit) as in Table 3-4

ESUN _λ =	Mean exoatmospheric solar irradiance (mW.cm ⁻² .μm ⁻¹) as in Table 3-3
θ _s =	Solar zenith angle (degrees)

Table 3-3 The parameters input to the model.

Band	L _λ 1%	ESUN _λ
Blue	-2.952287	2005.824
Green	-2.497447	1848.653
Red	-2.039939	1566.489
NIR	-1.126369	1064.725

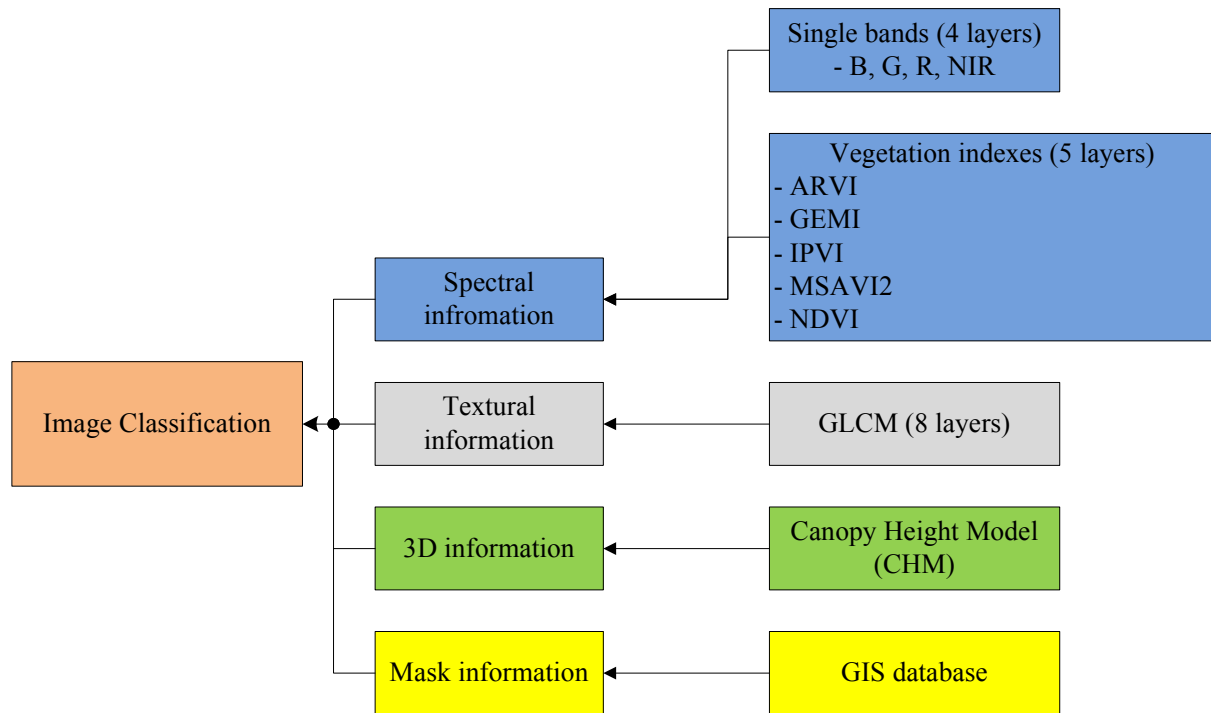
Source: Geo-Informatics and Space Technology Development Agency (GISTDA).

Table 3-4 Distance from Earth to the Sun (Astronomical Unit).

Julian Day	Distance	Julian Day	Distance	Julian Day	Distance	Julian Day	Distance	Julian Day	Distance
1	0.9832	74	0.9945	152	1.0140	227	1.0128	305	0.9925
15	0.9836	91	0.9993	166	1.0158	242	1.0092	319	0.9892
32	0.9853	106	1.0003	182	1.0167	258	1.0057	335	0.9860
46	0.9878	121	1.0076	196	1.0165	274	1.0011	349	0.9843
60	0.9909	135	1.0109	213	1.0149	288	0.9972	365	0.9833

3.4 Image Classification

Image classification technique was used for mapping Para rubber plantations and to estimate the girth and age of each plantation. The technique developed here uses combining multi-information of the spectral, textural, 3D and mask information. Then, the 18 layers obtained by image classification technique were stored in the geo-database for the Para rubber plantation Surface Extraction. The steps of processing are described as follows (illustrated in Figure 3-4):

Figure 3-4 The processes of Image Classification.

3.4.1 Spectral information

Five classical of broadband greenness Vegetation Indexes were calculated from the 4 spectral bands. Each index is a combination of the various bands ratios as follows:

- Atmospherically Resistant Vegetation Index (ARVI) [38] was determined using the Equation (3-6):

$$\frac{\text{NIR} - 2(\text{RED}) - \text{BLUE}}{\text{NIR} + 2(\text{RED}) - \text{BLUE}} \quad (3-6)$$

- Global Environment Monitoring Index (GEMI) [39] was determined using the Equation (3-7):

$$\frac{n(1-0.25n)-RED-0.125}{1-RED} \quad \text{where : } n = \frac{2[(NIR^2-RED^2)+1.5(NIR)]}{1-RED} \quad (3-7)$$

- Infrared Percentage Vegetation Index (IPVI) [40] was determined using the Equation (3-8):

$$\frac{NIR}{NIR + RED} \quad (3-8)$$

- Modified Soil Adjusted Vegetation Index² (MSAVI₂) [41] was determined using the Equation (3-9):

$$\frac{2NIR + 1 - \sqrt{(2NIR + 1)^2 - 8(NIR - RED)}}{2} \quad (3-9)$$

- Normalized Difference Vegetation Index (NDVI) [38] was determined using the Equation (3-10):

$$\frac{NIR - RED}{NIR + RED} \quad (3-10)$$

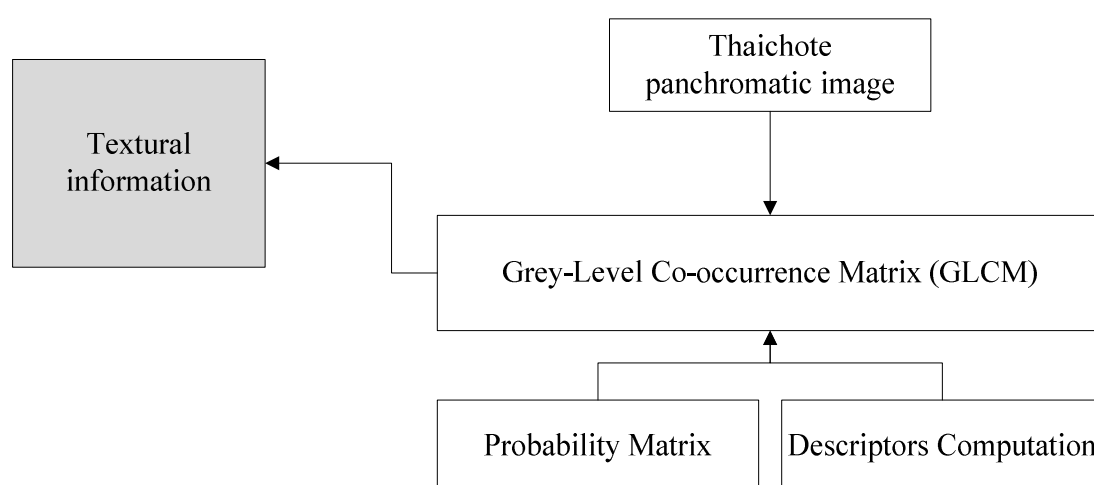
where:

- NIR = Near Infrared reflectance value (spectral band 0.77 – 0.9 μm)
- RED = Visible Red reflectance value (spectral band 0.62 – 0.69 μm)
- BLUE = Visible blue reflectance value (spectral band 0.53 – 0.6 μm)

3.4.2 Textural information

The texture of an image is related to the statistical characteristics of association of pixels at a given scale. The texture of an image is a good descriptor of the forest canopy [8, 9]. The Grey-Level Co-occurrence Matrix (GLCM) texture measurement [42, 43] was applied to THAICHOTE panchromatic image. The texture information illustrated in Figure 3-5.

Figure 3-5 The processes of textural information.



The GLCM is a tabulation of how often different combinations of pixel brightness values (grey levels) occur in the image. The GLCM is realized in 2 steps, the first one is the generation of the co-occurrence matrix called probability matrix, and the second one is the computation of texture descriptors. The probability matrix characterizes the texture of an image by calculating how often pairs of pixel with specific values and in a specified spatial relationship occur in an image, creating a GLCM, and then extracting statistical measures from this matrix [43]. A 15x15 pixels sliding window [8] was used to generate co-occurrence matrix. Four directions (0°, 45°, 90°, and 135°) of pixel neighborhood connections were considered. Texture descriptors were computed from GCLM. The Haralic et al. [42] equations were used for texture measurements. These equations refer to 3 groups of descriptors that are: the contrast group (Contras, Dissimilarity, and Homogeneity), the orderliness group (Angular

second moment, Entropy) and the descriptive statistics group (Mean, Variance, and Correlation). Eight textural layers were computed from the original image (Table 3-5).

Table 3-5 Textural information equations. [42]

Texture group	GLCM descriptor	Formula	Description
Contrast	Contrast (CON)	$f_{\text{CON}} = \sum_{i,j=0}^{N-1} P_{i,j} i - j ^2$	Quadratic measure of the local variation in the image. High values indicate large differences between neighbouring pixels.
	Dissimilarity (DIS)	$f_{\text{DIS}} = \sum_{i,j=0}^{N-1} P_{i,j} i - j $	Linear measure of the local variation in the image.
	Homogeneity (HOM)	$f_{\text{HOM}} = \sum_{i,j=0}^{N-1} \frac{P_{i,j}}{1 + (i - j)^2}$	Measure of the uniformity of tones in the image. A concentration of high values along the GLCM diagonal denotes to a high homogeneity.
Orderliness	Angular Second Moment (ASM)	$f_{\text{ASM}} = \sum_{i,j=1}^{N-1} P_{i,j}^2$	Measure of the order in the image. It is related to the energy required for arranging the elements in the system.
	Entropy (ENT)	$f_{\text{ENT}} = \sum_{i,j=0}^{N-1} P_{i,j} (-\ln P_{i,j})$	Measure of the disorder in the image. It is inversely related to ASM.
Descriptive	Mean	$f_{\mu i} = \mu_i \sum_{i,j=0}^{N-1} i(P_{i,j}),$	Mean of the probability

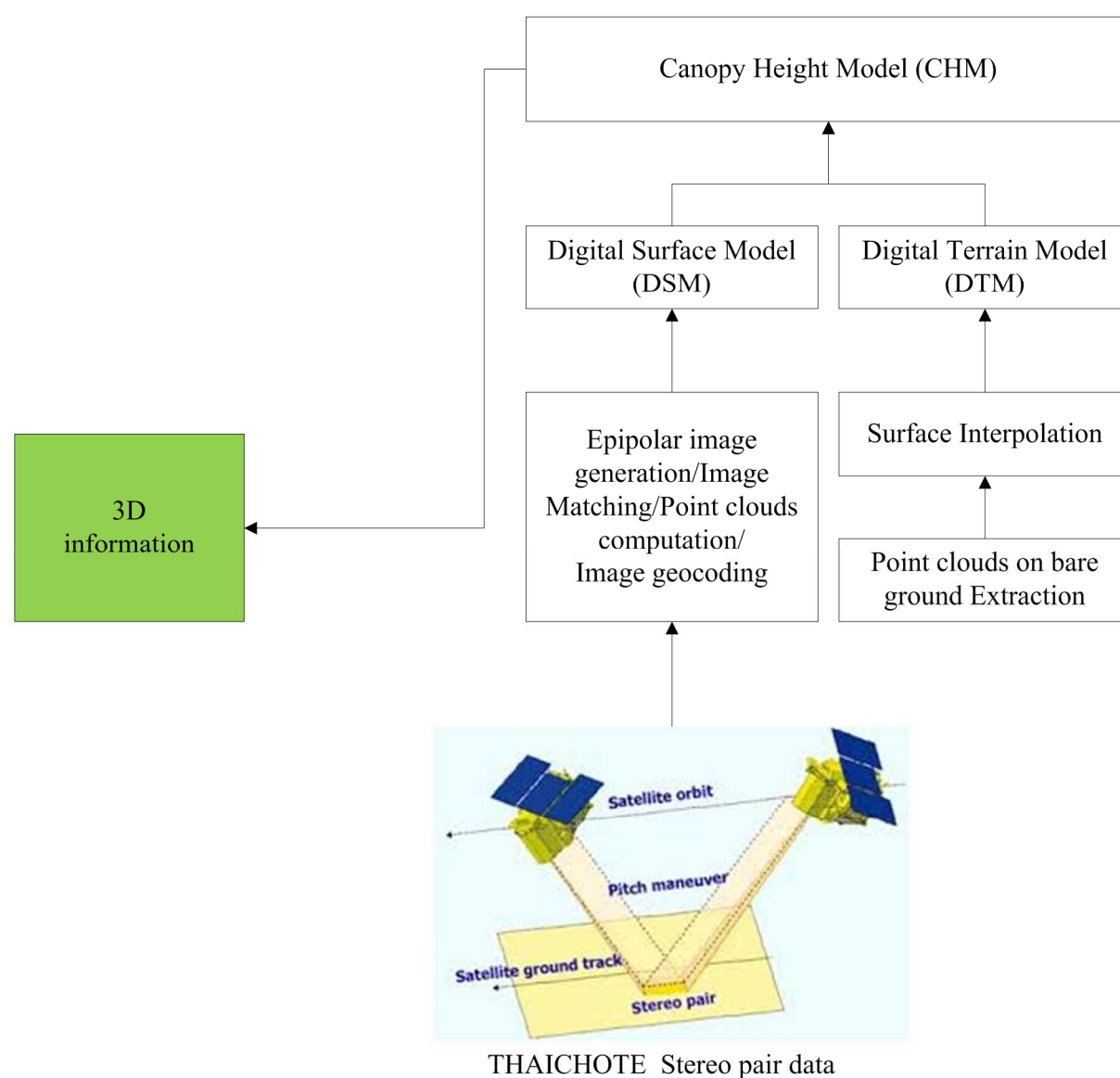
statistics		$f_{\mu_j} = \mu_j \sum_{i,j=0}^{N-1} j(P_{i,j})$	values from the GLCM. It is directly related to the image spectral heterogeneity.
	Variance (Var)	$f_{\text{variance}} = \sum_{i,j=0}^{N-1} P_{i,j} (i - \mu)^2$	Measure of the global variation in the image. Large values denote high levels of spectral heterogeneity.
	Correlation (Cor)	$f_{\text{correlation}} = \sum_{i,j=0}^{N-1} \left[\frac{(i - \mu_i)(j - \mu_j)}{\sqrt{(\sigma_i^2) + (\sigma_j^2)}} \right]$	Measure of the linear dependency between neighbouring pixels.

where:

$P_{i,j}$	=	The probability matrix
i	=	Reference pixel
j	=	Neighborhood pixel
$\mu_i, \mu_j, \sigma_i, \sigma_j$	=	The mean and standard deviation of $P_{i,j}$ respectively

3.4.3 Three dimensional (3D) information

The estimation of Para rubber tree height was obtained from the Canopy Height Model (CHM) and it was combined in the image classification layers. The CHM was estimated using the THAICHOTE stereo pair data. The Epipolar image, Digital Surface model (DSM) and Digital Terrain Model (DTM) were generated in this process. The 3D information generation is illustrated in Figure 3-6 and the steps of process are described as follows:

Figure 3-6 The processes of 3D information.

Firstly, the epipolar image was generated for setting the geometrical constraint between two frame images of a THAICHOTE stereo pair data. The Rational Polynomial Coefficients (RPCs) [47] and tie points obtained from the scale invariant feature transformation (SIFT) [49] were used for aligning the image orientation. SIFT was used for automatic tile point matching of the stereo pair data. The input parameters obtained from the THAICHOTE header file (sensor's model) were shown in Table 3-1. The focal length of 2,989 mm and camera lens pixel size of 0.0065 mm were used for calibrating the image.

Secondly, point cloud generation and image geocoding were used for the Digital Surface Model (DSM) generation. The point clouds (called depth information) were computed using the parallax equation [50]. Then, the DSM surface was interpolated using triangulated irregular network (TIN).

Finally, the CHM was generated from the different of height surface of Digital Surface Model (DSM) and Digital Terrain Model (DTM) was computed using the Equation (3-11):

$$CHM = DSM - DTM \quad (3-11)$$

where:

CHM	=	Canopy Height Model (m)
DSM	=	Digital Surface Model (m)
DTM	=	Digital Terrain Model (m)

The DTM was generated using the random point cloud (x, y, z) on the bare-ground surface. Without the areas of vegetation and human artifact, the inverse of Normalize Difference Vegetation Index (NDVI) was applied for extracting the point cloud. This process, the sparse points cloud was obtained. Therefore, the DTM surface was interpolated using inverse distance weighting method (IDW) [51].

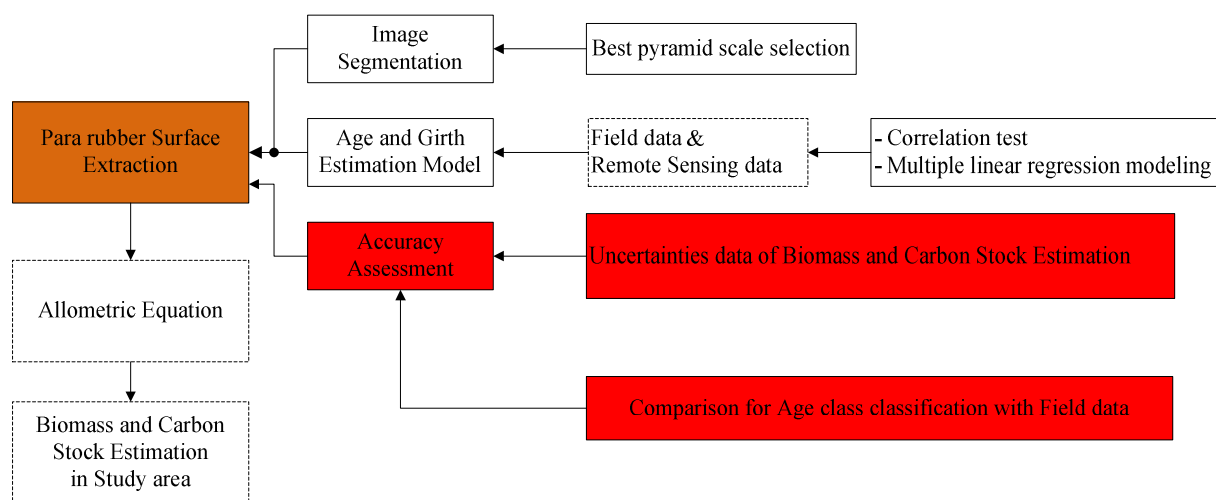
3.4.4 Mask information

The study used the NSDI (Thai National Spatial Data Infrastructure) GIS database 2011 obtained by the Geo-Informatics and Space Technology Development Agency (GISTDA, Thailand) to extract the Para rubber plantation areas and evaluate the areas not concerned by the study that the processes are: (1) the urban areas, other agricultural, natural forest areas and road were selected for build mask information, (2) the mask database was map referenced to the UTM WGS84, Z48, (3) the localization of bare soil and water bodies was evaluated by inverse of Normalized Different vegetation Index (NDVI). These areas were masked on the THAICHOTE pan-sharpened image.

3.5. Para rubber plantation Surface Extraction

The Object Based Image Analysis (OBIA) was used to classify the Rubber tree canopy properties (eg. reflectance data, texture data). Two results were extracted from image classification and modeling which are a map of the plantations and an estimation of girth and age of trees of each plantation. The map of plantation was realized using an image segmentation process. The girth and age of trees of each plantation were estimated from a linear regression equation build from the relationships between field data and image characteristics measured at the emplacement where field data were acquired. Finally, the results of biomass and carbon stock estimation over the Mae num Prasae watershed were calculated using the integration of Para rubber plantation surface map, Field data and Allometric equation. The Para rubber Surface Extraction illustrated in Figure 3-7.

Figure 3-7 The processes of Para rubber surface extraction.



This study process are described as follows:

3.5.1 Image Segmentation

Para rubber plantation limits (plantation boundaries) were extracted automatically from image multi-scale segmentation [52, 53] on THAICHOTE data. The results of multi scale segmentation were tested by empirically visualization [54] to find a suitable compromise

between precision and generalization. Therefore, the total number of tree was estimated by GIS area calculation from the tree density of plantations. The multi-scale segmentation shown in Equation (3-12):

$$E(\lambda) = D + \lambda \cdot C \quad (3-12)$$

where:

$E(\lambda)$	=	Multi-scale segmentation
D	=	Goodness of fit
λ	=	Pyramid scale
C	=	Complexity of the segmentation

The uncertainty data of Para rubber surface (plantation limit) was computed using the comparison of limit between manual digitization and multi-scale segmentation.

3.5.2 Para rubber Age class and Girth Estimation

Values of the various vegetation and textural indexes were extracted on the position of each plot measured in the field. From that data set using a multiple linear regression model, a set of linear equations relating the girth of tree and the characteristics of the layers was extracted in the form of the Tree Girth Model (called TGM). The confidence in this equation has been analyzed using Pearson's correlation coefficient. TGM was generated using linear multiple regression stepwise method for predicting tree girth and tree age. The tree girth is a function from multi-parameterization of spectral and textural information. The Pearson's correlation and TGM equations shown in Equation (3-13, 3-14):

- Pearson's correlation

$$r = \frac{S_{XY}}{\sqrt{S_{XX}S_{YY}}} \quad (3-13)$$

where:

r	=	Pearson's correlation
S_{XY}	=	Sum of the cross-products

$$S_{XX}, S_{YY} = \text{Sum of square of the X and Y values}$$

- Tree Girth Model (TGM)

$$Y = a + [b_1X_1 + b_2X_2 \dots + b_nX_n] \quad (3-14)$$

where:

Y = Tree girth (m)

a = Constant

b₁ to b_n = Coefficients of image parameters

X₁ to X_n = Image parameters (from spectral and textural indexes)

These parameters was applied the mean value of each plot using GIS zonal operation. The input dataset was shown in Appendix A.3.

The Equation (3-14) was used to estimate the girth of trees of each plantation delineated at the segmentation step. Knowing the surface of the plantations and the age of the plantation, the biomass of each plantation was calculated from the allometric equations (equation 3-1). Carbon stock was estimated using the conversion factor and carbon sequestration of Equations (3-2, 3-3).

The root mean square error (RMSE) and mean absolute percentage error (MAPE) were used to evaluate the model accuracy. These statistics was shown to Equation (3-15, 3-16). Additionally, the uncertainties data of the TGM was computed using root mean square error (RMSE), (Equation 3-15). Therefore, the total uncertainty of biomass and carbon stock estimation were combined using the uncertainty of Para rubber surface and the uncertainty of TGM.

- Root Mean Square Error (RMSE)

$$RMSE = \sqrt{\sum \left(\frac{Y_t - F_t}{n} \right)^2} \quad (3-15)$$

where:

RMSE	=	Root mean square error
Y_t	=	Reference observation for time period t
F_t	=	Predict for the same period
n	=	Time periods

- Mean Absolute Percentage Error (MAPE)

$$MAPE = \frac{1}{n} \sum_{t=1}^n \left| \left(\frac{Y_t - F_t}{Y_t} \right) \times 100 \right| \quad (3-16)$$

where:

MAPE	=	Mean absolute percentage error
Y_t	=	Reference observation for time period t
F_t	=	Predict for the same period
n	=	Time periods

3.5.3 Accuracy Assessment

The confusion matrix and kappa index [54] were employed to determine the accuracy of Para rubber tree age class map obtained by object based classification. The accuracy assessment manipulated using the combination of reference data and predict data. The confusion matrix and kappa index were shown in equation (3-17, 3-18).

- Overall Accuracy

$$Overall\ Accuracy = \left(\frac{\text{sum of major diagonal tاییies}}{\text{total number of samples}} \right) * 100 \quad (3-17)$$

- Kappa index

$$\hat{K} = \frac{N \sum_{i=1}^k X_{ii} - \sum_i^k (X_{i+} * X_{+i})}{N^2 - \sum_{i=1}^k (X_{i+} * X_{+i})} \quad (3-18)$$

where:

\hat{K}	=	Points in rows or types of land utilization and land cover
X_{ii}	=	Oblique points in of Row i and Column i
X_{i+}	=	All points in Row i
X_{+i}	=	All points in Column i
N	=	Total points

Denote : descriptive, $\hat{K} < 0$ Less than chance agreement, 0.01–0.20 Slight agreement, 0.21– 0.40 Fair agreement, 0.41–0.60 Moderate agreement, 0.61–0.80 Substantial agreement, 0.81–0.99 Almost perfect agreement.

RESULTS

&

DISCUSSION

CHAPTER IV

RESULTS AND DISCUSSION

The results following by: field data, ground biomass and carbon stock estimation are first explored. Secondly, the THAICHOTE image is calibrated. Then, the image classification, Para rubber surface extraction and biomass and carbon estimation are described. Finally, the consequences of the results of biomass and carbon estimation over the Mae num Prasae watershed are explored. Therefore, the results of this study are discussed.

4.1 Field data

A total sample 500 plots of Para rubber plantation were collected in the study area (from December 2011 to April 2012) (Figure 4-1). The relationship obtained from tree age and girth was shown to strongest than tree height with correlation R^2 of 0.95 and 0.86 respectively (Figure 4-2). The highest girth was shown on the tree age 25 years old (90 cm) while the lowest girth is shown on the tree age 4 years old (32 cm). The tree height was shown maximum to 26 m on age 25 years while shown minimum to 7 m on age 4 years. The Para rubber plantations in the study area were clustered to young age class (4 to 12 years old) was less than 53 cm while middle age class (12 to 18 years old) was 53 to 65 cm and old age class (> 18 years old) was more than 65 cm. The Para rubber plantation statistics show in Table 4-1. Cultivation of the Para rubber plantation has a traditional spatial distribution. Trees are spaced of 3 m on lines spaced of 7 m (Figure 4-3). Thus, the density of Para rubber plantation is averaged to around 475 trees.ha⁻¹.

Figure 4-1 The Mae num Prasae watershed on THAICHOTE satellite data (yellow boundary). The field data shown in green dots with UTM WGS 1984 Zone 48.

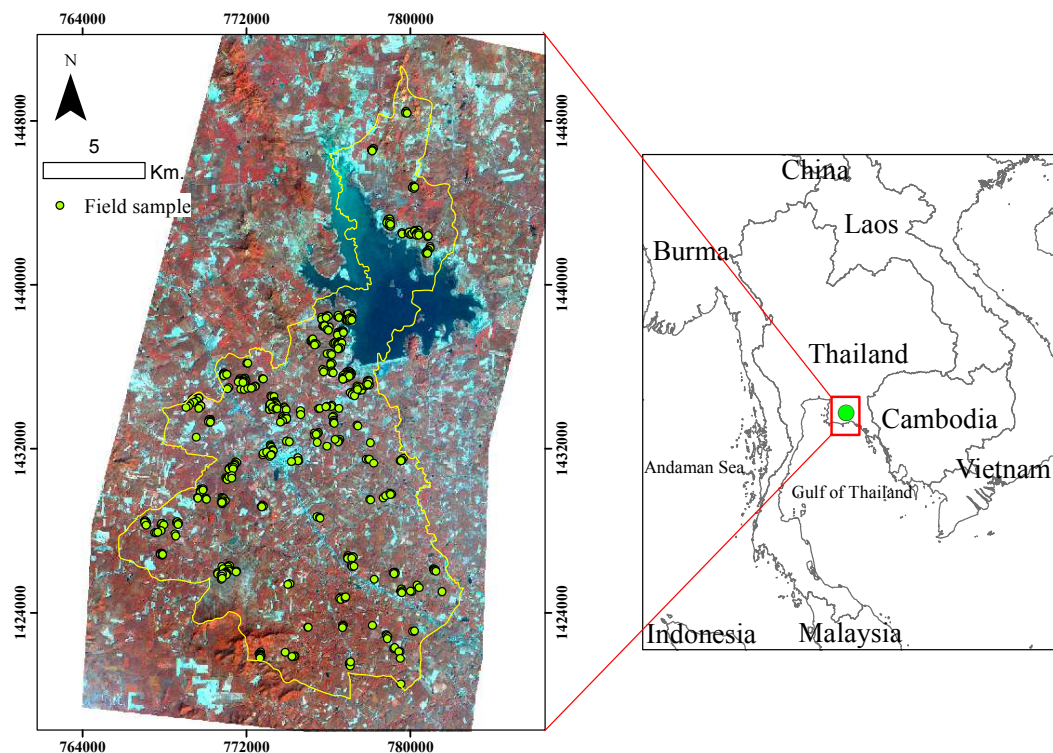


Figure 4-2 The relationships of tree age, girth and height.

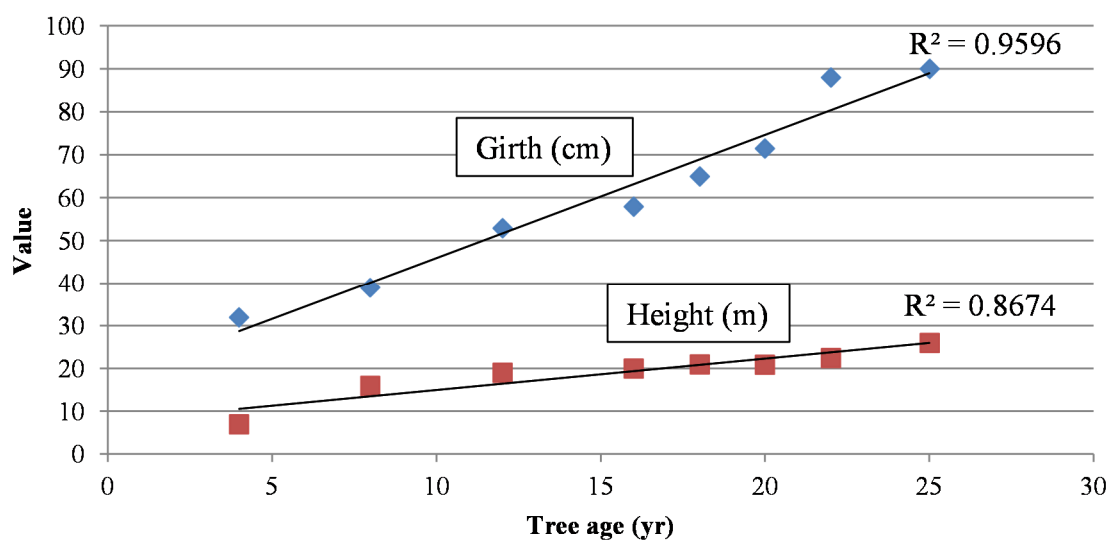


Table 4-1 Field data collected from December 2011 to April 2012: view from ground and view from THAICHOTE satellite data (band composite RGB:NIR, Red, Green) for the Para rubber ages used in this study.

Age (yr)		Girth (cm)	Height (m)
Young	4	32 (+/-6.5)	7 (+/-2)
	8	39 (+/-1.6)	16 (+/-2)
	12	53 (+/-4.26)	19 (+/-2.5)
Middle	16	58 (+/- 1)	20 (+/-3)
	18	65 (+- 3.2)	21 (+- 3.5)
Old	20	71.50 (+-2.7)	20.9 (+-3)
	22	88 (+-4.5)	22.5 (+-4)
	25	90 (+- 2)	26 (+-4)







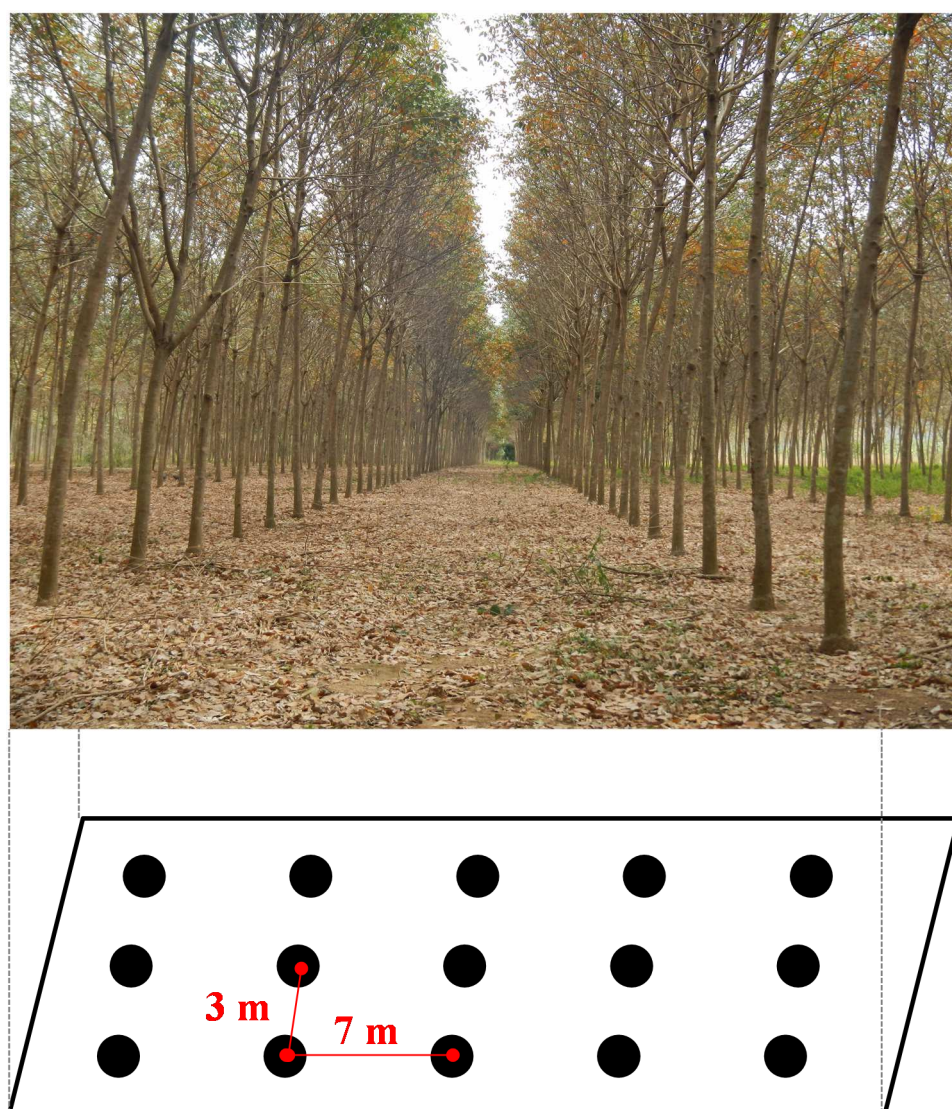
Age class	View from ground	THAICHOTE satellite data
(a) Young Age 4-12 years, Girth < 53 cm, Number of sample 117 plots		
(b) Middle Age 12-18 years, Girth 53 – 65 cm, Number of sample 28 plots		
(c) Old Age >18 years, Girth > 65 cm, Number of sample 355 plots		

Figure 4-3 Planting layout of Para rubber plantation in study area.

4.2 Ground Biomass and Carbon Stock Estimation

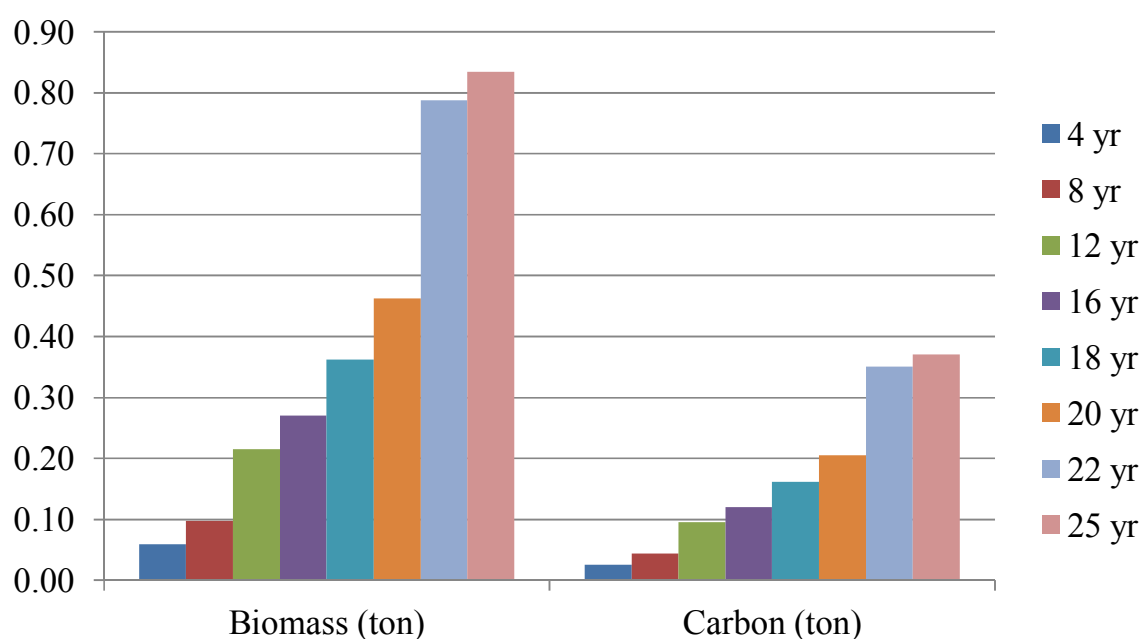
The estimation of a single tree stand biomass and carbon stock was used the allometric Equation (3-1), the Para rubber tree age at 25 years old is shown to have a maximum of biomass and carbon stocked (0.83 t, 0.37 tC) while a 4 years old is shown to have a minimum of biomass and carbon stocked (0.06 t, 0.03 tC). The Para rubber tree age 8, 12, 16, 18, 20 and 22 years old are stocked the biomass and carbon of (0.1 t, 0.04 tC), (0.21 t, 0.1 tC), (0.27 t, 0.12 tC), (0.36 t, 0.16 tC), (0.46 t, 0.21 tC) and (0.79 t, 0.35 tC) respectively. The rate of

carbon sequestration, biomass and carbon stock obtained by a single tree stand are shown in Table 4-2 and Figure 4-4.

Table 4-2 The rate capacity of carbon sequestration, biomass and carbon stock obtained by single tree stand of Para rubber tree.

Class	Age (yr)	Biomass (ton)	Carbon (ton)
Young	4	0.06	0.03
	8	0.10	0.04
	12	0.21	0.10
Middle	16	0.27	0.12
	18	0.36	0.16
Old	20	0.46	0.21
	22	0.79	0.35
	25	0.83	0.37

Figure 4-4 The biomass and carbon stocked in single tree of Para rubber.



4.3 THAICHOTE Satellite Image

THAICHOTE satellite image of 2 m spatial resolution was corrected radiometry using COST model. The reflectance of 1% was assumed to compensate the image. The statistical of THAICHOTE data were listed in Table 4-3. In data distribution, every single bands shown to slightly peak kurtosis (normal peak = 3) while they skewness are seem to normal distributed. THAICHOTE natural color (R, G, B) and false color (NIR, G, B) images were shown in Figure 4-5 and 4-6.

Table 4-3 Statistical of THAICHOTE satellite data. It was corrected radiometry using COST model (reflectance data)., SD = Standard deviation.

Wavelength	Min	Max	Mean	SD	Skewness	Kurtosis
Blue	0	0.2550	0.0539	0.0375	-0.108	4.361
Green	0	0.4299	0.0833	0.0590	0.081	4.182
Red	0	0.6087	0.1259	0.0929	0.5	3.660
NIR	0	0.8698	0.2227	0.1626	-0.185	4.178

Figure 4-5 THAICHOTE satellite natural color (R, G, B) image corrected. The UTM WGS 1984 Zone 48 was referenced.

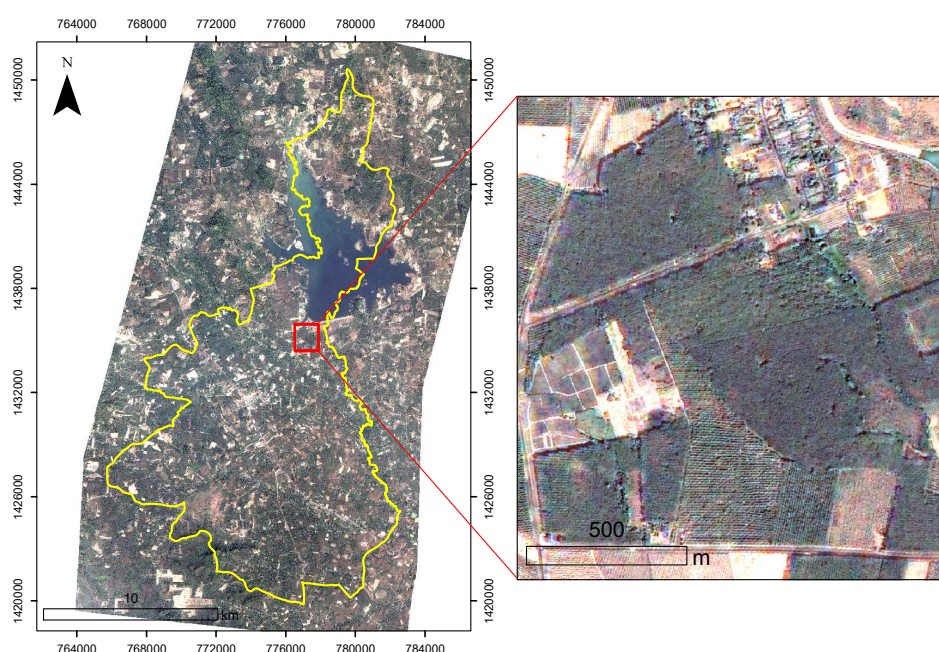
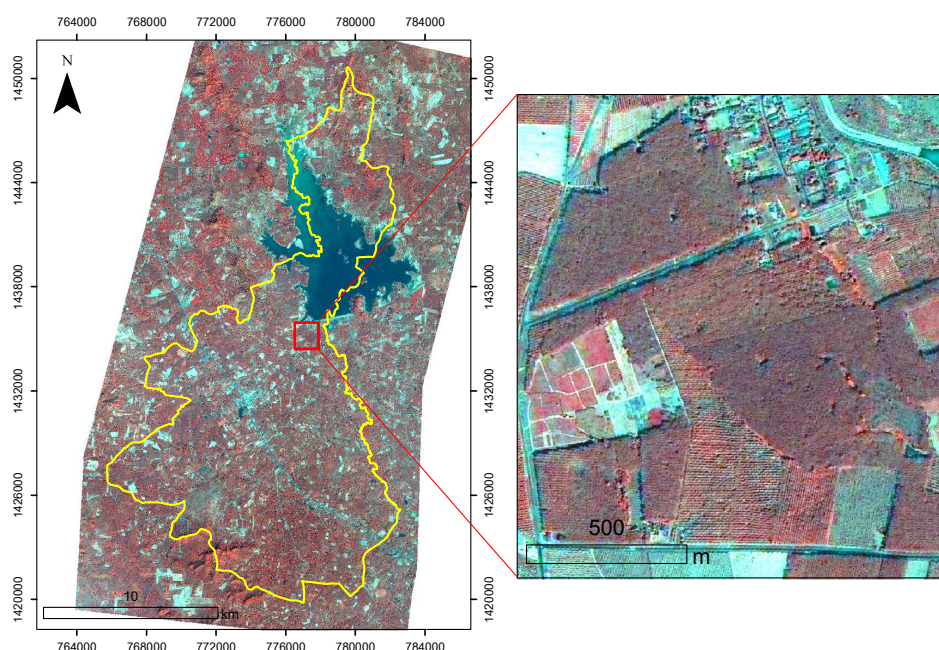


Figure 4-6 THAICHOTE satellite false color (NIR, G, B) image corrected. The UTM WGS 1984 Zone 48 was referenced.



Water, vegetation and bare soil were tested according to the reflectance of THAICHOTE image (Table 4-4, Figure 4-7). NIR band obtained from THAICHOTE image corrected was changed to high direction according to the vegetation and bare soil. The spectral signatures obtained from the reflectance of THAICHOTE non-corrected and corrected radiometry were shown in Figure 4-8, 4-9.

Table 4-4 The rate of carbon sequestration, biomass and carbon stock obtained by individual tree stand of Para rubber tree., Veg.1-3 is vegetation area 1-3.

Object	Blue		Green		Red		NIR	
	Non-Corrected	Corrected	Non-Corrected	Corrected	Non-Corrected	Corrected	Non-Corrected	Corrected
Water	97.41	0.08	77.22	0.11	85.24	0.14	33.27	0.10
Veg. 1	98.00	0.08	83.08	0.11	97.77	0.17	96.49	0.32
Veg. 2	95.95	0.07	79.61	0.11	92.79	0.16	95.87	0.31
Veg. 3	98.34	0.08	85.64	0.12	100.14	0.17	106.25	0.35
Bare soil	149.09	0.12	152.51	0.22	236.88	0.42	130.33	0.43

Figure 4-7 The sample reflectance data in the study area obtained by THAICHOTE image (a). non-corrected radiometry and (b). corrected radiometry.

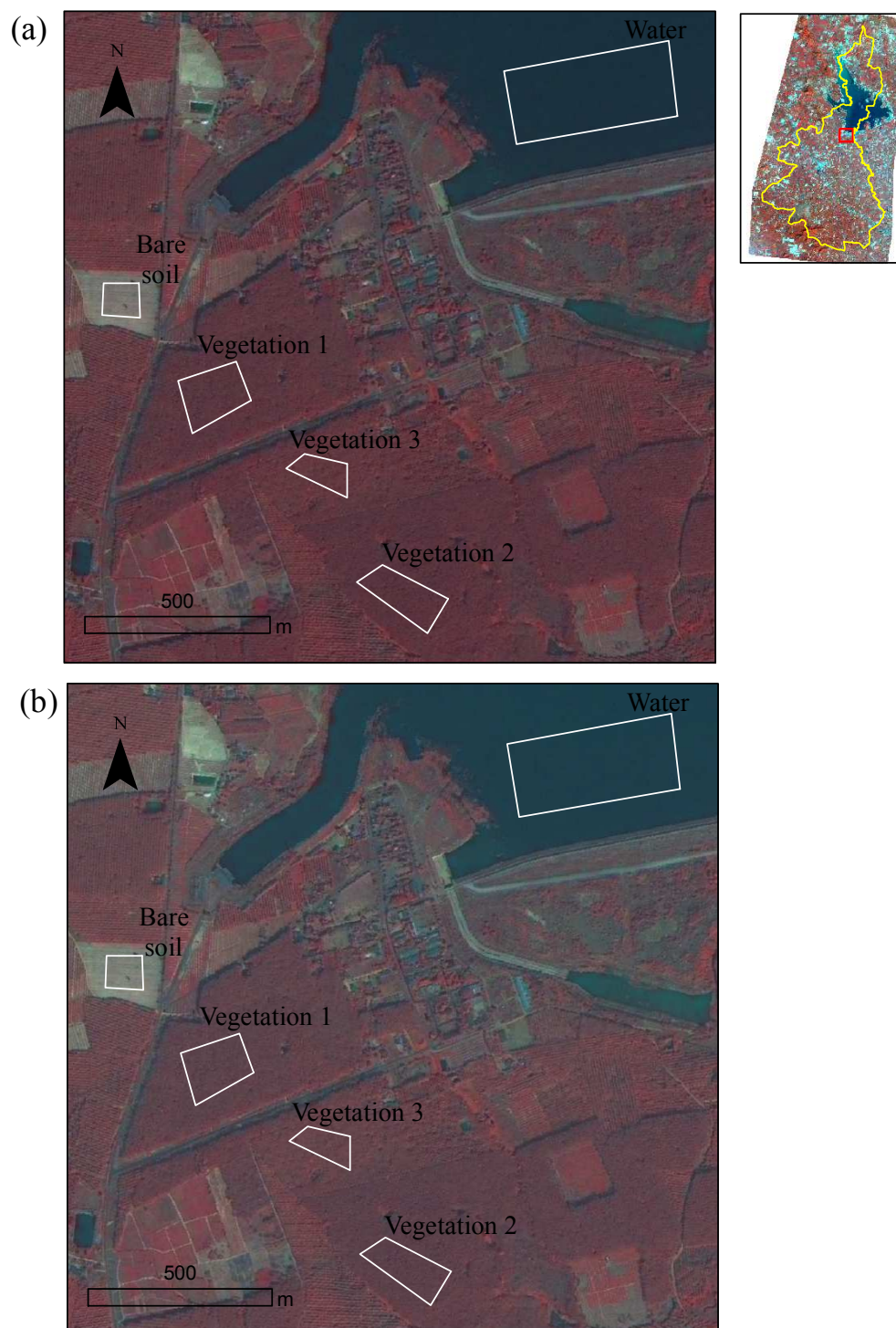


Figure 4-8 The spectral signature obtained by THAICHOTE satellite image non-corrected according to Water, Vegetation and Bare soil object.

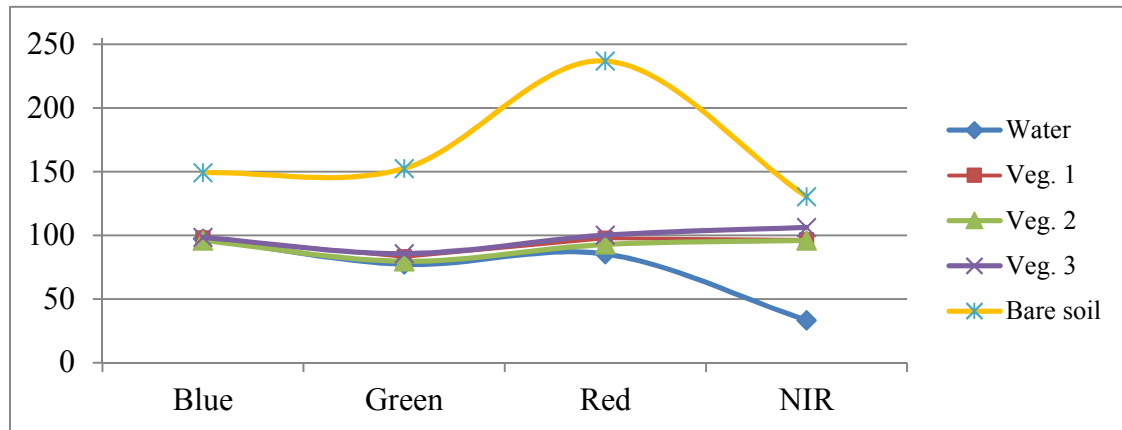
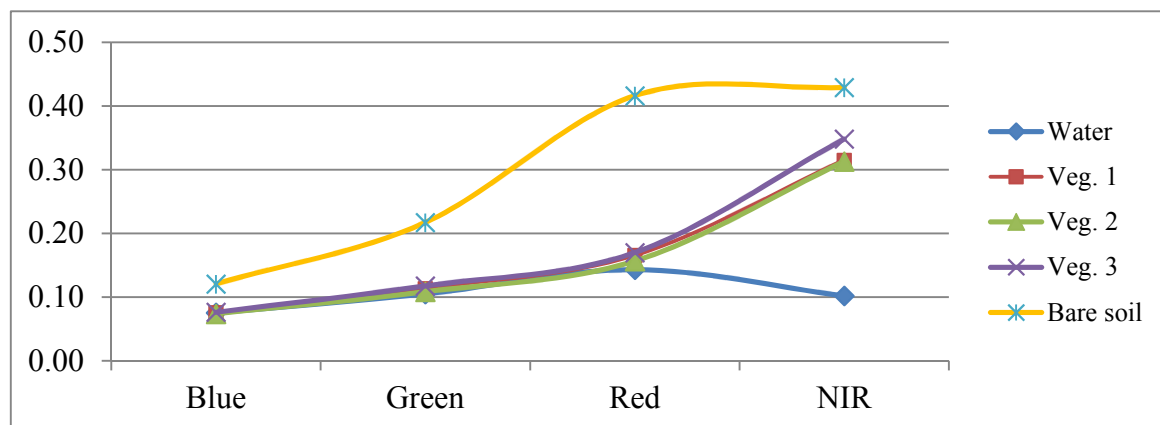


Figure 4-9 The spectral signature obtained by THAICHOTE satellite image corrected according to Water vegetation and bare soil object.



4.4 Image Classification

An 17 layers were computed in the image classification information of this study. Four single bands and five vegetation indexes were integrated in the spectral information. The vegetation indexes were computed using map algebra in Red and NIR bands ration. The spectral information was listed in Table 4-5 and sample layers were shown in Figure 4-10 to 4-12. The 8 texture indexes of textural information were computed using GLCM method. The textural information was listed in Table 4-5 and sample layers were shown in Figure 4-13 to 4-14.

In 3D information, the digital surface model (DSM) and digital terrain model (DTM) were first computed using THAICHOTE stereo pair data. DSM was shown a maximum height surface of 220 m and DTM was shown a maximum height surface of 195 m. The canopy height model (CHM) was not appropriated to build the image classification information for estimating the Para rubber biomass and carbon stock. The mean absolute percentage error (MAPE) was shown to 74% when compare the tree height data from field. 3D information were shown in Figure 4-15 and 4-16.

Additionally, the GIS database obtained by NSDI (Thai National Spatial Data Infrastructure) was evaluated to the mask information. The areas not concerned by the study were masked using urban areas, natural forest areas and other agricultural crops. Thus, the total surface of Para rubber plantation is shown to 154.34 km².

Table 4-5 Statistical of image classification layers obtained by spectral and textural information, For Spectral information: ARVI is Atmospherically Resistant Vegetation Index, GEMI is Global Environment Monitoring Index, IPVI is Infrared Percentage Vegetation Index, MSAVI2 is Modified Soil Adjusted Vegetation Index2 and NDVI is Normalized Difference Vegetation Index. For textural information (GLCM): CON is Contrast, DIS is Dissimilarity, HOM is Homogeneity, ASM is Angular second moment, ENT is Entropy, MEAN is Mean, VAR is Variance and COR is Correlation.

Image Classification Layer	Min	Max	Mean	SD
ARVI	-0.668	0.679	0.09	0.15
GEMI	-0.611	0.699	0.187	0.237
IPVI	0.042	0.928	0.632	0.079
MSAVI2	0.167	0.85	0.427	0.138
NDVI	-0.527	0.762	0.182	0.18
CON	0	18.8	2.413	2.846
DIS	0	9.47	0.9	0.746
HOM	0	1	0.662	0.249
ASM	0	1	0.374	0.43
ENT	0	5	2.02	1.474
MEAN	0	28.32	8.321	5.64
VAR	0	7.4	1.16	2.2
COR	-16.37	62.51	-2.64	35.44

Figure 4-10 Example layers of Spectral information (Single bands)., (a) Blue., (b) Green., (c) Red., (d) NIR., (z) THAICHOTE false color image (NIR, G, B).

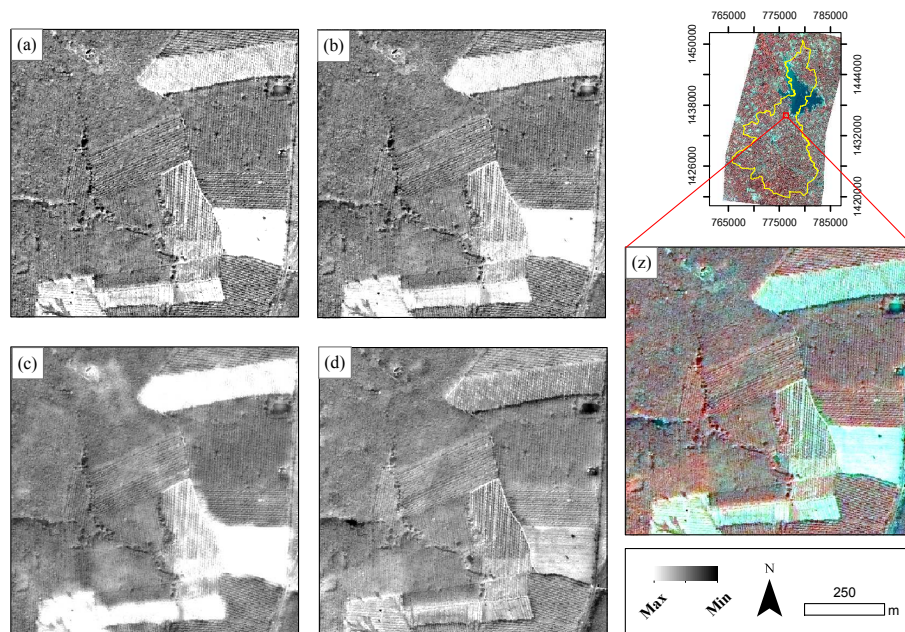


Figure 4-11 Example layers of Spectral information (Vegetation indexes)., (a) ARVI., (b) GEMI., (c) IRVI., (d) MSAVI2., (z) THAICHOTE false color image (NIR, G, B).

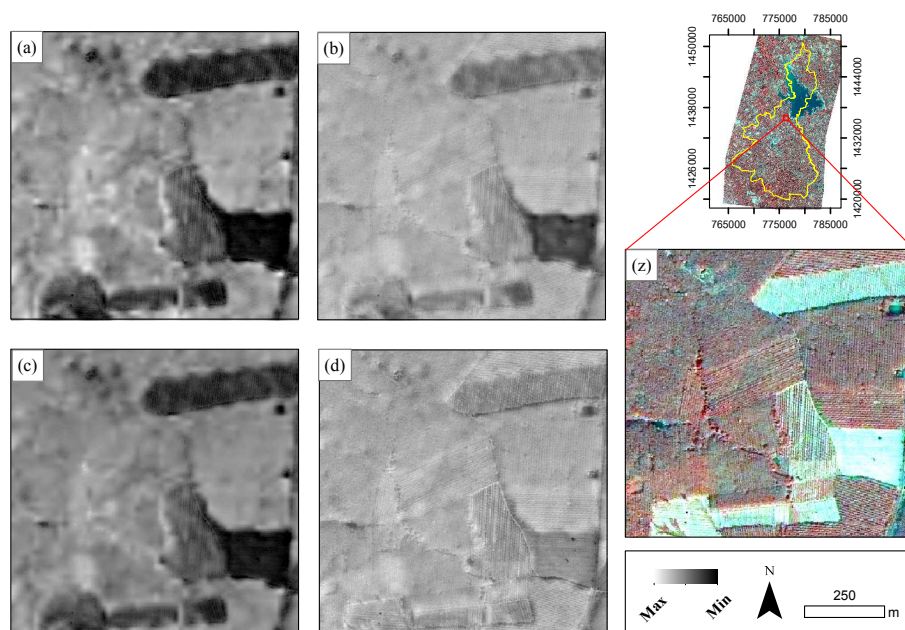


Figure 4-12 Example layers of Spectral information (Vegetation indexes)., (e) NDVI., (z) THAICHOTE false color image (NIR, G, B).

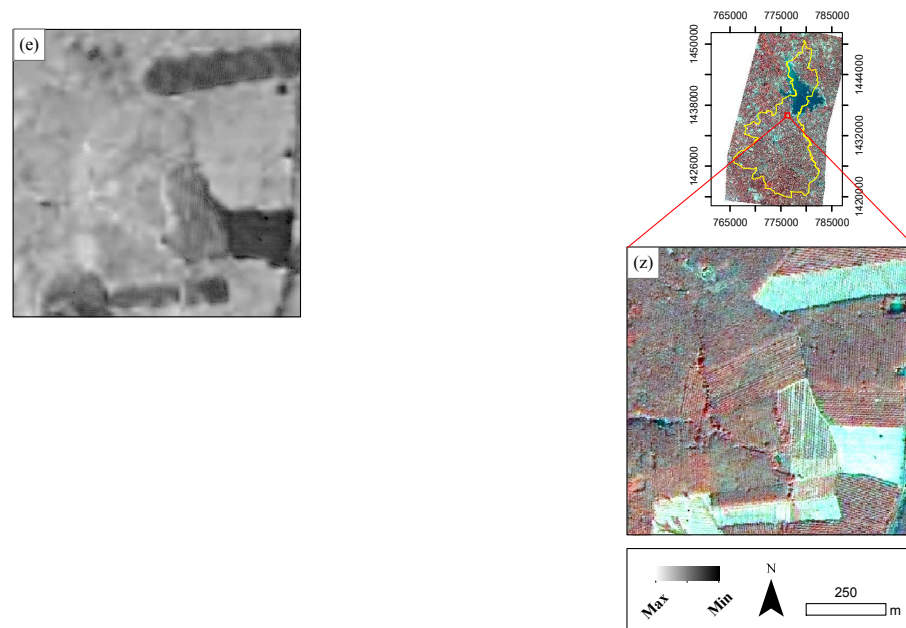


Figure 4-13 Example layers of Textural information (Texture measures)., (a) CON., (b) DIS., (c) HOMO., (d) ASM., (z) THAICHOTE false color image (NIR, G, B).

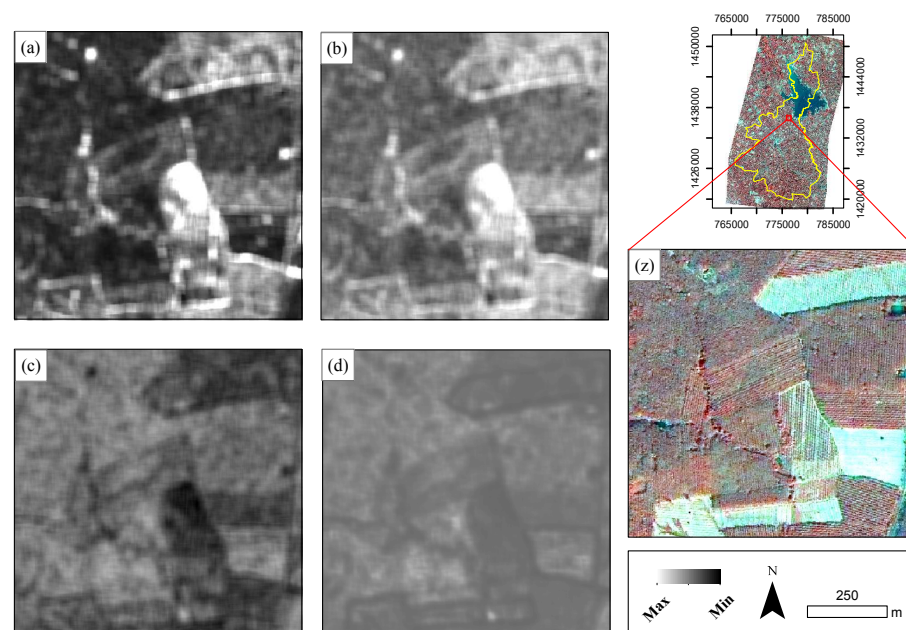


Figure 4-14 Example layers of Textural information (Texture measures)., (e) ENT., (f) Mean., (g) Var., (h) Cor., (z) THAICHOTE false color image (NIR, G, B).

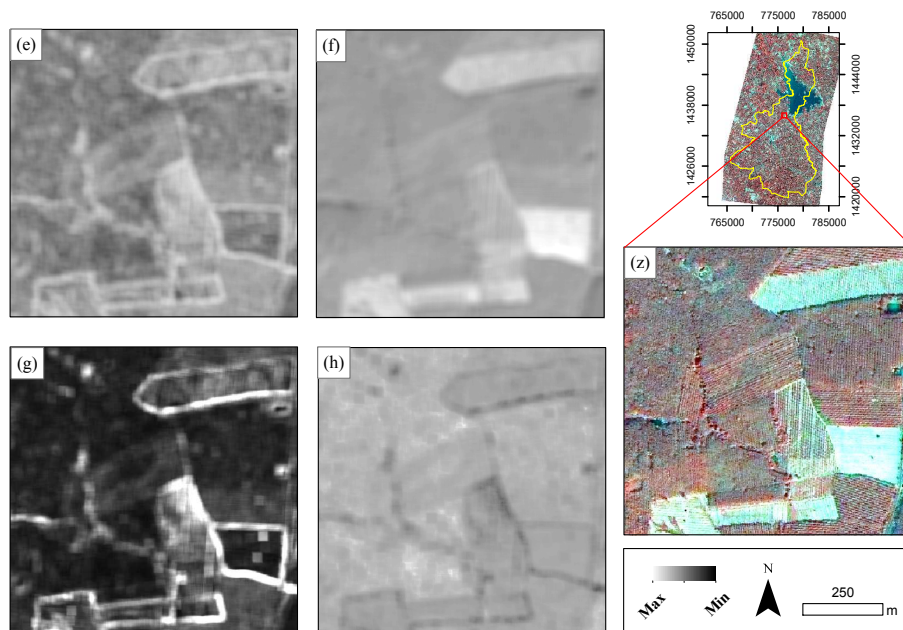


Figure 4-15 Example images of THAICHOTE stereo pair data., (a) Forward acquired (along -37.471443° , across 21.013978°), (b) Backward acquired (along 35.521264° , across 21.101122°).

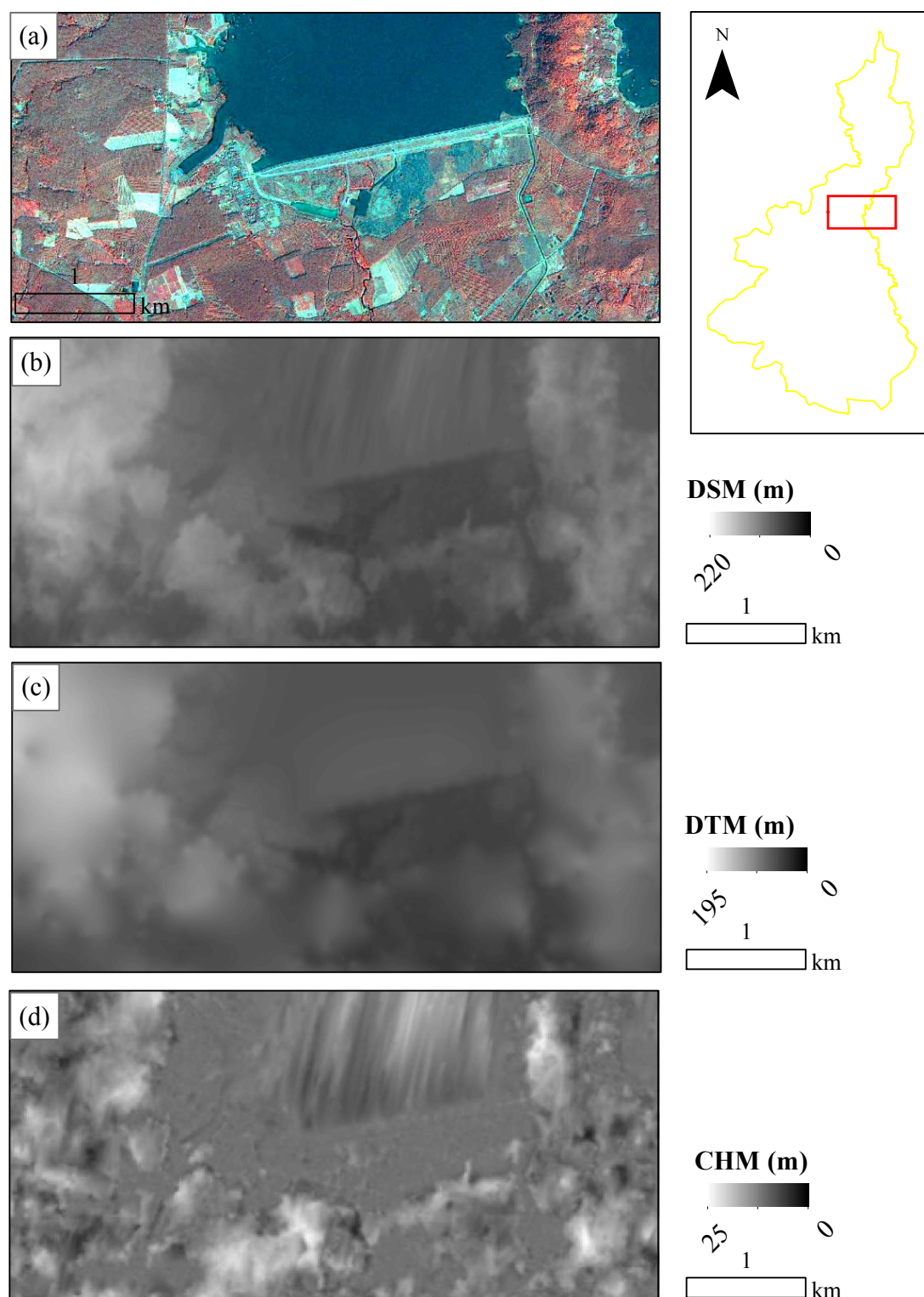
(a)



(b)



Figure 4-16 Example layers of 3D information., (a) THAICHOTE false color image (NIR, G, B)., (b) Digital Surface Model (DSM)., (c) Digital Terrain Model (DTM), (d) Canopy Height Model (CHM).



4.5 Map of Para rubber plantation limit

Ten thousand and sixty nine Para rubber plantations were identified with a maximum surface of 0.23 km² and a minimum surface of 1,600 m² while, the mean surface was 15,329 m². Figure 4-17 shows a sample of the map of Para rubber plantations obtained from the image segmentation process. The uncertainty of Para rubber plantation surface was calculated from comparison of multi scale segmentation and manual digitization (Figure 4-18). The total surface of plantation is 154.34 km² with an uncertainty of 11% (+/- 17 km²). The number of Para rubber tree stand was calculated using the constant value for 475 trees ha⁻¹ obtained by field measurement. Thus, the total number of tree stand is approximately of 7,321,444 trees (+/- 802,832 trees).

Figure 4-17 Example map of Para rubber plantations extracted from the multi-scale segmentation. Yellow polygon is Para rubber plantation limits.

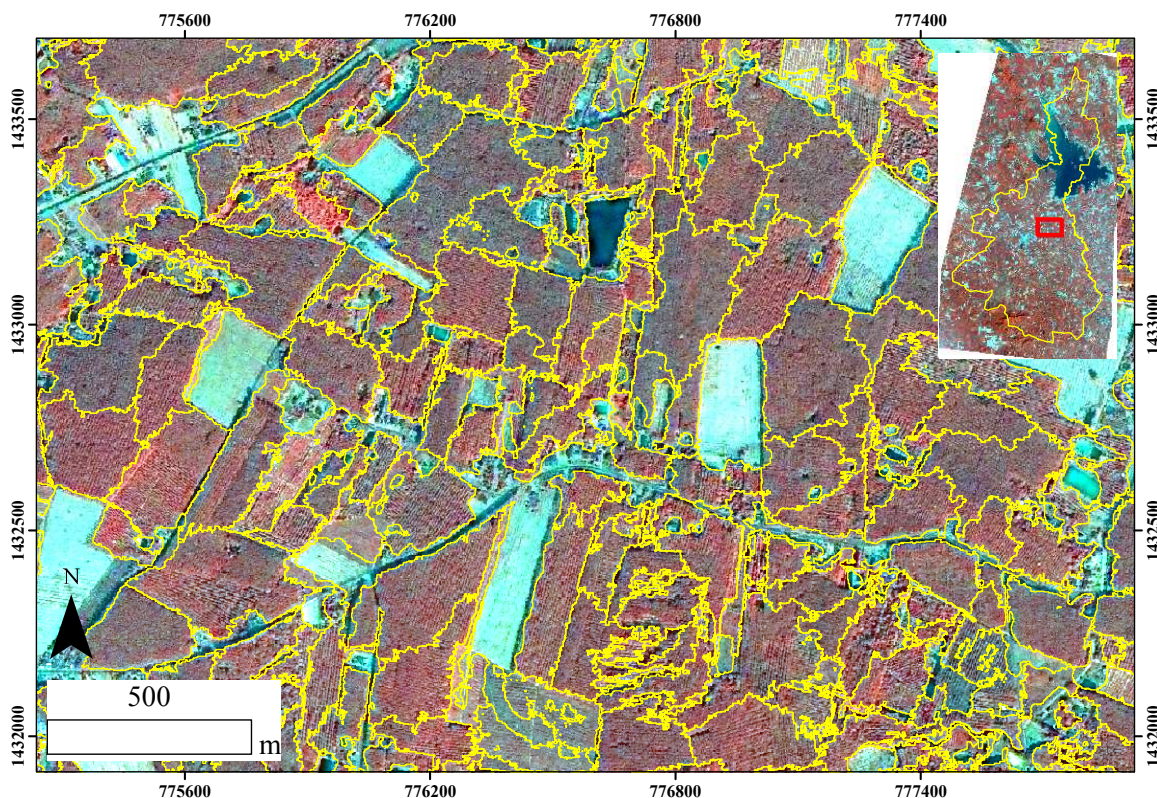
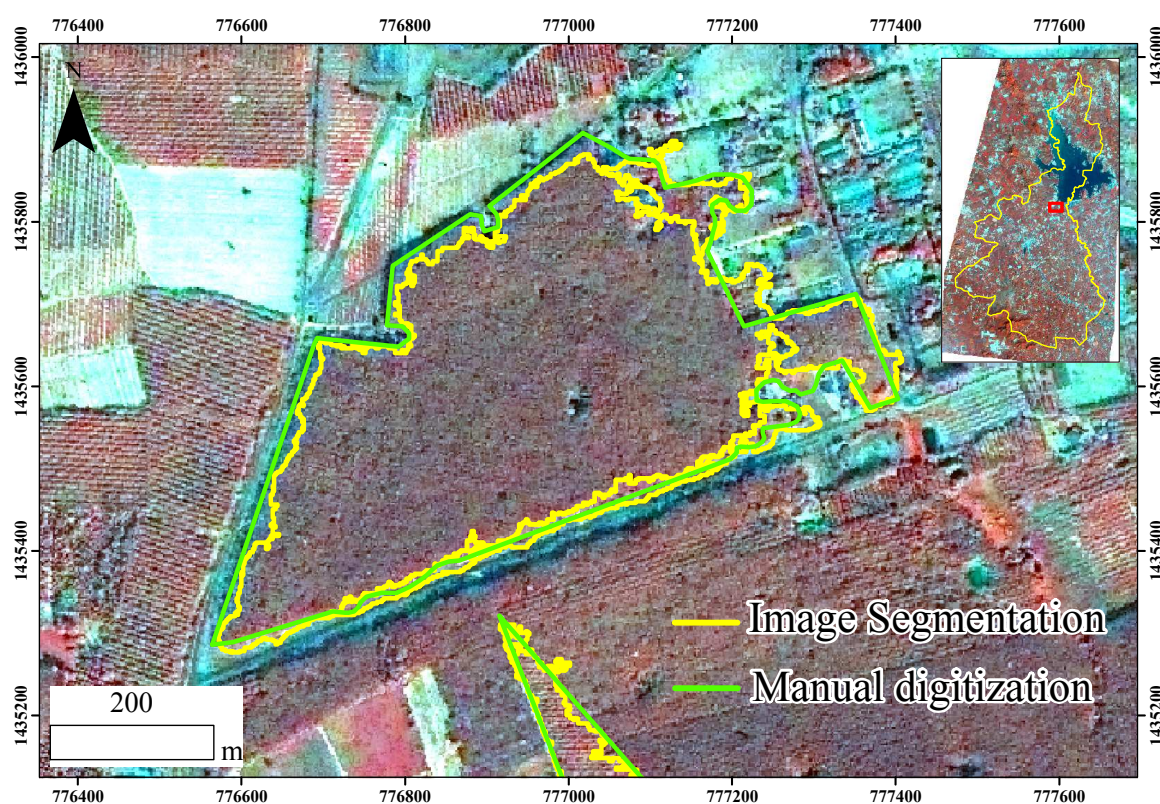


Figure 4-18 Example map of Para rubber plantations limit extracted from the multi-scale segmentation (Yellow polygon) and the manual digitization (Green polygon).



4.6 Tree girth model (TGM) and Para rubber tree Classification

Table 4-6a and 4-6b shows statistics of image characteristics measured (17 layers) at the emplacement where field data were acquired (see in Figure 4-1) association to the girth and age of trees of each plantation. In mean, the spectral layers were slightly differentiated value while the texture layers were extremely differentiated value of each age class. In the textural information, Young age class was shown to the highest value of CON, DIS and VAR while Old age class was shown to lowest. The data distribution is described by frequency histogram on the skewness and kurtosis using mean. Most cases, the kurtosis value was shown to higher than 3.00 (normal distribution). Young age class, maximum skew was shown in CON (1.44) while minimum was shown in COR (-1.93) and maximum kurtosis was shown in COR while minimum was shown in HOM. Middle age class, maximum skew was shown in Red (1.17) while minimum was shown in COR (-1.26) and maximum kurtosis was shown in

COR while minimum was shown in ASM (1.92). Old age class, maximum skew was shown in CON (1.3) while minimum was shown in IPVI (-1.73) and maximum kurtosis was shown in IPVI (12.66) or highest value of all while minimum was shown in ARVI (2.48). Figure 4-19 shown the graphics obtained from mean, skewness and kurtosis of the image classification layers of each age class of Para rubber plantation. Additionally, the graphics of frequency histogram are shown in appendix (Figure 3A-1).

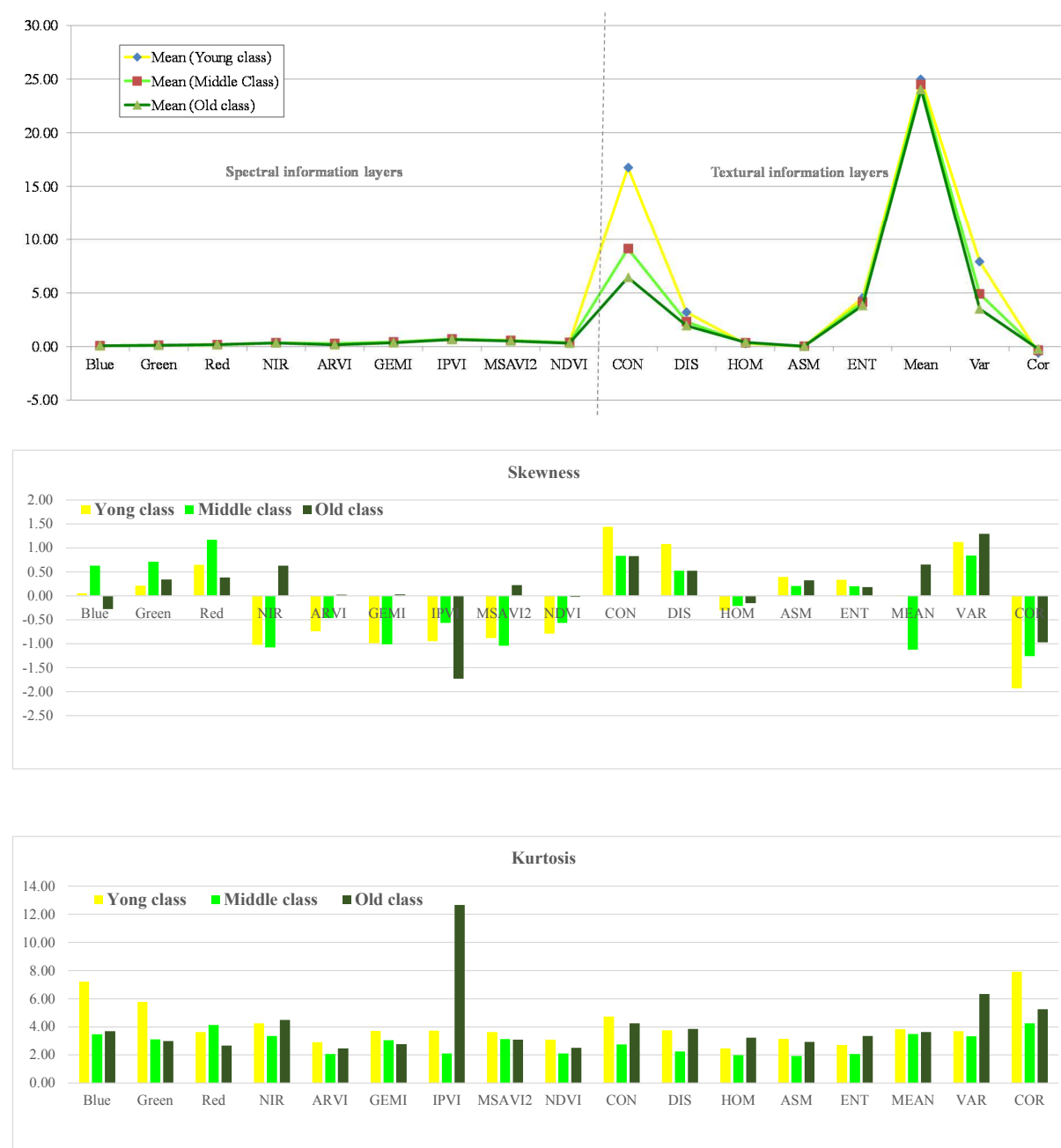
Table 4-6a Statistical of image characteristics measured at the emplacement where field data were acquired association to the girth and age of trees of each plantation (Min, Max, Mean, Standard deviation (SD)). For Spectral information : ARVI is Atmospherically Resistant Vegetation Index, GEMI is Global Environment Monitoring Index, IPVI is Infrared Percentage Vegetation Index, MSAVI2 is Modified Soil Adjusted Vegetation Index2 and NDVI is Normalized Difference Vegetation Index. For textural information (GLCM) : CON is Contrast, DIS is Dissimilarity, HOM is Homogeneity, ASM is Angular second moment, ENT is Entropy, MEAN is Mean, VAR is Variance and COR is Correlation.

Layer	Young class				Middle class				Old class			
	Min	Max	Mean	SD	Min	Max	Mean	SD	Min	Max	Mean	SD
Blue	0.06	0.09	0.08	0.00	0.07	0.08	0.08	0.00	0.07	0.08	0.08	0.00
Green	0.10	0.14	0.12	0.01	0.11	0.12	0.11	0.00	0.11	0.13	0.12	0.00
Red	0.13	0.22	0.17	0.01	0.15	0.17	0.16	0.01	0.15	0.21	0.17	0.01
NIR	0.30	0.38	0.35	0.02	0.31	0.38	0.35	0.02	0.29	0.37	0.32	0.01
ARVI	0.05	0.33	0.23	0.06	0.21	0.31	0.27	0.03	0.06	0.29	0.16	0.05
GEMI	0.28	0.46	0.41	0.04	0.35	0.46	0.42	0.03	0.29	0.43	0.35	0.03
IPVI	0.61	0.72	0.68	0.02	0.66	0.71	0.69	0.01	0.47	0.70	0.65	0.02
MSAVI2	0.47	0.59	0.56	0.03	0.51	0.59	0.56	0.02	0.47	0.57	0.51	0.02
NDVI	0.21	0.43	0.36	0.05	0.33	0.41	0.38	0.02	0.22	0.40	0.30	0.04
CON	7.49	42.32	16.76	7.41	6.02	15.36	9.12	2.61	3.76	11.51	6.44	1.31
DIS	2.10	5.59	3.20	0.73	1.89	3.00	2.32	0.34	1.49	2.74	1.93	0.20
HOM	0.14	0.37	0.27	0.05	0.28	0.39	0.35	0.04	0.28	0.46	0.39	0.03
ASM	0.01	0.03	0.01	0.00	0.01	0.03	0.02	0.01	0.02	0.05	0.03	0.01
ENT	4.01	5.12	4.54	0.24	3.74	4.62	4.12	0.25	3.42	4.49	3.84	0.18
MEAN	23.53	26.83	24.99	0.52	22.73	25.58	24.50	0.72	22.58	26.03	24.04	0.65
VAR	3.96	15.36	7.92	2.75	2.98	8.85	4.90	1.41	1.99	7.43	3.51	0.84
COR	-2.02	-0.29	-0.61	0.29	-0.75	-0.20	-0.35	0.13	-0.58	-0.08	-0.23	0.07

Table 4-6b Statistical of image characteristics measured at the emplacement where field data were acquired association to the girth and age of trees of each plantation (Skewness and Kurtosis).

Layer	Young class		Middle class		Old class	
	Skewness	Kurtosis	Skewness	Kurtosis	Skewness	Kurtosis
Blue	0.05	7.22	0.63	3.48	-0.27	3.70
Green	0.22	5.77	0.71	3.11	0.34	2.99
Red	0.65	3.63	1.17	4.12	0.38	2.67
NIR	-1.03	4.25	-1.08	3.35	0.63	4.49
ARVI	-0.75	2.91	-0.47	2.06	0.02	2.48
GEMI	-0.99	3.70	-1.01	3.05	0.03	2.77
IPVI	-0.95	3.74	-0.57	2.10	-1.73	12.66
MSAVI2	-0.89	3.62	-1.04	3.13	0.23	3.08
NDVI	-0.79	3.09	-0.57	2.10	-0.02	2.52
CON	1.44	4.74	0.84	2.75	0.83	4.26
DIS	1.08	3.75	0.52	2.24	0.52	3.85
HOM	-0.31	2.48	-0.21	1.99	-0.15	3.24
ASM	0.40	3.14	0.21	1.92	0.33	2.92
ENT	0.34	2.72	0.20	2.08	0.18	3.35
MEAN	0.00	3.82	-1.12	3.49	0.65	3.62
VAR	1.12	3.70	0.84	3.34	1.30	6.34
COR	-1.93	7.91	-1.26	4.25	-0.97	5.26

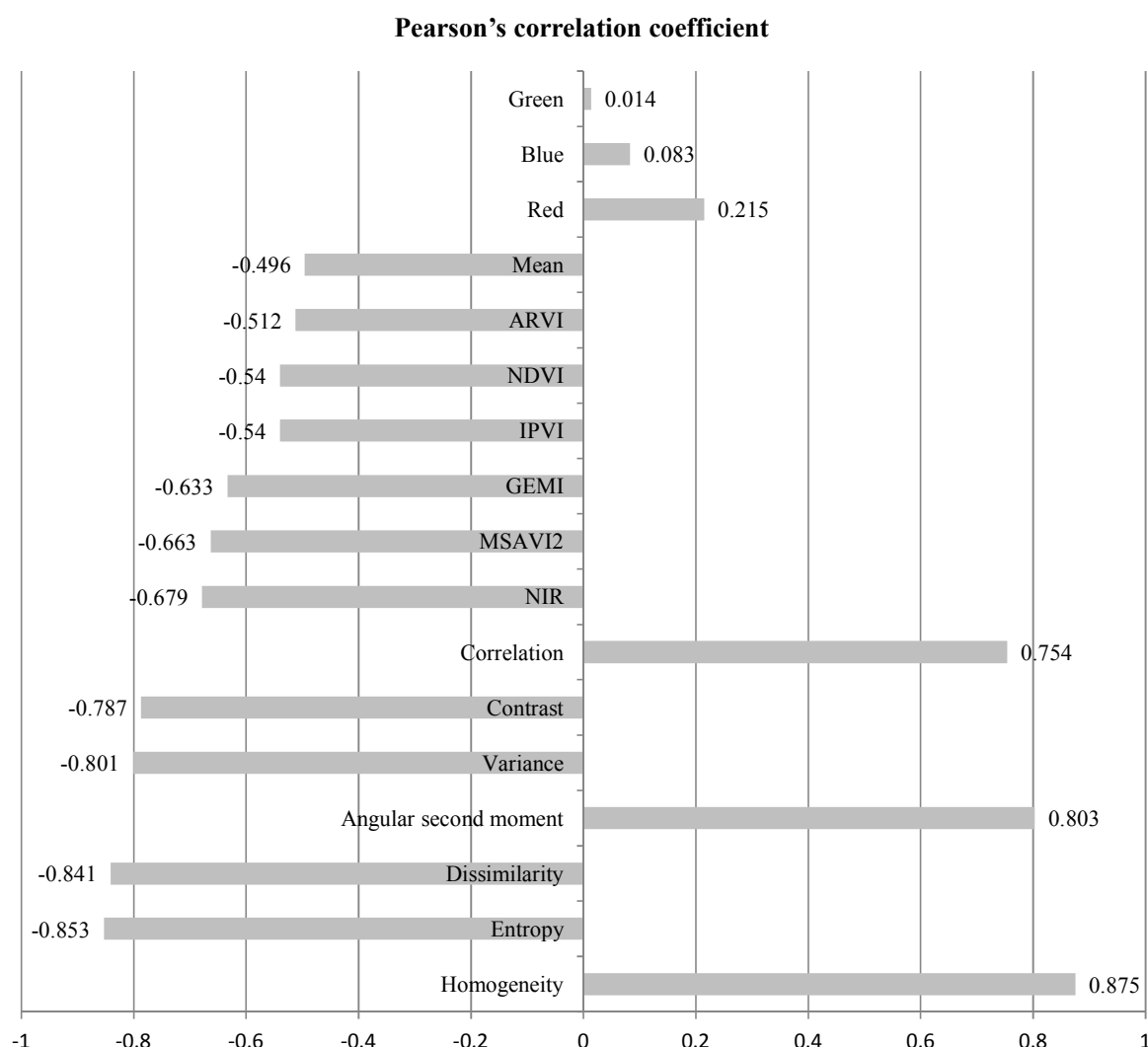
Figure 4-19 The graphics obtained from mean, skewness and kurtosis of the image classification layers of each age class of Para rubber plantation. Broadband vegetation indexes: NIR is near infrared band, ARVI is Atmospherically Resistant Vegetation Index, GEMI is Global Environment Monitoring Index, IPVI is Infrared Percentage Vegetation Index, MSAVI2 is Modified Soil Adjusted Vegetation Index2 and NDVI is Normalized Difference Vegetation Index. Texture measurement: GLCM CON is Contrast, DIS is Dissimilarity, HOM is Homogeneous, ASM is Angular second moment, ENT is Entropy, MEAN is Mean, VAR is Variance and COR is Correlation.



The correlation between tree girth and values of the different layers obtained from the remote sensing image was tested by Pearson's correlation. All the Parameters of texture and vegetation indexes were correlated to the tree girth (Table 4-7, Figure 20). The Homogeneity has the highest correlation with tree girth (0.875) while lowest is the Mean (-0.496). For vegetation index, MSAVI2 has the highest correlation with tree girth (-0.663) while ARVI has the lowest (-0.512). For the single bands of the satellite image, NIR (near infrared) is highest correlated with tree girth (correlation coefficient of -0.679).

Table 4-7 Pearson's correlation between tree girth and layer Parameters measured at field plot positions. Only the layers with an absolute value of correlation coefficient better than 0.4 were integrated in the final multi linear regression model.

Parameter	Pearson's correlation coefficient	Sig.
Homogeneity	0.875	0.000
Entropy	-0.853	0.000
Dissimilarity	-0.841	0.000
Angular second moment	0.803	0.000
Variance	-0.801	0.000
Contrast	-0.787	0.000
Correlation	0.754	0.000
NIR	-0.679	0.000
MSAVI2	-0.663	0.000
GEMI	-0.633	0.000
IPVI	-0.540	0.000
NDVI	-0.540	0.000
ARVI	-0.512	0.000
Mean	-0.496	0.000
Red	0.215	0.000
Blue	0.083	0.105
Green	0.014	0.778

Figure 4-20 Pearson's correlation coefficient graph.

Different models were built from the different layers (Table 4-8). A first model (TGM#1) used only the spectral information. The coefficient of correlation of this model was poor ($R^2 = 0.53$) and RMSE = 11.4 cm. The integration of the textural layers improved strongly of the model. The better fit called here the TGM#2 achieved a coefficient of regression of $R^2 = 0.87$ and RMSE = 6.32 cm. Thus, the model (TGM#1) was inappropriate. The multicollinearity of TGM#2 was tested. Dissimilarity, Contrast and Homogeneity in the textural information were shown to high VIF (variance inflation factor) of 1,168, 498 and 183 respectively while GEMI and Variance were gave small VIF. The study purposed to use the 5 parameters (GEMI, HOMO, DIS, CON and VAR) for estimation of tree girth and age of Para rubber trees.

The equation of TGM#2 is shown to Equation (4-1):

$$Y = 3.694 - 1.29(\text{GEMI}) - 2.740(\text{HOMO}) - 0.933(\text{DIS}) + 0.068(\text{CON}) - 0.015(\text{VAR}) \quad (4-1)$$

where Y is the tree girth (m) and R^2 is 0.87., Scatter plot of TGM#1 and TGM#2 is shown in Figure 4-21.

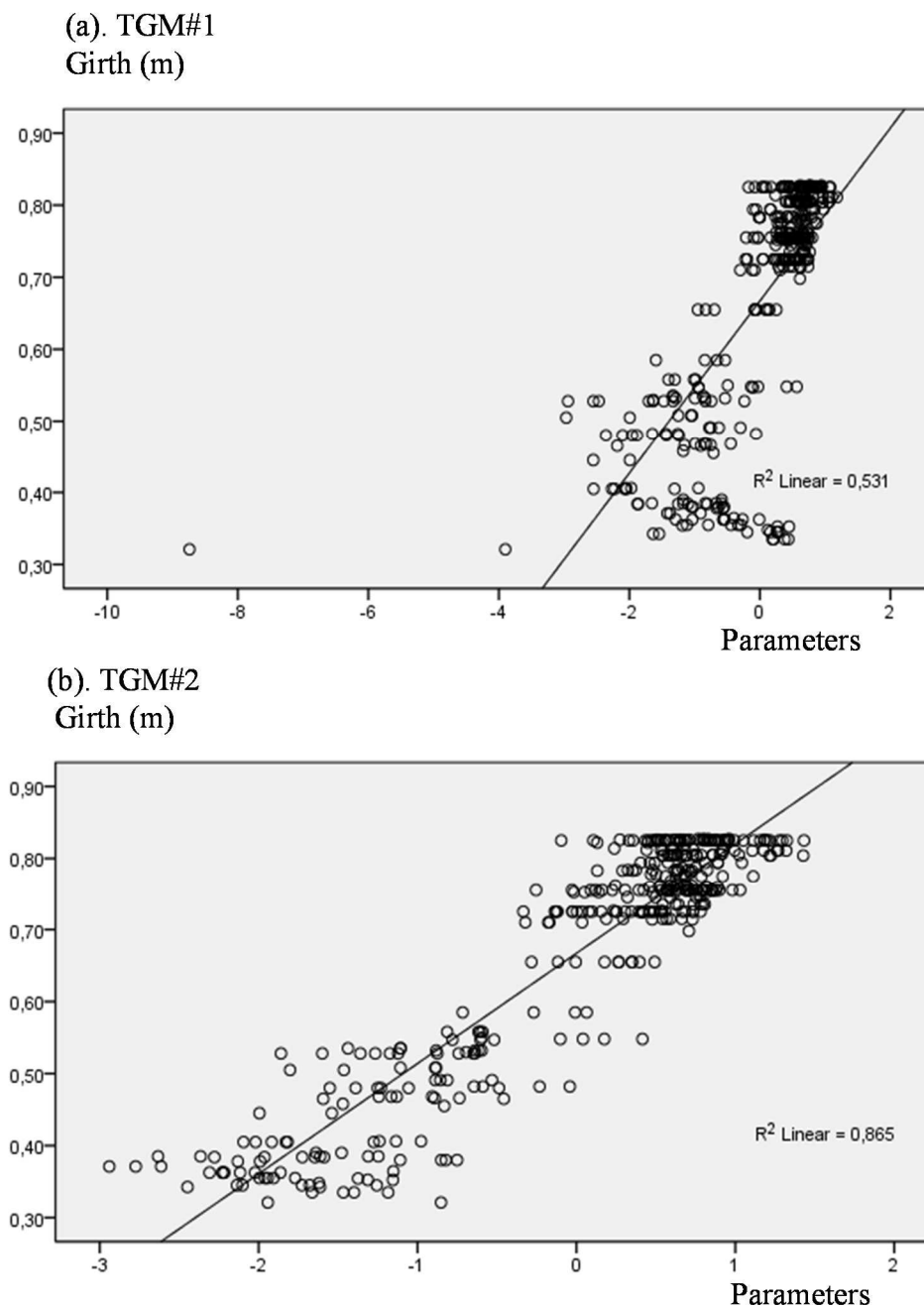
Table 4-8 Model summary. The number of girth measurements is 388 samples. Method Stepwise regression, Criteria = Probability in(.05), Probability out(.10). Spectral information: NIR = Near-infrared band, RED = Red band, GEMI = Global Environment Monitoring Index, MSAVI2 = Modified Soil Adjusted Vegetation Index2. Textural information: HOMO = Homogeneous, DIS = Dissimilarity, CON = Contrast, VAR = Variance.

Model	R^2	Adj. R^2	RMSE Tree girth (cm)	Constant	Coefficient		Collinearity Statistics	
							Tolerance	VIF
TGM#1	0.531	0.526	11.40	-16.435	NIR	-95.441	0.000	2,816.797
					RED	73.826	0.001	759.217
					MSAVI2	55.867	0.000	2,877.383
					GEMI	18.064	0.001	693.770
TGM#2	0.865	0.863	6.32	3.694	GEMI	-1.290	0.680	1.471
					HOMO	-2.740	0.005	183.046
					DIS	-0.933	0.001	1,167.832
					CON	0.068	0.002	497.873
					VAR	-0.015	0.056	17.926

Table 4-9 Excluded Variables. Spectral information: RED = Red band, NIR = Near-infrared band, ARVI = Atmospheric Resistance Vegetation Index, IPVI = Infrared Percentage Vegetation Index, MSAVI2 = Modified Soil Adjusted Vegetation Index2. NDVI = Normalized Different Vegetation. Textural information: COR = Correlation, ENT = Entropy, MEAN = Mean, ASM = Angular Second Moment.

Parameter	Sig.	Partial Correlation	Collinearity Statistics		
			Tolerance	VIF	Minimum Tolerance
BLUE	.105	-.083	.761	1.313	.001
GREEN	.460	-.038	.763	1.311	.001
RED	.997	.000	.484	2.067	.001
NIR	.936	-.004	.210	4.752	.001
ARVI	.972	.002	.093	10.789	.001
IPVI	.688	.021	.065	15.489	.001
MSAVI2	.903	.006	.014	72.879	.001
NDVI	.688	.021	.065	15.489	.001
COR	.836	-.011	.020	50.387	.001
ENT	.733	-.017	.023	43.936	.001
MEAN	.988	-.001	.666	1.501	.001
ASM	.252	-.059	.048	20.871	.001

Figure 4-21 (a) TGM#1 derived from a spectral information., (b) TGM#2 derived from a combination of spectral and textural information.



This equation was applied of the layers defining each plantation in order to estimate the girth of the trees of each plantation. The model (TGM#2) was realized in the GIS built for this study. From the tree girth map, a map of tree ages has been drawn (Figure 4-22).

Old age classes (more than 18 years old) cover a surface of 54.55 km² (35%, 5,455 ha), Young age classes (less than 12 years old) cover a surface of 51.12 km² (33%, 5,112 ha)

while Middle age classes (from 12 to 18 years old) cover a surface of 48.68 km² (32%, 4,868 ha). The areas of each age classes are listed in Table 4-10.

Table 4-10 Area summary of the Para rubber plantation.

Age (yr)	Area (ha)	Age Class	Area (ha)
4	52.05	Young	5,111.65
8	899.26		
12	4,160.34		
16	1,965.42	Middle	4,868.12
18	2,902.70		
20	2,658.79	Old	5,455.09
22	2,791.13		
25	5.17		
Total	15,434.86	Total	15,434.86

The confusion matrix was used to evaluate the accuracy of Para rubber age class map. Table 4-11 was shown the quality from object based classification of this study. A total 25,437 m² were used to compare data between object base and ground truth. The overall accuracy is 90% for all age classes and Kappa index is shown to almost perfect agreement (0.83).

Table 4-11. Confusion matrix of Para rubber classification.

		Ground truth			
		Young age	Middle age	Old age	Overall
Object based	Young age	10,733	442	10	11,185
	Middle age	1,465	1,473	365	3,303
	Old age	43	154	10,752	10,949
	Overall	12,241	2,069	11,127	25,437
Overall accuracy = 90.25%, Kappa = 0.83					

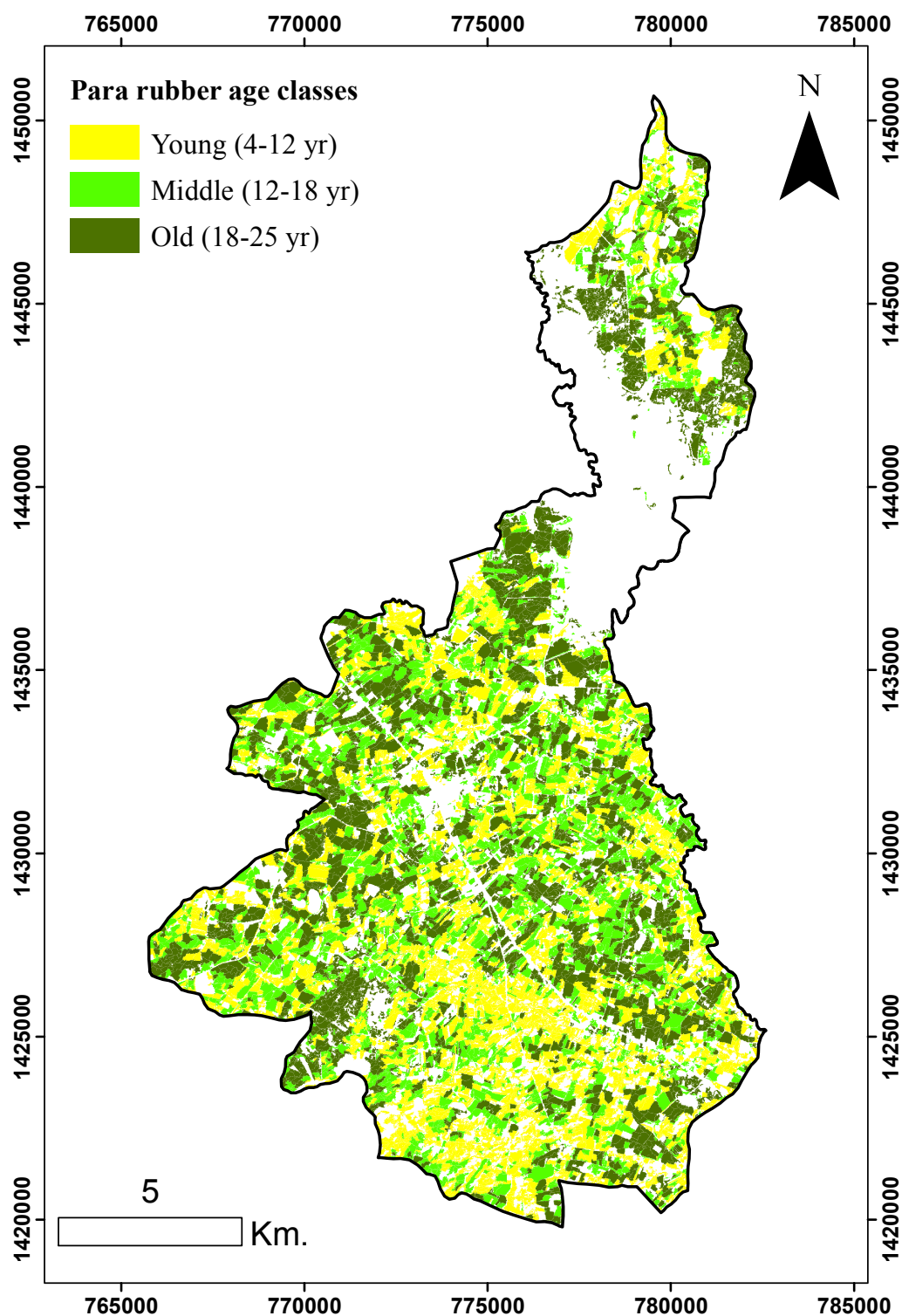
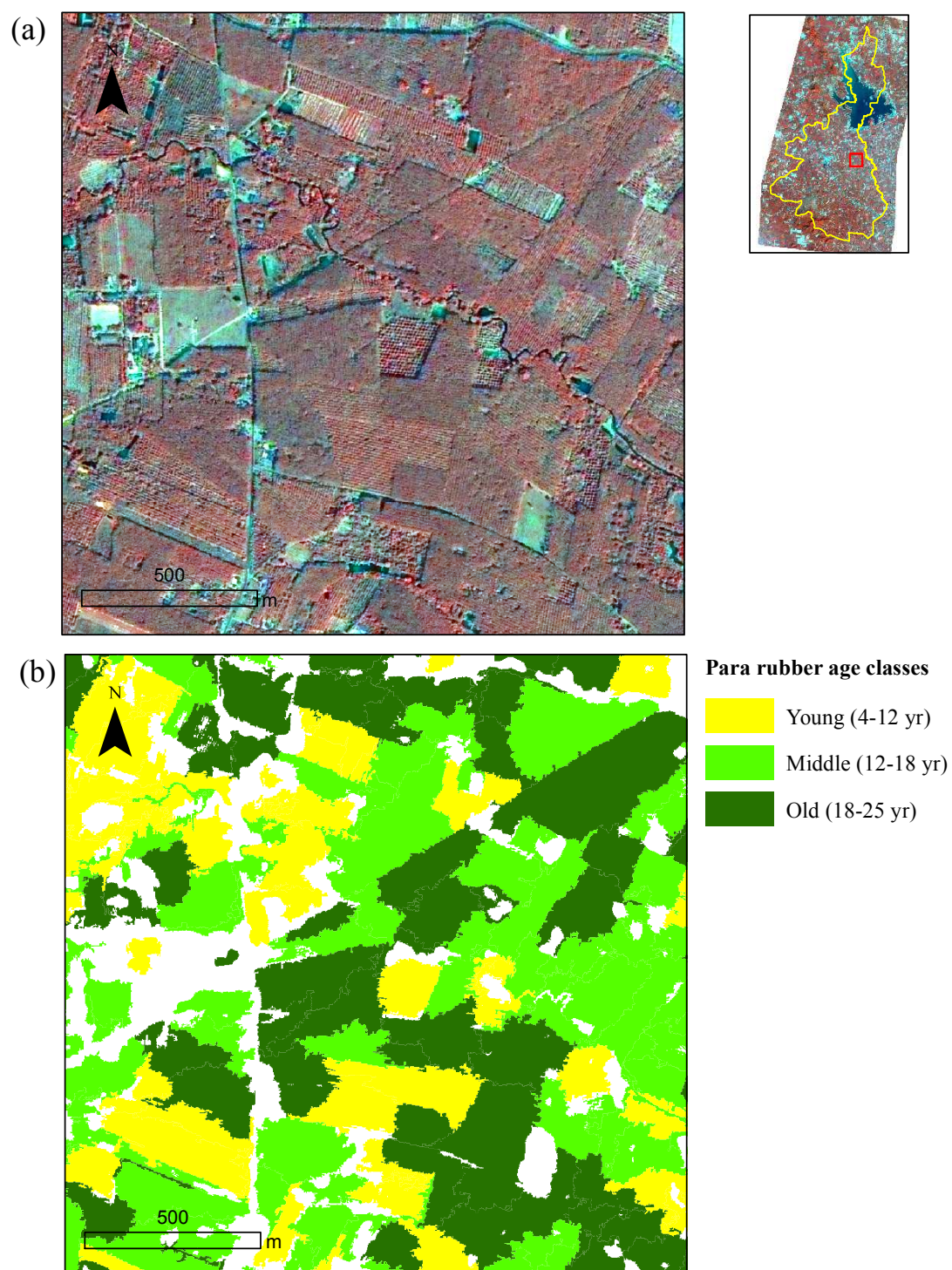
Figure 4-22 Map of Para rubber age class.

Figure 4-22 (cont.) (a) THAICHOTE false color image., (b) Map of Para rubber age class.



4.7 Estimation of Biomass and Carbon Stock

The accuracy of the model TGM#2 was evaluated using the root mean square error (RMSE) and the mean absolute percentage (MAPE). The RMSE and MAPE are given to 0.17 tC ha⁻¹ and 8.33% respectively. The errors from the surface and the model were summarized. Consequently, the total uncertainty of the biomass and carbon stock estimation is given to 111,656.32 tons (or 11.3%).

The total amount of biomass stock in Mae Num Prasae watershed was estimated by the allometric equation (Equation 3-1). The highest biomass stocked in Para rubber plantations is obtained for 22 years old trees that sequester approximately 32% of the total biomass (703,766 tons). The lowest biomass stock is found at 4 years (approximate 0.1% or 1,276 tons) while at the age class of 20, 18, 12, 16, 8 and 25 years for the amount of biomass stocked is 23%, 20%, 14%, 10%, 1% and 0.1% respectively, (Table 4-12, Figure 4-23).

The rate carbon stock of investigated area is average stocked 64 tC ha⁻¹. The age for 4 years old is lowest stocked biomass (11 tC ha⁻¹) while the age for 25 years is highest stocked (229 tC ha⁻¹). The ages of 8, 12, 16, 18, 20 and 22 years old are expressed to 17, 33, 51, 67, 86 and 112 tC ha⁻¹ respectively, (Table 4-12, Figure 4-23). The carbon stock map can be drawn in Figure 4-24. The total biomass stocked in the study area is 2.23 Megatons corresponding to 0.99 Megatons of carbon stocked.

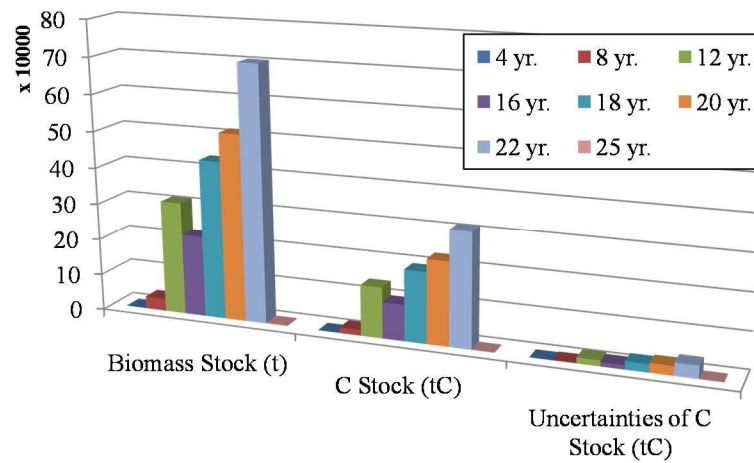
The evaluation of CO₂ sequestration by Para rubber age is reported in Table 4-12. The study found that Para rubber has the higher C sequestration at 25 years (33.53 tC ha⁻¹yr⁻¹), while the lower C sequestration is found at 8 years (7.79 tC ha⁻¹yr⁻¹). In 2011, the investigated area sequestered 33.05 tC corresponding to 121.28 t CO₂ by Para rubber plantation assuming that 1 tC represents 3.676 t of CO₂.

Table 4-12 Biomass and Carbon stocked in study area 2011. The uncertainty on the Carbon Stock comes from the uncertainty on the surface and the uncertainty of the model.

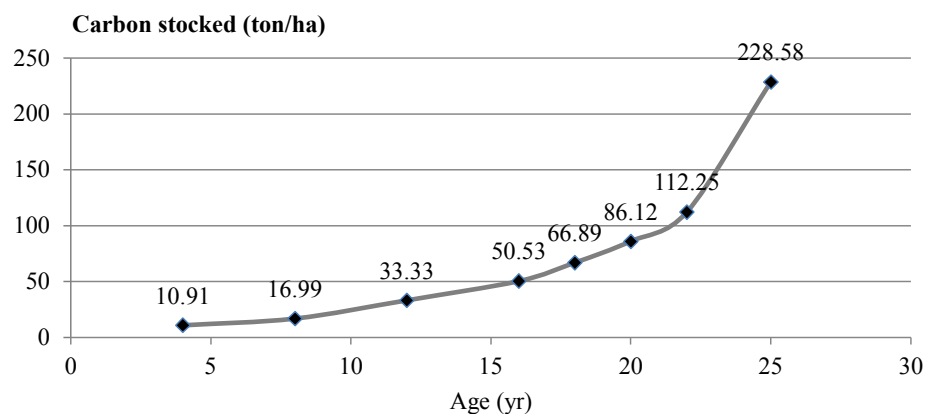
Class	Age (yr)	Biomass Stock (t)	C Stock (tC)	Rate C Stock (tC ha⁻¹)	Uncertainty of C Stock (tC)	C Sequestered (tC ha⁻¹ yr⁻¹)	CO₂ Sequestered (tCO₂ ha⁻¹ yr⁻¹)
Young	4	1,275.55	567.88	10.91	72.16	2.73	10.01
	8	34,309.54	15,274.61	16.99	1,845.45	2.12	7.79
	12	311,479.13	138,670.51	33.33	15,987.87	2.78	10.19
Middle	16	223,062.92	99,307.61	50.53	11,363.43	3.16	11.59
	18	436,121.53	194,161.30	66.89	21,820.70	3.72	13.64
Old	20	514,323.60	228,976.87	86.12	25,588.01	4.31	15.8
	22	703,766.39	313,316.80	112.25	34,847.56	5.1	18.73
	25	2,654.43	1,181.75	228.58	131.13	9.14	33.53
Grand Total		2,226,993.09	991,457.32	64.23 (average)	111,656.32 (11.3%)	33.05	121.28

Figure 4-23 (a) Bar graphs: biomass, carbon stock and uncertainties data., (b) The rate of C stocking., (c) The rate of CO₂ sequestration by Para rubber of each age class.

(a)



(b)



(c)

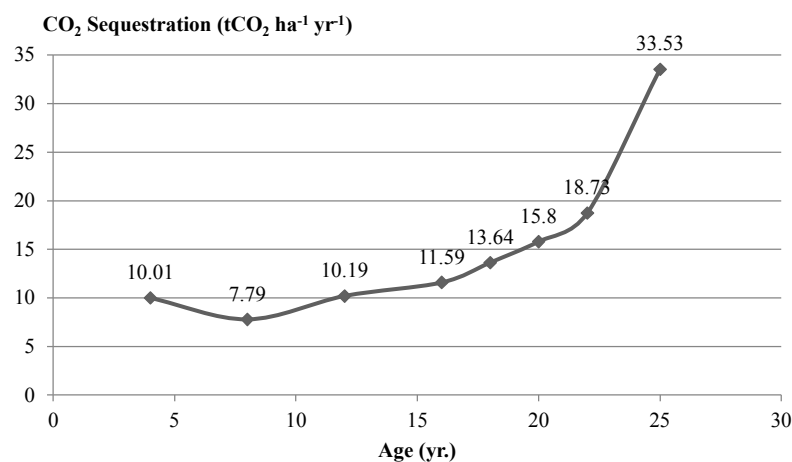


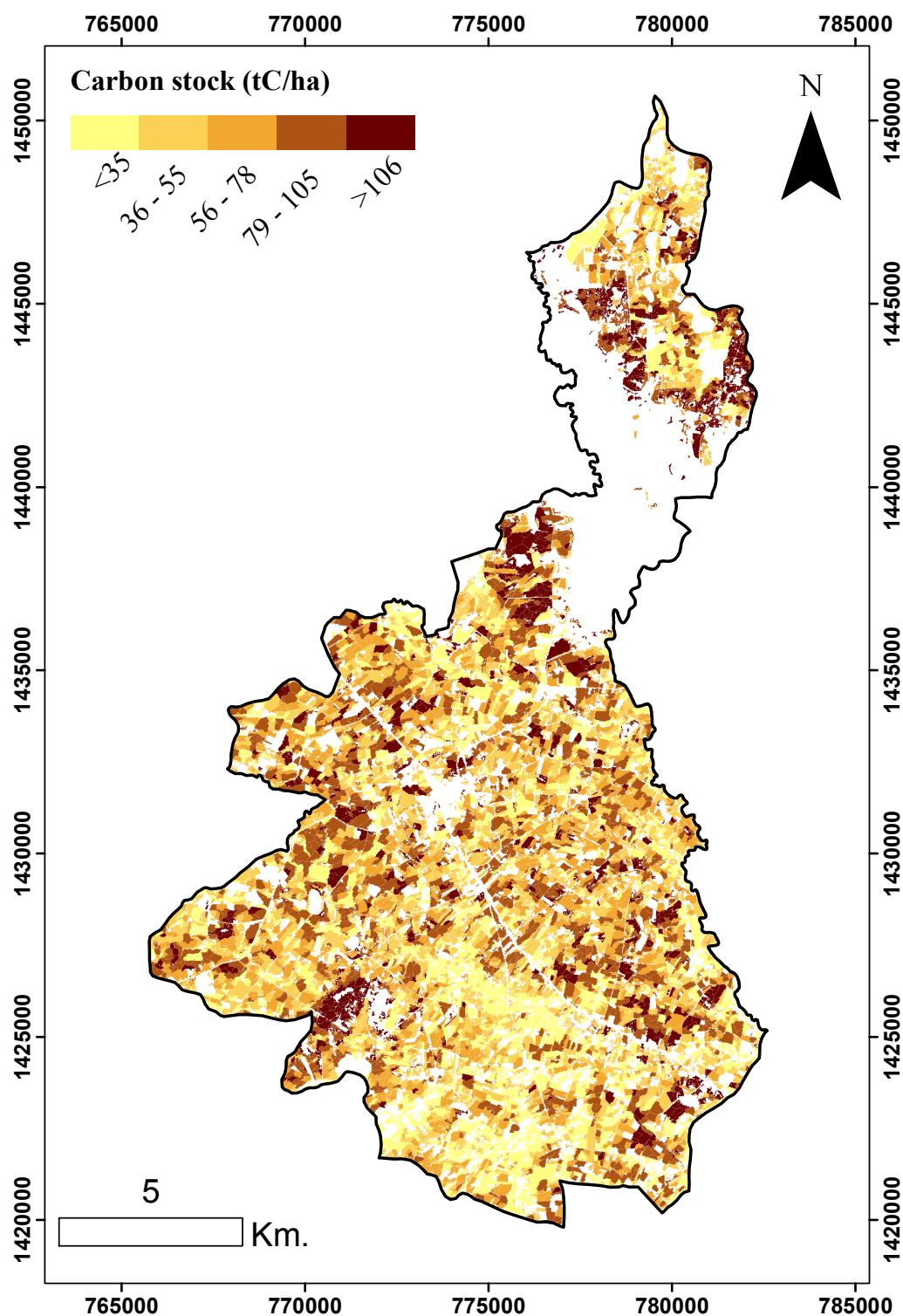
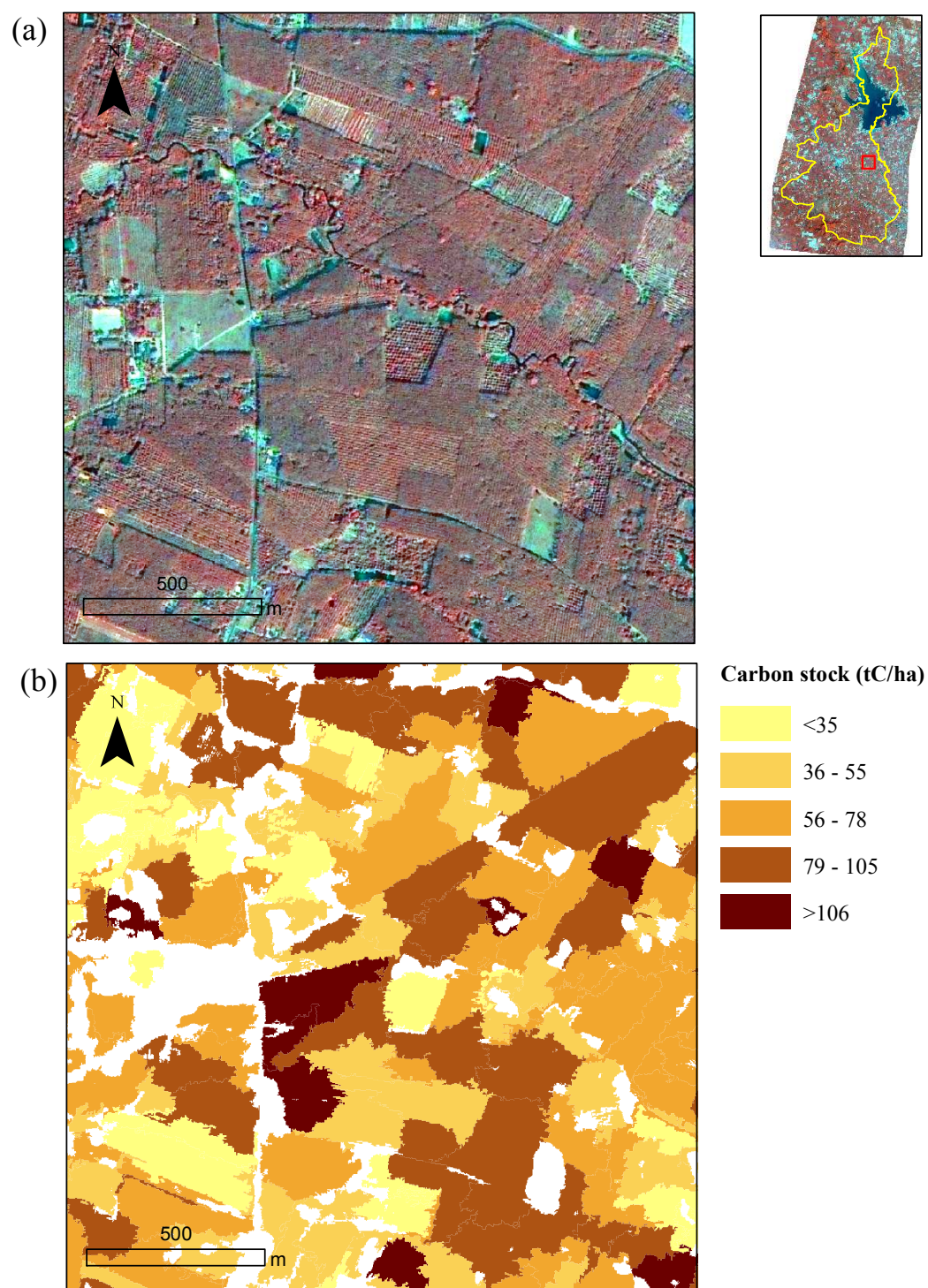
Figure 4-24 Map of Para rubber carbon stock.

Figure 4-24 (contin.) (a) THAICHOTE false color image (b) Map of Para rubber carbon stock.



4.8 Result's Discussion

The objective of this study was to connect biomass and carbon inventory data to THAICHOTE satellite image and to develop a tree girth model (TGM) to improve biomass and carbon stocks estimation in Para rubber plantations in East Thailand. The accuracy of Para rubber biomass and carbon stock estimation at large-surface realized on many interacting factors that might be distributed by:

(1) Remote sensing techniques

- Image quality (Spatial resolution, Camera sensor, Data acquisition)
- Image classification techniques (Tree counting, Tree age and girth identification)

(2) Plantation Management

- Tree species (clone of Rubber plantation)
- Planting layout (density of tree stand per area)
- Planting location (environmental conditions eg.soil, climate)

(3) Statistical Analysis for connecting ground data and remote sensing data

- Fitted Modeling (Tree sampling, Parameterization, Relationship, Empirically and Globally models, Multicollinearity data)
- Allometric equation (Empirically and Globally models)
- Carbon concentration (ratio)

• Tree Girth Modeling and Spectral, Textural information

The obtain relationships between tree girth and layers used for image classification show that texture parameters are better correlated than single bands and vegetation indices as shown by the Pearson's correlation coefficient values. The results of this study are in agreement with Eckert, (2012) [8] findings who observed the degraded forest stratum with high resolution WorldView-2 data. The textures are better parameters than spectral data to estimate the age of the canopy. The present work shows that the textural information has to be added to the spectral one for a precise inventory of characteristics of forest or plantations in agreement with the works of Eckert, (2012) [8] and Sarker et al., (2011) [9] with high resolution WORLDVIEW-2 and ALOS AVNIR-2 used in Madagascar, Hong Kong and Central Siberia for forest biomass estimations.

Despite the single bands in the spectral information are inappropriated to estimate biomass in Para rubber plantation, the vegetation indexes obtained by the Red and NIR combination have shown a high potential on forest biomass evaluation in agreement of Eckert, (2012) [8] and shown a substantial to extraction Para rubber surface by the vegetation indexes on the mask information.

In the model TGM#2 (Table 4-8), the texture parameters of homogeneity, dissimilarity and contrast were gave poor values of the VIF (Variance Inflation Factor) on the multicollinearity analysis as in agreement with the works of Eckert, (2012) [8] and Sarker et al., (2011) [9] recommended to the good VIF value is less than ten. Thus, these texture parameters may unsuitable for tree girth and age prediction. In contrast, the empirical model TGM#2 obtained by five parameters (equation 4-18) is shown the R^2 of 0.87 higher than the model TGM#3 (R^2 of 0.82) when the GEMI (Global Environment Monitoring Index) and texture variance are considered. Thus in this studied, the empirical model TGM#2 is appropriated for connecting field data and remote sensing data and may show a limitation for publishing to the global model. The model summary of TGM#3 is shown in Table 4-13.

Table 4-13 Model summary of TGM#3. The number of girth measurements is 388 samples. Method Stepwise regression, Criteria = Probability in(.05), Probability out(.10). GEMI = Global Environment Monitoring Index, Textural information: VAR = Variance.

Model	R^2	Adj. R^2	RMSE Tree girth (cm)	Constant	Coefficient		Collinearity Statistics	
							Tolerance	VIF
TGM#3	0.817	0.816	7.07	1.462	GEMI	-1.653	0.917	1.091
					VAR	-0.04	0.917	1.091

Several allometric relationship methods have been used for ground evaluation to biomass in Para rubber plantation. The allometric equation of Chuntuma et al., (2012) [7] show high relationship in the same order magnitude (R^2 0.86 – 0.99) to other works of Shorrocks et al., (1965) [55] and Wauters et al., (2008) [56] were tested in the biomass estimation of *Hevea brasiliensis* on Malaysia and Brazil respectively. Thus, the way in which

ground biomass estimation using allometric relationship method varied as a function of tree components, tree species (clone of Para rubber) and study sites [55, 56].

- **THAICHOTE satellite data, canopy height model**

Despite THAICHOTE data do not contain Medium Infrared data (MIR) as used in other studies [57, 58], the results of this study have shown a high potential on forest biomass evaluation. The multispectral (4 bands) and panchromatic data (2 m) were shown a good to build the broadband vegetation indexes (VIs) and grey level co-occurrence measurement (GLCM).

The forest CHM (canopy height model) obtained by the photogrammetric techniques is very complex, high variation in reflectance anisotropy, and the matching accuracy for such a surface may be flawed by:

- (1) little or no texture (corresponding to photographic quality);
- (2) moving objects (such as leaves, tree apex and shadows);
- (3) occlusions;
- (4) radiometric artifacts
- (5) high angle or wide baseline [59 - 62].

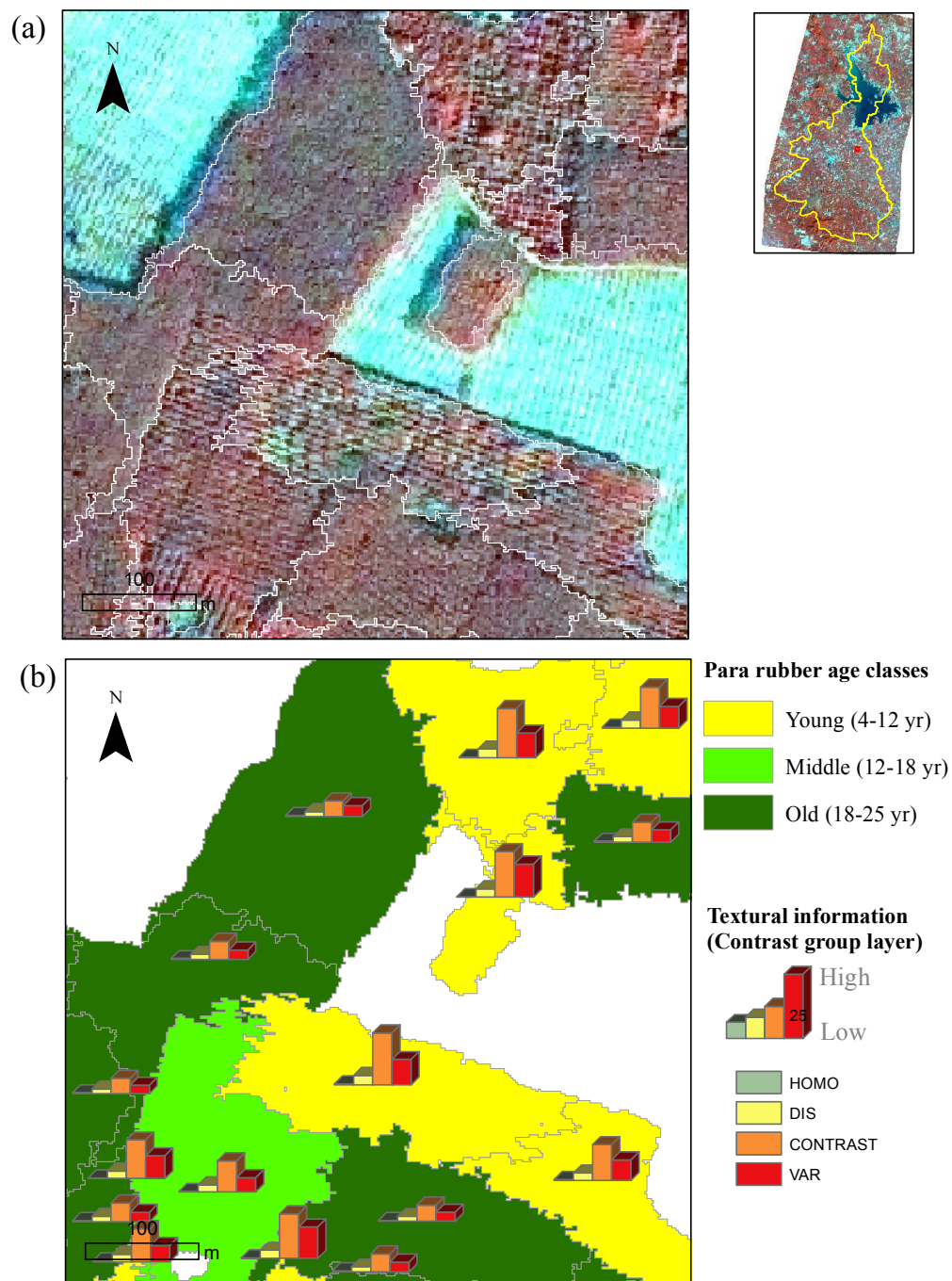
Nevertheless, the CHM quality is not editing by hand and beyond in the scope of this studied. The accuracy CHM was tested using the mean absolute percentage error (MAPE) and shown up to 70% thus the CHM obtained by THAICHOTE stereo data is unsuited for biomass forest evaluation.

The Para rubber plantation surface extraction is depended on the NSDI (Thai National Spatial Data Infrastructure) data for establishing the mask information that the Para rubber may increasing and decreasing for a surface calculation. To minimizing the uncertainty data, the good quality and lasted NSDI data are needed to build the mask information.

The Para rubber plantation is non-evergreen forest type. In study area, the leaves of Para rubber fall on between February and May. The method developed in this study consider green plantation that the GEMI, HOMO, DIS and VAR are shown to negative for the canopy age of tree while the CON is shown to positive (Figure 4-25). Additional work remains to be

done to test the potentialities of THAICHOTE data acquired in the period during which trees have no leaves.




Figure 4-25 (a) Para rubber plantation limits (segmentation)., (b) Bar graph: textural information and age class map.



- **Rate capacity of C stocked by Plantations**

The Para rubber plantation is a one candidate to stocking carbon, the result of this estimation shown the high potentiality carbon stocked of 112.5 – 228.58 tC ha⁻¹ at mature stage (rotation stage) when comparing for the other plantations in Thailand [12, 14]. Table 4-14 shows the capacity of carbon storage at rotation age (old age) in Eucalyptus (*E. camaldulensis*), Teak (*Tectona grandis*) and Para rubber plantation RRIM 600 (*Hevea brasiliensis*). Moreover, the results of the study are confirmed on the carbon stocking in the same order magnitude (214 tC ha⁻¹) from the work of Kongsager et al., (2013) [63] for estimation of rate carbon stock in tree clone *Hevea brasiliensis* using allometric equations.

Table 4-14 The rate of carbon storage at rotation age in Eucalyptus (*E. camaldulensis*), Teak (*Tectona grandis*) and Para rubber plantation RRIM 600 (*Hevea brasiliensis*).

	Eucalyptus (<i>E. camaldulensis</i>)	Teak (<i>Tectona grandis</i>)	Para rubber RRIM600 (<i>Hevea brasiliensis</i>)
Carbon stored	25.9 tC ha ⁻¹	38.5 tC ha ⁻¹	112.5 – 228.58 tC ha ⁻¹
Rotation age	5 yr.	25-38 yr.	22 - 25yr.
Ground view			
Reference	Onida Iglesias [12]	Noiruksar [14]	The study
Location tested	East Thailand	North Thailand	East Thailand

These amount of CO₂ captured by Para rubber plantations can be compared to natural carbon sequestration estimated for the ocean. Borges *et al.*, (2005) [64] show that the sequestration of CO₂ by ocean is around 4.45 gC m⁻² yr⁻¹, while Para rubber plantation can sequester up to 914.3 gC m⁻² yr⁻¹. The study believe that agriculture and human intervention may play a critical role in the extraction of CO₂ from the atmosphere and thus in the short carbon cycle.

CONCLUSIONS

&

PERSPECTIVES

CHAPTER V

CONCLUSIONS AND PERSPECTIVES

5.1 Conclusions

This study explored the potential of THAICHOTE satellite data to estimate Para rubber biomass and carbon stock. The method developed here used the object based classification combining the spectral, textural and 3D information on THAICHOTE satellite data. Two hypotheses of the study are accepted by H1. The textural information can be improved the relationship of Para rubber plantation biomass between field and remote sensing data and the precision measuring of Para rubber biomass and carbon stock can be done using the object based classification. The conclusions of the study are listed in below.

The correlation between tree girth and values of the different layers obtained from the remote sensing image was tested by Pearson's correlation. The texture parameters were shown high correlation of absolute 0.75 to 0.88, excluded the texture mean that it shown to absolute 0.5. The broadband greenness vegetation indexes were shown medium correlation of absolute 0.51 to 0.66. The single bands were shown poor correlation (absolute value 0.01 to 0.21), excluded the NIR that it shown to absolute 0.68.

The canopy height model (CHM) is not appropriated to build the image classification layers and it shown to high error (MAPE = 74%) for estimating the Para rubber biomass and carbon stock.

The results of this study show that these data can be used to map Para rubber plantation and distinguish age classes of trees in the plantations. The study propose that textural information is more useful than spectral information to capture tree canopy architecture and thus the age of the canopy. Moreover, it has been possible to build a empirical model equation relating some textural parameters to the age of the plantation. In the

study, the tree girth model (TGM#2) obtained from multiple linear regression analysis (stepwise method) was shown correlation coefficient of $R^2=0.87$ with accepted five layers (excluded twelve layers) and thus can be used with confidence on the study area. The TGM is written in formula:

$$Y = 3.694 - 1.29(\text{GEMI}) - 2.740(\text{HOMO}) - 0.933(\text{DIS}) + 0.068(\text{CON}) - 0.015(\text{VAR})$$

where Y is Tree girth (m), From spectral information: GEMI is Global Environment Monitoring Index, Form textural information: HOMO is Homogeneity, DIS is Dissimilarity, CON is Contrast and VAR is Variance.

Around 154 km² of the 232 km² of the studied area are covered by Para rubber plantations. The class of age of each plantation has been estimated to be 33% of the crop surface belong to the young class (from 4 to 12 years), 34% of the crop surface belong to the middle class (from 12 to 18 years) and 33% belong to the old class (older than 18 years).

The rate of biomass stock, the age for four years old is lowest stocked biomass (11 tC ha⁻¹) while the age for twenty-five years is highest stocked biomass (229 tC ha⁻¹). The average value for the rate of biomass stock in the study area is 64 tC ha⁻¹. The way in which the rate increasing of biomass stock varied as a function of the girth and age of tree.

The total amount of biomass and carbon stocks are 2.23 Megatons and 0.99 Megatons C respectively with uncertainty of 11%. In 2011, the total area sequestered 121 tCO₂ by Para rubber plantations. Moreover, the results of this studied show that the Para rubber plantation (914.3 gC m⁻² yr⁻¹) has higher potential CO₂ sequestration than the Ocean (4.45 gC m⁻² yr⁻¹) for around 200 time.

5.2 Perspectives

Despite, the THAICHOTE satellite data, the object based classification and the tree girth model developed here are appropriated for estimation biomass and carbon stock in Para rubber plantation, the problems and the limitations of the study are needed to improve for minimizing the uncertainty data of forest biomass-carbon mapping. The study recommended for further research as following areas:

- Use of this study method in other Para rubber plantation areas could provide basis of comparison in terms of accuracy.
- Consideration of the ground measuring CO₂ flux in the Para rubber plantation by Eddy Covariance (EC) method, multi-spectral/hyper-spectral imageries and Light Detection and Ranging (LiDAR) from Unmanned Aerial System (UAS) for high precision of biomass and carbon stock and source estimation at large-surface.

REFERENCES

1. R. Sales, D. Lasco, and M. R. Banaticla, “Carbon storage and sequestration potential of smallholder tree farms on Leyte Island, the Philippines,” in ACIAR Smallholder Forestry Project ASEM 200/008 Redevelopment of a Timber Industry Following Extensive Land Clearing: Proceedings from the End-of Project Workshop, Ormoc City, Philippines (2004).
2. S. Backeus, Wikstrom. P, and T. Lamas, “A model for regional analysis of carbon sequestration and timber production,” *Forest Ecology and Management*. 216, 28-40 (2005).
3. R. Sedjo, “Forest carbon sequestration: some issues for forest investment,” Discussion Paper 01-34, Resources for the Future (2001).
4. “United Nation Framework Convention on Climate Change, Kyoto Protocol,” <http://unfccc.int/2860.php> accessed (20 October 2014).
5. “Production of Natural Rubber”, Rubber Research Institute of Thailand, 2011, http://www.rubberthai.com/statistic/stat_index.htm accessed (20 October 2014).
6. C. Viriyabuncha, Handbook of Stand Biomass Estimation, pp. 1–11, Department of National Parks, Wildlife and Plant Conservation, Thailand (2003).
7. A. Chantuma, T. Wichitchonlachai, and P. Chantuma, “Rubber new planting in Thailand: towards the world affected on climate change,” *Rubber Thai*. 1, 40–47 (2012).
8. S. Eckert, “Improved forest biomass and carbon estimations using texture measures from WorldView-2 Satellite data,” *Remote Sens*. 4, 810–829 (2012).
9. L. R. Sarker and J. E. Nichol, “Improved forest biomass estimates using ALOS AVNIR-2 texture indices,” *Remote Sens. Environ*. 115, 968–977 (2011).
10. H. Fuchs et al., “Estimating aboveground carbon in a catchment of the Siberian forest tundra: combining satellite imagery and field inventory,” *Remote Sens. Environ*. 113, 518–531 (2009).
11. D. Lu et al., “Relationships between forest stand parameters and Landsat TM spectral responses in the Brazilian Amazon Basin,” *For. Ecol. Manage*. 198, 149–167 (2004).

12. C. O. Iglesias, "Determination of carbon sequestration and storage capacity of eucalyptus plantation in Sra Kaew Province," Thailand using remote sensing, MSc Thesis, Mahidol University, Thailand (2007).
13. J. Nilubol, "Geo-Informatics Technology for Age Class Identification for Para rubber Plantation in Krabi Province," MSc Thesis, Mahidol University (2007).
14. S. Noiruksar, "Application of Remote Sensing for Aboveground Carbon Storage Determination of Teak in Khun Mae Kham Mee Plantation, Prae province, Thailand." MSc Thesis, Mahidol University (2011).
15. G. Zheng et al., "Combining remote sensing imagery and forest age inventory for biomass mapping," *J. Environ. Manage.* 85, 616–623 (2007).
16. L. Arko, "Uncertainties in segmentation and their visualisation application of geoinformatics," PhD Thesis, Universiteit Utrecht (2004).
17. N. Picard, L. Saint-André, and M. Henry, Manual for Building Tree Volume and Biomass Allometric Equations, Food and Agriculture Organization of the United Nations (2012).
18. C. Mongkolsawat, W. Putklang, "An approach for Estimating Area of Rubber Plantation: Integrating Satellite and Physical Data Over the North East Thailand." Proceeding 31st Asian Conference on Remote Sensing (ACRS) (2010).
19. A. Benzie, "Canopy Height Modeling for Improved Forest Biomass Inventory." Msc Thesis, Queen's University (2013).
20. Zhang et al., "Estimation of forest aboveground biomass in California using canopy height and leaf area index estimated from satellite data." *Remote Sensing of Environment.* (2014) <http://dx.doi.org/10.1016/j.rse.2014.01.025>.
21. Q. Guo, M. Kelly, P. Gong and D. Liu, "An Object-Based Classification Approach in Mapping Tree Mortality Using High Spatial Resolution Imagery." *GIScience & Remote Sensing.* 1, 24-27 (2007).
22. M. Kim, M. Madden and T. A. Warner, "Forest Type Mapping using Object-specific Texture Measures from Multispectral Ikonos Imagery: Segmentation Quality and Image Classification Issues." *Photogrammetric Engineering & Remote Sensing.* 75 Vol. 75, No.7, 819–829 (2009).
23. UNFCCC/CCNUCC, "Project design document: Clean Development Mechanism (CDM) Implementation in Natural Rubber Plantations." Version 1, 22th May, 2012.

24. P. Rao and K. R. Vijayakumar, "Climatic requirements," in *Natural Rubber: Biology, Cultivation and Technology*, Developments in Crop Science 23, Elsevier, Netherlands (1992).
25. J. Morison, R. Matthews, G. Miller, M. Perks, T. Randle, E. Vanguelova, M. White and S. Yamulki, "Understanding the carbon and greenhouse gas balance of forests in Britain." Forestry Commission (2012).
26. Food and Agriculture Organization, "State of the World's Forests." Food and Agriculture Organization of the United Nations, Rome, Italy (1997).
(2001a). Committee on Forestry. Climate Change and the Kyoto Protocol: Key Forestry-Related Issues. Rome, Italy.
(2001b). Global Forest Resource Assessment 2000. FAO Forestry Paper 140. Food and Agriculture Organization. Rome, Italy.
(2006). FAO Newsroom. Forests and climate change.
27. S. Brown, "Estimating biomass and biomass change of tropical forests: a primer." FAO Forestry Paper 134. Food and Agriculture Organization. Rome, Italy (1997).
28. "Global Environment Outlook Three: Past, present and future perspective." London: Earthscan Publication Ltd (2003).
29. Intergovernmental Panel on Climate "Change. Second Assessment Report 2001." http://www.grida.no/climate/ipcc_tar/wg1/index.htm accessed (20 October 2014).
30. T.Kira and T. Shidei, "Primary production and turnover of organic matter in different ecosystems of the Western Pacific." *Jap. Journal of Ecology*. 17(2), 70-87 (1967).
31. R.N.(Ed.). Colwell, *Manual of Remote Sensing*. Second Edition, Vol I: Theory, Instruments and Techniques. American Society of Photogrammetry and Remote Sensing ASPRS, Falls Church (1983).
32. P.J. Curran, *Principles of Remote Sensing*, Longman Group: UK (1985).
33. P.M. Mather and M. Koch, "Computer processing of remotely-sensed images: an introduction." 4th ed. Singapore: Markono (2011).
34. M. Kaewmanee, T. Choomnoommanee, and R. Fraisse, "Thailand Earth Observation System: Mission and Products," in *Proc. ISPRS Commission I Symposium*, July 4-6 (2006).
35. J.R. Jensen, "Remote sensing of environment: an earth resource perspective." Prentice-hall: USA (2000).
36. "Exelis VIS product documentation." <http://www.exelisvis.com/docs/BroadbandGreenness.html> accessed (1 December 2014).

37. J. W. Rouse et al., "Monitoring vegetation systems in the great plains with ERTS," in Third ERTS Symposium, NASA SP-351, Vol. 1, pp. 309–317, NASA, Washington, DC (1973).
38. Y. J. Kaufman and D. Tanré, "Atmospherically resistant vegetation index (ARVI) for EOSMODIS," [IEEE Trans. Geosci. Remote Sens.](#) 30, 261–270 (1992).
39. B. Pinty and M. M. Verstraete, "GEMI: a non-linear index to monitor global vegetation from satellites," *Vegetation* 101, 15–20 (1992).
40. R. E. Crippen, "Calculating the vegetation index faster," [Remote Sens. Environ.](#) 34, 71–73 (1990).
41. J. Qi et al., "Modified soil adjusted vegetation index (MSAVI)," [Remote Sens. Environ.](#) 48, 119–126 (1994).
42. R. M. Haralick, K. Shanmugan, and I. Dinstein, "Textural features for image classification," [IEEE Trans. Syst. Man Cybern.](#) 3, 610–621 (1973).
43. H. Anys et al., "Texture analysis for the mapping of urban areas using airborne MEIS-II images," in Proc. First Int. Airborne Remote Sens. Conf. Exhibition, pp. 231–245, Strasbourg, France (1994).
44. S. Rawlinson, "Design and Implementation of a Spatially Enabled Panoramic Virtual Reality Prototype." Msc. Thesis, University of New Brunswick, Canada (2002).
45. The Exelis Visual Information Solutions product documentation center (2014).
46. B. Thomas, L. Stefan, H. Geoffrey (Eds.), *Object-Based Image Analysis Spatial Concepts for Knowledge-Driven Remote Sensing Applications Series: Lecture Notes in Geoinformation and Cartography*, 817 p. XVII (2008).
47. G. Jacek and D. Gene, "Block adjustment of high-resolution satellite images described by rational polynomials," [Photogramm. Eng. Remote Sens.](#) 69(1), 59–68 (2003).
48. P. S. Chavez, Jr., "Image-based atmospheric corrections—revisited and revised," [Photogramm. Eng. Remote Sens.](#) 62(9), 1025–1036 (1996).
49. D. Lowe, "Distinctive image features from scale-invariant keypoints" [International Journal of Computer Vision.](#) 60, 2, 91–110 (2004).
50. P.R. Wolf, "Elements of Photogrammetry." McGraw-Hill (1983).
51. D.F. Watson and P., G. M., "A Refinement of Inverse Distance Weighted Interpolation." [Geoprocessing.](#) 2, 315–327 (1985).
52. L. Guigues, J.-P. Cocquerez, and H. Le Men, "Scale sets image analysis," [Int. J. Comput. Vision.](#) 68(3), 289–317 (2006).

53. A. Le Bris, "Extraction of vineyards out of aerial ortho-image using texture information," in *ISPRS Annals of the Photogrammetry, Remote Sensing and Spatial Information Sciences*, XXII ISPRS Congress, Volume I-3, Melbourne, Australia (2012).
54. J. Cohen J, "A coefficient of agreement for nominal scales." *Educational and Psychological Measurement*. 20(1), 37-40 (19620).
55. V.M. Shorrocks, "Mineral nutrition, growth and nutrient cycle of *Hevea brasiliensis*. Growth and nutrient content." *Journal of Rubber Research Institute of Malaysia*. **19**, 32-47 (1965).
56. J.B. Wauters, S. Coudert, E. Grallien, M. Jonard and Q. Ponette, Q. "Carbon stock in rubber plantation in Western Ghana and Mato Grosso (Brazil)." *Forest Ecology and Management*. **255**(7), 2347-2361 (2008).
57. D. Lu, "Aboveground biomass estimation using Landsat TM data in the Brazilian Amazon," *Int. J. Remote Sens*. 26, 2509–2525 (2005).
58. S. A. Eckert, "Contribution to Sustainable Forest Management in Patagonia: Object-Oriented Classification and Forest Parameter Extraction based on ASTER and Landsat ETM+ Data," PhD Thesis, University of Zurich, Zurich, Switzerland (2005).
59. J. Lisein, M. Pierrot-Deseilligny, S. Bonnet and P. Lejeune, "A Photogrammetric Workflow for the Creation of a Forest Canopy Height Model from Small Unmanned Aerial System Imagery." *Forests*. 4, 922-944 (2013).
60. E.Baltsavias, A. Gruen, H. Eisenbeiss, L. Zhang and L.T. Waser, "High-quality image matching and automated generation of 3D tree models." *Int. J. Remote Sens*. 29, 1243–1259 (2008).
61. J. White, M. Wulder, M. Vastaranta, N. Coops, D. Pitt and M. Woods, "The utility of image-based point clouds for forest inventory: A comparison with airborne laser scanning." *Forests*. 4, 518–536 (2013).
62. J. Jarnstedt, A. Pekkarinen, S. Tuominen, C. Ginzler, M. Holopainen and R. Viitala, "Forest variable estimation using a high-resolution digital surface model." *ISPRS J. Photogram. Remote Sens*. 74, 78–84 (2012).
63. R. Kongsager, J. Napier J., and O. Mertz, "The carbon sequestration potential of tree crop plantations." *Mitig Adapt Strateg Glob Change*. 18, 1197–1213 (2013). DOI [10.1007/s11027-012-9417-z](https://doi.org/10.1007/s11027-012-9417-z).

-
64. A. V. Borges, B. Delille, and M. Frankignoulle, “Budgeting sinks and sources of CO² in the coastal ocean: diversity of ecosystems counts,” [Geophys. Res. Lett.](#) 32, L14601 (2005).

APPENDIX

APPENDIX

A.1 Field measurement: Tree height measurement using Haga altimeter

Haga is a device to measure tree heights within fixed distances of 15, 20, 25 and 30m to the tree by the trigonometric principle and slope in percent. The suitable scale can be selected by rotating the adjustment disk at the front of the device. A reference tape can be installed at the tree to determine the distance optically.

Figure 1A-1 Tree height measurement., (a) distance measurement using field tape., (b) height measurement using Haga altimeter.

(a)



(b)



Distance measurement

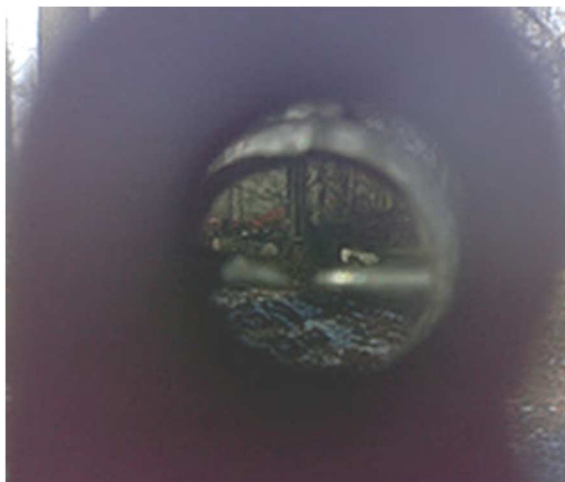
- Place the reference tape at the tree,
- Determine an optimal distance to the tree by checking the view field to tree bottom and top within the forest stand - preferably 15, 20, 25 or 30m.

Height measurement

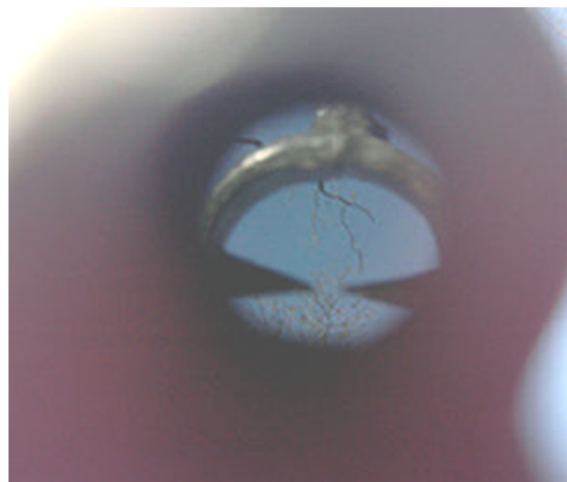
- Select the corresponding height scale by turning the adjustment disk,
- Sight tree bottom, lock the pointer needle and remember the value,
- Sight tree crown, lock the pointer needle and remember the value,
- The difference between the measurements will be tree height : $h_{\text{tree}} = h_{\text{canopy}} - h_{\text{bottom}}$

Figure 1A-2 Tree height measurement., (a) live view measuring tree bottom., (b) live view measuring tree canopy.

(a)



(b)



Source: <http://wiki.awf.forst.uni-goettingen.de/wiki/index.php?title=Haga&oldid=10014>

A.2 Field measurement: Data sheet for collecting forest inventory data

DATE (DD/MM/YY) :		COLLECTIVE DATA SHEET						
COORDINATE REFERENCE: DIRECTION: SLOPE (%): ELEVATION (M):								
		GPS					CANOPY COVER	
ID	REMARK/ ENVIRONMEN T	X	Y	AGE (YEA R)	DIAMETER(C M.)	HEIGH T (M.)	N,S	E,W

A.3 The input dataset for tree girth modeling (TGM) and Histogram

Table A3-1 shown the input dataset (N = 388 samples) for establishing the tree girth model (TGM).

Table A3-1 The input data set of TGM., Girth (cm), B1, B2, B3 and B4 are Blue, Green, Red and Near infrared bands (reflectance unitless)., ARVI is Atmospherically Resistant Vegetation Index., GEMI is Global Environment Monitoring Index., IPVI is Infrared Percentage Vegetation Index., MSAVI2 is Modified Soil Adjusted Vegetation Index2., NDVI is Normalized Difference Vegetation Index., txt_CON is texture Contrast., txt_Cor is texture Correlation., txt_DIS is texture Dissimilarity., txt_ENT is texture Entropy., txt_HOM is texture Homogeneity., txt_Mean is texture Mean., txt_ASM is texture Angular second moment., txt_Var is texture variance.

Girth (cm)	B1	B2	B3	B4	ARVI	GEMI	IPVI	MSAVI	NDVI	txt_CON	txt_Cor	txt_DIS	txt_ENT	txt_HOM	txt_Mean	txt_ASM	txt_Var
32.10	0.09	0.14	0.22	0.42	0.17	0.44	0.66	0.59	0.32	9.44	-0.33	2.37	4.42	0.34	29.46	0.02	6.15
32.10	0.08	0.13	0.19	0.46	0.29	0.52	0.70	0.65	0.41	12.93	-0.56	2.76	4.58	0.30	29.29	0.01	8.08
33.50	0.08	0.12	0.19	0.33	0.12	0.34	0.64	0.51	0.27	22.28	-0.82	3.90	4.82	0.20	24.81	0.01	10.37
33.50	0.08	0.12	0.20	0.33	0.07	0.32	0.62	0.50	0.24	22.27	-0.80	3.94	4.82	0.19	24.81	0.01	9.92
33.50	0.08	0.12	0.19	0.32	0.12	0.33	0.64	0.51	0.27	19.19	-0.68	3.61	4.73	0.22	24.12	0.01	9.05
33.50	0.08	0.12	0.18	0.33	0.15	0.36	0.65	0.52	0.30	16.08	-0.63	3.22	4.70	0.26	24.48	0.01	8.10
34.25	0.08	0.12	0.19	0.38	0.19	0.41	0.67	0.56	0.33	34.55	-1.31	4.84	5.08	0.17	26.53	0.01	14.77
34.25	0.08	0.12	0.19	0.37	0.18	0.40	0.66	0.55	0.32	45.09	-1.74	5.47	5.17	0.17	26.30	0.01	16.88
34.49	0.08	0.12	0.18	0.34	0.17	0.37	0.65	0.53	0.31	15.35	-0.73	3.13	4.78	0.26	24.68	0.01	9.28
34.50	0.08	0.12	0.18	0.32	0.11	0.33	0.63	0.50	0.27	37.63	-1.17	5.18	5.00	0.16	24.14	0.01	14.18
34.50	0.08	0.12	0.19	0.29	0.05	0.28	0.61	0.47	0.21	40.13	-1.19	5.38	4.96	0.15	23.47	0.01	14.77
34.50	0.08	0.12	0.18	0.31	0.11	0.32	0.63	0.50	0.26	39.10	-1.19	5.31	4.99	0.15	24.04	0.01	14.39
34.50	0.08	0.12	0.19	0.31	0.07	0.30	0.61	0.48	0.23	41.63	-1.45	5.45	5.06	0.15	24.02	0.01	15.75
34.80	0.08	0.12	0.18	0.32	0.15	0.34	0.64	0.51	0.28	30.04	-0.96	4.43	4.91	0.20	24.71	0.01	12.49
35.25	0.08	0.12	0.19	0.33	0.13	0.34	0.63	0.51	0.27	18.48	-0.53	3.53	4.62	0.23	25.32	0.01	8.12
35.25	0.08	0.12	0.18	0.33	0.17	0.36	0.65	0.52	0.30	15.93	-0.39	3.27	4.44	0.24	24.79	0.01	6.47
35.44	0.08	0.12	0.17	0.36	0.23	0.41	0.68	0.56	0.35	15.55	-0.56	3.12	4.60	0.27	25.75	0.01	7.80
35.49	0.08	0.12	0.18	0.35	0.19	0.39	0.66	0.54	0.32	21.40	-0.73	3.80	4.80	0.21	25.76	0.01	10.29
35.49	0.08	0.12	0.18	0.36	0.22	0.41	0.67	0.56	0.35	18.76	-0.56	3.58	4.67	0.21	25.66	0.01	8.55

Girth (cm)	B1	B2	B3	B4	ARVI	GEMI	IPVI	MSAVI	NDVI	txt_CON	txt_Cor	txt_DIS	txt_ENT	txt_HOM	txt_Mean	txt_ASM	txt_Var
35.49	0.08	0.12	0.18	0.34	0.15	0.36	0.65	0.53	0.30	33.78	-1.23	4.71	5.02	0.19	25.11	0.01	13.76
35.49	0.08	0.12	0.19	0.35	0.16	0.38	0.65	0.54	0.31	35.36	-1.31	4.83	5.04	0.19	25.49	0.01	14.22
35.49	0.08	0.12	0.19	0.34	0.14	0.36	0.64	0.52	0.29	37.55	-1.39	5.08	5.10	0.17	25.19	0.01	14.99
36.25	0.08	0.12	0.18	0.35	0.19	0.39	0.66	0.54	0.33	27.59	-0.62	4.41	4.72	0.18	25.29	0.01	9.65
36.25	0.08	0.12	0.18	0.34	0.19	0.38	0.66	0.54	0.32	35.39	-0.96	4.98	4.93	0.16	24.89	0.01	12.48
36.25	0.08	0.12	0.18	0.35	0.19	0.39	0.66	0.54	0.32	26.29	-0.69	4.29	4.76	0.18	25.13	0.01	9.72
36.25	0.07	0.11	0.17	0.33	0.20	0.38	0.67	0.53	0.33	24.48	-0.70	4.13	4.72	0.19	24.58	0.01	9.50
36.25	0.08	0.12	0.17	0.36	0.23	0.41	0.68	0.56	0.36	21.63	-0.49	3.89	4.57	0.20	25.32	0.01	8.00
36.25	0.08	0.12	0.19	0.34	0.13	0.35	0.64	0.52	0.28	24.83	-0.64	4.18	4.74	0.18	25.29	0.01	9.34
36.25	0.08	0.12	0.18	0.37	0.21	0.41	0.67	0.56	0.35	21.58	-0.64	3.82	4.72	0.21	26.00	0.01	8.85
36.43	0.08	0.12	0.17	0.35	0.21	0.40	0.67	0.55	0.34	13.69	-0.46	2.99	4.50	0.27	24.86	0.01	6.63
37.10	0.08	0.12	0.17	0.35	0.22	0.40	0.67	0.55	0.35	30.02	-0.88	4.59	4.85	0.17	25.45	0.01	12.75
37.10	0.08	0.12	0.17	0.37	0.23	0.42	0.68	0.56	0.36	28.97	-1.03	4.53	4.87	0.17	26.31	0.01	15.05
37.10	0.08	0.12	0.19	0.37	0.20	0.40	0.67	0.56	0.34	25.88	-0.83	4.25	4.84	0.19	26.44	0.01	13.53
37.80	0.08	0.12	0.16	0.34	0.24	0.40	0.68	0.55	0.35	22.78	-0.69	3.99	4.76	0.19	24.87	0.01	9.24
37.80	0.08	0.12	0.17	0.35	0.24	0.40	0.68	0.55	0.36	20.08	-0.67	3.71	4.75	0.21	25.21	0.01	9.14
38.00	0.08	0.12	0.16	0.35	0.25	0.41	0.68	0.56	0.37	10.41	-0.34	2.56	4.37	0.31	24.91	0.02	5.89
38.00	0.08	0.12	0.17	0.36	0.25	0.42	0.68	0.56	0.36	11.80	-0.40	2.70	4.45	0.31	25.17	0.01	6.35
38.00	0.08	0.12	0.17	0.35	0.23	0.41	0.68	0.55	0.35	10.48	-0.36	2.61	4.42	0.29	25.22	0.01	5.86
38.00	0.08	0.12	0.17	0.36	0.26	0.42	0.69	0.56	0.37	10.62	-0.41	2.55	4.39	0.32	24.96	0.02	5.98
38.40	0.08	0.11	0.16	0.37	0.28	0.45	0.70	0.58	0.40	15.42	-0.40	3.22	4.46	0.24	25.36	0.01	6.32
38.40	0.08	0.12	0.16	0.37	0.30	0.45	0.70	0.59	0.41	13.88	-0.37	3.05	4.42	0.25	25.35	0.01	5.81
38.40	0.08	0.12	0.16	0.36	0.28	0.43	0.69	0.57	0.39	15.09	-0.61	3.15	4.61	0.25	24.56	0.01	7.49
38.40	0.08	0.12	0.17	0.36	0.24	0.42	0.68	0.56	0.37	21.03	-0.71	3.72	4.75	0.22	25.28	0.01	8.95
38.40	0.08	0.12	0.17	0.35	0.22	0.40	0.67	0.55	0.35	29.14	-1.09	4.44	4.99	0.18	24.92	0.01	12.47
38.50	0.08	0.12	0.17	0.35	0.23	0.40	0.67	0.55	0.35	14.13	-0.50	3.03	4.48	0.26	24.69	0.01	6.76
38.50	0.08	0.11	0.16	0.35	0.25	0.41	0.69	0.56	0.37	13.87	-0.50	3.03	4.41	0.26	24.29	0.02	6.65
38.50	0.08	0.12	0.17	0.37	0.26	0.43	0.69	0.57	0.37	17.91	-0.71	3.38	4.59	0.24	25.65	0.01	8.17
38.50	0.08	0.12	0.17	0.35	0.22	0.40	0.67	0.55	0.34	27.38	-0.66	4.44	4.76	0.17	25.21	0.01	10.63
38.50	0.08	0.12	0.16	0.36	0.26	0.42	0.69	0.57	0.38	22.18	-0.62	3.93	4.71	0.20	24.67	0.01	8.96
39.00	0.08	0.12	0.18	0.36	0.22	0.41	0.67	0.56	0.34	17.23	-0.63	3.30	4.65	0.25	25.95	0.01	8.57
39.00	0.08	0.12	0.18	0.36	0.19	0.39	0.66	0.55	0.32	20.11	-0.72	3.58	4.76	0.23	25.82	0.01	9.88
40.50	0.07	0.11	0.15	0.38	0.32	0.46	0.71	0.59	0.43	17.43	-0.70	3.38	4.61	0.23	24.73	0.01	9.04
40.50	0.08	0.11	0.16	0.38	0.29	0.46	0.70	0.59	0.40	15.23	-0.32	3.23	4.34	0.23	25.68	0.02	5.73
40.50	0.08	0.12	0.16	0.38	0.30	0.46	0.71	0.59	0.41	16.55	-0.38	3.39	4.43	0.22	25.77	0.01	6.37
40.50	0.08	0.12	0.17	0.37	0.25	0.42	0.68	0.57	0.37	13.07	-0.33	2.94	4.35	0.27	25.50	0.02	5.55
40.50	0.08	0.12	0.17	0.38	0.27	0.45	0.69	0.58	0.39	16.74	-0.45	3.34	4.52	0.24	25.83	0.01	6.93
40.50	0.08	0.11	0.16	0.38	0.30	0.46	0.70	0.59	0.41	14.89	-0.36	3.17	4.39	0.25	25.57	0.02	6.01
40.60	0.07	0.11	0.16	0.36	0.26	0.42	0.69	0.56	0.38	11.49	-0.45	2.68	4.36	0.30	24.64	0.02	5.95
40.60	0.07	0.12	0.17	0.38	0.27	0.45	0.69	0.58	0.39	11.19	-0.35	2.70	4.30	0.29	25.54	0.02	5.32

Girth (cm)	B1	B2	B3	B4	ARVI	GEMI	IPVI	MSAVI	NDVI	txt_CON	txt_Cor	txt_DIS	txt_ENT	txt_HOM	txt_Mean	txt_ASM	txt_Var
40.60	0.07	0.11	0.16	0.38	0.29	0.45	0.70	0.59	0.40	11.69	-0.38	2.72	4.34	0.30	25.49	0.02	5.44
44.50	0.07	0.11	0.15	0.37	0.32	0.46	0.71	0.59	0.42	20.32	-1.02	3.57	4.84	0.23	24.68	0.01	10.26
44.50	0.07	0.11	0.15	0.38	0.33	0.47	0.72	0.60	0.43	12.48	-0.49	2.82	4.51	0.28	25.01	0.01	6.48
45.50	0.08	0.12	0.16	0.35	0.25	0.41	0.68	0.56	0.36	11.26	-0.43	2.66	4.35	0.30	24.57	0.02	6.14
45.80	0.08	0.12	0.16	0.36	0.26	0.43	0.69	0.57	0.38	14.78	-0.56	3.04	4.54	0.28	24.91	0.01	7.20
46.50	0.08	0.12	0.17	0.38	0.28	0.45	0.70	0.59	0.39	14.43	-0.41	3.09	4.44	0.25	25.81	0.01	6.08
46.50	0.08	0.12	0.17	0.36	0.24	0.42	0.68	0.56	0.36	8.78	-0.25	2.33	4.06	0.33	25.37	0.02	3.95
46.60	0.08	0.12	0.16	0.35	0.25	0.41	0.68	0.56	0.37	11.77	-0.60	2.63	4.51	0.31	25.04	0.01	8.19
46.60	0.08	0.12	0.17	0.36	0.24	0.42	0.68	0.56	0.36	9.84	-0.39	2.45	4.33	0.33	25.33	0.02	5.90
46.80	0.08	0.11	0.15	0.34	0.27	0.40	0.69	0.55	0.38	12.31	-0.44	2.82	4.33	0.27	24.00	0.02	6.55
46.80	0.07	0.11	0.15	0.36	0.31	0.44	0.71	0.57	0.41	11.27	-0.29	2.74	4.26	0.28	24.27	0.02	4.88
46.80	0.08	0.11	0.15	0.35	0.29	0.43	0.70	0.57	0.40	12.62	-0.38	2.91	4.38	0.26	24.27	0.02	5.52
46.80	0.07	0.11	0.15	0.35	0.29	0.43	0.70	0.57	0.40	11.96	-0.31	2.83	4.22	0.27	24.31	0.02	4.90
48.00	0.08	0.12	0.16	0.37	0.31	0.45	0.70	0.58	0.41	10.86	-0.31	2.67	4.30	0.28	24.79	0.02	5.05
48.00	0.07	0.11	0.15	0.37	0.34	0.46	0.71	0.59	0.43	10.85	-0.31	2.64	4.28	0.30	25.09	0.02	4.93
48.00	0.08	0.12	0.16	0.38	0.31	0.46	0.71	0.59	0.41	12.85	-0.40	2.91	4.47	0.27	25.50	0.01	6.13
48.00	0.08	0.11	0.15	0.38	0.34	0.47	0.72	0.60	0.43	11.46	-0.34	2.70	4.34	0.30	25.33	0.02	5.27
48.00	0.08	0.12	0.16	0.37	0.27	0.43	0.69	0.57	0.38	8.11	-0.29	2.20	4.10	0.36	25.41	0.02	4.36
48.00	0.07	0.11	0.15	0.37	0.31	0.46	0.71	0.59	0.42	11.38	-0.34	2.70	4.33	0.29	25.33	0.02	5.41
48.20	0.08	0.13	0.19	0.34	0.15	0.36	0.64	0.52	0.29	8.42	-0.44	2.22	4.30	0.36	24.98	0.02	6.29
48.20	0.07	0.11	0.16	0.36	0.28	0.44	0.70	0.57	0.39	8.36	-0.30	2.23	4.11	0.36	24.96	0.02	4.44
48.20	0.08	0.12	0.17	0.37	0.25	0.43	0.68	0.57	0.37	8.76	-0.34	2.28	4.20	0.35	25.56	0.02	5.42
48.20	0.08	0.11	0.16	0.37	0.29	0.45	0.70	0.58	0.40	5.70	-0.16	1.84	3.78	0.40	25.38	0.03	2.97
49.10	0.08	0.11	0.17	0.36	0.23	0.41	0.68	0.56	0.36	11.39	-0.40	2.66	4.35	0.30	25.03	0.02	5.40
49.10	0.08	0.11	0.17	0.35	0.23	0.41	0.68	0.55	0.35	12.89	-0.44	2.84	4.42	0.28	25.14	0.02	6.05
49.10	0.08	0.12	0.17	0.36	0.23	0.41	0.68	0.56	0.35	11.64	-0.40	2.73	4.35	0.28	25.21	0.02	5.57
49.10	0.08	0.12	0.17	0.35	0.22	0.40	0.67	0.55	0.35	10.17	-0.32	2.53	4.24	0.31	24.79	0.02	4.82
50.50	0.07	0.11	0.16	0.38	0.31	0.46	0.71	0.59	0.41	11.92	-0.43	2.76	4.42	0.29	24.87	0.02	5.88
50.50	0.07	0.11	0.15	0.39	0.34	0.48	0.72	0.61	0.44	15.18	-0.53	3.10	4.54	0.26	25.35	0.01	6.82
50.80	0.07	0.11	0.17	0.36	0.25	0.42	0.69	0.56	0.37	10.76	-0.35	2.63	4.33	0.30	24.93	0.02	5.26
50.80	0.07	0.11	0.16	0.36	0.26	0.43	0.69	0.57	0.38	10.81	-0.34	2.61	4.29	0.30	25.08	0.02	5.00
50.80	0.07	0.11	0.16	0.36	0.25	0.43	0.69	0.57	0.38	11.91	-0.44	2.74	4.47	0.29	25.25	0.01	6.16
52.80	0.07	0.11	0.16	0.37	0.28	0.44	0.70	0.58	0.40	14.87	-0.65	2.97	4.56	0.28	25.11	0.01	8.21
52.80	0.07	0.11	0.15	0.39	0.33	0.48	0.72	0.60	0.44	14.99	-0.57	3.10	4.60	0.26	25.34	0.01	7.48
52.80	0.07	0.11	0.16	0.37	0.27	0.44	0.69	0.58	0.39	12.75	-0.49	2.79	4.44	0.29	25.12	0.02	6.87
52.80	0.07	0.11	0.15	0.37	0.31	0.45	0.71	0.59	0.42	13.53	-0.49	2.92	4.43	0.27	24.99	0.02	6.33
52.80	0.07	0.11	0.16	0.36	0.27	0.44	0.69	0.57	0.39	10.69	-0.39	2.58	4.31	0.31	24.84	0.02	5.26
52.80	0.07	0.11	0.16	0.38	0.30	0.46	0.71	0.59	0.41	13.74	-0.56	2.87	4.44	0.28	25.28	0.02	6.55
52.80	0.07	0.11	0.16	0.38	0.29	0.46	0.70	0.59	0.41	18.52	-0.92	3.31	4.69	0.26	25.05	0.01	9.05
52.80	0.08	0.12	0.17	0.36	0.22	0.41	0.67	0.56	0.35	9.53	-0.34	2.43	4.31	0.33	24.86	0.02	5.17

Girth (cm)	B1	B2	B3	B4	ARVI	GEMI	IPVI	MSAVI	NDVI	txt_CON	txt_Cor	txt_DIS	txt_ENT	txt_HOM	txt_Mean	txt_ASM	txt_Var
52.80	0.08	0.12	0.18	0.36	0.21	0.41	0.67	0.56	0.35	10.42	-0.30	2.57	4.31	0.31	25.25	0.02	5.10
52.80	0.08	0.12	0.18	0.35	0.19	0.38	0.66	0.54	0.32	10.94	-0.41	2.60	4.42	0.31	24.90	0.02	6.43
52.98	0.08	0.12	0.16	0.37	0.28	0.45	0.70	0.58	0.39	8.24	-0.30	2.26	4.18	0.34	25.06	0.02	4.37
53.20	0.08	0.11	0.15	0.35	0.28	0.42	0.69	0.56	0.39	9.22	-0.30	2.43	4.17	0.32	24.21	0.02	4.43
53.20	0.08	0.11	0.15	0.36	0.29	0.43	0.70	0.57	0.40	8.43	-0.29	2.30	4.12	0.34	24.63	0.02	4.64
53.20	0.08	0.11	0.15	0.36	0.30	0.44	0.70	0.58	0.41	9.92	-0.31	2.49	4.21	0.32	24.90	0.02	4.61
53.20	0.08	0.11	0.15	0.36	0.30	0.44	0.70	0.57	0.40	8.33	-0.24	2.29	4.06	0.34	24.61	0.02	3.87
53.50	0.08	0.11	0.16	0.36	0.26	0.42	0.69	0.56	0.37	12.44	-0.46	2.82	4.46	0.28	24.76	0.01	6.20
53.50	0.08	0.11	0.16	0.36	0.28	0.44	0.69	0.57	0.39	11.72	-0.41	2.71	4.38	0.30	25.05	0.02	5.90
53.50	0.08	0.11	0.16	0.36	0.27	0.43	0.69	0.57	0.39	13.71	-0.45	3.01	4.52	0.26	25.11	0.01	6.79
54.70	0.08	0.11	0.16	0.33	0.25	0.39	0.68	0.54	0.36	10.78	-0.53	2.54	4.37	0.32	24.08	0.02	6.74
54.70	0.08	0.11	0.16	0.36	0.27	0.43	0.69	0.57	0.38	9.36	-0.37	2.35	4.19	0.34	24.74	0.02	4.76
54.70	0.08	0.12	0.17	0.36	0.24	0.41	0.68	0.56	0.35	13.32	-0.62	2.72	4.44	0.32	25.49	0.02	7.41
54.80	0.07	0.11	0.15	0.31	0.24	0.37	0.68	0.52	0.36	8.22	-0.31	2.17	3.92	0.36	22.54	0.03	4.02
54.80	0.07	0.11	0.15	0.32	0.24	0.38	0.68	0.53	0.36	5.88	-0.18	1.92	3.77	0.38	22.97	0.03	2.84
54.80	0.07	0.11	0.15	0.33	0.28	0.41	0.69	0.55	0.39	8.10	-0.30	2.14	3.93	0.37	23.30	0.03	4.00
54.80	0.07	0.11	0.15	0.34	0.26	0.41	0.69	0.55	0.38	6.94	-0.23	2.04	3.86	0.37	23.56	0.03	3.20
54.98	0.08	0.12	0.18	0.35	0.19	0.38	0.66	0.54	0.32	10.55	-0.48	2.49	4.41	0.33	25.16	0.02	7.41
55.80	0.07	0.11	0.15	0.36	0.29	0.44	0.70	0.57	0.40	8.54	-0.31	2.32	4.15	0.33	24.60	0.02	4.70
55.80	0.07	0.11	0.15	0.36	0.30	0.44	0.70	0.57	0.41	8.40	-0.26	2.28	4.08	0.34	24.59	0.02	3.96
55.80	0.07	0.11	0.15	0.37	0.31	0.45	0.71	0.58	0.41	8.73	-0.35	2.29	4.14	0.34	25.06	0.02	5.62
55.80	0.07	0.11	0.15	0.36	0.31	0.45	0.71	0.58	0.41	8.14	-0.29	2.21	4.10	0.35	24.84	0.02	4.23
58.50	0.08	0.11	0.15	0.35	0.29	0.43	0.70	0.57	0.39	6.91	-0.28	1.98	3.88	0.39	24.44	0.03	4.42
58.50	0.08	0.12	0.16	0.35	0.28	0.42	0.69	0.56	0.38	5.37	-0.16	1.79	3.69	0.41	24.69	0.04	2.67
58.50	0.08	0.11	0.15	0.37	0.32	0.45	0.71	0.58	0.41	8.92	-0.29	2.26	4.05	0.36	25.09	0.03	4.22
58.50	0.08	0.11	0.16	0.35	0.26	0.42	0.69	0.56	0.38	6.68	-0.25	1.97	3.91	0.38	24.90	0.03	3.57
65.50	0.08	0.11	0.16	0.33	0.24	0.39	0.68	0.54	0.35	5.61	-0.15	1.84	3.66	0.40	23.96	0.04	2.56
65.50	0.08	0.11	0.16	0.34	0.25	0.40	0.68	0.54	0.36	5.03	-0.13	1.75	3.55	0.41	23.93	0.04	2.29
65.50	0.08	0.11	0.16	0.34	0.26	0.40	0.68	0.55	0.37	5.61	-0.15	1.86	3.65	0.39	24.04	0.04	2.50
65.50	0.08	0.11	0.16	0.36	0.26	0.43	0.69	0.57	0.38	7.81	-0.28	2.14	4.01	0.36	24.99	0.03	3.94
65.50	0.08	0.12	0.16	0.33	0.23	0.38	0.67	0.53	0.34	5.45	-0.18	1.79	3.69	0.41	23.99	0.04	2.76
65.50	0.08	0.12	0.16	0.34	0.24	0.40	0.68	0.55	0.35	6.02	-0.18	1.87	3.71	0.40	24.53	0.03	2.81
65.50	0.08	0.11	0.16	0.33	0.25	0.40	0.68	0.54	0.36	5.07	-0.12	1.75	3.55	0.42	23.89	0.04	2.29
65.50	0.08	0.12	0.17	0.36	0.22	0.41	0.67	0.56	0.35	7.65	-0.24	2.12	3.96	0.36	25.52	0.03	3.82
65.50	0.08	0.11	0.16	0.34	0.26	0.40	0.68	0.55	0.37	5.91	-0.19	1.89	3.80	0.39	24.31	0.03	2.93
65.50	0.08	0.12	0.16	0.36	0.27	0.43	0.69	0.57	0.38	6.11	-0.17	1.93	3.75	0.38	25.05	0.03	2.79
69.80	0.08	0.12	0.18	0.32	0.16	0.35	0.65	0.51	0.29	5.54	-0.19	1.83	3.75	0.40	24.50	0.03	3.13
71.00	0.07	0.11	0.15	0.34	0.28	0.41	0.69	0.55	0.39	7.57	-0.24	2.16	3.93	0.35	23.68	0.03	3.42
71.00	0.07	0.11	0.15	0.32	0.26	0.39	0.68	0.53	0.37	7.42	-0.29	2.14	4.01	0.36	23.04	0.03	3.70
71.00	0.08	0.11	0.15	0.34	0.29	0.42	0.70	0.56	0.39	8.18	-0.28	2.22	3.98	0.35	23.80	0.03	3.76

Girth (cm)	B1	B2	B3	B4	ARVI	GEMI	IPVI	MSAVI	NDVI	txt_CON	txt_Cor	txt_DIS	txt_ENT	txt_HOM	txt_Mean	txt_ASM	txt_Var
71.00	0.08	0.11	0.15	0.34	0.26	0.40	0.69	0.55	0.38	8.02	-0.29	2.19	3.99	0.36	23.88	0.03	3.91
71.40	0.07	0.11	0.16	0.31	0.21	0.36	0.66	0.52	0.33	6.54	-0.24	1.96	3.83	0.38	23.25	0.03	3.41
71.40	0.08	0.12	0.17	0.32	0.17	0.35	0.65	0.51	0.30	5.33	-0.21	1.74	3.71	0.42	23.71	0.04	3.14
71.50	0.08	0.12	0.17	0.32	0.18	0.36	0.66	0.52	0.31	5.39	-0.19	1.78	3.73	0.41	23.89	0.03	2.80
71.50	0.08	0.11	0.16	0.30	0.17	0.34	0.65	0.50	0.30	6.32	-0.19	1.97	3.80	0.38	22.97	0.03	2.93
71.50	0.08	0.11	0.16	0.32	0.22	0.37	0.67	0.53	0.34	5.07	-0.20	1.73	3.66	0.42	23.40	0.04	2.72
71.50	0.07	0.11	0.16	0.32	0.23	0.38	0.67	0.53	0.35	6.91	-0.25	1.95	3.88	0.40	23.76	0.03	3.42
71.50	0.08	0.11	0.17	0.33	0.20	0.38	0.67	0.53	0.33	4.54	-0.13	1.63	3.56	0.44	24.06	0.04	2.33
71.50	0.07	0.11	0.17	0.31	0.16	0.34	0.65	0.51	0.30	9.02	-0.34	2.33	4.11	0.34	23.11	0.02	4.92
72.40	0.07	0.11	0.18	0.33	0.14	0.35	0.64	0.51	0.29	7.09	-0.25	2.07	4.00	0.37	24.04	0.03	3.66
72.50	0.08	0.12	0.18	0.33	0.15	0.35	0.64	0.52	0.29	5.34	-0.16	1.79	3.73	0.41	24.50	0.03	2.73
72.50	0.08	0.11	0.17	0.33	0.19	0.37	0.66	0.53	0.32	6.45	-0.22	1.97	3.91	0.39	24.05	0.03	3.30
72.50	0.08	0.12	0.18	0.32	0.14	0.34	0.64	0.51	0.28	6.38	-0.25	1.96	3.98	0.38	24.07	0.03	3.62
72.50	0.08	0.11	0.17	0.33	0.20	0.37	0.66	0.53	0.33	6.91	-0.24	2.07	3.95	0.36	23.74	0.03	3.41
72.50	0.07	0.11	0.16	0.30	0.17	0.34	0.65	0.50	0.31	5.71	-0.16	1.88	3.75	0.39	22.52	0.03	2.76
72.50	0.07	0.11	0.16	0.31	0.20	0.36	0.66	0.51	0.33	6.50	-0.22	2.00	3.86	0.38	22.72	0.03	3.14
72.50	0.07	0.11	0.17	0.30	0.16	0.33	0.65	0.50	0.29	5.85	-0.19	1.89	3.82	0.39	22.88	0.03	3.03
72.50	0.07	0.11	0.16	0.31	0.19	0.35	0.66	0.51	0.32	5.65	-0.17	1.85	3.74	0.40	22.83	0.03	2.77
72.50	0.07	0.11	0.15	0.31	0.22	0.37	0.67	0.52	0.34	6.12	-0.24	1.88	3.82	0.40	22.79	0.03	3.36
72.50	0.07	0.11	0.15	0.32	0.27	0.39	0.69	0.54	0.37	6.76	-0.26	2.01	3.91	0.38	23.01	0.03	3.64
72.50	0.07	0.11	0.15	0.33	0.28	0.41	0.69	0.55	0.39	7.75	-0.25	2.20	3.98	0.34	23.51	0.03	3.63
72.50	0.07	0.11	0.15	0.33	0.26	0.40	0.69	0.54	0.37	6.35	-0.19	1.96	3.79	0.38	23.47	0.03	2.91
72.50	0.07	0.11	0.15	0.32	0.24	0.38	0.68	0.53	0.35	7.49	-0.26	2.13	3.99	0.36	23.01	0.02	3.67
72.50	0.08	0.11	0.15	0.31	0.24	0.37	0.68	0.52	0.35	8.60	-0.34	2.26	4.08	0.35	23.04	0.02	4.23
72.50	0.08	0.11	0.16	0.32	0.23	0.37	0.67	0.52	0.34	8.89	-0.38	2.32	4.12	0.33	22.94	0.02	4.46
72.50	0.08	0.11	0.16	0.31	0.20	0.35	0.66	0.51	0.32	6.98	-0.26	2.06	3.89	0.36	23.00	0.03	3.39
72.50	0.08	0.11	0.16	0.32	0.21	0.37	0.66	0.52	0.33	6.87	-0.24	1.97	3.89	0.39	23.80	0.03	3.60
72.50	0.07	0.11	0.16	0.32	0.23	0.38	0.67	0.53	0.35	6.78	-0.23	2.03	3.87	0.37	23.30	0.03	3.28
72.50	0.08	0.11	0.15	0.32	0.24	0.37	0.67	0.53	0.35	5.81	-0.18	1.87	3.74	0.39	23.19	0.03	2.84
72.50	0.08	0.12	0.18	0.32	0.14	0.34	0.64	0.51	0.28	10.29	-0.55	2.44	4.43	0.34	24.07	0.02	6.81
72.50	0.08	0.11	0.16	0.32	0.20	0.37	0.66	0.52	0.33	7.20	-0.26	2.06	3.89	0.37	23.62	0.03	3.50
72.50	0.08	0.11	0.16	0.32	0.22	0.37	0.67	0.52	0.33	5.73	-0.21	1.86	3.75	0.40	23.22	0.03	2.87
72.50	0.08	0.12	0.17	0.31	0.17	0.34	0.65	0.51	0.30	5.46	-0.19	1.79	3.72	0.41	23.57	0.03	2.76
72.50	0.08	0.11	0.16	0.31	0.22	0.37	0.67	0.52	0.34	5.64	-0.17	1.82	3.69	0.40	23.22	0.03	2.77
72.50	0.08	0.12	0.16	0.32	0.21	0.36	0.66	0.52	0.33	6.13	-0.20	1.91	3.79	0.39	23.49	0.03	2.91
72.50	0.08	0.11	0.16	0.32	0.23	0.38	0.67	0.53	0.34	5.39	-0.15	1.82	3.70	0.40	23.41	0.03	2.60
72.50	0.08	0.12	0.17	0.33	0.21	0.37	0.66	0.53	0.33	9.92	-0.35	2.50	4.27	0.32	24.14	0.02	4.84
72.50	0.07	0.11	0.15	0.33	0.27	0.40	0.69	0.55	0.37	7.25	-0.23	2.10	3.91	0.36	23.79	0.03	3.40
72.50	0.07	0.11	0.15	0.34	0.28	0.41	0.69	0.55	0.38	6.24	-0.18	1.94	3.81	0.39	23.92	0.03	2.89
72.50	0.07	0.11	0.15	0.34	0.28	0.41	0.69	0.55	0.38	7.34	-0.23	2.12	3.92	0.36	23.87	0.03	3.47

Girth (cm)	B1	B2	B3	B4	ARVI	GEMI	IPVI	MSAVI	NDVI	txt_CON	txt_Cor	txt_DIS	txt_ENT	txt_HOM	txt_Mean	txt_ASM	txt_Var
72.60	0.08	0.11	0.16	0.32	0.20	0.37	0.66	0.52	0.33	7.46	-0.25	2.15	3.98	0.35	23.42	0.03	3.62
72.60	0.08	0.11	0.17	0.32	0.18	0.36	0.66	0.52	0.31	6.41	-0.20	1.99	3.79	0.37	23.55	0.03	2.95
73.50	0.08	0.11	0.17	0.31	0.17	0.35	0.65	0.51	0.31	6.48	-0.20	1.99	3.79	0.38	23.35	0.03	2.96
73.50	0.08	0.12	0.17	0.32	0.16	0.35	0.65	0.51	0.29	5.37	-0.14	1.81	3.66	0.40	23.79	0.03	2.53
73.50	0.08	0.11	0.17	0.31	0.15	0.34	0.65	0.50	0.29	5.49	-0.17	1.84	3.77	0.39	23.46	0.03	2.79
73.50	0.08	0.11	0.17	0.32	0.15	0.34	0.65	0.51	0.29	6.14	-0.18	1.93	3.80	0.39	23.69	0.03	2.91
73.50	0.08	0.12	0.18	0.32	0.15	0.35	0.65	0.51	0.29	5.46	-0.17	1.82	3.75	0.40	23.93	0.03	2.85
73.50	0.08	0.12	0.17	0.33	0.18	0.36	0.66	0.52	0.31	5.09	-0.16	1.75	3.67	0.41	24.03	0.04	2.56
73.50	0.08	0.11	0.17	0.32	0.16	0.35	0.65	0.51	0.30	5.15	-0.15	1.79	3.69	0.40	23.62	0.03	2.60
74.50	0.07	0.11	0.16	0.32	0.21	0.37	0.67	0.52	0.34	5.05	-0.16	1.72	3.64	0.42	23.30	0.04	2.53
74.50	0.08	0.11	0.17	0.31	0.17	0.34	0.65	0.50	0.30	5.40	-0.18	1.78	3.73	0.41	23.05	0.03	2.78
74.50	0.07	0.11	0.16	0.33	0.23	0.39	0.67	0.54	0.35	4.63	-0.15	1.64	3.59	0.44	23.61	0.04	2.38
74.50	0.08	0.12	0.18	0.32	0.14	0.34	0.64	0.50	0.28	9.83	-0.41	2.29	4.18	0.36	23.52	0.02	5.82
74.60	0.07	0.11	0.17	0.32	0.18	0.36	0.66	0.51	0.31	5.01	-0.12	1.74	3.54	0.41	23.43	0.04	2.25
75.20	0.08	0.12	0.17	0.33	0.19	0.37	0.66	0.53	0.32	3.85	-0.08	1.52	3.36	0.45	24.32	0.05	1.84
75.20	0.08	0.12	0.18	0.33	0.18	0.36	0.65	0.52	0.31	9.41	-0.46	2.20	4.12	0.38	23.94	0.03	5.82
75.20	0.08	0.12	0.17	0.33	0.19	0.36	0.66	0.52	0.31	5.81	-0.16	1.87	3.66	0.40	24.09	0.04	2.61
75.20	0.08	0.12	0.17	0.33	0.21	0.38	0.67	0.53	0.33	7.10	-0.28	1.99	3.89	0.39	24.28	0.03	4.13
75.20	0.08	0.12	0.18	0.30	0.09	0.29	0.62	0.48	0.23	11.33	-0.64	2.50	4.46	0.34	24.77	0.02	10.53
75.20	0.08	0.12	0.18	0.32	0.16	0.34	0.64	0.51	0.29	6.67	-0.24	1.95	3.83	0.39	24.10	0.03	3.40
75.50	0.08	0.12	0.17	0.33	0.17	0.36	0.65	0.52	0.30	4.52	-0.15	1.62	3.56	0.44	24.11	0.04	2.40
75.50	0.08	0.12	0.17	0.33	0.20	0.38	0.66	0.53	0.33	3.84	-0.11	1.49	3.42	0.46	24.27	0.05	2.03
75.50	0.08	0.12	0.17	0.33	0.18	0.36	0.65	0.52	0.31	3.97	-0.10	1.53	3.41	0.45	24.08	0.05	1.97
75.50	0.08	0.12	0.18	0.33	0.17	0.37	0.65	0.53	0.31	4.18	-0.11	1.56	3.46	0.45	24.40	0.04	2.07
75.50	0.08	0.11	0.16	0.34	0.23	0.40	0.68	0.54	0.35	5.26	-0.16	1.78	3.71	0.41	24.41	0.03	2.65
75.50	0.08	0.12	0.17	0.33	0.18	0.37	0.66	0.53	0.31	5.09	-0.15	1.75	3.71	0.41	24.42	0.03	2.72
75.50	0.07	0.11	0.16	0.32	0.19	0.36	0.66	0.52	0.32	5.64	-0.19	1.84	3.77	0.40	23.49	0.03	2.89
75.50	0.07	0.11	0.16	0.34	0.23	0.40	0.68	0.54	0.35	6.44	-0.25	1.89	3.83	0.41	24.27	0.03	3.47
75.50	0.08	0.12	0.17	0.35	0.22	0.40	0.67	0.55	0.34	4.69	-0.14	1.66	3.59	0.43	24.77	0.04	2.39
75.50	0.07	0.11	0.17	0.31	0.16	0.34	0.65	0.50	0.30	6.06	-0.19	1.91	3.76	0.39	22.97	0.03	3.07
75.50	0.08	0.11	0.17	0.32	0.16	0.35	0.65	0.51	0.30	5.09	-0.14	1.77	3.63	0.41	23.78	0.04	2.47
75.50	0.07	0.11	0.15	0.32	0.24	0.38	0.68	0.53	0.36	8.12	-0.41	2.18	4.13	0.36	22.58	0.02	4.92
75.50	0.07	0.11	0.15	0.32	0.23	0.38	0.68	0.53	0.35	7.70	-0.30	2.16	4.02	0.35	22.62	0.02	4.11
75.50	0.07	0.11	0.16	0.32	0.21	0.38	0.67	0.53	0.34	7.28	-0.27	2.11	4.00	0.36	23.18	0.02	3.77
75.50	0.07	0.11	0.16	0.34	0.23	0.39	0.68	0.54	0.36	9.47	-0.37	2.36	4.16	0.34	23.65	0.02	4.75
75.50	0.07	0.11	0.16	0.32	0.22	0.38	0.67	0.53	0.35	6.38	-0.20	1.97	3.87	0.38	23.12	0.03	3.13
75.50	0.08	0.12	0.17	0.32	0.18	0.36	0.65	0.52	0.31	5.17	-0.16	1.77	3.66	0.41	23.89	0.04	2.55
75.50	0.08	0.12	0.18	0.32	0.14	0.35	0.64	0.51	0.29	4.61	-0.14	1.63	3.57	0.44	24.19	0.04	2.43
75.50	0.08	0.12	0.17	0.33	0.18	0.36	0.66	0.52	0.31	5.10	-0.16	1.74	3.64	0.42	23.95	0.04	2.76
75.50	0.08	0.11	0.17	0.31	0.17	0.35	0.65	0.51	0.30	4.42	-0.12	1.61	3.49	0.44	23.49	0.04	2.18

Girth (cm)	B1	B2	B3	B4	ARVI	GEMI	IPVI	MSAVI	NDVI	txt_CON	txt_Cor	txt_DIS	txt_ENT	txt_HOM	txt_Mean	txt_ASM	txt_Var
75.50	0.08	0.12	0.17	0.32	0.17	0.35	0.65	0.51	0.30	4.05	-0.11	1.53	3.40	0.46	23.66	0.05	1.98
75.50	0.08	0.12	0.18	0.33	0.16	0.36	0.65	0.52	0.30	4.66	-0.17	1.59	3.52	0.46	24.10	0.04	2.58
75.50	0.08	0.12	0.18	0.32	0.15	0.34	0.64	0.51	0.29	3.83	-0.11	1.44	3.27	0.48	23.83	0.05	1.95
75.50	0.08	0.11	0.16	0.32	0.19	0.36	0.66	0.51	0.32	3.98	-0.11	1.51	3.44	0.46	23.43	0.05	2.07
75.50	0.08	0.11	0.17	0.32	0.19	0.36	0.66	0.52	0.32	5.92	-0.22	1.81	3.72	0.41	23.54	0.03	3.09
75.50	0.08	0.12	0.17	0.32	0.18	0.35	0.65	0.51	0.31	5.39	-0.17	1.79	3.68	0.41	23.54	0.03	2.63
75.50	0.08	0.11	0.17	0.32	0.18	0.35	0.65	0.51	0.31	3.89	-0.09	1.53	3.41	0.45	23.45	0.04	1.99
75.50	0.08	0.12	0.18	0.31	0.14	0.33	0.64	0.50	0.27	5.54	-0.18	1.81	3.73	0.41	23.42	0.03	2.88
75.50	0.08	0.12	0.17	0.31	0.17	0.35	0.65	0.51	0.30	5.07	-0.15	1.71	3.59	0.43	23.51	0.04	2.45
75.50	0.08	0.12	0.17	0.32	0.20	0.36	0.66	0.52	0.32	4.94	-0.13	1.73	3.60	0.42	23.60	0.04	2.40
75.50	0.08	0.11	0.17	0.32	0.19	0.37	0.66	0.52	0.32	5.50	-0.19	1.76	3.68	0.42	23.84	0.04	2.82
75.50	0.08	0.11	0.16	0.32	0.19	0.36	0.66	0.52	0.32	4.23	-0.10	1.58	3.44	0.44	23.42	0.04	2.03
75.50	0.08	0.11	0.16	0.32	0.20	0.37	0.66	0.52	0.32	4.19	-0.12	1.56	3.44	0.45	23.54	0.05	2.11
75.50	0.08	0.11	0.16	0.33	0.21	0.38	0.67	0.53	0.34	5.20	-0.18	1.72	3.62	0.42	23.96	0.04	2.78
75.50	0.08	0.12	0.17	0.32	0.20	0.36	0.66	0.52	0.32	4.33	-0.13	1.60	3.50	0.44	23.77	0.04	2.20
75.50	0.08	0.11	0.16	0.33	0.23	0.39	0.67	0.54	0.35	5.48	-0.18	1.79	3.65	0.41	23.83	0.04	2.76
75.50	0.08	0.11	0.17	0.33	0.20	0.37	0.66	0.53	0.33	4.16	-0.12	1.56	3.41	0.44	23.78	0.05	2.16
75.50	0.08	0.12	0.17	0.33	0.21	0.38	0.67	0.53	0.33	4.40	-0.15	1.57	3.54	0.46	23.98	0.04	2.42
76.00	0.08	0.11	0.17	0.33	0.19	0.37	0.66	0.52	0.32	5.27	-0.18	1.74	3.70	0.42	24.04	0.04	3.04
76.00	0.08	0.11	0.17	0.31	0.16	0.34	0.65	0.51	0.30	5.08	-0.21	1.76	3.74	0.41	23.20	0.03	3.37
76.00	0.08	0.11	0.17	0.32	0.18	0.36	0.65	0.51	0.31	4.23	-0.12	1.59	3.47	0.44	23.56	0.04	2.07
76.00	0.08	0.11	0.17	0.32	0.18	0.36	0.66	0.52	0.32	4.34	-0.13	1.62	3.53	0.43	23.73	0.04	2.21
76.00	0.08	0.11	0.17	0.31	0.15	0.33	0.64	0.50	0.28	7.16	-0.26	2.09	3.96	0.36	23.28	0.03	3.77
76.00	0.08	0.11	0.17	0.32	0.15	0.34	0.65	0.51	0.29	5.97	-0.22	1.90	3.84	0.39	23.87	0.03	3.34
76.00	0.08	0.11	0.17	0.32	0.19	0.37	0.66	0.52	0.32	5.94	-0.21	1.89	3.76	0.39	23.76	0.03	2.99
76.20	0.07	0.11	0.16	0.31	0.21	0.36	0.66	0.51	0.33	5.16	-0.17	1.72	3.58	0.43	22.66	0.04	2.50
76.20	0.07	0.11	0.16	0.32	0.22	0.37	0.67	0.52	0.34	5.06	-0.18	1.73	3.68	0.42	23.19	0.04	2.71
76.20	0.07	0.11	0.16	0.32	0.21	0.37	0.67	0.52	0.34	4.75	-0.13	1.67	3.52	0.43	23.03	0.04	2.21
76.20	0.07	0.11	0.16	0.33	0.22	0.38	0.67	0.53	0.34	4.84	-0.14	1.68	3.58	0.43	23.57	0.04	2.38
76.20	0.08	0.11	0.16	0.33	0.22	0.38	0.67	0.53	0.34	6.02	-0.25	1.84	3.88	0.41	24.04	0.03	3.56
76.20	0.08	0.12	0.17	0.33	0.20	0.37	0.66	0.53	0.33	4.41	-0.13	1.59	3.57	0.45	24.07	0.04	2.51
76.20	0.07	0.11	0.17	0.31	0.15	0.34	0.65	0.50	0.30	6.13	-0.20	1.94	3.83	0.38	22.94	0.03	3.01
76.50	0.08	0.12	0.17	0.33	0.18	0.37	0.66	0.53	0.31	4.92	-0.14	1.72	3.63	0.42	24.34	0.04	2.48
76.80	0.08	0.12	0.17	0.32	0.17	0.35	0.65	0.51	0.30	5.69	-0.25	1.84	3.85	0.40	23.54	0.03	3.89
77.50	0.08	0.12	0.17	0.30	0.14	0.33	0.64	0.50	0.28	4.18	-0.11	1.56	3.43	0.45	23.53	0.05	2.09
77.50	0.08	0.12	0.17	0.31	0.15	0.33	0.64	0.50	0.28	4.95	-0.18	1.68	3.63	0.43	23.88	0.04	2.93
77.50	0.08	0.12	0.17	0.33	0.19	0.37	0.66	0.53	0.32	4.81	-0.16	1.67	3.60	0.43	24.17	0.04	2.66
77.50	0.08	0.12	0.18	0.34	0.18	0.38	0.66	0.53	0.32	3.24	-0.07	1.36	3.29	0.49	24.63	0.05	1.70
77.50	0.08	0.12	0.17	0.33	0.18	0.37	0.66	0.53	0.32	4.43	-0.13	1.63	3.55	0.43	24.34	0.04	2.26
77.80	0.07	0.11	0.17	0.31	0.17	0.34	0.65	0.51	0.30	6.74	-0.27	2.00	3.92	0.38	22.98	0.03	3.88

Girth (cm)	B1	B2	B3	B4	ARVI	GEMI	IPVI	MSAVI	NDVI	txt_CON	txt_Cor	txt_DIS	txt_ENT	txt_HOM	txt_Mean	txt_ASM	txt_Var
77.80	0.08	0.12	0.18	0.32	0.14	0.35	0.64	0.51	0.28	5.28	-0.17	1.77	3.72	0.42	23.79	0.03	2.86
77.80	0.07	0.11	0.17	0.32	0.17	0.35	0.65	0.51	0.30	6.37	-0.20	1.99	3.88	0.38	23.45	0.03	3.23
78.00	0.08	0.12	0.18	0.32	0.15	0.35	0.64	0.51	0.29	6.18	-0.17	1.93	3.74	0.39	24.10	0.03	2.86
78.00	0.08	0.12	0.18	0.32	0.15	0.34	0.64	0.51	0.29	5.72	-0.14	1.89	3.66	0.39	23.88	0.04	2.55
78.30	0.08	0.12	0.18	0.32	0.12	0.33	0.63	0.50	0.27	6.45	-0.26	1.95	3.90	0.39	23.89	0.03	4.04
78.30	0.08	0.12	0.19	0.35	0.16	0.37	0.65	0.53	0.30	7.28	-0.22	2.14	3.96	0.35	25.44	0.03	3.64
78.30	0.08	0.12	0.19	0.35	0.16	0.37	0.65	0.53	0.30	6.35	-0.17	1.98	3.85	0.38	25.60	0.03	3.08
78.30	0.08	0.12	0.19	0.35	0.15	0.37	0.65	0.53	0.29	7.24	-0.20	2.12	3.92	0.35	25.62	0.03	3.43
78.30	0.08	0.12	0.20	0.35	0.12	0.35	0.64	0.52	0.27	5.37	-0.14	1.82	3.71	0.40	25.82	0.03	2.64
78.40	0.08	0.11	0.17	0.33	0.18	0.36	0.66	0.52	0.32	6.68	-0.21	2.04	3.90	0.36	23.80	0.03	3.23
78.40	0.08	0.12	0.18	0.34	0.18	0.37	0.66	0.53	0.32	5.42	-0.17	1.80	3.76	0.41	24.50	0.03	2.85
78.40	0.08	0.11	0.17	0.33	0.20	0.38	0.67	0.53	0.33	6.08	-0.19	1.91	3.82	0.39	23.95	0.03	3.05
78.40	0.08	0.12	0.18	0.33	0.15	0.35	0.64	0.51	0.29	4.94	-0.13	1.73	3.58	0.41	24.33	0.04	2.34
78.40	0.08	0.12	0.18	0.33	0.16	0.36	0.65	0.52	0.30	4.89	-0.13	1.70	3.58	0.43	24.40	0.04	2.33
78.40	0.08	0.12	0.18	0.33	0.17	0.36	0.65	0.52	0.31	5.38	-0.16	1.82	3.75	0.40	24.33	0.03	2.82
78.50	0.08	0.11	0.17	0.32	0.16	0.35	0.65	0.51	0.30	6.24	-0.20	1.94	3.78	0.38	23.54	0.03	2.93
78.70	0.08	0.11	0.17	0.32	0.16	0.35	0.65	0.51	0.30	5.59	-0.20	1.80	3.70	0.41	23.52	0.04	3.10
78.70	0.08	0.12	0.18	0.33	0.15	0.35	0.65	0.52	0.29	5.05	-0.15	1.73	3.61	0.42	24.16	0.04	2.43
79.40	0.08	0.12	0.17	0.34	0.22	0.40	0.67	0.54	0.34	4.24	-0.12	1.58	3.52	0.44	24.61	0.04	2.24
79.40	0.08	0.12	0.16	0.34	0.23	0.39	0.67	0.54	0.35	4.66	-0.15	1.63	3.59	0.44	24.46	0.04	2.47
79.40	0.08	0.12	0.16	0.33	0.23	0.38	0.67	0.53	0.34	5.77	-0.23	1.72	3.62	0.44	24.04	0.04	3.39
79.40	0.08	0.12	0.17	0.34	0.22	0.39	0.67	0.54	0.34	5.91	-0.21	1.68	3.55	0.45	24.59	0.05	2.90
79.40	0.08	0.12	0.18	0.31	0.13	0.32	0.64	0.50	0.27	5.96	-0.20	1.90	3.83	0.39	23.55	0.03	3.15
79.40	0.08	0.12	0.17	0.31	0.14	0.33	0.64	0.50	0.28	5.51	-0.18	1.83	3.74	0.40	23.42	0.03	2.86
79.40	0.08	0.12	0.18	0.31	0.13	0.33	0.64	0.50	0.27	5.57	-0.18	1.82	3.74	0.40	23.57	0.03	2.77
79.40	0.08	0.12	0.19	0.31	0.08	0.31	0.62	0.49	0.24	5.32	-0.17	1.78	3.74	0.41	23.96	0.03	2.80
80.40	0.08	0.11	0.17	0.31	0.16	0.34	0.65	0.50	0.30	5.99	-0.25	1.87	3.81	0.40	22.89	0.03	3.95
80.40	0.08	0.11	0.16	0.32	0.21	0.37	0.67	0.52	0.33	5.28	-0.17	1.76	3.68	0.42	23.60	0.04	2.67
80.40	0.08	0.11	0.17	0.31	0.17	0.34	0.65	0.50	0.30	5.38	-0.23	1.77	3.77	0.42	23.08	0.03	3.40
80.40	0.08	0.12	0.18	0.33	0.15	0.35	0.65	0.51	0.29	5.22	-0.19	1.73	3.72	0.42	24.44	0.04	3.18
80.40	0.08	0.11	0.17	0.31	0.17	0.34	0.65	0.51	0.30	6.15	-0.21	1.92	3.85	0.39	23.55	0.03	3.26
80.40	0.08	0.12	0.18	0.32	0.15	0.34	0.64	0.51	0.29	5.60	-0.17	1.84	3.79	0.40	24.21	0.03	2.88
80.40	0.08	0.12	0.18	0.32	0.15	0.35	0.64	0.51	0.29	6.10	-0.17	1.94	3.78	0.38	24.22	0.03	2.92
80.40	0.08	0.12	0.18	0.32	0.14	0.34	0.64	0.51	0.28	5.33	-0.19	1.79	3.74	0.41	23.92	0.03	3.18
80.40	0.08	0.12	0.20	0.31	0.05	0.29	0.60	0.48	0.21	4.96	-0.16	1.71	3.79	0.42	24.57	0.03	2.95
80.40	0.08	0.13	0.20	0.31	0.05	0.29	0.61	0.48	0.21	4.38	-0.13	1.63	3.66	0.43	24.45	0.03	2.53
80.40	0.08	0.12	0.21	0.31	0.05	0.29	0.60	0.48	0.21	5.16	-0.18	1.77	3.85	0.41	24.53	0.03	3.19
80.50	0.08	0.11	0.16	0.31	0.19	0.35	0.66	0.51	0.31	4.43	-0.17	1.59	3.57	0.45	23.31	0.04	2.75
80.50	0.08	0.11	0.16	0.32	0.20	0.37	0.66	0.52	0.32	4.12	-0.11	1.55	3.45	0.45	23.61	0.04	2.03
80.50	0.08	0.11	0.17	0.31	0.18	0.35	0.65	0.51	0.31	5.60	-0.33	1.74	3.76	0.43	23.12	0.04	4.43

Girth (cm)	B1	B2	B3	B4	ARVI	GEMI	IPVI	MSAVI	NDVI	txt_CON	txt_Cor	txt_DIS	txt_ENT	txt_HOM	txt_Mean	txt_ASM	txt_Var
80.50	0.08	0.11	0.16	0.33	0.21	0.38	0.67	0.53	0.33	4.15	-0.13	1.55	3.44	0.46	23.84	0.05	2.10
80.50	0.08	0.11	0.16	0.33	0.21	0.38	0.67	0.53	0.33	4.67	-0.16	1.67	3.58	0.43	23.85	0.04	2.36
80.50	0.08	0.11	0.16	0.32	0.20	0.37	0.66	0.52	0.32	3.57	-0.09	1.45	3.32	0.47	23.62	0.05	1.80
80.50	0.08	0.11	0.16	0.32	0.22	0.37	0.67	0.53	0.34	4.04	-0.12	1.50	3.34	0.47	23.63	0.05	1.94
80.50	0.08	0.12	0.17	0.33	0.19	0.36	0.66	0.52	0.32	5.14	-0.14	1.75	3.67	0.42	24.00	0.03	2.50
80.50	0.08	0.11	0.17	0.32	0.17	0.36	0.65	0.52	0.31	5.29	-0.16	1.77	3.65	0.42	23.90	0.04	2.48
80.50	0.08	0.11	0.18	0.32	0.13	0.34	0.64	0.50	0.28	4.34	-0.12	1.63	3.54	0.43	23.99	0.04	2.21
80.50	0.08	0.11	0.18	0.31	0.13	0.33	0.64	0.50	0.27	5.49	-0.21	1.76	3.72	0.42	23.64	0.04	3.25
80.60	0.08	0.12	0.18	0.30	0.12	0.31	0.63	0.49	0.26	5.54	-0.22	1.75	3.67	0.43	23.70	0.04	4.33
80.60	0.08	0.11	0.17	0.31	0.17	0.35	0.65	0.51	0.30	4.46	-0.13	1.61	3.48	0.44	23.47	0.04	2.15
81.10	0.08	0.13	0.22	0.32	0.01	0.27	0.59	0.48	0.18	6.03	-0.25	1.83	3.87	0.41	25.02	0.03	3.87
81.10	0.08	0.12	0.19	0.32	0.10	0.32	0.63	0.50	0.25	5.31	-0.19	1.75	3.77	0.42	24.58	0.03	3.30
81.10	0.08	0.13	0.21	0.31	0.04	0.28	0.60	0.48	0.20	5.98	-0.20	1.90	3.86	0.39	24.59	0.03	3.34
81.10	0.08	0.12	0.20	0.30	0.05	0.28	0.61	0.47	0.21	5.17	-0.19	1.73	3.80	0.42	24.11	0.03	3.14
81.10	0.08	0.13	0.20	0.31	0.06	0.29	0.61	0.48	0.22	4.75	-0.16	1.65	3.72	0.44	24.74	0.03	2.72
81.10	0.08	0.12	0.18	0.30	0.09	0.30	0.62	0.48	0.24	5.37	-0.21	1.78	3.86	0.41	23.68	0.03	3.70
81.10	0.08	0.12	0.19	0.32	0.10	0.32	0.62	0.49	0.25	4.07	-0.12	1.55	3.54	0.45	24.47	0.04	2.36
81.10	0.08	0.12	0.18	0.32	0.13	0.34	0.64	0.51	0.27	4.76	-0.14	1.64	3.60	0.44	24.26	0.04	2.54
81.20	0.08	0.12	0.18	0.32	0.14	0.34	0.64	0.51	0.28	7.57	-0.28	2.14	4.00	0.36	23.94	0.03	3.71
81.20	0.08	0.11	0.17	0.32	0.15	0.34	0.65	0.51	0.29	6.52	-0.23	1.97	3.88	0.38	23.70	0.03	3.26
81.20	0.08	0.12	0.18	0.32	0.14	0.34	0.64	0.51	0.28	6.58	-0.22	1.99	3.88	0.38	24.24	0.03	3.21
81.20	0.08	0.12	0.17	0.32	0.16	0.35	0.65	0.51	0.29	5.01	-0.18	1.69	3.66	0.43	23.90	0.04	2.86
81.40	0.08	0.12	0.18	0.33	0.16	0.36	0.65	0.52	0.30	5.80	-0.19	1.90	3.85	0.38	24.30	0.03	3.09
81.40	0.08	0.12	0.18	0.34	0.17	0.37	0.65	0.53	0.31	6.84	-0.26	2.02	4.04	0.38	24.48	0.02	3.87
81.40	0.08	0.12	0.18	0.33	0.15	0.35	0.65	0.52	0.29	5.29	-0.17	1.77	3.70	0.41	24.40	0.03	2.70
82.20	0.08	0.11	0.17	0.32	0.17	0.36	0.65	0.52	0.31	8.25	-0.29	2.24	4.08	0.35	23.67	0.02	3.97
82.20	0.08	0.11	0.17	0.31	0.17	0.34	0.65	0.51	0.30	6.86	-0.23	2.04	3.93	0.37	23.22	0.03	3.38
82.20	0.08	0.11	0.17	0.31	0.16	0.34	0.65	0.51	0.30	5.96	-0.20	1.90	3.82	0.39	23.55	0.03	3.05
82.50	0.08	0.12	0.19	0.32	0.10	0.33	0.63	0.50	0.26	4.94	-0.15	1.72	3.69	0.42	24.25	0.03	2.64
82.50	0.08	0.12	0.19	0.32	0.10	0.33	0.63	0.50	0.26	4.18	-0.12	1.58	3.50	0.44	24.08	0.04	2.21
82.50	0.07	0.11	0.18	0.31	0.12	0.33	0.63	0.50	0.27	5.37	-0.17	1.78	3.72	0.41	23.53	0.03	2.76
82.50	0.08	0.12	0.18	0.30	0.11	0.31	0.63	0.49	0.26	3.63	-0.09	1.45	3.35	0.47	23.23	0.05	1.87
82.50	0.08	0.11	0.17	0.30	0.15	0.33	0.64	0.50	0.29	3.33	-0.05	1.40	3.25	0.47	22.93	0.05	1.67
82.50	0.08	0.11	0.17	0.30	0.15	0.33	0.64	0.49	0.28	4.36	-0.14	1.59	3.51	0.45	22.94	0.04	2.27
82.50	0.08	0.11	0.18	0.31	0.12	0.32	0.63	0.49	0.27	4.33	-0.11	1.62	3.51	0.43	23.36	0.04	2.17
82.50	0.08	0.11	0.17	0.29	0.10	0.29	0.62	0.47	0.24	5.21	-0.19	1.75	3.71	0.41	22.47	0.04	2.92
82.50	0.08	0.12	0.18	0.31	0.12	0.32	0.63	0.50	0.27	4.20	-0.13	1.60	3.54	0.43	23.55	0.04	2.22
82.50	0.08	0.11	0.18	0.30	0.11	0.31	0.63	0.49	0.26	4.04	-0.10	1.52	3.40	0.46	23.27	0.05	1.96
82.50	0.08	0.12	0.20	0.31	0.06	0.29	0.61	0.48	0.22	4.64	-0.14	1.65	3.64	0.43	24.31	0.04	2.48
82.50	0.08	0.13	0.22	0.32	0.02	0.28	0.60	0.48	0.19	4.70	-0.14	1.70	3.75	0.42	25.22	0.03	2.87

Girth (cm)	B1	B2	B3	B4	ARVI	GEMI	IPVI	MSAVI	NDVI	txt_CON	txt_Cor	txt_DIS	txt_ENT	txt_HOM	txt_Mean	txt_ASM	txt_Var
82.50	0.08	0.12	0.18	0.33	0.16	0.36	0.65	0.52	0.30	5.32	-0.15	1.80	3.79	0.41	24.71	0.03	2.95
82.50	0.08	0.12	0.18	0.34	0.17	0.37	0.65	0.53	0.31	5.02	-0.15	1.71	3.65	0.42	25.06	0.04	2.61
82.50	0.08	0.12	0.18	0.35	0.17	0.38	0.65	0.53	0.31	5.32	-0.17	1.73	3.67	0.43	25.29	0.04	2.71
82.50	0.08	0.11	0.17	0.32	0.16	0.35	0.65	0.51	0.30	5.62	-0.15	1.84	3.69	0.40	23.90	0.03	2.59
82.50	0.08	0.12	0.20	0.33	0.10	0.33	0.63	0.51	0.26	5.42	-0.17	1.81	3.83	0.40	25.28	0.03	3.04
82.50	0.08	0.13	0.21	0.34	0.08	0.33	0.62	0.51	0.24	6.16	-0.21	1.94	4.02	0.38	25.69	0.02	3.75
82.50	0.08	0.13	0.20	0.34	0.09	0.33	0.62	0.51	0.25	5.58	-0.17	1.88	3.89	0.38	25.65	0.03	3.26
82.50	0.08	0.12	0.18	0.32	0.14	0.34	0.64	0.51	0.28	5.02	-0.13	1.75	3.62	0.41	23.87	0.04	2.41
82.50	0.08	0.12	0.17	0.32	0.15	0.34	0.64	0.51	0.29	5.17	-0.15	1.78	3.61	0.40	23.78	0.04	2.40
82.50	0.08	0.11	0.18	0.32	0.15	0.34	0.64	0.51	0.29	5.71	-0.18	1.83	3.73	0.41	23.96	0.03	2.75
82.50	0.08	0.12	0.18	0.32	0.13	0.33	0.64	0.50	0.27	4.61	-0.15	1.63	3.54	0.44	24.11	0.04	2.26
82.50	0.08	0.12	0.18	0.32	0.13	0.33	0.64	0.50	0.27	6.80	-0.18	2.08	3.87	0.36	24.04	0.03	3.13
82.50	0.08	0.12	0.18	0.32	0.12	0.33	0.63	0.50	0.27	4.89	-0.15	1.70	3.59	0.43	24.19	0.04	2.37
82.50	0.08	0.12	0.18	0.32	0.14	0.34	0.64	0.50	0.28	6.96	-0.19	2.11	3.88	0.35	23.95	0.03	3.24
82.50	0.08	0.12	0.19	0.31	0.10	0.31	0.62	0.49	0.25	5.87	-0.24	1.86	3.78	0.40	23.78	0.03	3.44
82.50	0.08	0.12	0.19	0.32	0.10	0.32	0.62	0.49	0.25	5.67	-0.20	1.87	3.84	0.39	24.28	0.03	3.06
82.50	0.08	0.12	0.18	0.33	0.14	0.35	0.64	0.52	0.28	7.52	-0.22	2.12	3.95	0.36	24.82	0.03	3.67
82.50	0.08	0.12	0.19	0.33	0.13	0.34	0.64	0.51	0.27	4.17	-0.11	1.58	3.53	0.44	24.83	0.04	2.26
82.50	0.08	0.12	0.19	0.34	0.15	0.36	0.65	0.52	0.29	6.26	-0.18	1.93	3.84	0.39	25.08	0.03	3.08
82.50	0.08	0.12	0.19	0.35	0.17	0.38	0.65	0.53	0.31	5.39	-0.14	1.79	3.72	0.41	25.60	0.03	2.76
82.50	0.08	0.12	0.18	0.35	0.19	0.39	0.66	0.54	0.32	6.01	-0.19	1.87	3.85	0.40	25.35	0.03	3.34
82.50	0.08	0.12	0.17	0.32	0.17	0.35	0.65	0.51	0.30	6.34	-0.25	1.92	3.88	0.40	23.62	0.03	3.76
82.50	0.08	0.12	0.18	0.33	0.17	0.36	0.65	0.52	0.30	6.74	-0.20	2.03	3.92	0.37	24.33	0.03	3.34
82.50	0.08	0.12	0.18	0.35	0.18	0.38	0.66	0.54	0.32	8.30	-0.27	2.27	4.11	0.34	25.12	0.02	4.21
82.50	0.08	0.12	0.19	0.35	0.15	0.36	0.65	0.53	0.29	7.93	-0.30	2.14	4.05	0.37	25.47	0.03	4.41
82.50	0.08	0.13	0.20	0.34	0.12	0.35	0.64	0.52	0.27	5.83	-0.19	1.86	3.82	0.40	25.92	0.03	4.08
82.60	0.07	0.11	0.16	0.32	0.23	0.38	0.67	0.53	0.34	6.50	-0.26	1.95	3.88	0.39	23.62	0.03	3.61
82.60	0.08	0.12	0.18	0.34	0.15	0.36	0.65	0.52	0.29	4.28	-0.14	1.59	3.56	0.44	24.80	0.04	2.27
82.60	0.08	0.13	0.21	0.34	0.07	0.33	0.62	0.51	0.24	6.65	-0.22	2.01	4.02	0.37	26.00	0.02	3.73
82.60	0.08	0.13	0.22	0.34	0.06	0.32	0.61	0.50	0.22	7.02	-0.26	2.07	4.14	0.37	26.24	0.02	4.36
82.60	0.08	0.12	0.18	0.32	0.15	0.34	0.64	0.50	0.28	5.96	-0.19	1.89	3.81	0.40	24.18	0.03	2.98
82.60	0.08	0.13	0.20	0.33	0.10	0.32	0.62	0.50	0.25	6.75	-0.23	2.01	3.99	0.38	25.32	0.03	3.65
82.60	0.08	0.14	0.24	0.34	-0.02	0.26	0.58	0.48	0.16	9.06	-0.31	2.39	4.30	0.32	27.23	0.02	5.24
82.60	0.08	0.12	0.17	0.32	0.17	0.35	0.65	0.51	0.30	5.45	-0.21	1.76	3.73	0.42	23.85	0.04	2.89
82.60	0.08	0.12	0.17	0.33	0.19	0.36	0.66	0.52	0.32	5.80	-0.22	1.83	3.79	0.41	24.09	0.03	3.13
82.60	0.08	0.13	0.22	0.34	0.05	0.30	0.61	0.50	0.21	8.19	-0.36	2.22	4.31	0.35	25.87	0.02	5.49
82.60	0.08	0.12	0.19	0.30	0.09	0.30	0.62	0.48	0.24	5.87	-0.26	1.85	3.99	0.40	24.46	0.03	4.21
82.60	0.08	0.14	0.24	0.34	0.01	0.28	0.59	0.49	0.18	7.11	-0.23	2.07	4.08	0.37	26.87	0.02	4.18
82.60	0.08	0.13	0.21	0.33	0.07	0.31	0.62	0.50	0.23	6.59	-0.21	2.01	3.95	0.37	25.47	0.03	3.59
82.60	0.08	0.12	0.19	0.32	0.10	0.32	0.62	0.50	0.25	6.90	-0.24	2.02	3.95	0.37	24.49	0.03	3.58

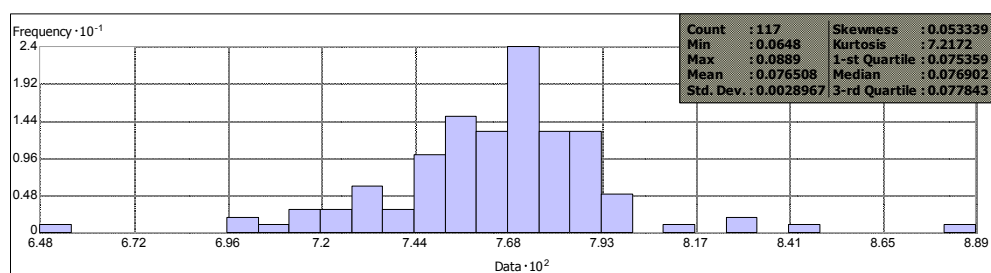
Girth (cm)	B1	B2	B3	B4	ARVI	GEMI	IPVI	MSAVI	NDVI	txt_CON	txt_Cor	txt_DIS	txt_ENT	txt_HOM	txt_Mean	txt_ASM	txt_Var
82.60	0.08	0.13	0.21	0.33	0.05	0.31	0.61	0.49	0.22	6.44	-0.21	1.96	3.94	0.38	25.82	0.03	3.63
82.60	0.08	0.13	0.20	0.33	0.09	0.32	0.62	0.50	0.25	6.80	-0.22	2.05	4.00	0.37	25.38	0.02	3.80
82.60	0.08	0.12	0.16	0.33	0.22	0.38	0.67	0.53	0.33	4.90	-0.16	1.70	3.65	0.42	24.06	0.04	2.55
82.60	0.08	0.12	0.20	0.32	0.08	0.31	0.62	0.49	0.24	5.47	-0.17	1.81	3.76	0.41	24.49	0.03	2.87
82.60	0.08	0.12	0.19	0.31	0.08	0.30	0.62	0.49	0.24	4.85	-0.16	1.71	3.75	0.42	23.85	0.03	2.91
82.70	0.08	0.12	0.20	0.32	0.08	0.31	0.62	0.49	0.24	5.96	-0.18	1.89	3.78	0.39	24.40	0.03	2.88
82.70	0.08	0.12	0.19	0.33	0.10	0.33	0.63	0.51	0.26	5.75	-0.17	1.87	3.73	0.40	24.69	0.03	2.74
82.70	0.08	0.12	0.19	0.33	0.10	0.33	0.63	0.50	0.26	5.52	-0.17	1.83	3.75	0.40	24.74	0.03	2.76
82.70	0.08	0.12	0.20	0.34	0.10	0.34	0.63	0.51	0.26	5.21	-0.16	1.77	3.79	0.41	25.47	0.03	3.16

Figure A3-1 shown the frequency histograms on skewness and kurtosis associated to three age classes of Para rubber plantation.

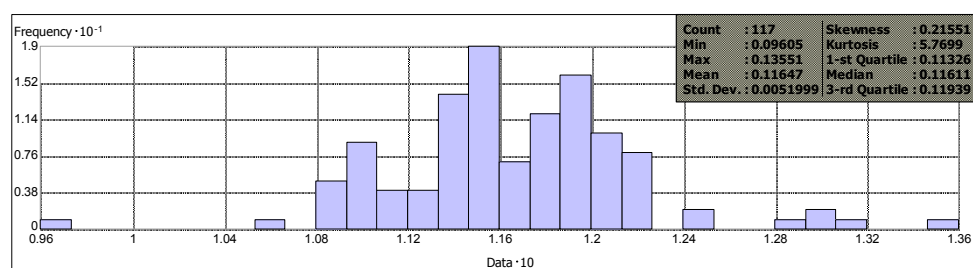
Table A3-1 The graphics of frequency histogram on age classes of Para rubber plantation (skewness and kurtosis were calculated by mean).

Young age class (Girth < 53 cm, Age 4-12 years)

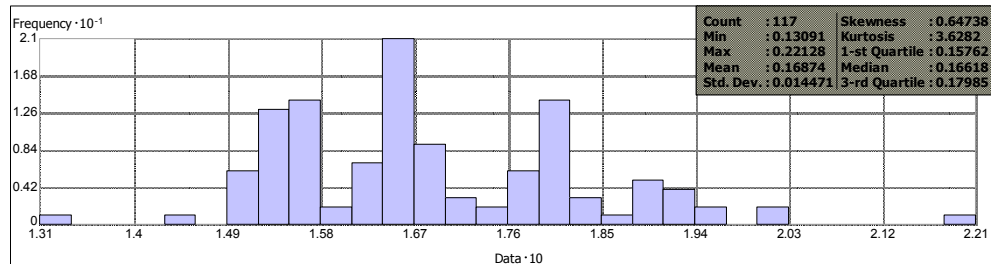
Blue



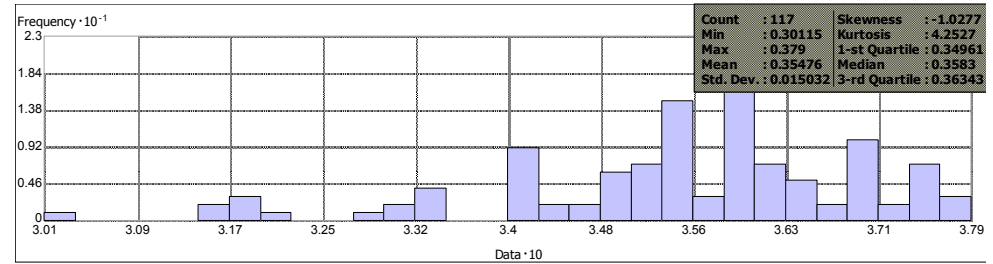
Green



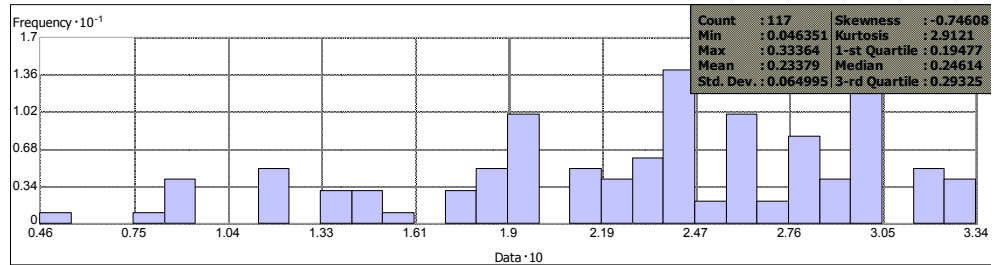
Red



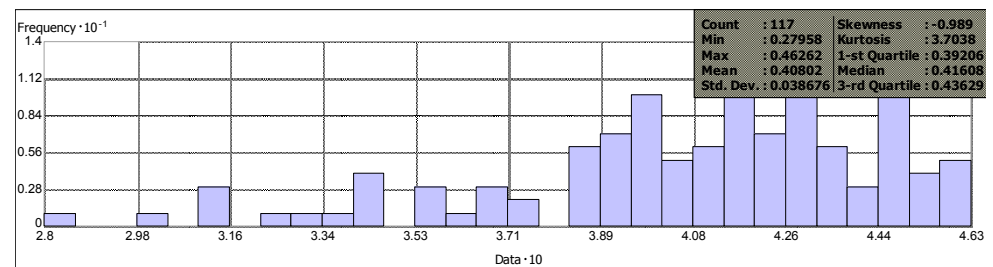
NIR



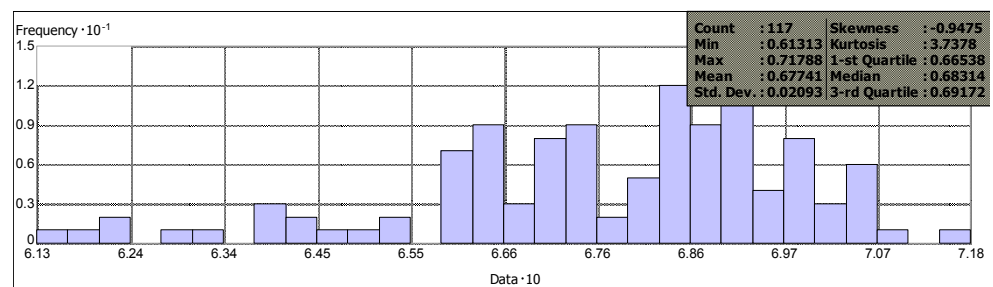
ARVI



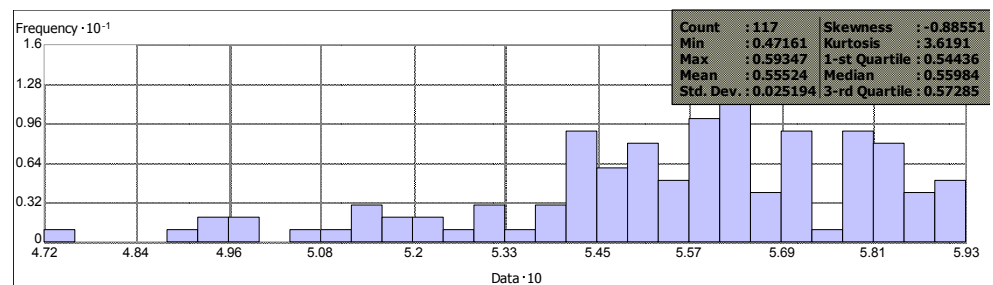
GEMI



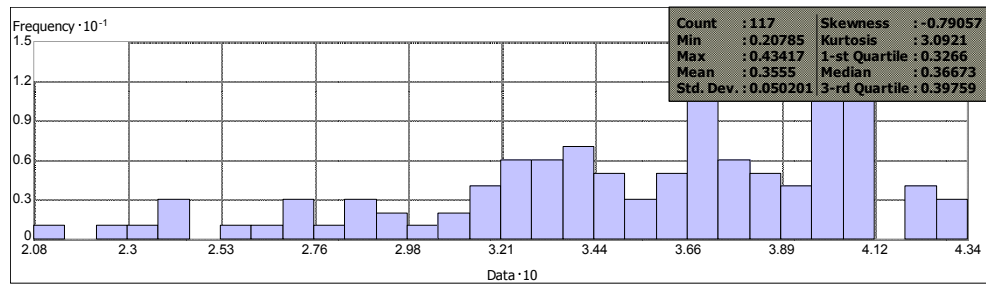
IPVI



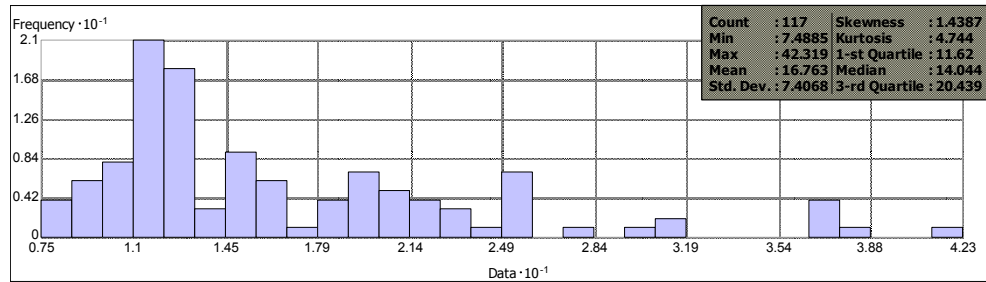
MSAVI2



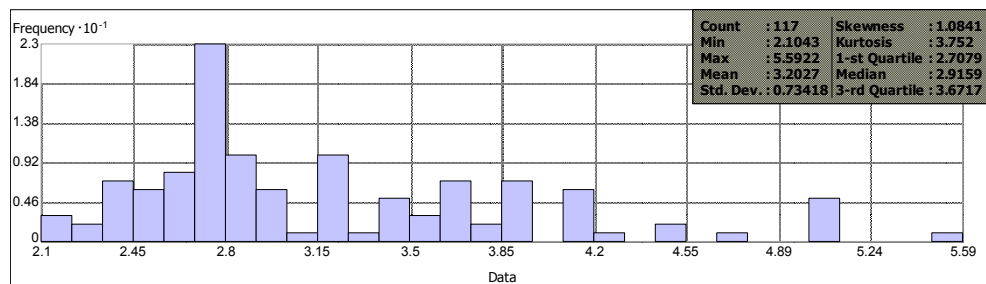
NDVI



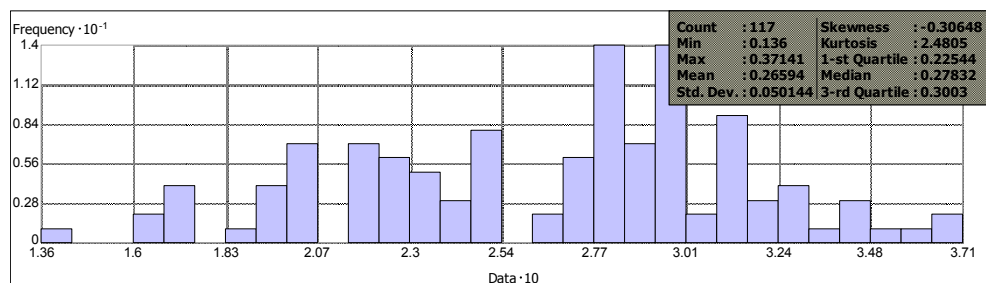
CON



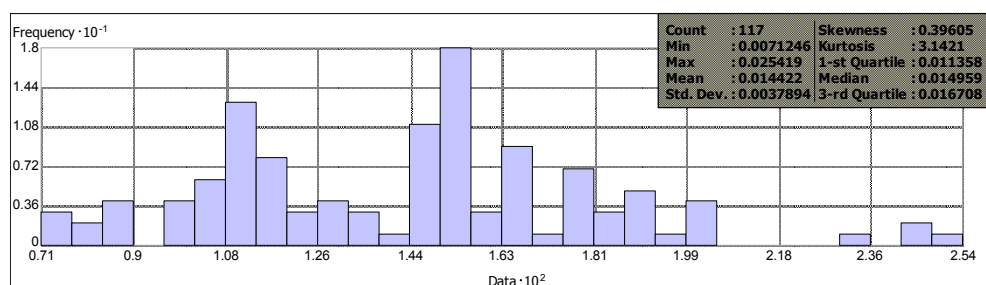
DIS



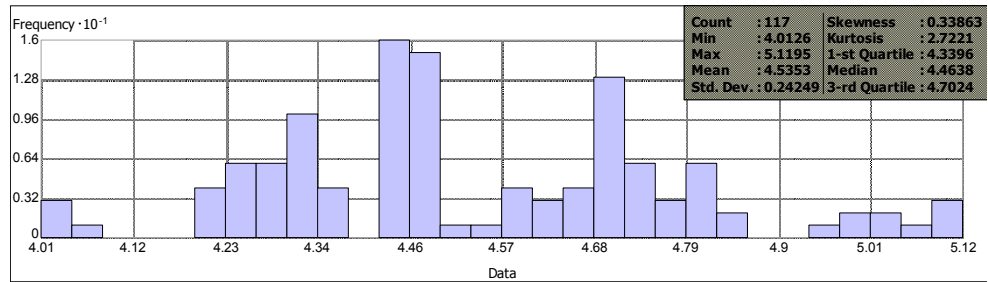
HOMO



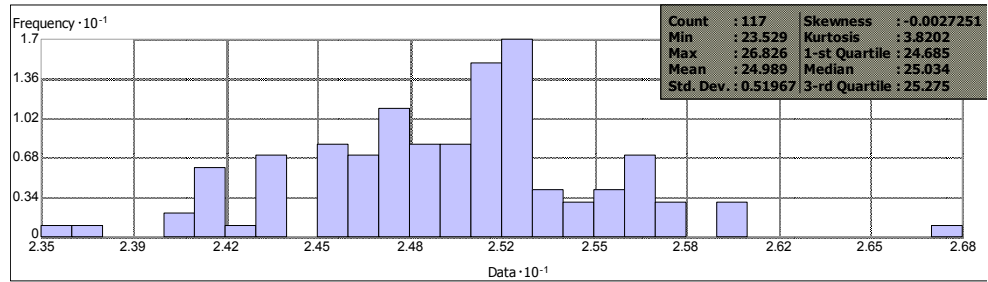
ASM



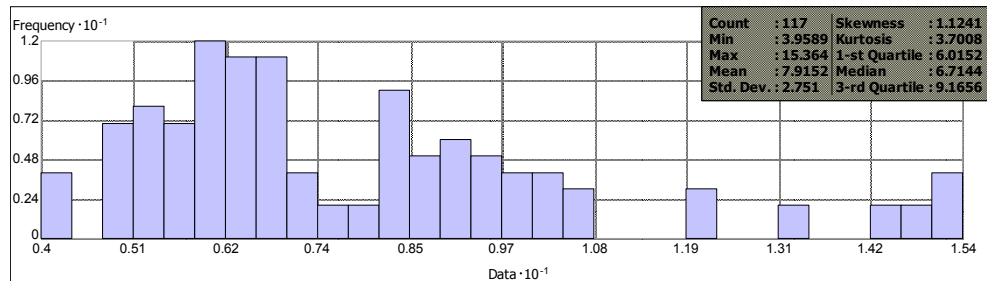
ENT



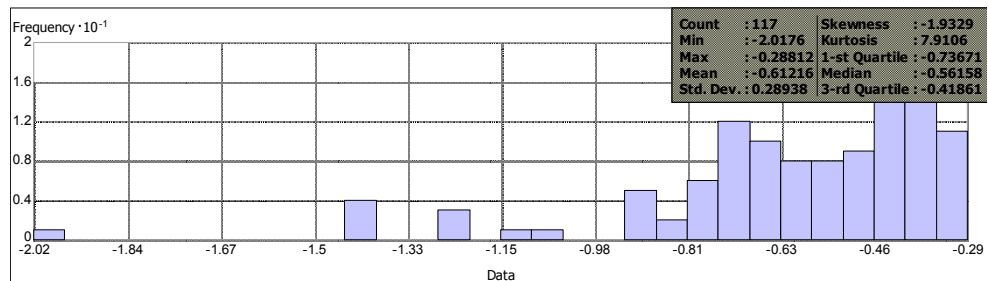
MEAN



VAR

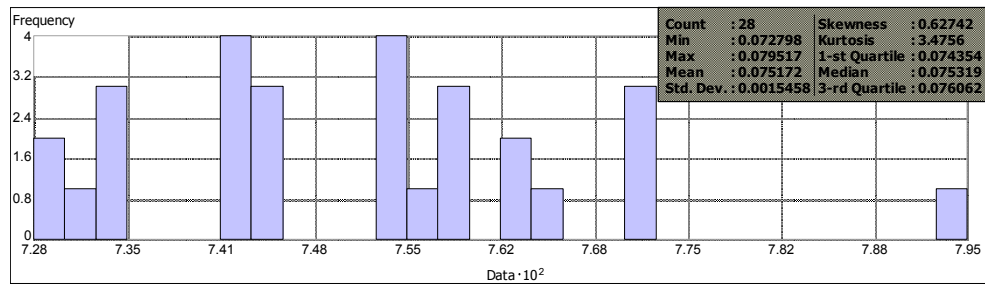


COR

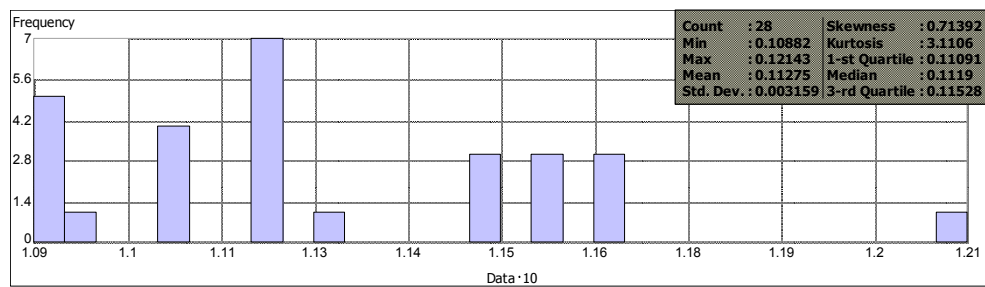


Middle age class (Girth 53-65 cm, Age 12-18 years)

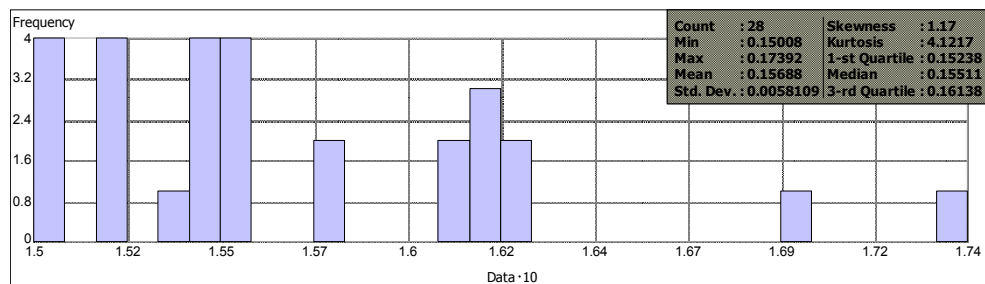
Blue



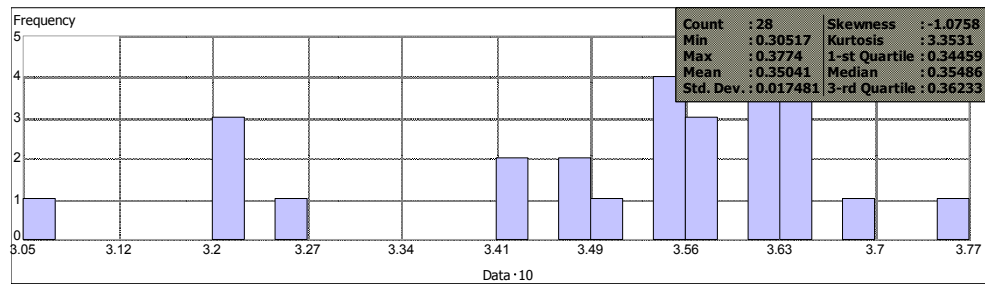
Green



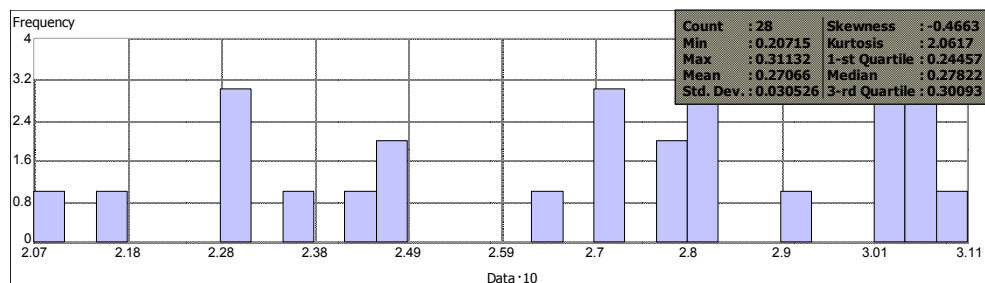
Red



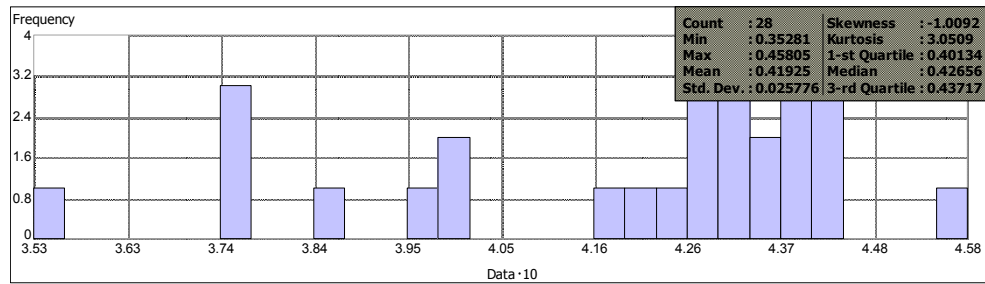
NIR



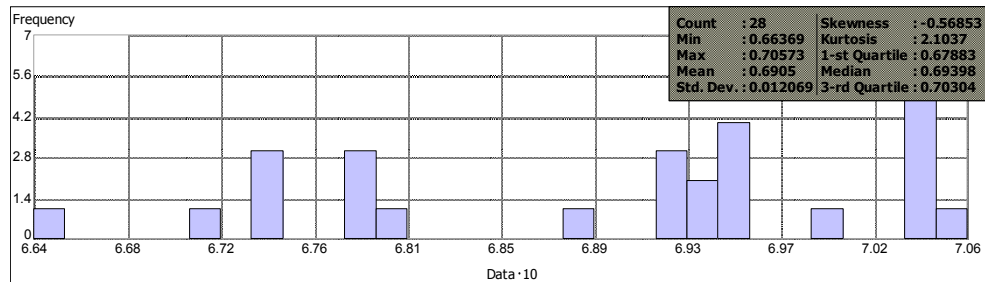
ARVI



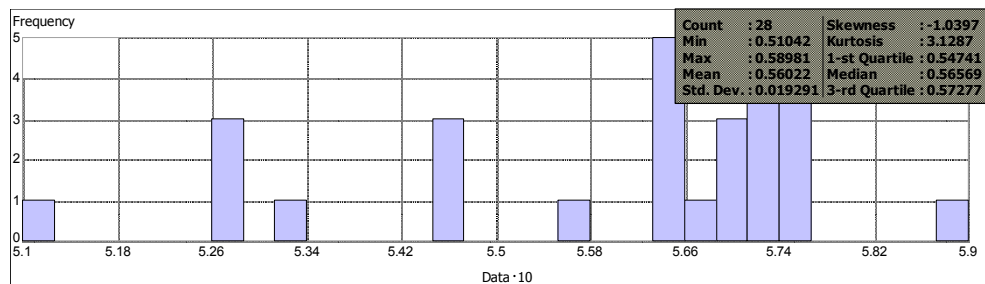
GEMI



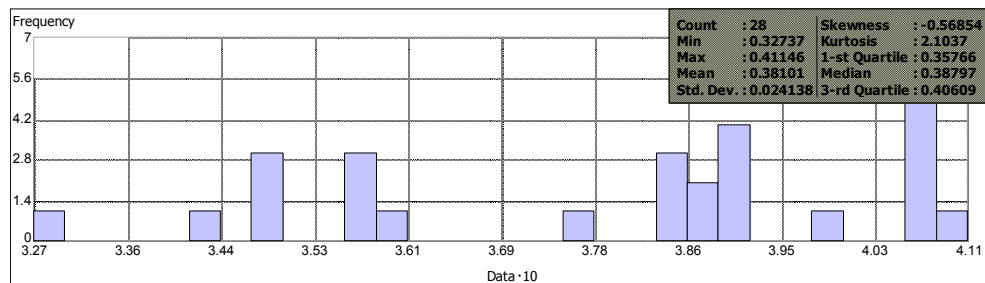
IPVI



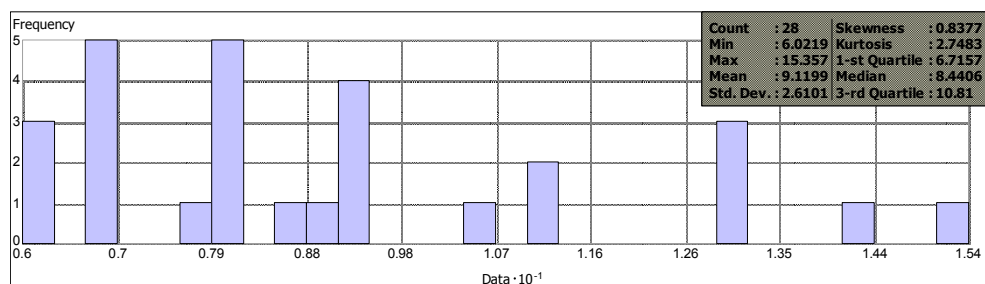
MSAVI2



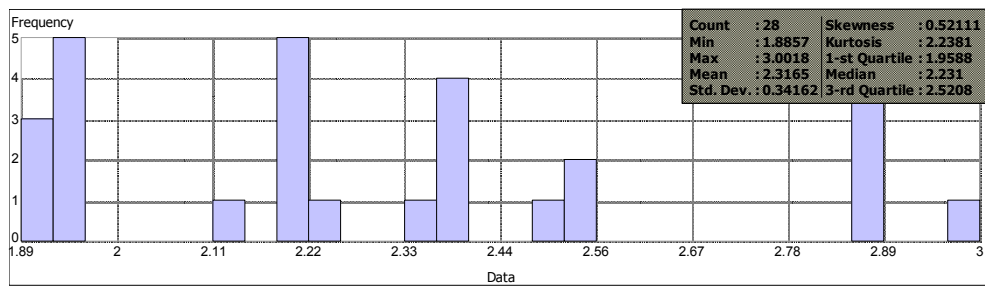
NDVI



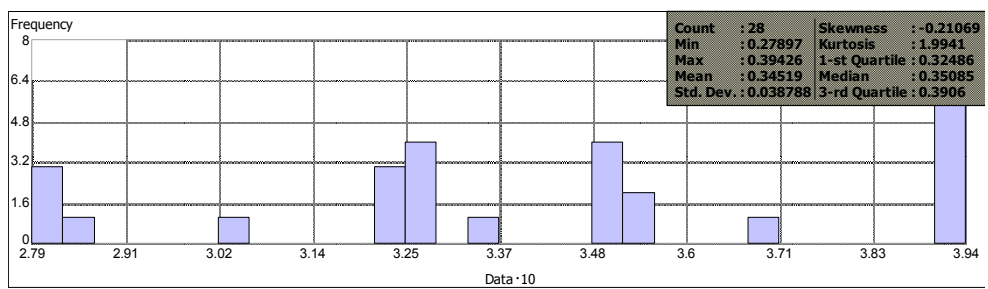
CON



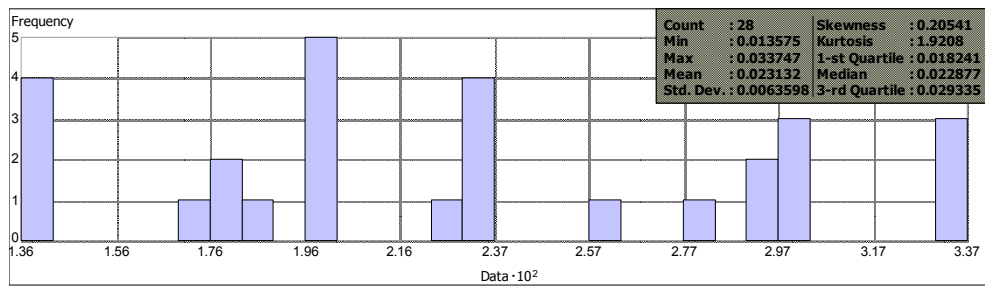
DIS



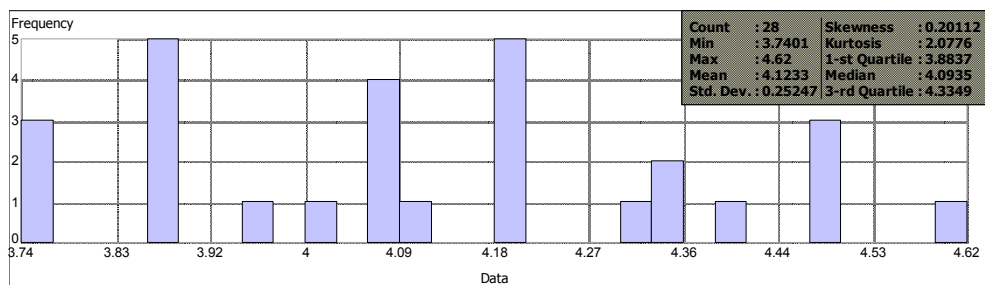
HOMO



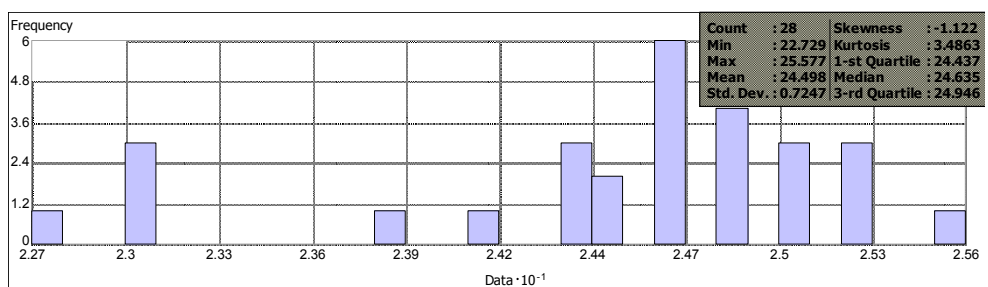
ASM



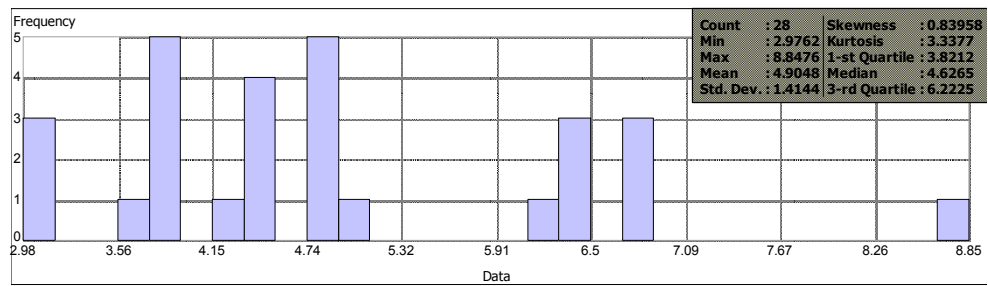
ENT



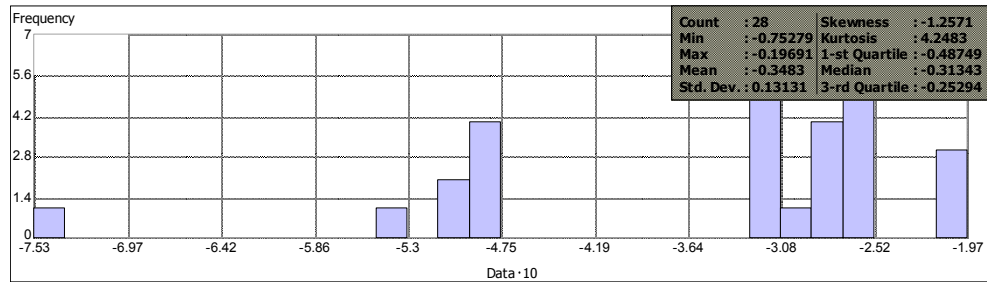
MEAN



VAR

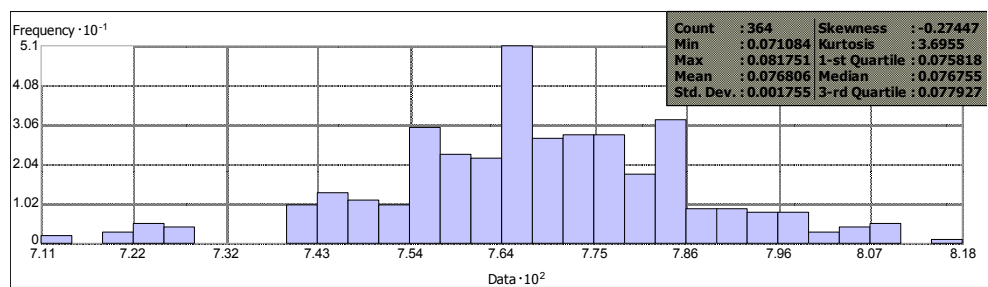


COR

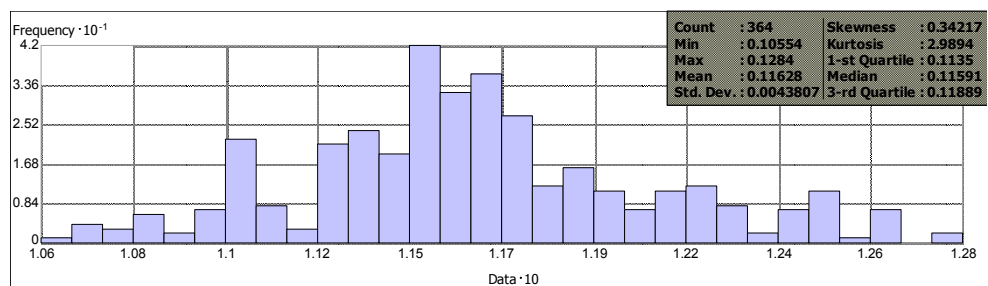


Old age class (Girth > 65 cm, Age > 18 years)

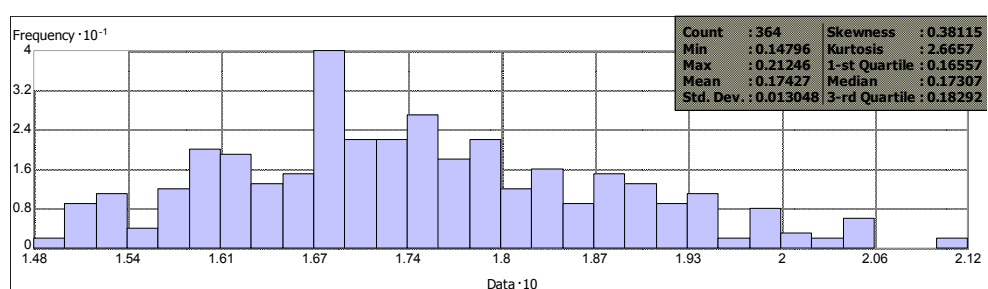
Blue



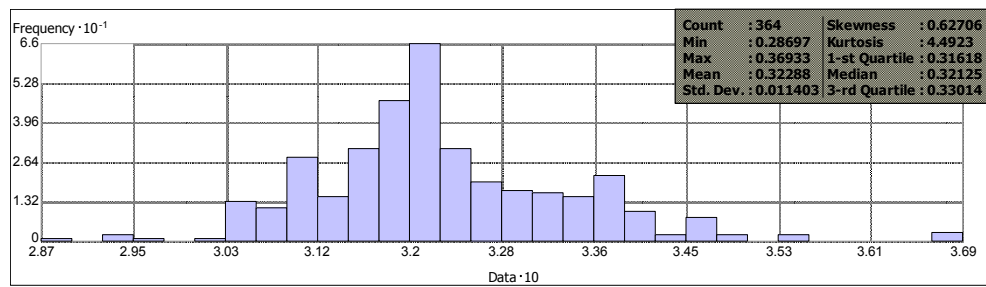
Green



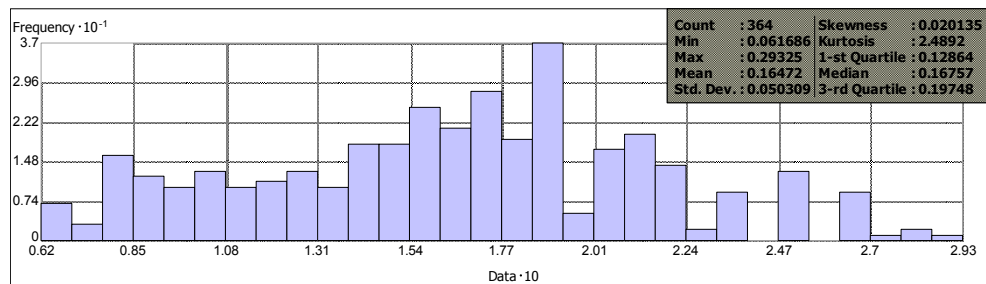
Red



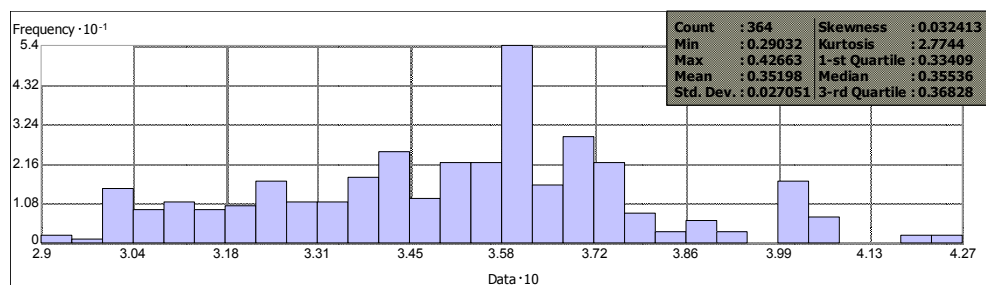
NIR



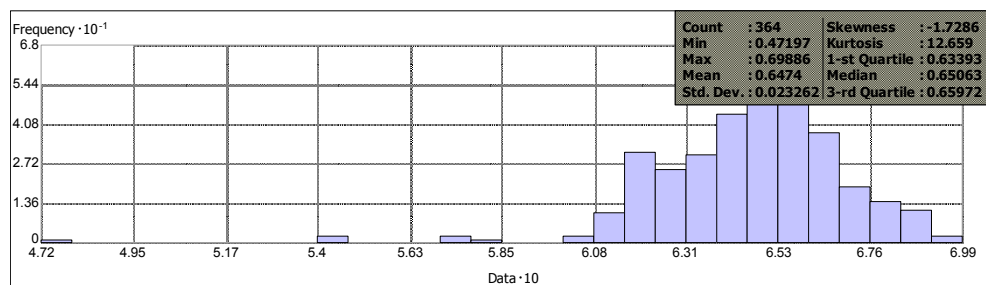
ARVI



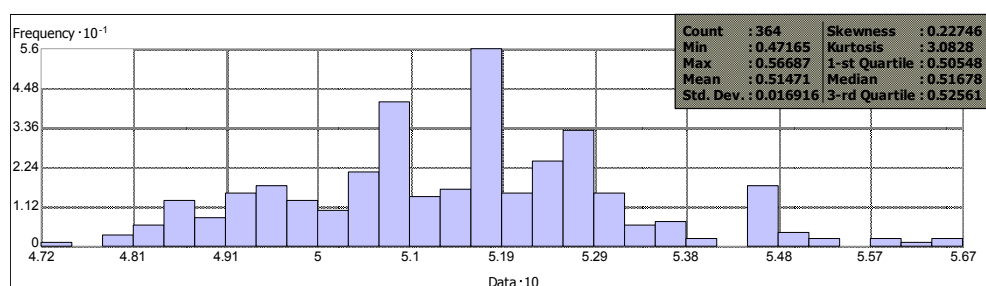
GEMI



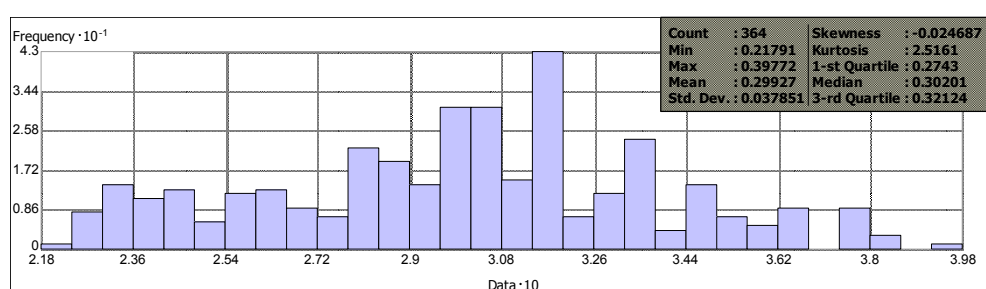
IPVI



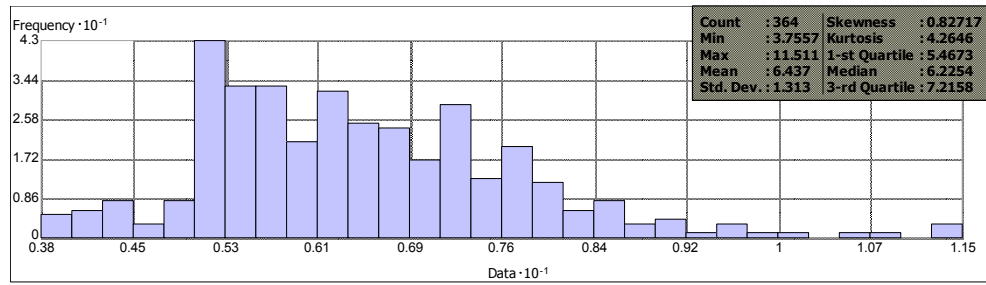
MSAVI2



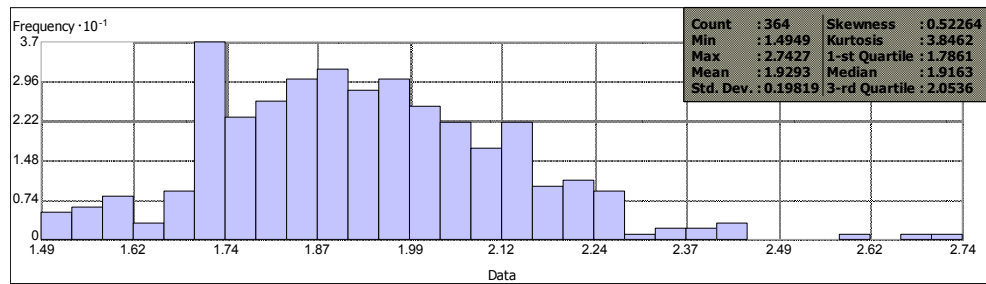
NDVI



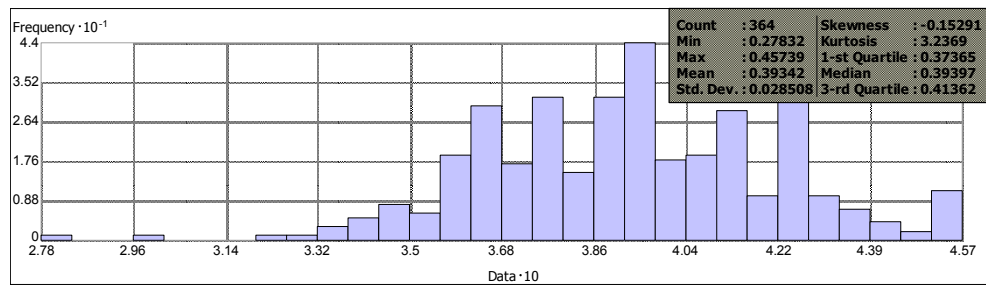
CON



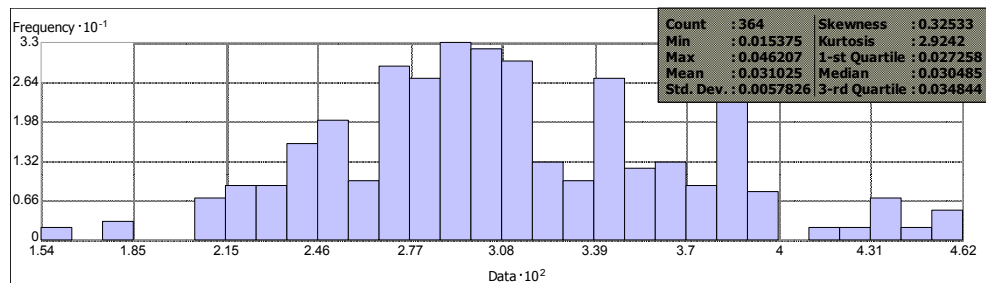
DIS



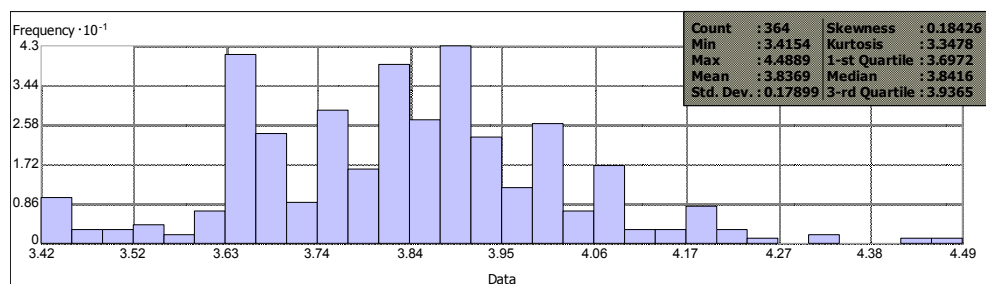
HOMO



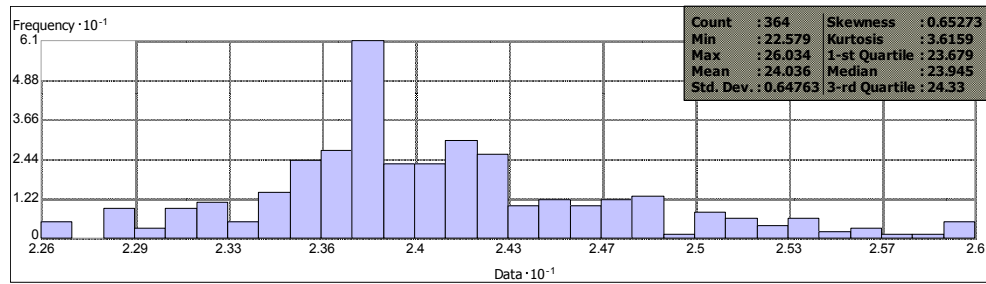
ASM



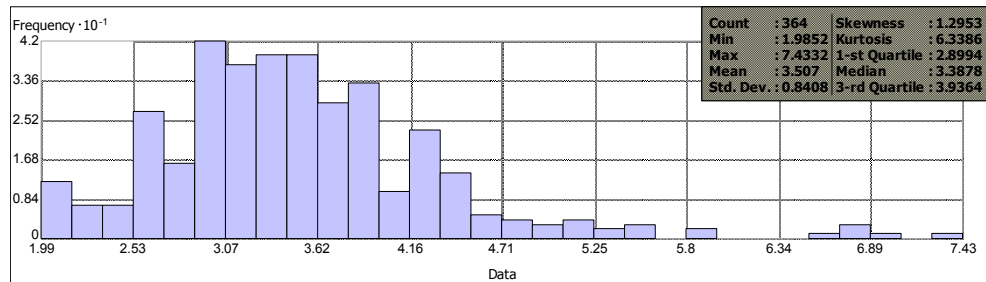
ENT



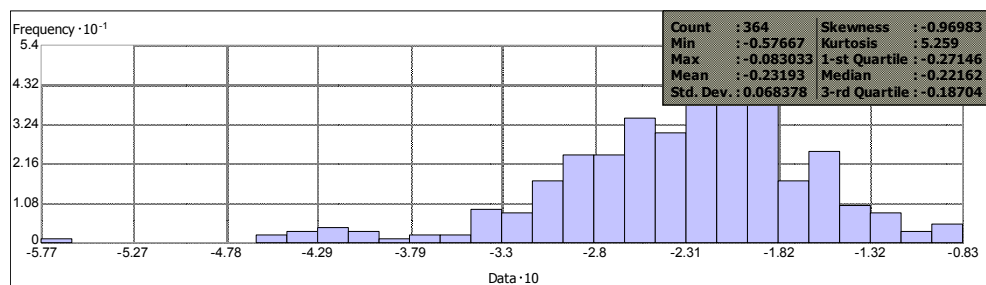
MEAN



VAR



COR



A.4 Articles publication

The study has been published in 2 articles following as below:

- The partial result of the study has been published in e-proceeding on 14th International Symposium on Water - Rock Interaction, June 2013., Avignon France.

K.Charoenjit, P. Zuddas, P. Allemand, “Estimation of natural carbon sequestration in eastern Thailand: preliminary results.” *Procedia Earth and Planetary Science* 1, 139-142 (2013).



Available online at www.sciencedirect.com

SciVerse ScienceDirect

Procedia Earth and Planetary Science 7 (2013) 139 – 142

Procedia
Earth and Planetary Science

Water Rock Interaction [WRI 14]

Estimation of natural carbon sequestration in eastern Thailand: preliminary results

K. Charoenjit^{a,*}, P. Zuddas^{a,*}, P. Allemand^b

^a*Institut des Sciences de la Terre de Paris (ISTeP, UMR 7193), Université Pierre et Marie Curie, Paris-Sorbonne, Tour 56-55, 4 place Jussieu 75252 Paris cedex 05, France*

^b*Laboratoire de Géologie de Lyon, Terre, Planètes, Environnement (LGLTPE, UMR 5276) Université Claude Bernard, Lyon1, bât. GEODE, 2 rue Raphaël Dubois 69622 Villeurbanne Lyon, France*

Abstract

We estimated carbon sequestration in Pará rubber tree plantations using a remote sensing approach and then compared the results to known figures for carbon sequestration resulting from soil-water interaction. The preliminary zone investigated is in Wangchun, eastern Thailand, and covers about 20 km².

Carbon sequestrated during soil-water interaction was estimated using a hydrological model taking into account variations in alkalinity and topography. We found that soil-water interaction resulted in the sequestration of 0.04 tons C/km²/year. The amount of naturally stored carbon in the Pará rubber plantation using THAICHOTE satellite imagery and specific biomass equations, was found to be 645 tons C/km²/year.

The magnitude of these preliminary results suggests that the flux of carbon storage in Pará rubber plantations could play a substantial role in the global carbon cycle.

© 2013 The Authors. Published by Elsevier B.V.

Selection and/or peer-review under responsibility of the Organizing and Scientific Committee of WRI 14 – 2013

Keywords: carbon sequestration; remote sensing; Pará rubber; Eastern Thailand.

1. Introduction

Pará rubber is a perennial plantation with a very high growth rate and is economically important in southeast Asia. Quantifying the high biomass rapid growth may allow us to evaluate the potential plant ability to sink CO₂ from the atmosphere. If that ability is confirmed, Pará rubber plantations could then be considered as long term carbon storage sites.

* Corresponding author. Tel.: +33 (0)14427 4965.

E-mail address: pierpaolo.zuddas@upmc.fr.

However, the flux of CO₂ in the earth's surface is shared between biochemical and geochemical processes [1]. In this study, we estimated the amount of carbon stored in Pará rubber trees during their growth and compared it to the amount of carbon sequestered by the process of soil-water interaction in the same zone.

2. Carbon storage in Pará rubber plantations

We estimated the total biomass and carbon content in Pará rubber tree plantations using THAICHOTE satellite imagery. The zone, located in Wangchun - eastern Thailand (coordinates 773149 E, 1470376 N and 778149 E, 1434376 N) covers about 20 km². Data collected from December 2011 to April 2012 (dry season), includes multispectral, panchromatic, and stereo pair images.

The images were initially corrected for topographic and atmospheric conditions [2-3] and we then applied vegetation indices, texture and color (IHS). We defined specific balance equations to determine the total biomass and carbon content in Pará rubber plantations. A total of 60 sample plots, measuring 20 x 20 meters, were identified with an average density of 48,750 trees/km². The mean diameter-at-breast height (DBH) was 1.7 meters and the total height of individual trees was measured in the field. For every individual tree, a stage class was evaluated by the *RRIM600* species-specific biomass model [4].

The results of our calculations indicate that the net surface area occupied by Pará rubber tree plantations is 13.38 Km² and that the mature stage class covers 40% of the area, while young and harvested stage classes cover 13% and 20% respectively of the "green" surface area. We found the amount of C storage in our field conditions to be 203,800 tons.

The mature stage class has the highest capacity for carbon sequestration, corresponding to 890.8 tons C/km²/year while the younger stage class has the least capacity for storage, 467.6 tons C/km²/year, and the harvested stage sequester 576.9 tons C/km²/year. The average carbon sequestration is estimated to be 645 tons C/km²/year.

3. Carbon Storage in soil –water interaction

Geochemical processes in soil-water interaction involve dissolution and precipitation of mineral phases and complex biogeochemical reactions [5]. We observed variations in alkalinity between the different soil layers of between 2 and 4 mmol/L, in agreement with previous variations observed in East Thailand [6, 7]. We assumed that alkalinity variations, resulting in mineral dissolution and precipitation reflect the soil-water geochemical net carbon storage [8].

The variation in soil water fluxes was evaluated by the physically-based hydrological model SWAT (Soil Water Assessment Tool) [9] operating on a daily time step. Based on water balance, the water storage per year in pore soil can be evaluated by the following Eq. 1:

$$SW_t = SW_o + \sum_{i=1}^t (R_{day} - Q_{surf} - E_a - W_{seep} - Q_{gw}) \quad (1)$$

Where SW_t is the final soil water content expressed in mm of H₂O, SW_o is the initial soil water content, R_{day} is the amount of daily precipitation on day, Q_{surf} is the daily surface runoff, W_{seep} is percolation and by pass flow in soil profile bottom and Q_{gw} is the daily return flow of the water, t is the time integration (1 year). The SWAT model requires input on topography, soils, land use and

meteorological data. These were provided by the Thailand Spatial Data Infrastructure: Thai SDI (<http://thaisdi.gistda.or.th/>). The Arc-SWAT software interface (version 2012) [5] was used to compile the SWAT input files.

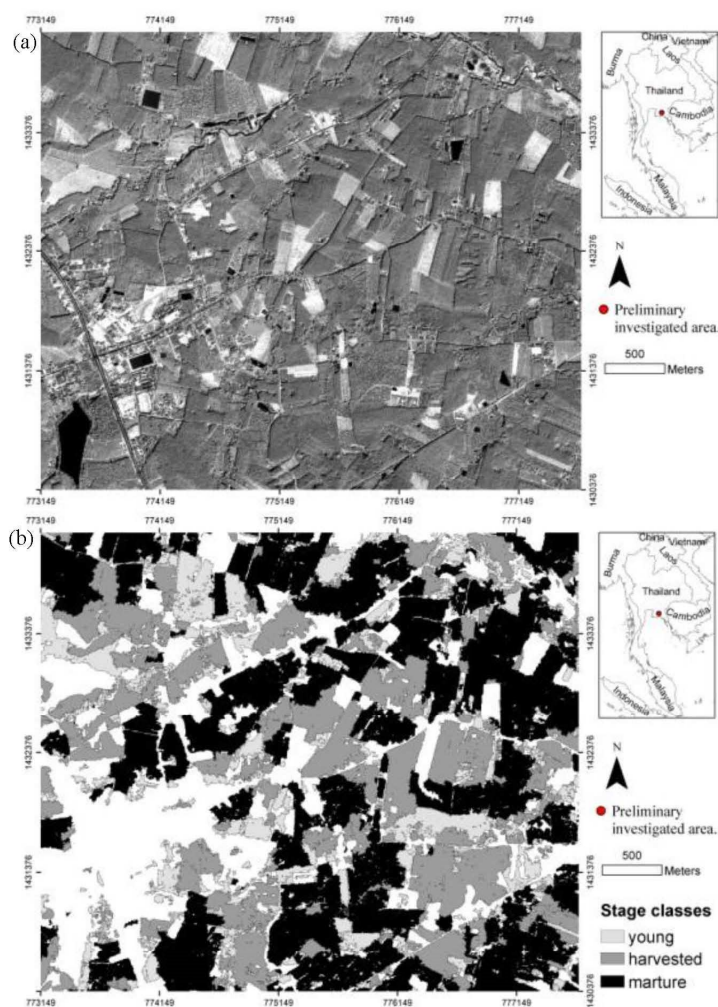


Fig. 1. (a) The preliminary investigate area of Wangchun district, Rayong province (false color composite RGB = NIR, R, G, map scale 1:20,000), © THAICHOTE Image Copyright 2011 GISTDA. (b) Thematic map of Para rubber classification.

Where SW_t is the final soil water content expressed in mm of H_2O , SW_o is the initial soil water

content, R_{day} is the amount of daily precipitation on day, Q_{surf} is the daily surface runoff, W_{seep} is percolation and by pass flow in soil profile bottom and Q_{gw} is the daily return flow of the water, t is the time integration (1 year). The SWAT model requires input on topography, soils, land use and meteorological data. These were provided by Thailand Spatial Data Infrastructure: ThaiSDI (<http://thaisdi.gistda.or.th/>). The Arc-SWAT software interface (version 2012) [5] was used to compile the SWAT input files.

Our estimations, based on pore soil water balance from 2011, in the studied area of 33,008 m³ (or 1,650.4 m³/km²) yield a carbon sequestration of 0.04 tons C/km²/year [6, 7].

4. Conclusions

Our preliminary results indicate that Pará rubber trees may store amount of carbon 2 orders of magnitude higher than that resulting from soil-water reaction; suggesting that Pará rubber tree plantations are a potential candidate for the artificial regulation of atmospheric CO₂.

References

- [1] Falkowski P, Scholes RJ, Boyle E, Canadell J. The Global Carbon Cycle: A Test of Our Knowledge of Earth as a System. *Science* 2000 ; **290**(5490): 291–296.
- [2] Grodecki J, Dial G. Block Adjustment of High-Resolution Satellite Images Described by Rational Polynomials. *Photogrammetric Engineering and Remote Sensing* 2003; **69**(1): 59-68.
- [3] Chavez PS Jr. Image-based atmospheric corrections-revisited and revised. *Photogrammetric Engineering and Remote Sensing* 1996; **62**(9): 1025-1036.
- [4] Chantuma A, Wichitchonlachai T, Chantuma P. Carbon Sequestration in Rubber plantation, Thailand. *Project Promotion of Chachungso Rubber Research Center* 2005. Chachungso, Thailand.
- [5] Juliet S, Johnson L, Baker A, Fox P. Geochemical Transformations During Artificial Groundwater Recharge : Soil-Water Interactions of Inorganic Constituents. *Wat Res* 1999; **33**(1): 196-206.
- [6] Silapajarn K, Silapajarn O, Boyd CE, 2005. Evaluation of Lime Requirement Procedures and Liming Materials for Aquaculture Ponds in Thailand. *Journal of Applied Aquaculture* 2005; **17**(3).
- [7] Kone YJM, Borges AV. Dissolved inorganic carbon dynamics in the waters surrounding forested mangroves of the Ca Mau Province (Vietnam). *Estuarine, Coastal and Shelf Science* 2008; **77**: 409-421.
- [8] Millero FJ, Roy RN. A chemical equilibrium model for the carbonate system in natural waters. *Croatia Chemica Acta* 1997; **70**: 1-38.
- [9] Winchell M, Srinivasan R, Di Luzio M, Arnold J. *ArcSWAT Interface for SWAT User's Guide*. Blackland Research Center, Texas Agricultural Experiment station and USDA Agricultural Research Service, 2012.

- The study has been published on Journal of Applied Remote Sensing.

K. Charoenjit, P. Zuddas, P. Allemand, S. Pattanakiat, K. Pachana, "Estimation of biomass and carbon stock in Para rubber plantations using object-based classification from Thaichote satellite data in Eastern Thailand," J. Appl. Remote Sens., 9(1), 096072 (2015).
doi:10.1117/1.JRS.9.096072.



Estimation of biomass and carbon stock in Para rubber plantations using object-based classification from Thaichote satellite data in Eastern Thailand

Kitsanai Charoenjit
Pierpaolo Zuddas
Pascal Allemand
Sura Pattanakiat
Katavut Pachana

SPIE.

Downloaded From: <http://remotesensing.spiedigitallibrary.org/> on 03/21/2015 Terms of Use: <http://spiedigitallibrary.org/terms>

Estimation of biomass and carbon stock in Para rubber plantations using object-based classification from Thaichote satellite data in Eastern Thailand

Kitsanai Charoenjit,^{a,*} Pierpaolo Zuddas,^a Pascal Allemand,^b
Sura Pattanakiat,^c and Katavut Pachana^d

^aUPMC–Sorbonne Universités, Institut des Sciences de la Terre de Paris, 4 Place Jussieu, 75252 Paris, France

^bUniversité Claude Bernard Lyon1, Laboratoire de Géologie de Lyon, Terre, Planètes, Environnement (LGL–TPE), 2 rue Raphaël Dubois, 69622 Villeurbanne Lyon, France

^cMahidol University, Geo-Informatics in Resource and Environment Research and Training Center (GIREN), Faculty of Environment and Resource Studies, 999 Salaya, Phutthamonthon, Nakhon Pathom 73170, Thailand

^dBurapha University, Faculty of Science, Department of Chemistry, 169 Long-Hard Bangsaen Road, Saen Sook Subdistrict, Chonburi 20131, Thailand

Abstract. This paper deals with the efficiency of measurements of carbon stock by remote sensing techniques on Para rubber plantations in Thailand. These plantations could play an important role in carbon budget and thus are part of the Clean Development Mechanism of the Kyoto Protocol. Current methods of carbon stock estimations use middle resolution images and produce results with a large uncertainty. We use very high resolution images from the Thaichote satellite, associated with field measurements to estimate the carbon stock and its evolution in the Mae num Prasae watershed, Eastern Thailand. Using object-based classifications, the plantations have been mapped and their age has been estimated from a parametric model derived from both spectral and textural information and field data. The total biomass and carbon stocked are 2.23 and 0.99 Megaton with an uncertainty of 11%. One hundred and twenty one tons of carbon are sequestered annually in the Para rubber plantations of the studied area. © The Authors. Published by SPIE under a Creative Commons Attribution 3.0 Unported License. Distribution or reproduction of this work in whole or in part requires full attribution of the original publication, including its DOI [DOI: 10.1117/1.JRS.9.096072]

Keywords: carbon stock estimation; object-based classification; Para rubber plantation; Thaichote satellite; Eastern Thailand.

Paper 14701 received Nov. 19, 2014; accepted for publication Feb. 24, 2015; published online Mar. 19, 2015.

1 Introduction

CO₂ is the most abundant atmospheric gas related to global warming. CO₂ is responsible for more than half of the radiative forces associated with the greenhouse effect.¹ Forest may play an important role in the short carbon dioxide cycle. In particular, tropical forests have the potential capacity to sequester and to conserve carbon permanently.^{2,3} This is why the Clean Development Mechanism recommended by the Kyoto Protocol advocates evaluating tree capacity of CO₂ storage in humid tropical forest plantations.⁴ Para rubber is a perennial tree of economic importance in Indonesia, Malaysia, and particularly in Thailand for producing latex for the world-market. The Para rubber has a high biomass, high growth rate, and strong potential for carbon storage.⁵ Thailand is the leader of rubber production in the world; it produces around 37% of the world's annual rubber production.⁶

Today, very high resolution (VHR) sensors on board satellites can map tropical forest plantations and provide valuable data to evaluate forest biomass and carbon stock evolution. VHR

*Address all correspondence to: Kitsanai Charoenjit, E-mail: kitsanai.charoenjit@upmc.fr

Charoenjit et al.: Estimation of biomass and carbon stock in Para rubber plantations...

data has overcome the limitation of spatial resolution of the medium-low resolution sensors such as Landsat 8 OLI (15 m) or MODIS (250 m). These sensors cannot capture tree characteristics such as the crown canopy. Therefore, estimations of plantation biomass and carbon stocks from low resolution remote sensing data were inaccurate.⁷ The Thaichote satellite camera (previously named THEOS) is a high resolution sensor with a 2-m resolution. It is the first Earth observation satellite of Thailand. Its data are potentially an important data source for biomass and carbon stock estimation of large surfaces. However, the evaluation of forest carbon stock is a complex task. Numerous approaches have been proposed to estimate biomass using remote sensing techniques.⁷⁻¹³ The spectral information contained in satellite data is classically used.¹⁰⁻¹³ The methods developed with these data cannot differentiate biomass according to the tree species or tree age.⁷⁻⁹

We have identified two major problems in biomass estimation by remote sensing classification techniques. The first problem is the noise in the image classification on VHR data. Figure 1 shows “the salt-pepper noise problem” on the Para rubber plantation mapping. The Thaichote image [Fig. 1(a)] was classified with a classical pixel based technique [Fig. 1(b)]. The result shows inaccuracies in terms of the surface geometry of the age class boundary (or plantation limit). The legacy technique is derived from supervised and unsupervised methods for assigning a class label to an individual pixel based on distance or similarity measures in feature space.¹⁴ This approach was used as simple spectral information for class identification.

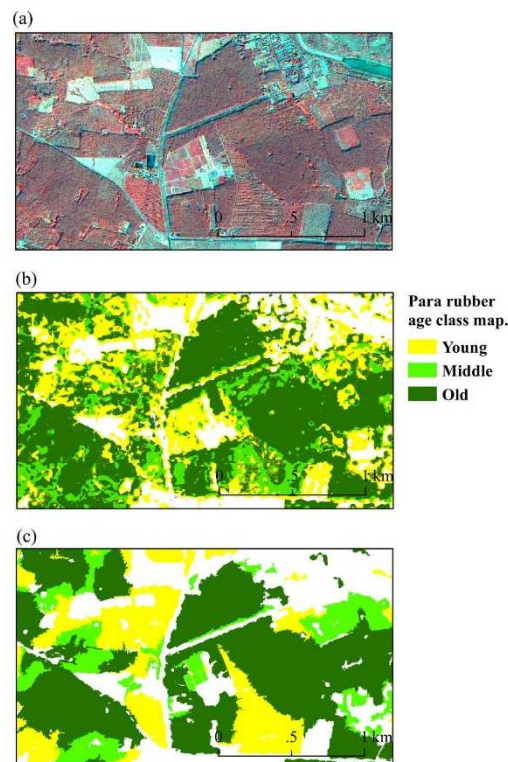


Fig. 1 (a) Thaichote false-color image (RGB: NIR, red, blue, spatial resolution of 2 m). (b) Para rubber age-class map derived from pixel-based classification with coverage by “salt-pepper noise” and misclassification of some age classes of Para rubber plantations. (c) Para rubber age-class map derived from object-based classification.

Charoenjit et al.: Estimation of biomass and carbon stock in Para rubber plantations...

By contrast, the object-based classification [object-based image analysis (OBIA)] overcomes the limitation of pixel-based classification. Figure 1(c) revised the Para rubber plantation mapping derived from the OBIA approach. The OBIA process is done in two steps: image segmentation and modeling for object identification. Segmentation can remove the image noise while the model can identify the object by analyzing more information such as reflectance distribution, shape, size, and texture.¹⁴ The second problem is the poor-quality relationship between field data and VHR data when using spectral information for biomass estimation. Recently, methods based on the texture measurement were developed to obtain better results than those using only spectral information.⁷⁻⁹ The texture of image is a good description of the forest canopy architecture. It was shown to have a certain relation with biomass volume.⁷⁻⁹ Classical pixel-based classification is not a good candidate to determine the characteristics of the canopy. Most of the previous works were used as simple spectral information for forest biomass estimation using medium-resolution satellite images.¹¹⁻¹³ Consequently, the established relationships between field data and remote sensing data were weak.

The goal of this study is to improve the Para rubber biomass and carbon stocks estimation using object-based classification combining both spectral and textural information from a Thaichote satellite image that was acquired in December 2011 over the Mae num Prasae watershed (Thailand). In the following, the study area and the Para rubber tree characteristics are first described. Then, the data and the remote sensing techniques are described and the results are given and commented on. Finally, the consequences of the results are discussed.

2 Study Area and Para Rubber Plantation

The area chosen in this study is the Mae num Prasae watershed located near 12°58'22"N/101°32'56"E (Rayong province, East Thailand) covering a surface of 232 km² (Fig. 2). The average elevation of the watershed is around 43 m above MSL and the average slope is 6 deg. Rainfalls occur around 120 days/year and the cumulative rainfall is 1900 mm. The average temperature is 28°C and humidity ranges from 60% to 90%.¹⁵

The rubber clone of *Hevea brasiliensis* RRIM 600 (Rubber Research Institute of Malaysia No. 600) is planted in this area (Fig. 3). In 2011, 34% of the Rayong province area was occupied

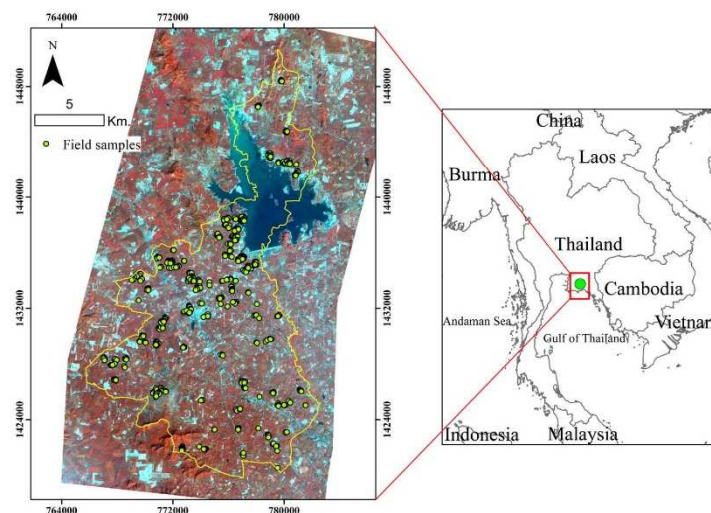


Fig. 2 The Mae num Prasae watershed in Thaichote satellite data (band composite RGB:NIR, red, green). The field data is shown in green dots.

Charoenjit et al.: Estimation of biomass and carbon stock in Para rubber plantations...



Fig. 3 Ground-view characteristics of Para rubber plantations, latex extraction and crop management (tree layout is approximately 3×7 m).

by Para rubber plantations. A rubber tree life cycle is around 25 to 30 years, after which the latex production from the rubber is decreased. Replanting is thus necessary to maintain latex production. *Hevea brasiliensis* needs a rainfall of 2000 mm (or more) with no severe dry season and 125 to 150 raining days/year. The minimum and maximum temperatures should be 20°C and 35°C, respectively, and atmospheric humidity should be 80% to 90% with moderate wind and bright sunshine for about 2000 h a year.¹⁶

3 Data and Methods

Classical methods are based on identification of forest plantations from classification of spectral pixel information on remote sensing images. Our purpose is to improve the classification by OBIA by combining both spectral and textural information from the images. The method developed here needs field data that will permit the building of a transfer equation model between field and remote sensing data.

The girths of trees were measured in the field according to their age in 500 randomly chosen plots. In each plot, the characteristics of 10 to 15 trees were measured and evaluated. The biomass and the carbon storage for a single tree were estimated from already published allometric equations.^{17,18} In parallel, the Thaichote satellite image (2 m) was corrected from atmospheric artifacts and then classified according to the OBIA method.¹⁴ The first step of OBIA consists of the image segmentation in order to identify the Para rubber plantations and to estimate the number of trees available per plantation. In a second step, textural and vegetation indices were constructed from the images using classical descriptors. The new images combined with the initial bands were used as inputs in a classification process to extract a numerical relation between the girths and ages of trees and the indicator values of the sampled plots. The empirical model obtained from a simple linear multiple regression technique was used to estimate the age of every plantation. Finally, the biomass and carbon stocked by Para rubbers in the Mae num Prasae watershed were estimated from the map of the plantation, the age estimated for each plantation and the relationship between the age and carbon stock for a single tree.

3.1 Field Data

In December 2011, field data were randomly collected on 500 sample plots (shown in Fig. 2 by green dots). In the field, the diameter at breast height (DBH), girth, and age were measured on

Charoenjit et al.: Estimation of biomass and carbon stock in Para rubber plantations...


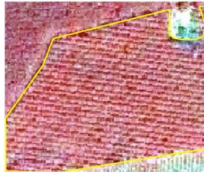



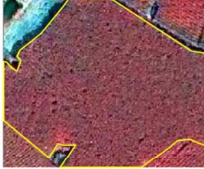
Age class	View from ground	THAICHOTE satellite data
(a) Young Age 4-12 years, Girth < 53 cm Number of sample 117 plots Age (yr) Girth (cm) 4 32 (+/-6.5) 8 39 (+/-1.6) 12 53 (+/-4.26)		
(b) Middle Age 12-18 years, Girth 53 – 65 cm Number of sample 28 plots Age (yr) Girth (cm) 16 58 (+/- 1) 18 65 (+/- 3.2)		
(c) Old Age >18 years, Girth > 65 cm Number of sample 355 plots Age (yr) Girth (cm) 20 71.50 (+/-2.7) 22 88 (+/-4.5) 25 90 (+/- 2)		

Fig. 4 Field data collected from December 2011 to April 2012: view from ground and view from Thaichote satellite data (band composite RGB: NIR, red, green) for the Para rubber ages used in this study.

about 10 to 15 trees per plot. Random plots were used for the forest inventory associated to tree age range from 4 to 25 years old. The age data were classified in eight classes (Fig. 4). DBH and tree girth were measured with a diameter tape at heights of 1.3 to 1.7 m above the ground according to the position of the latex tap on the skin of the trunk (Fig. 3). Cultivation of the Para rubber plantation has a traditional spatial distribution. Trees are spaced 3 m apart in lines spaced 7 m apart (Fig. 3). The density of a Para rubber tree stand is ~76 trees per 1600 m² or 0.0475 tree m⁻². Data were managed in a GIS database which included a topographic map and satellite image projected in the Universal Transverse Mercator (UTM) 48N Zone on World Geodetic System 1984 (WGS84). The Para rubber plantation statistics are shown in Fig. 4.

3.2 Ground Biomass and Carbon Estimation

Biomass estimation was derived from the empirically allometric equation relating geometric parameters of trees to their biomass and carbon content. The study used the allometric equation proposed by Chantuma et al.¹⁸ specifically for Para rubber to estimate the biomass Eq. (1):

$$Y = 0.0082X^{2.5623}, \quad (1)$$

where Y is the tree dry biomass in kg and X is the girth of a tree in cm. The coefficient of correlation (R^2) is 0.96. This equation was developed by measurements realized on plots located in the North, North East, South and East of Thailand. The carbon mass of a given tree is proportional to the biomass by a conversion factor of 0.4452.¹⁸ The rate of carbon sequestration (in tC ha⁻¹ y⁻¹) is given by the following Eq. (2):

Charoenjit et al.: Estimation of biomass and carbon stock in Para rubber plantations...

Table 1 Thaichote instrument characteristics. Thaichote was launched on October 2008.

Characteristics	Multispectral	Panchromatic
Spectral range	Blue band 0.45 to 0.52 μm . Green band 0.53 to 0.60 μm . Red band 0.62 to 0.69 μm . NIR band 0.77 to 0.90 μm . (Nadir looking)	0.45 to 0.90 μm . (Nadir looking)
Spatial resolution	15 m	2 m
Swath width	90 km	22 km
Pixel depth	8 bits	8 bits

$$\text{Carbon sequestration} = \frac{\text{Carbon mass in 1 ha}}{\text{Age of trees}}, \quad (2)$$

where carbon sequestration is the amount of carbon sequestered by each age class per year expressed as tons of C per hectare per year ($\text{tC ha}^{-1} \text{yr}^{-1}$). Carbon density is a total amount of carbon stored by each age (years) expressed as tons of C per hectare (tC ha^{-1}).

3.3 Thaichote Satellite Images Preprocessing

The Thaichote satellite image at level 1A containing both multispectral (Table 1) and panchromatic data was acquired on December 27, 2011, at 03:22 GMT, during the dry season where cloud cover was <10%. The sun azimuth was 143.21 deg and the sun elevation was 44.42 deg. The image was first pan-sharpened (2 m) and georeferenced¹⁹ in the Universal Transverse Mercator projection Zone 48 North on World Geodetic System 1984 ellipsoid (UTM WGS-1984 Z48N) and corrected from topographic distortion using ASTER Global Digital Elevation (GDEM Version 2). The cosine of the solar zenith corrections²⁰ was used to correct the radiometry of the image.

3.4 Image Classification

The image classification technique was used to map Para rubber plantations and estimate the age of each plantation. The technique developed here uses a combination of spectral information (data from spectral bands and band ratios called in the following vegetation indices), textural information and mask information.

Five classical vegetation indices obtained by Refs. 21–25 were calculated from the four spectral bands (Table 2). Each index is a combination of the various bands' ratios. The resulting complete spectral dataset contained nine layers.

The texture of an image is related to the statistical characteristics of association of pixels at a given scale. The texture of an image is a good descriptor of the forest canopy.^{7–9} The gray-level co-occurrence matrix (GLCM) texture measurement^{26,27} was applied to the Thaichote image. A 15×15 pixels sliding window⁷ was used to generate a co-occurrence matrix. The Haralick et al.²⁶ equations were used for building texture descriptors. These equations refer to three groups of descriptors that are the contrast group (contrast, dissimilarity, and homogeneity), the orderliness group (angular second moment, entropy), and the descriptive statistics group (mean, variance, and correlation) (Table 2). Eight textural layers were computed from the original image.

We also used the Thai National Spatial Data Infrastructure GIS database 2011 obtained by the Geo-Informatics and Space Technology Development Agency (GISTDA, Thailand) to extract the Para rubber plantation areas and evaluate the areas that not considered in the study: (1) the urban areas, other agricultural, natural forest areas and roads were selected for building mask information, (2) the mask database was map referenced to the UTM WGS84, Z48, (3) the localization of bare soil and water bodies was evaluated by the inverse of normalized different vegetation index. These areas were masked on the Thaichote pan-sharpened image.

Charoenjit et al.: Estimation of biomass and carbon stock in Para rubber plantations...

Table 2 Layers used for image classification.

Image mining	Formula	References
^a Single bands	Blue, Green, Red, NIR	
^a ARVI	$\frac{\text{NIR}-2(\text{RED})-\text{BLUE}}{\text{NIR}+2(\text{RED})-\text{BLUE}}$	Ref. 21
^a GEMI	$\frac{n(1-0.25n)-\text{RED}-0.125}{1-\text{RED}}$ where $n = \frac{2(\text{NIR}^2-\text{RED}^2)+1.5(\text{NIR})}{1-\text{RED}}$	Ref. 22
^a IPVI	$\frac{\text{NIR}}{\text{NIR}+\text{RED}}$	Ref. 23
^a MSAVI2	$\frac{2\text{NIR}+1-\sqrt{(2\text{NIR}+1)^2-8(\text{NIR}-\text{RED})}}{2}$	Ref. 24
^a NDVI	$\frac{\text{NIR}-\text{RED}}{\text{NIR}+\text{RED}}$	Ref. 25
^b GLCM contrast (CON)	$f_{\text{CON}} = \sum_{i,j=0}^{N-1} P_{i,j} i-j ^2$	Ref. 26
^b GLCM dissimilarity (DIS)	$f_{\text{DIS}} = \sum_{i,j=0}^{N-1} P_{i,j} i-j $	
^b GLCM homogeneity (HOM)	$f_{\text{HOM}} = \sum_{i,j=0}^{N-1} \frac{P_{i,j}}{1+ i-j ^2}$	
^b GLCM angular second moment (ASM)	$f_{\text{ASM}} = \sum_{i,j=0}^{N-1} P_{i,j}^2$	
^b GLCM entropy (ENT)	$f_{\text{ENT}} = \sum_{i,j=0}^{N-1} P_{i,j} (-\ln P_{i,j})$	
^b GLCM mean	$f_{\mu_i} = \mu_i \sum_{i,j=0}^{N-1} i(P_{i,j}), f_{\mu_j} = \mu_j \sum_{i,j=0}^{N-1} j(P_{i,j})$	
^b GLCM variance	$f_{\text{variance}} = \sum_{i,j=0}^{N-1} P_{i,j} (i-\mu)^2$	
^b GLCM correlation	$f_{\text{correlation}} = \sum_{i,j=0}^{N-1} \left[\frac{(i-\mu_i)(j-\mu_j)}{\sqrt{(\sigma_i^2)(\sigma_j^2)}} \right] P_{i,j}$	

^aFor spectral information: NIR is near infrared band, ARVI is atmospherically resistant vegetation index, GEMI is global environment monitoring index, IPVI is infrared percentage vegetation index, MSAVI2 is modified soil adjusted vegetation index2 and NDVI is normalized difference vegetation index.

^bFor textural information, GLCM: where $P_{i,j}$ is the probability matrix, i = reference pixel, j = neighborhood pixel and $\mu_i, \mu_j, \sigma_i, \sigma_j$ = the mean and standard deviation of $P_{i,j}$, respectively.

3.5 Para Rubber Age Class and Tree-Girth Classification

OBIAS was used to classify the Para rubber tree canopy properties. A complete description of the OBIAS is beyond the scope of the paper and can be found in Ref. 14. Two results were extracted from image classification and modeling which are a map of the plantations and an estimation of the girths and ages of the trees of each plantation. The map of the plantation was realized using an image segmentation process. The girths and ages of trees of each plantation were estimated from a linear regression equation built from the relationships between field data and image characteristics measured at the emplacement where field data were acquired.

Para rubber plantation limits were automatically extracted from image multiscale segmentation^{28,29} on Thaichote data. After the multiscale segmentation, the limits of the plantations were obtained. The results of multiscale segmentation were tested by empirical visualization.²⁹ Therefore, the total number of trees was estimated by GIS area calculation from the classical density of plantations.

Values of the various vegetation and textural indices were extracted at the position of each plot measured in the field. From that dataset and using a multiple linear regression model, a set of linear equations relating the girth of the tree and the characteristics of the layers was extracted in the form of Eq. (3). The confidence in this equation has been analyzed using Pearson's correlation coefficient.

The tree girth model (TGM) was generated using a linear multiple regression stepwise method^{7,8} for predicting tree girth and tree age. The tree girth is a function of multiparameterization of spectral and textural information. This is shown in Eq. (3):

$$Y = a + [b_1X_1 + b_2X_2 \dots + b_nX_n], \quad (3)$$

where Y is Tree girth (m), a is a constant, (b_1b_n) are coefficients of image parameters, and $(X_1 \dots X_n)$ are spectral and textural parameters (from four single bands, five vegetation indices,

Charoenjit et al.: Estimation of biomass and carbon stock in Para rubber plantations...

and eight GLCM). The mean value of these parameters was assigned to each plantation. The root mean square error (RMSE) and mean absolute percentage error (MAPE) were used to evaluate the model accuracy. Equation (3) was used to estimate the girth of trees of each plantation delineated at the segmentation step. Knowing the surface of the plantation and the age of the plantation, the biomass of each plantation was calculated from the allometric equation. Carbon stock was estimated using the conversion factor and carbon sequestration was estimated using Eq. (2).

4 Results and Discussion

4.1 Map of Para Rubber Plantation Limits

Ten thousand and sixty-nine crops of Para rubber plantation were identified with a maximum surface of 0.23 km² and a minimum surface of 1600 m², while the mean surface was 15,329 m². The uncertainty of Para rubber plantation surface was calculated from a comparison of multiscale segmentation and manual digitization. The total surface of plantations is 154.34 km² (15,434 ha) with an uncertainty of 11% (± 17 km²). The number of Para rubber tree stands was calculated using a constant value of 475 trees ha⁻¹ obtained by field measurement. Thus, the total number of tree stands is approximately 7,321,444 trees ($\pm 802,832$ trees). Figure 5 shows a sample of the map of Para rubber plantations obtained from the image segmentation process.

4.2 TGM and Para Rubber Tree Classification

The correlation between tree girth and values of the different layers obtained from the remote sensing image was tested by Pearson's correlation. All the parameters of texture and vegetation indices were correlated to the tree girth (Table 3). The homogeneity has the highest correlation with tree girth (0.875), while lowest is the mean (-0.496). For vegetation index, MSAVI2 has the highest correlation with tree girth (-0.663), whereas ARVI has the lowest (-0.512). For the bands of the satellite image, NIR (near infrared) is the band that correlates better with tree girth (correlation coefficient of -0.679).

Different models were built from different layers (Table 4). A first model (TGM#1) used only the spectral information. The coefficient of correlation of this model was poor (0.53). Thus, the

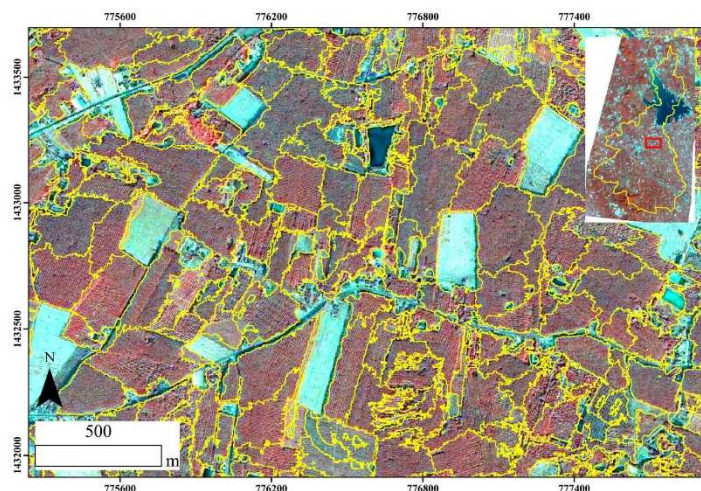


Fig. 5 Example of map of Para rubber plantations extracted from the multiscale segmentation. Yellow line is Para rubber plantation limits.

Charoenjit et al.: Estimation of biomass and carbon stock in Para rubber plantations...

model (TGM#1) was rejected. The integration of the textural layers improved strongly improved the model. The better fit by TGM#2 achieved a coefficient of regression of 0.87. It used the layers GEMI, HOMO, DIS, CON and VAR. The equation of TGM#2 is shown in Eq. (4):

$$Y = 3.694 - 1.29(\text{GEMI}) - 2.740(\text{HOMO}) - 0.933(\text{DIS}) + 0.068(\text{CON}) - 0.015(\text{VAR}), \quad (4)$$

where Y is the tree girth (m) and R^2 is 0.87. The scatter plots of TGM#1 and TGM#2 are shown in Fig. 6.

This equation was applied to the layers defining each plantation in order to estimate the girth of the trees of each plantation. The model (TGM#2) was realized in the GIS built for this study. From the tree girth map, a map of tree ages has been drawn (Fig. 7).

Old age classes (more than 18 years old) cover a surface of 54.55 km² (35%, 5455 ha), Young age classes (less than 12 years old) cover a surface of 51.12 km² (33%, 5112 ha), and middle age classes (from 12 to 18 years old) cover a surface of 48.68 km² (32%, 4868 ha). The areas of each age class are listed in Table 5.

The obtained relationships between tree girth and layers used for image classification show that texture parameters are better correlated than single bands and vegetation indices as shown by the Pearson's correlation coefficient values. The results of our study are in agreement with Eckert⁷ findings who observed the degraded forest stratum with high resolution WorldView-2 data.

The textures are better parameters than spectral data to estimate the age of the canopy. The present work shows that the textural information has to be added to the spectral one for a precise inventory of characteristics of forest or plantations in agreement with the works of Eckert⁷ and Sarker and Nichol⁸ with high resolution WorldView-2 and ALOS AVNIR-2 used in Madagascar, Hong Kong and Central Siberia for forest biomass modeling.

Table 3 Pearson's correlation between tree girth and layer parameters measured at field plot positions. Only the layers with an absolute value of correlation coefficient better than 0.4 were integrated in the final multilinear regression model.

Parameter	Pearson's correlation coefficient	Sig.
GLCM homogeneity	0.875	0.000
GLCM entropy	-0.853	0.000
GLCM dissimilarity	-0.841	0.000
GLCM angular second moment	0.803	0.000
GLCM variance	-0.801	0.000
GLCM contrast	-0.787	0.000
GLCM correlation	0.754	0.000
NIR	-0.679	0.000
MSAVI2	-0.663	0.000
GEMI	-0.633	0.000
IPVI	-0.540	0.000
NDVI	-0.540	0.000
ARVI	-0.512	0.000
GLCM mean	-0.496	0.000
Red	0.215	0.000
Blue	0.083	0.052
Green	0.014	0.389

Charoenjit et al.: Estimation of biomass and carbon stock in Para rubber plantations...

Table 4 Model summary. The number of girth measurements is 388 samples. Method: Stepwise regression, Criteria = Probability in (0.05), Probability out(.10). Spectral information; NIR = near-infra red band, RED = red band, GEMI = global environment monitoring index, MSAVI2 = modified soil adjusted vegetation index2. Textural information; HOMO = homogeneous, DIS = dissimilarity, CON = contrast, VAR = variance.

Model	R^2	Adj. R^2	RMSE tree girth (cm)	RMSE biomass (t/ha)	RMSE carbon (tC/ha)	MAPE (%)	Coefficient
TGM#1	0.531	0.526	11.26	1.93	0.86	15.43	(Constant) -16.435 NIR -95.441 RED 73.826 MSAVI2 55.867 GEMI 18.064
TGM#2	0.865	0.863	6.05	0.39	0.17	8.33	(Constant) 3.694 GEMI -1.290 HOMO -2.740 DIS -0.933 CON 0.068 VAR -0.015

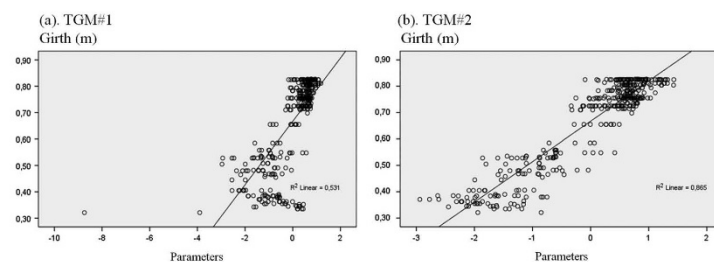


Fig. 6 (a) TGM#1 derived from spectral information. (b) TGM#2 derived from a combination of spectral and textural information.

Table 5 Para rubber classification, biomass and carbon stock in study area 2011. The uncertainty on the carbon stock comes from the uncertainty on the surface and the uncertainty of the model.

Class	Age (yr)	Area (ha)	Biomass stock (t)	C Stock (tC)	Uncertainty of C stock (tC)	C sequestered (tC ha ⁻¹ yr ⁻¹)	CO ₂ sequestered (tCO ₂ ha ⁻¹ yr ⁻¹)
Young	4	52.05	1,275.55	567.88	72.16	2.73	10.01
	8	899.26	34,309.54	15,274.61	1,845.45	2.12	7.79
	12	4,160.34	311,479.13	138,670.51	15,987.87	2.78	10.19
Middle	16	1,965.42	223,062.92	99,307.61	11,363.43	3.16	11.59
	18	2,902.70	436,121.53	194,161.30	21,820.70	3.72	13.64
Old	20	2,658.79	514,323.60	228,976.87	25,588.01	4.31	15.8
	22	2,791.13	703,766.39	313,316.80	34,847.56	5.1	18.73
	25	5.17	2,654.43	1,181.75	131.13	9.14	33.53
Grand total	15,434.87	2,226,993.09	991,457.32	111,656.32 (11.3%)	33.05	121.28	

4.3 Estimation of Biomass and Carbon Stocks

The total amount of biomass stock in the study area was estimated using the field data and remote sensing data. The field data and Eq. (4) were used to predict the girth and age of every plantation. Then the biomass stock was calculated using the allometric Eq. (1). In the study area, the highest biomass stock in Para rubber plantations is obtained for 22 years old trees that sequester

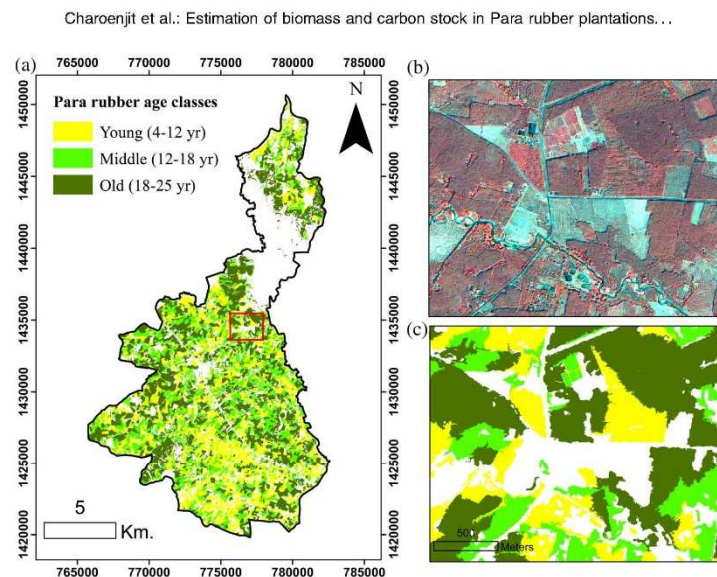


Fig. 7 (a) Map of Para rubber age classes. (b) Thaichote false color-image. (c) Zoom map of Para rubber age classes.

approximately 32% of the total biomass (703,766 tons). The lower biomass stock is found at 4 years (approximate 0.1% or 1276 tons) while at the age classes of 20, 18, 12, 16, 8 and 25 years, the amount of biomass stocked is 23%, 20%, 14%, 10%, 1% and 0.1% respectively (Table 5, Fig. 8). The carbon stock map is given in Fig. 9. The total biomass stock in the study area is 2.23 Megatons corresponding to 0.99 Megatons of carbon stock.

The accuracy of the model was evaluated using the RMSE and the MAPE. The RMSE and MAPE are 0.17 tC ha^{-1} and 8.33%, respectively. The errors from the surface and the model were summarized. Consequently, the total uncertainty of the carbon stock estimation is 111,656.32 tons (11.3%) (Table 5).

The evaluation of CO_2 sequestration by Para rubber trees by age is reported in Table 5. We found that Para rubber has the higher C sequestration at 25 years ($33.53 \text{ tC ha}^{-1} \text{ yr}^{-1}$), whereas the lower C sequestration is found at 8 years ($7.79 \text{ tC ha}^{-1} \text{ yr}^{-1}$). In 2011, the investigated area sequestered 33.05 tC corresponding to 121.28 t CO_2 by Para rubber plantation assuming that 1 tC represents 3.676 t of CO_2 .

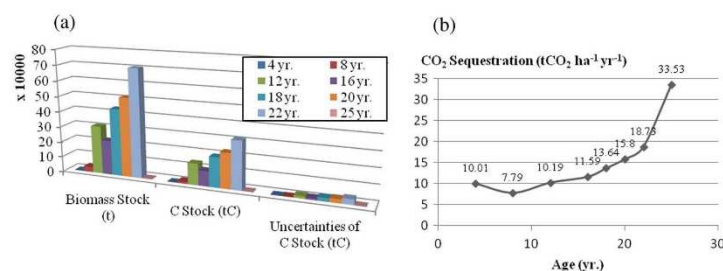


Fig. 8 (a) Bar graphs: biomass, carbon stock, and uncertainties data. (b) The rate of CO_2 sequestration by Para rubber of each age class.

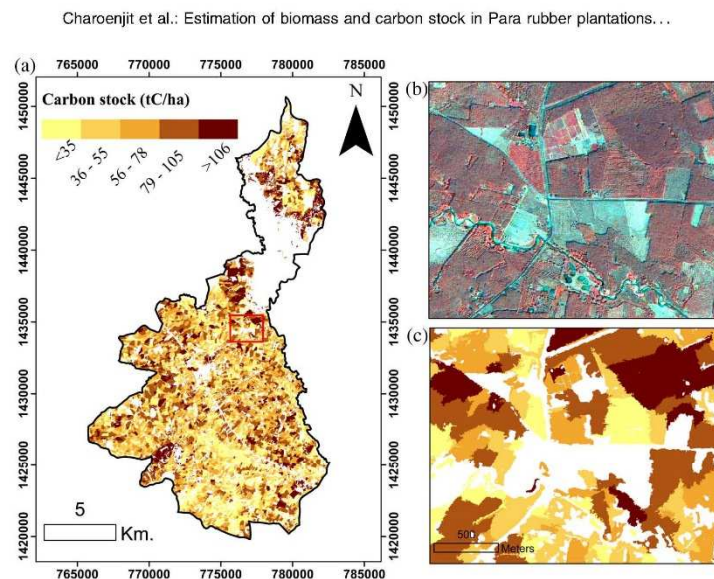


Fig. 9 (a) Map of Para rubber carbon stock. (b) Thaichote false color-image. (c) Zoom map of Para rubber carbon stock.

The result of our estimation confirms the strong potential of Para rubber for CO₂ capture as suggested by Chuntuma et al.¹⁸ based on the tree physiological characteristics. Our results show that the rate capture of CO₂ is 33.53 tCO₂ ha⁻¹ yr⁻¹ that is on the same order of magnitude of the values of CO₂ capture found in Ghana (35.30 tCO₂ ha⁻¹ yr⁻¹), Malaysia (38.33 tCO₂ ha⁻¹ yr⁻¹) and Indonesia (29.30 tCO₂ ha⁻¹ yr⁻¹) for Para rubber.³⁰

These amounts of CO₂ captured by Para rubber plantations can be compared to natural carbon sequestration estimated for the ocean. Borges et al.³¹ show that the sequestration of CO₂ by the ocean is around 4.45 gC m⁻² yr⁻¹, while Para rubber plantation can sequester up to 914.3 gC m⁻² yr⁻¹. We believe that agriculture and human intervention may play a critical role in the extraction of CO₂ from the atmosphere and thus in the short carbon cycle.

5 Conclusions and Further Research

This study explored the potential of Thaichote satellite data to estimate Para rubber biomass and carbon stock. Despite the fact that Thaichote data do not contain medium infrared data (MIR) as used in other studies,^{32,33} the results of our study have shown a high potential for forest biomass evaluation. The Para rubber plantation is a non-evergreen forest type. In the study area, the leaves of Para rubber fall between February and May. The method developed in this paper considered green plantations. Additional work remains to be done to test the potential of Thaichote data acquired during the period when trees have no leaves.

The results of this study show that these data can be used to map Para rubber plantations and distinguish the age classes of trees in the plantations. We propose that textural information is more useful than spectral information to capture tree canopy architecture and thus the age of the canopy. Moreover, it has been possible to build a model equation relating some textural parameters to the age of the plantation. This equation has been obtained from multiple linear regression analysis with a correlation coefficient of 0.87 and thus can be used with confidence on the study area. Around 154 km² of the 232 km² of the studied area are covered by Para rubber plantations. The class of age for each plantation has been estimated as follows: 33% of the crop surface belongs to the young class (from 4 to 12 years), 34% of the crop surface belongs to the middle class (from 12 to 18 years), and 33% belongs to the old class (older than 18 years). The total amount of biomass and carbon stock is 2.23 Megatons and 0.99 Megatons C, respectively, with

Charoenjit et al.: Estimation of biomass and carbon stock in Para rubber plantations...

an uncertainty of 11%. In 2011, the total area sequestered 121 tCO₂ by Para rubber plantations. Such a value is two orders of magnitude higher than the carbon sequestered in the ocean.

Acknowledgments

We would like to thank the Geo-Informatics and Space Technology Development Agency (GISTDA) for providing Thaichote satellite data without charge, and the team of GIREN, Mahidol University and Faculty of Forestry, Kasetsart University for the help on establishing the biomass and carbon forest inventory. We also thank two anonymous reviewers and the associate editor Dr. Feng Gao for suggestions that improved the quality and the clarity of the manuscript.

Financial support was partially provided through a scholarship to Kitsanai Charoenjit by the Franco-Thai program from Pierre et Marie Curie and Burapha Universities.

References

1. R. Sales, D. Lasco, and M. R. Banaticla, "Carbon storage and sequestration potential of smallholder tree farms on Leyte Island, the Philippines," in *ACIAR Smallholder Forestry Project ASEM 200/008 Redevelopment of a Timber Industry Following Extensive Land Clearing: Proceedings from the End-of Project Workshop*, Ormoc City, Philippines (2004).
2. S. Backeus, P. Wikstrom, and T. Lamas, "A model for regional analysis of carbon sequestration and timber production," *For. Ecol. Manage.* **216**, 28–40 (2005).
3. R. Sedjo, "Forest carbon sequestration: some issues for forest investment," Discussion Paper 01-34, *Resources for the Future* (2001).
4. "United Nation Framework Convention on Climate Change, Kyoto Protocol," <http://unfccc.int/2860.php> (20 October 2014).
5. C. Viriyabuncha, *Handbook of Stand Biomass Estimation*, pp. 1–11, Department of National Parks, Wildlife and Plant Conservation, Thailand (2003).
6. "Production of Natural Rubber," Rubber Research Institute of Thailand, 2011, http://www.rubberthai.com/statistic/stat_index.htm accessed (20 October 2014).
7. S. Eckert, "Improved forest biomass and carbon estimations using texture measures from WorldView-2 Satellite data," *Remote Sens.* **4**, 810–829 (2012).
8. L. R. Sarker and J. E. Nichol, "Improved forest biomass estimates using ALOS AVNIR-2 texture indices," *Remote Sens. Environ.* **115**, 968–977 (2011).
9. H. Fuchs et al., "Estimating aboveground carbon in a catchment of the Siberian forest tundra: combining satellite imagery and field inventory," *Remote Sens. Environ.* **113**, 518–531 (2009).
10. D. Lu et al., "Relationships between forest stand parameters and Landsat TM spectral responses in the Brazilian Amazon basin," *For. Ecol. Manage.* **198**, 149–167 (2004).
11. C. O. Iglesias, "Determination of carbon sequestration and storage capacity of eucalyptus plantation in Sra Kaew Province," Thailand using remote sensing, MSc Thesis, Mahidol University, Thailand (2007).
12. J. Nilubol, "Geo-informatics technology for age class identification for Para rubber plantation in Krabi province," MSc Thesis, Mahidol University (2007).
13. G. Zheng et al., "Combining remote sensing imagery and forest age inventory for biomass mapping," *J. Environ. Manage.* **85**, 616–623 (2007).
14. L. Arko, "Uncertainties in segmentation and their visualisation application of geoinformatics," PhD Thesis, Universiteit Utrecht (2004).
15. "Annual weather summary of Thailand in 2011," Thai Meteorological Department http://www.tmd.go.th/programs%5Cuploads%5CyearlySummary%5CAnnual2011_up.pdf accessed (October 20 2014).
16. P. Rao and K. R. Vijayakumar, "Climatic requirements," in *Natural Rubber: Biology, Cultivation and Technology, Developments in Crop Science*, Vol. 23, Elsevier, Netherlands (1992).
17. N. Picard, L. Saint-André, and M. Henry, *Manual for Building Tree Volume and Biomass Allometric Equations*, Food and Agriculture Organization of the United Nations (2012).
18. A. Chantuma, T. Wichitchonlachai, and P. Chantuma, "Rubber new planting in thailand: towards the world affected on climate change," *Rubber Thai.* **1**, 40–47 (2012).

Charoenjit et al.: Estimation of biomass and carbon stock in Para rubber plantations...

19. G. Jacek and D. Gene, "Block adjustment of high-resolution satellite images described by rational polynomials," *Photogramm. Eng. Remote Sens.* **69**(1), 59–68 (2003).
20. P. S. Chavez, Jr., "Image-based atmospheric corrections—revisited and revised," *Photogramm. Eng. Remote Sens.* **62**(9), 1025–1036 (1996).
21. Y. J. Kaufman and D. Tanré, "Atmospherically resistant vegetation index (ARVI) for EOS-MODIS," *IEEE Trans. Geosci. Remote Sens.* **30**, 261–270 (1992).
22. B. Pinty and M. M. Verstraete, "GEMI: a non-linear index to monitor global vegetation from satellites," *Vegetation* **101**, 15–20 (1992).
23. R. E. Crippen, "Calculating the vegetation index faster," *Remote Sens. Environ.* **34**, 71–73 (1990).
24. J. Qi et al., "Modified soil adjusted vegetation index (MSAVI)," *Remote Sens. Environ.* **48**, 119–126 (1994).
25. J. W. Rouse et al., "Monitoring vegetation systems in the great plains with ERTS," in *Third ERTS Symposium, NASA SP-351*, Vol. 1, pp. 309–317, NASA, Washington, DC (1973).
26. R. M. Haralick, K. Shanmugan, and L. Dinstein, "Textural features for image classification," *IEEE Trans. Syst. Man Cybern.* **3**, 610–621 (1973).
27. H. Anys et al., "Texture analysis for the mapping of urban areas using airborne MEIS-II images," in *Proc. First Int. Airborne Remote Sens. Conf. Exhibition*, pp. 231–245, Strasbourg, France (1994).
28. L. Guigues, J.-P. Cocquerez, and H. Le Men, "Scale sets image analysis," *Int. J. Comput. Vision* **68**(3), 289–317 (2006).
29. A. Le Bris, "Extraction of vineyards out of aerial ortho-image using texture information," in *ISPRS Annals of the Photogrammetry, Remote Sensing and Spatial Information Sciences, XXII ISPRS Congress*, Volume I-3, Melbourne, Australia (2012).
30. IRRDB, "The effects of climate change on NR cultivation and productivity," *International Rubber Research and Development*, Malaysian Rubber Board Building, Malaysia (2009).
31. A. V. Borges, B. Delille, and M. Frankignoulle, "Budgeting sinks and sources of CO₂ in the coastal ocean: diversity of ecosystems counts," *Geophys. Res. Lett.* **32**, L14601 (2005).
32. D. Lu, "Aboveground biomass estimation using Landsat TM data in the Brazilian Amazon," *Int. J. Remote Sens.* **26**, 2509–2525 (2005).
33. S. A. Eckert, "Contribution to sustainable forest management in Patagonia: object-oriented classification and forest parameter extraction based on ASTER and Landsat ETM+ data," PhD Thesis, University of Zurich, Zurich, Switzerland (2005).

Kitsanai Charoenjit is a PhD candidate in the Institute of Sciences de la Terre de Paris at UPMC–Sorbonne Universités. His research focuses on forest carbon sequestration with emphasis on remote sensing technology and unmanned aerial systems (UAS). He is also an associate researcher at the Faculty of Geoinformatics, Burapha University.

Pierpaolo Zuddas is a professor of geochemistry in the Institute des Sciences de la Terre de Paris at UPMC–Sorbonne Universités. He made substantial contributions on carbon sequestration processes in both natural and artificial conditions. Prior to joining Sorbonne Universités, he was chair of the Institute of Environmental Engineering and Eco-Development and director of the Environment and Risk Program at the University of Lyon.

Pascal Allemand is a professor of earth sciences and remote sensing in the Laboratoire de Géologie de Lyon: Terre, Planète, Environnement at Université de Lyon 1. His main research concerns the development of methods for landscape monitoring using remote sensing data, geospatial modeling, LiDAR, and unmanned aerial systems (UAS).

Sura Pattanakiat is an associate professor of forestry ecology and remote sensing and director of the Geo-Informatics in Resource and Environment Research and Training Center (GIREN), Mahidol University. His main research concerns development methods for land use and land cover on watershed monitoring and natural-disaster management using geoinformation.

Katavut Pachana is an assistant professor of the Department of Chemistry at Burapha University. His research is focused on environment and risk management.

BIOGRAPHY

NAME	Kitsanai CHAROENJIT
DATE OF BIRTH	February 11 st , 1983
PLACE OF BIRTH	Bangkok, Thailand
INSTITUTIONS ATTENDED	<p>Rajabhat Suandusit University, 2002-2006: Bachelor of Science (Environmental Science)</p> <p>Mahidol University, 2006-2009: Master of Science (Appropriate Technology for Resources and Environmental Development)</p> <p>Université Pierre et Marie CURIE, 2011-2015: Doctor of Philosophy (Geosciences, Natural Resources and Environment)</p>
RESEARCH-GRANT	<p>Franco-Thai Scholarship Program (From Burapha University, Thailand 2011-2014)</p>
HOME ADDRESS	<p>534 Soi.Sukumvit soi 54 Sukumvit Rd., Prakanhong, Bangkok 10260, Thailand. E-mail:kitsanai.charoenjit@upmc.fr, kitsanai@buu.ac.th</p>